JOURNAL OF RESEARCH

OF THE U.S. GEOLOGICAL SURVEY

NOVEMBER–DECEMBER 1975
VOLUME 3, NUMBER 6

Scientific notes and summaries of investigations in geology, hydrology, and related fields

U.S. DEPARTMENT OF THE INTERIOR

UNITED STATES DEPARTMENT OF THE INTERIOR

GEOLOGICAL SURVEY

V. E. McKelvey, Director

For sale by the Superintendent of Documents, U.S. Government Printing Office, Washington, DC 20402. Annual subscription rate $18.90 (plus $4.75 for foreign mailing). Single copy $3.15. Make checks or money orders payable to the Superintendent of Documents.

Send all subscription inquiries and address changes to the Superintendent of Documents at the above address.

Purchase orders should not be sent to the U.S. Geological Survey library.

Library of Congress Catalog-card No. 72-600241.

The Journal of Research is published every 2 months by the U.S. Geological Survey. It contains papers by members of the Geological Survey and their professional colleagues on geologic, hydrologic, topographic, and other scientific and technical subjects.

Correspondence and inquiries concerning the Journal (other than subscription inquiries and address changes) should be directed to Anna M. Orellana, Managing Editor, Journal of Research, Publications Division, U.S. Geological Survey, National Center 321, Reston, VA 22092.

Papers for the Journal should be submitted through regular Division publication channels.

The Secretary of the Interior has determined that the publication of this periodical is necessary in the transaction of the public business required by law of this Department. Use of funds for printing this periodical has been approved by the Director of the Office of Management and Budget through June 30, 1980.

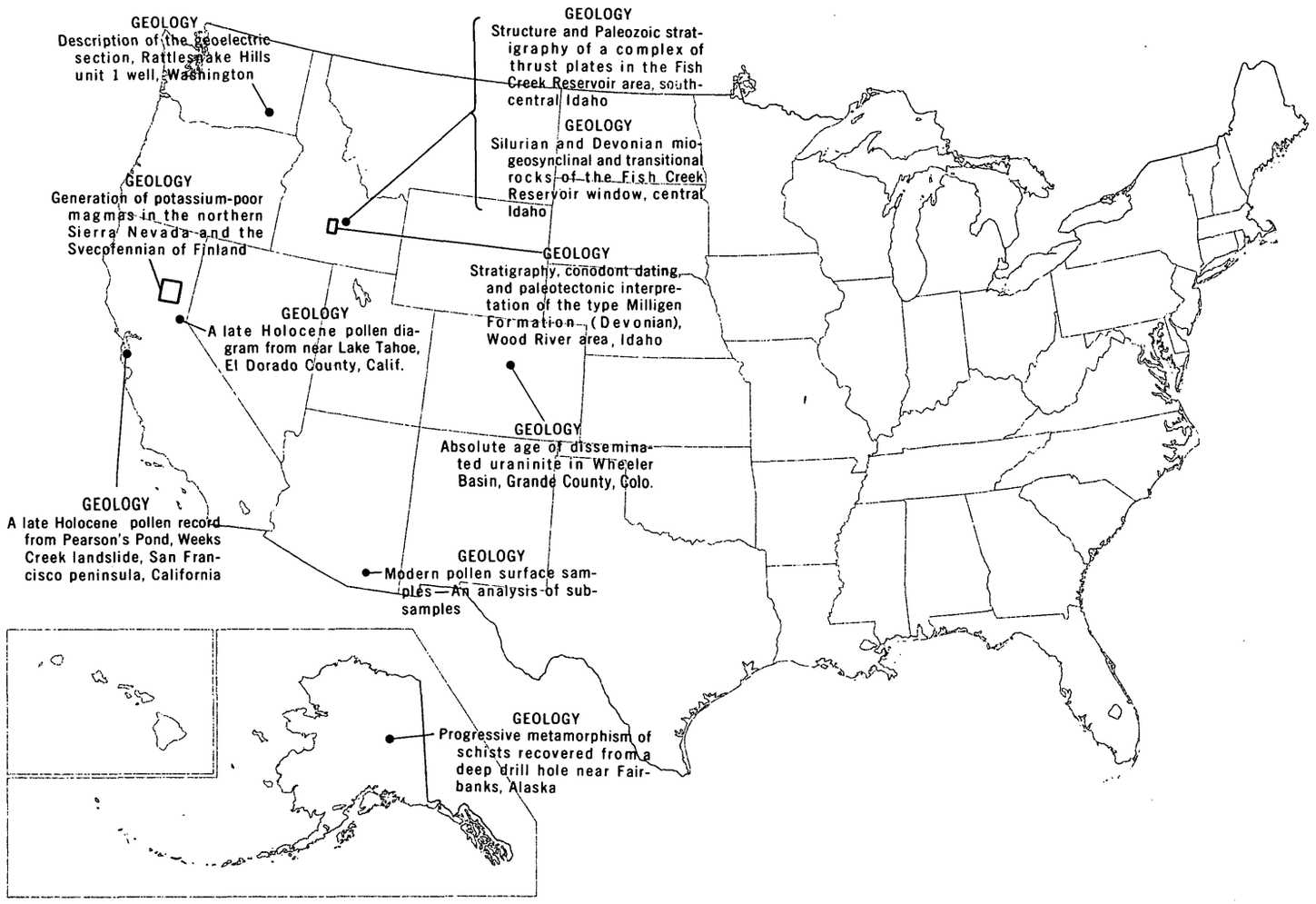

GEOGRAPHIC INDEX TO ARTICLES

See "Contents" for articles concerning areas outside the United States and articles without geographic orientation.

JOURNAL OF RESEARCH

of the

U.S. Geological Survey

Vol. 3 No. 6 Nov.–Dec. 1975

CONTENTS

ABBREVIATIONS

A ——— angstrom
a_0 ——— unit cell edge
acre-ft ——— acre-foot
A.D. ——— anno Domini
alt ——— altitude
atm ——— atmosphere
avg ——— average
bbl ——— barrel
B.C. ——— before Christ
B.P. ——— before present
b.y. ——— billion years
°C ——— degree Celsius
cal ——— calorie
calc ——— calculated
cm ——— centimetre
cm^2 ——— square centimetre
COD ——— chemical oxygen demand
colln. ——— collection
concd ——— concentrated
concn ——— concentration
cP ——— centipoise
c/s ——— counts per second; cycles per second
D ——— debye unit
d ——— day
dB ——— decibel
d.f. ——— degree of freedom
diam ——— diameter
DO ——— dissolved oxygen
DSDP ——— Deep Sea Drilling Project
Eh ——— oxidation-reduction potential
eq ——— equation
EROS ——— Earth Resources Observation System
ERTS ——— Earth Resources Technology Satellite (now LANDSAT)
eU ——— equivalent uranium
exp ——— exponential of
°F ——— degree Fahrenheit
ft ——— foot
ft^2 ——— square foot
ft-c ——— foot-candle
g ——— gram
gal ——— gallon
h ——— hour
ha ——— hectare
hm ——— hectometre
in. ——— inch
inf ——— inferior
J ——— joule
K ——— kelvin
keV ——— kiloelectronvolt
kg ——— kilogram
km ——— kilometre
km^2 ——— square kilometre
kV ——— kilovolt
kWh ——— kilowatt-hour
l ——— litre
lat ——— latitude
lb ——— pound
LDMW ——— locally derived meteoric water
lim ——— limit
lm ——— lumen
log ——— logarithm (common)
long ——— longitude
M ——— molarity, molar (concentration)
m ——— molality, molal (concentration)
m ——— metre
m^2 ——— square metre
mA ——— milliampere
max ——— maximum
MBAS ——— methylene blue active substance
MeV ——— megaelectron volt
mg ——— milligram
Mgal ——— million gallons
mGal ——— milligal
mi ——— mile
mi^2 ——— square mile
MIBK ——— methyl isobutyl ketone
min ——— minute
Ml ——— million litres
ml ——— millilitre
mm ——— millimetre
mo ——— month
mol ——— mole
mV ——— millivolt
m.y. ——— million years
μcal ——— microcalorie
μg ——— microgram
μm ——— micrometre
μmho ——— micromho
N ——— normality
n ——— neutron
NASA ——— National Aeronautics and Space Administration
NBS ——— National Bureau of Standards
NOAA ——— National Oceanic and Atmospheric Administration
nm ——— nanometre
ohm-m ——— ohm-metre
oz ——— ounce
p ——— proton
P.d.t. ——— Pacific daylight time
pH ——— measure of hydrogen ion activity
ppb ——— part per billion
ppm ——— part per million
r/min ——— revolutions per minute
s ——— second
(s) ——— solid
SEM ——— scanning electron microscope
SI ——— Système International (International System)
SMOW ——— standard mean ocean water
std ——— standard
σ ——— population standard deviation
t ——— tonne
U.S.P. ——— United States Pharmacopeia
UTM ——— Universal Transverse Mercator
var ——— variance
W ——— watt
w/v ——— weight per volume
yd ——— yard
yr ——— year

Jour. Research U.S. Geol. Survey
Vol. 3, No. 6, Nov.–Dec. 1975, p. 631–645

GENERATION OF POTASSIUM-POOR MAGMAS IN THE NORTHERN SIERRA NEVADA AND THE SVECOFENNIAN OF FINLAND

By ANNA HIETANEN, Menlo Park, Calif.

Abstract.—Comparison of the evolution of magmas in the Precambrian of southwestern Finland with that in the Paleozoic and Mesozoic of the northern Sierra Nevada brings out features that may clarify the origin of potassium-poor silicic magmas. In the northern Sierra Nevada, Paleozoic sodarhyolitic effusive rocks and associated trondhjemite represent silicic differentiates of andesitic magmas formed near a Benioff zone. These potassium-poor magmas were formed early, before thickening of the crust, and were followed by basaltic and rhyolitic magmas with normal potassium content. In southwestern Finland, where 70 percent of the area is covered by silicic and intermediate plutonic rocks, the early synkinematic intrusive masses are trondhjemitic and the later ones are granitic with eutectic ratios of quartz, plagioclase, and potassium feldspar. The latest granites are exceptionally rich in potassium feldspar. The oldest rocks, cordierite-garnet-sillimanite gneisses and interbedded metavolcanic rocks, are folded on gently plunging axes that steepen diapirically around large late kinematic plutonic masses. Trondhjemite occurs as thin sheetlike masses parallel to the folded bedding and could not have traveled far without losing its initial heat. Therefore it seems that the trondhjemitic magma was formed at shallow depths. By analogy with the shallow depth of early magma generation in the northern Sierra Nevada, it is suggested that the trondhjemitic magmas in Finland formed at mantle depths near a Benioff zone or at the base of the early thin crust at pressures where phlogopite or biotite was stable. Later, after thickening of the crust above, potassium from the biotite was released, making the late kinematic magmas rich in potassium. A plate-tectonic model of an island-arc environment explains the coeval age of the Svecofennian and "Karelian" foldbelts and the increase of potassium with decreasing age in the extrusive and intrusive magmas.

Studies of Cenozoic volcanic rocks in island arcs and continental margins indicate that the composition of magmas changes regularly across these structures, particularly the potassium content, which, at a given silica content, increases toward the continent. This feature has been related to the depth of the Benioff zone and associated melting of the subducted lithospheric slab (Dickinson and Hatherton, 1967; Dickinson, 1970). Moore (1959, 1962) has called attention to the increase of potassium in plutonic as well as in volcanic rocks eastward in western North America. Bateman and Dodge (1970) have shown that the K_2O:SiO_2 ratio in plutonic sequences across the central Sierra Nevada generally increases to the east with decreasing age. Some plutonic rocks richer in potassium and older than the main batholith are, however, exposed on the east side. In detail, the distribution of potassium-poor and potassium-rich plutonic rocks is complicated by a time factor similar to that found for volcanic rocks by Gill (1970) and Jakes and White (1972).

Jakes and White (1970, 1971, 1972), in discussing the variation of major and minor elements in the extrusive rocks of orogenic zones, showed that the abundances of potassium and of certain trace elements (rubidium, barium, strontium, and light rare earths) increase not only with the depth of the seismic zone but also with time, the stratigraphically younger rocks being richer in these elements. The earliest magmas, which come from shallow depths, are poor in potassium and related trace elements and have chrondritic rare-earth elements (REE). Jakes and Gill (1970) suggested the name "island arc tholeiitic series" for the rocks differentiated from these magmas as contrasted with the normal calc-alkaline series, which have high concentrations of potassium and differentiated REE patterns.

A similar increase in the potassium content has seemingly been repeated through geologic time during various periods of magmatic evolution, not only during volcanism but also during plutonism. Viljoen and Viljoen (1969a, b) have described a steady increase in the potassium content of plutonic rocks in the Barberton region, South Africa, some of the oldest in the Precambrian. There, the oldest silicic plutonic rocks (3.2–3.4 b.y.) are low in potassium (<0.6 K:Na) and related trace elements and are thus tonalitic or trondhjemitic in composition, whereas the youngest (3.07 b.y.) granitic plutons of this region are rich in potassium and have a 2.2 K:Na ratio. The tonalitic magmas are thought by these authors to be complementary to the ultrabasic lavas, the komatiites, which were extruded prior to the plutonism.

Goodwin (1968) and Baragar and Goodwin (1969) have stressed a uniformity in the evolution of early magmas (>2.5 b.y.) in the Archean volcanic belts of the Canadian Shield. In each of the four belts studied, the volcanism began with eruption of tholeiitic magmas, followed by andesitic and silicic magmas, all low in potassium, titanium, barium, and strontium. The trace-element content of the salic rocks was found to be different from that of the average crust in the shield area, thus excluding the possibility that these magmas were formed by melting of the crust.

In the western part of the Fennoscandian shield in central Sweden, soda-rich hälleflinta and leptite predominate in the lowest part of the stratigraphic column, whereas the upper part includes silicic volcanogenic rocks rich in potassium (Geijer, 1963). The leptite formation continues from Sweden to southern Finland, where it includes much sedimentary material. The evolution of plutonic magmas (1.7–1.9 b.y.) in southwestern Finland greatly resembles the evolution of Archean plutonic magmas in South Africa. The geologically oldest synkinematic plutonic rocks are trondhjemite and related potassium-poor intermediate rocks, whereas the youngest late kinematic granites are exceptionally rich in potassium (Heitanen, 1943, 1947).

In the northern Sierra Nevada, igneous activity in Paleozoic (Devonian?) time began with the eruption of potassium-poor magmas of the andesite-sodarhyolite suite followed in the Permian (?) by eruptions of potassium-rich rhyolite and basalt (Hietanen, 1973a, b). Small trondhjemitic masses that were emplaced early during the orogeny represent deep-seated equivalents of sodarhyolites. The large postorogenic plutons have quartz dioritic border zones but have granitic centers that contain 2–4 percent potassium.

The trend from potassium-poor to potassium-rich silicic magmas seems to be repeated during each magmatic cycle through geologic time. It is hoped that this comparison of the evolution of magmas in the Precambrian of Finland with that in the northern Sierra Nevada will better our understanding of reasons underlying this trend and its repetitional nature.

GENERATION OF MAGMAS IN THE NORTHERN SIERRA NEVADA

The sequence of major events in the northern Sierra Nevada is (1) Paleozoic island-arc-type volcanism and sedimentation, (2) deformation culminating in the Jurassic, (3) postorogenic plutonism in the Late Jurassic and Early Cretaceous, uplift, and (4) renewed volcanism in the Cenozoic.

Paleozoic extrusive magmas

The earliest Paleozoic (Devonian?) magmas in the northern Sierra Nevada are represented by a suite of metavolcanic rocks, called the Franklin Canyon Formation (fig. 1; Hietanen, 1973b), that have the chemical characteristics of island-arc andesites. They range in composition from calcium-rich basaltic andesite to dacite and sodarhyolite, all exceptionally poor in potassium (<0.15 K_2O, Hietanen, 1973b, table 1) and contain less barium and strontium than the Mesozoic plutonic rocks of the same area (Hietanen, 1973b, tables 5 and 6). The silica content of the andesitic suite is notably low. Jakes and Gill (1970) have pointed out that similar chemical features together with chondritic rare-earth element (REE) patterns are characteristic of the early stages in island-arc evolution. In the northern Sierra Nevada, the potassium-poor andesitic suite was deposited on a sequence of interbedded chert and shale, typical of sediments deposited on ocean floors. The Franklin Canyon Formation is overlain by the Horseshoe Bend Formation, which consists of Permian(?) basaltic and rhyolitic rocks and interbedded metachert, phyllite, and shallow-water carbonates. The metarhyolites of the Horseshoe Bend Formation contain as much as 4.5 percent K_2O and thus differ markedly from the potassium-

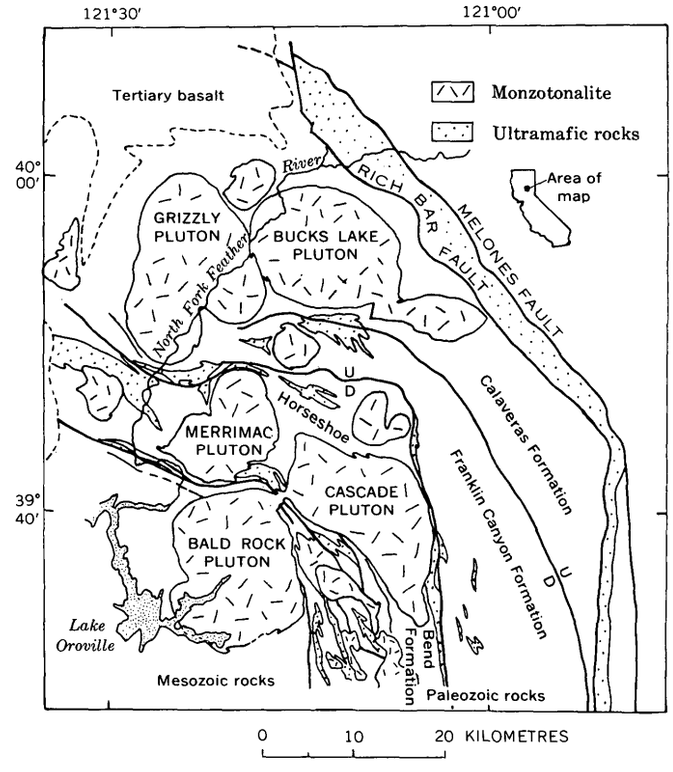

FIGURE 1.—The major geologic units in the northern Sierra Nevada, Calif. Modified from Hietanen (1973b).

poor silicic volcanic rocks of the Franklin Canyon Formation.

A similar sequence of potassium-poor to potassium-rich magmas erupted during Mesozoic time. The oldest of the Early Jurassic metavolcanic rocks are chemically and mineralogically similar to those of the Devonian(?) andesite-sodarhyolite suite, but the textures and structures are markedly different, the Mesozoic rocks being less deformed and better preserved. The cause of the repetition in compositional trend is not known, but it could be associated with a repetition of tectonic events. The northern Sierra Nevada is cut by several large northwest-trending faults, some of which are thrusts (figs. 1 and 2); all dip steeply to the east and may have been rotated to the vertical (Davis, 1969). The presence of ultramafic rocks along these fault zones is consistent with both the concept of large-scale underthrusting to the east and the hypothesis of an oceanic plate subducting under the North American continental plate during Paleozoic and Mesozoic time. Trench deposits related to the inferred Paleozoic subduction zone have not been recognized in the northern Sierra Nevada but are known in the Klamath Mountains, 150 km to the northwest (Burchfiel and Davis, 1972). In the northern Sierra Nevada, the Mesozoic volcanic rocks are west of the Paleozoic rocks. They are probably related to a younger Mesozoic subduction zone that evolved to the west of the Paleozoic zone and probably surfaced somewhere within, or west of, the present Coast Ranges. Such seaward steppings of subduction zones are reflected in the repetition of blueschist belts in the Coast Ranges (Ernst, 1973). After subduction, there must have been considerable vertical displacement along the Coast Range faults to bring the blueschist-facies rocks up from a depth of at least 30 km.

Two fundamentally different ways for generation of calc-alkaline andesitic and dacitic magmas in an island-arc environment have been suggested by experimentalists. Green (1972) has suggested that quartz-normative liquids could be formed in the basaltic layer of down-going oceanic lithosphere at temperatures >700°C and depths of 70–100 km or by two-stage melting of the mantle peridotite, the first liquid being tholeiitic. Yoder (1969), Kushiro and Yoder (1972), and Kushiro (1972) report a quartz-normative melt from a simple peridotitic mixture under hydrous conditions at temperatures of 1000°–1025°C and pressures of 10–26 kbar. Green (1973, p. 290) has refuted these reports, pointing out that the composition of the quench glass is not the composition of liquid formed in equilibrium with primary minerals of the

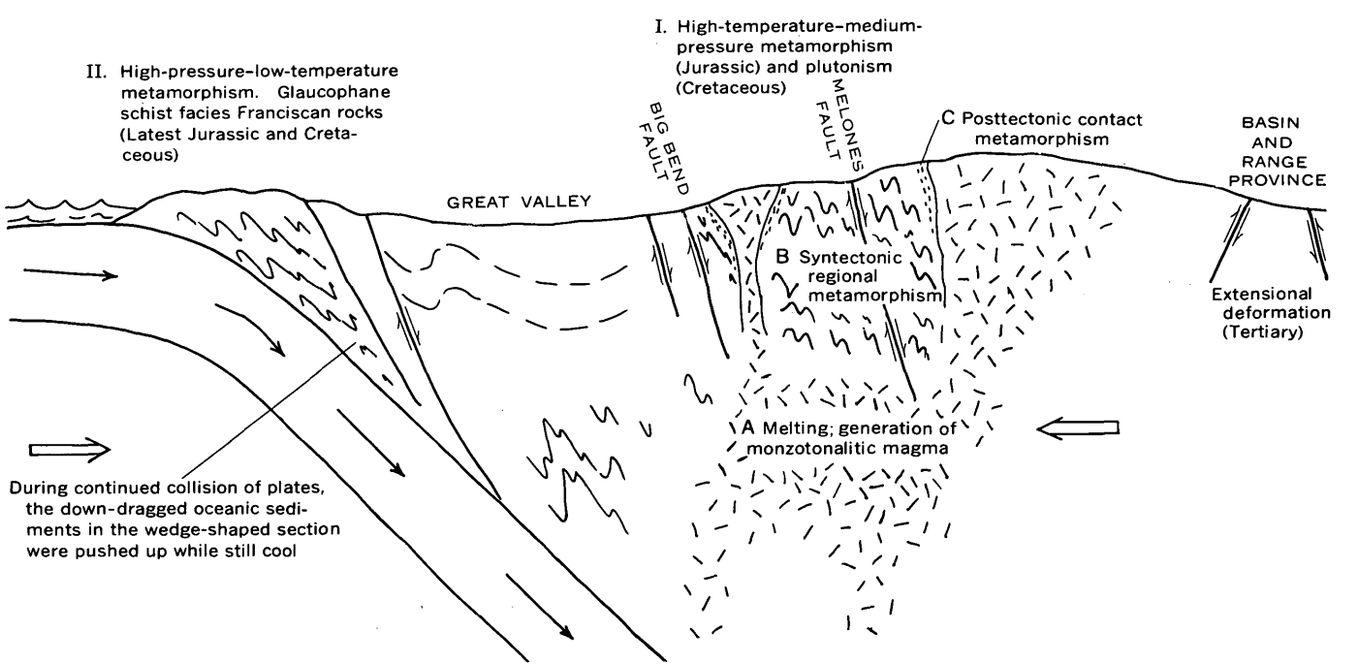

FIGURE 2.—Relations between deformation, metamorphism, and plutonism in the northern Sierra Nevada. In relation to magma chamber A, B is regional contact metamorphism. At the level presently exposed, zone B was metamorphosed to the border line between the greenschist and epidote amphibolite facies, and contact zone C to andalusite-cordierite (-staurolite) subfacies of the epidote amphibolite facies (Hietanen, 1967).

peridotite. In similar experiments he found quench amphibole and quench clinopyroxene crystals in the glass and concluded that the primary melt is quartz tholeiitic and the silicic glass a production of fractionation. This argument was supported by the observation of magnesium-iron disequilibrium partitioning between the glass and the primary minerals of the peridotite, olivine and orthopyroxene. Boettcher (1973) recently reported that olivine together with clinopyroxene and spinel is a liquidus phase if a magnetite-würstite-water buffer ($f_{O_2} \approx 10^{-11}$atm) is used in the experiments. The work of Modreski and Boettcher (1972) shows further that at high pressures quartz-normative liquids in equilibrium with olivine are produced from enstatite plus phlogopite plus water. Inasmuch as these minerals are common phases in mantle peridotite, this relationship would indicate that under certain conditions quartz-normative magmas can be generated from the wet mantle peridotite. The model of Nichols and Ringwood (1973) also is based on the expansion of the stability field of olivine under hydrous conditions. The trend of differentiation of the tholeiitic magma in their model is toward a potassium-rich calc-alkaline series and would not apply directly to the origin of the potassium-poor magmas.

The average composition of the andesitic magma of the Franklin Canyon Formation in the northern Sierra Nevada was estimated on the basis of areal distribution and chemical composition of its various members. This weighted mean composition (table 1, col. 1) is remarkably close to the composition of the metadiorite in the same area (table 1, col. 2). Both contain less silicon and alkalies, especially potassium, than average calc-alkaline andesites, and more aluminum, calcium, and magnesium. The composition is close to the island-arc basaltic andesite (table 1, col. 3) except for an exceptionally low amount of alkalies and high calcium and magnesium. These peculiarities of composition are discussed below under "Plutonic Magmas."

Alteration of extreme mafic and silicic layers is typical of parts of the Franklin Canyon Formation. The silicic layers are rich in quartz and albite (An_5) and contain muscovite, chlorite, and epidote. The presence of numerous phenocrysts of quartz and albite in these layers proves that they crystallized from silicic magmas. The interbedded metadacite has hornblende and chlorite as dark constituents, and quartz is in the groundmass and in amygdules. Intercalated with the silicic metavolcanic rocks are basic layers that consist of hornblende, chlorite, and epidote with minor albite. Pseudomorphs of chlorite and epidote after pyroxene and those of albite and epidote after plagioclase are common. These layers are extremely rich in calcium (15 percent CaO) and aluminum (20 percent Al_2O_2) and contain only about 40 percent SiO_2. They probably represent accumulations of clinopyroxene, hornblende, and calcic plagioclase from the basaltic andesite magma of the early island-arc type. No potassium-bearing minerals occur in any of the rocks of the Franklin Canyon Formation, and the K_2O content is consistently below 0.2 percent.

TABLE 1.—*Comparison of composition of magmas in the northern Sierra Nevada, island arc, and southwestern Finland*

[Values are given in percentage]

	Franklin Canyon Formation (estimated average)[1] (1)	Metadiorite in northern Sierra Nevada[2] (2)	Basaltic andesite in New Britain[3] (3)	Plutonic rocks in northern Sierra Nevada (estimated average)[4] (4)	Trondhjemite mite series in Finland (estimated average)[5] (5)
SiO_2	51.63	53.36	53.83	66.0	67.6
TiO_2	.58	.54	1.01	----	.04
Al_2O_3	17.81	15.20	15.42	16.0	16.1
Fe_2O_3	2.02	2.56	5.00	----	0.6
FeO	4.70	4.95	6.74	2.0	2.6
MnO	.13	.17	.20	----	0.1
MgO	5.83	7.58	4.36	1.5	1.5
CaO	10.52	10.36	8.83	4.0	3.6
Na_2O	1.96	1.80	2.99	4.5	5.0
K_2O	.06	.03	.92	1.8	1.8
P_2O_5	.13	..16	.21	----	0
H_2O	3.11	2.89	.44	----	0.8
Total	98.48	99.60	99.95	100.1	---

[1] Hietanen, 1973b.
[2] Hietanen, 1973b, table 1, sample 465.
[3] Lowder and Carmichael, 1970.
[4] Hietanen, 1973b, table 3.
[5] Hietanen, 1943.

The chemistry and stratigraphy of the Permian(?) metavolcanic rocks in the northern Sierra Nevada—the Horseshoe Bend Formation—are very different from those of the Devonian(?) meta-andesite suite—the Franklin Canyon Formation. The Permian(?) lavas are mainly basaltic with discontinuous interlayers of potassium-rich rhyolite in the lower part of the section and only a few small occurrences of andesite, dacite, and sodarhyolite within the interlayered sedimentary rocks. The occurrence of potassium-rich metarhyolite as discontinuous layers and lens-shaped bodies within the metabasalt indicates contemporaneous eruption of these two end members. Yoder (1973), in reviewing several field occurrences of contemporaneous basalt and rhyolite, suggested, on the basis of Kushiro's (1969) study of the diopside-forsterite-silica system, that melting of a quartz-normative parent rock would yield a rhyolitic melt until all quartz is exhausted. Upon removal of this melt, the bulk position would move to the diopside-enstatite join. Further melting would require a higher tem-

perature, and the liquid formed would be basaltic. No intermediate compositions would occur.

The transition from Devonian(?) to Permian(?) volcanism involves a radical change in the potassium content of the magmas from potassium-poor to potassium-rich, a trend not explained by these experiments. The potassium content is apparently time dependent, as in the stratigraphic columns of some modern island arcs that do not have a clearly developed seismic plane or where this plane is steep, as discussed by White, Jakes, and Christie (1971) and Jakes and White (1972). Individual volcanoes in the Fiji Islands show similar trends (Gill, 1970). Glikson (1972) has pointed out that the pattern of evolution of magmas in early Precambrian time was similar to that in the Fiji volcanoes and suggested that the increase in the potassium content was brought about by repeated partial fusion, first of oceanic crust, then of its differentiation products. The details of the possible mechanism were not discussed.

The recent experimental work by Allen, Modreski, Haygood, and Boettcher (1972), Modreski and Boettcher (1972), and Boettcher (1973) on the stabilities of amphiboles and biotite or phlogopite at high pressures and temperatures provides a possible explanation for the increase in potassium with time. On the basis of their experimental work, they suggest that amphiboles are stable down to depths of 75 km, whereas phlogopite does not begin to decompose until depths of about 100 km and ceases to be stable at depths greater than 175 km. When the subducting oceanic lithosphere reaches depths of 60–90 km, amphiboles would break down, releasing water for magma generation from basaltic rocks. Most of the sodium would be incorporated into the magma, whereas potassium might remain as phlogopite or biotite. This would yield a high Na:K ratio for the early magmas. After the oceanic plate had descended to depths of 100 km, biotite would begin to decompose, releasing potassium into the magma. Inasmuch as oceanic plates have been traced down to depths of 600–700 km as cool rigid bodies (Barazangi and others, 1970), it is likely that the earliest quartz normative magmas are generated from the mantle peridotite of the contental plate above the Benioff zone by adding only water from the subducting, oceanic lithosphere below. The relative stabilities of amphiboles and phlogopite could still give rise to the formation first of sodium-rich, and, somewhat later of potassium-rich magmas. According to the experimental work of Huang and Wyllie (1973), muscovite is not stable at high pressures and could not contribute to the change of the Na:K ratio across island arcs.

According to the stability relations between hornblende and biotite, the change from potassium-poor Devonian(?) to potassium-rich Permian(?) magmas in the northern Sierra Nevada would require an increase in the pressure of magma generation. Such an increase could be brought about by stepping of the Benioff zone to the west or by thickening of the crust above the magma chamber by accumulation and deformation, as suggested earlier (Hietanen, 1973a). Seaward steppings of the Benioff zone in the island-arc systems are common. Such an event seems the most likely cause for the repetition of potassium-poor andesitic volcanism west from the Paleozic volcanic rocks in Mesozoic time (figs. 1 and 2). Thickening of the crust by accumulation and tectonism is indicated by the stratigraphy and structure of the area. All these mechanisms could have been in operation to increase the load pressure above the zone of partial fusion. Thickening of the crust of the continental plate from Devonian(?) to Permian(?) by accumulation, folding, and faulting could have been of order of 10–20 km and could alone have produced the increase in pressure necessary to break down phlogopite and release potassium into the magma.

Plutonic magmas

The earliest plutonic rocks in the northern Sierra Nevada are small synkinematic bodies of gabbro, quartz diorite, and trondhjemite that were deformed and recrystallized with the Paleozoic metavolcanic rocks (Hietanen, 1973b). In their chemical composition and trace-element content, these rocks are similar to the equivalent effusive rocks, suggesting a common origin. The plutonic magmas intruded their own volcanic pile.

Large quantities of plutonic magmas were generated later, at the end of the peak of Jurassic deformation. These magmas contain more potassium than the earliest ones, the average (table 1, col. 4, estimated on basis of areal distribution of analyzed rocks; Hietanen, 1973b, tables 3, 4) being similar to the western sequences in the central Sierra Nevada (Bateman and Dodge, 1970). Members of a typical calc-alkaline differentiation series from hornblende gabbro and quartz diorite to monzotonalite and granite crystallized from these magmas. Comparison with the earliest group shows that there was a notable increase in the potassium content of the plutonic magmas with decreasing age (as was true also for the extrusive magmas). Generation of large quantities of quartz dioritic magma most likely resulted from partial melting of basaltic rocks attached to the seafloor of the

downgoing slab during early stages of subduction. These rocks could have been dehydrated during the generation of andesitic extrusive magmas and would consist of eclogite and gabbro, and therefore, according to the models of Hanson and Goldich (1972) and Arth and Hanson (1972) would yield quartz dioritic, tonalitic, and trondhjemitic magmas.

An explanation for the low potassium content of these magmas could be the same as that proposed by Allen, Modreski, Haygood, and Boettcher (1972) for the low potassium content of early island-arc andesites, that is, retention of potassium in the form of phlogopite in the residue. Under these conditions the partial melting that produced trondhjemitic magmas would have occurred at depths of less than 100 km.

An alternative model for the origin of trondhjemites is by the separation of abundant biotite at an early stage during the crystallization differentiation of "wet" gabbroic (or dioritic) magma. This origin was first proposed by Goldschmidt (1922) for trondhjemites in the type locality in Norway and thought by Hietanen (1943) to explain the origin of similar rocks in Finland. The difficulty in this model in Finland, however, is the relative amounts of trondhjemite (60 percent) and associated tonalite (30 percent) and diorite (10 percent) and the absence of exceptionally large amounts of biotite in the tonalitic rocks. The chemical analyses (Hietanen, 1943; see figs. 5, 6) show that all members of the differentiation series are low in potassium, the weighted average (table 1, col. 5) being close to the average of plutonic magmas in the northern Sierra Nevada. This leads to the conclusion that the parent magma, formed by partial melting of an unknown source rock, was low in potassium. In essence, the problem is once more returned to the rentention of potassium in a residue. Inasmuch as phlogopite (or biotite) is the only potassium-rich mineral stable at mantle depths, it seems that this mineral played a dual role in generation of trondhjemitic magmas.

Only some of the quartz dioritic plutons in the northern Sierra Nevada differentiated toward a trondhjemitic center or are cut by trondhjemitic dikes in which the potassium feldspar content is 2 to 10 percent. Crystallization of large quantities of biotite at an earlier stage explains the scarcity of potassium feldspar in these late-stage trondhjemites. Numerous hexagonal biotite phenocrysts are common in rhyolitic sheetlike bodies along the eastern border of the Merrimac pluton (Hietanen, 1951, pl. 2). Most of the potassium in this rock (4.3 percent) is in these early biotite phenocrysts. Some other plutons have a trondhjemitic core surrounded by a zone of biotite-rich (10 percent) tonalite. These relations suggest that an early fractionation of biotite in a dioritic or granodioritic magma can yield only a small amount of trodhjemitic end product unless the parent magma is low in potassium.

The simultaneity of the cessation of deformation and formation of large quantities of calc-alkaline plutonic magmas supports the concept that both these events resulted from a large-scale partial fusion of the subducted oceanic lithosphere as well as of the deeper part of the continental plate above it. Neither plate supported a further deformation. As suggested earlier (Hietanen, 1973a), magmas rising from the mantle initiated partial or total melting in deeper parts of the downfolded metavolcanic and interbedded metasedimentary rocks, resulting in mixed origin of most plutonic magmas. In support of this mixed origin, the 0.703–0.708 Sr^{87}/Sr^{86} ratios of the plutonic rocks (Hurley and others, 1965; Kistler and Peterman, 1973) are somewhat higher than those of the mantle-derived basalts and andesites. Trondhjemitic affinities of the Bald Rock pluton (Hietanen, 1951; Compton, 1955) were probably enhanced by digestion of large quantities of the Mesozoic potassium-poor metavolcanic rocks into which this pluton was emplaced. Soda-rhyolitic layers among these rocks contain only 0.9 percent K_2O but 4.7 percent Na_2O (Hietanen, 1951).

At the present level of erosion, selective partial fusion of the metamorphic rocks is reflected in their chemical composition. Comparison with unmetamorphosed island-arc andesite (table 1) and the average of andesites and dacites as given by Daly (1933) and Chayes (1969) suggests that the metavolcanic rocks have lost much of their alkalies and silicon and have been enriched in calcium and magnesium. Their mineralogy and textures indicate that these changes took place during regional metamorphism (B in fig. 2). In many layers large amounts of amphibole and epidote minerals, which form stable mineral assemblages with albite at low to medium metamorphic temperatures, increase the amount of calcium and magnesium to several percent more than is common in average andesite and dacite. Silica is notably low (41 percent, Hietanen, 1973b) and there is less than 0.1 percent K_2O. Yet in many dacitic and rhyolitic layers relict phenocrysts of quartz are preserved. There must have been extensive outward migration of silicon and alkalies during the metamorphism. Comparison of the mean composition of the plutonic rocks (table 1, col. 4) with that of calc-alkaline andesites shows that the plutonic rocks contain considerably more silicon and alkalies and less calcium, iron, and magnesium than the average andesite (table 1, col. 4).

The elements lost (Si, Na, K) and gained (Ca, Fe, Mg) by the metavolcanic rocks during metamorphism should be added to, and subtracted from the andesitic magma to yield magma of the same composition as the plutonic rocks. This supports the hypothesis of migration of silicon and alkalies from the surrounding rocks into a eutectic melt forming in the lower part of the crust.

Mineral assemblages in the metamorphic contact aureoles of the plutons provide some limiting values to the possible pressure-temperature conditions of the generation of the monzotonalitic magmas. The andalusite-cordierite-biotite assemblage is common in pelitic layers next to the plutons. Staurolite occurs in the outer contact aureole but has been pseudomorphosed to mica in the highest grade zone. Pressures during metamorphism were lower than at the triple point of the three aluminum silicates and temperatures higher than the upper stability limit of staurolite. Temperatures of about 600°C and pressures around 4 kbar seem reasonable and could have been reached 12 to 15 km below the surface. The region of melting was at a lower level. Assuming a geothermal gradient of 30°–25°C/km, monzotonalitic magma could be formed by differential melting at about 700°C (Piwinskii, 1968) at depths of 25–30 km. Textures of the plutonic rocks suggest that this magma contained crystals of plagioclase (An_{40-45}), epidote, hornblende, and biotite. Oscillatory zoning and resorption of early plagioclase phenocrysts indicate fluctuations in the pressure-temperature conditions and in the composition of the melt. Large amounts of early epidote may have been inherited from the metavolcanic rocks digested by the magma.

Cenozoic volcanism

Volcanism in the western Cordilleran region was renewed after the large deep-seated batholiths solidified and were exposed by erosion when the crust of the continental margin was cool and rigid again. The evolution of this late volcanism is related to a renewed subduction of the Pacific floor under the North American continent in Cenozoic time (Dickinson, 1970; Lipman and others, 1972). A change from predominantly island-arc type andesitic volcanism to a bimodal basalt-rhyolite phase occurred in late Cenozoic time (Christiansen and Lipman, 1972).

Late Cenozoic basaltic lavas east of the Sierra Nevada are thought by Scholz, Barazangi, and Sbar (1971) to be related to an extensional deformation typical of interarc basins behind the island arcs similar to the process suggested by Karig (1971) for development of marginal basins in the western Pacific. An interarc-type spreading in the Basin and Range province could be a direct result of the termination of subduction of the Pacific floor under the North American continent. Scholz, Barazangi, and Sbar (1971) have suggested the following mechanism for the related volcanism: Partially melted material from the upper part of the subducting slab rises diapirically through the mantle, is trapped beneath the lithosphere, flattens there, and spreads outward; extensional deformation accompanied by volcanism occurs when the stress is released.

SVECOFENNIAN IGNEOUS ROCKS

Outline of general geology

Radiometric age data obtained in recent years from rocks in all parts of the Fennoscandian Shield have radically changed the formerly accepted concept of an Archean age for the highly migmatized Svecofennian foldbelt and its tectonic relation with the "Karelian" foldbelt to the east. The "Karelian belt" consists mainly of well-preserved shelf type sedimentary rocks, such as quartzite, dolomite, and pelite, and was considered to be younger than the more highly metamorphosed and migmatized Svecofennian eugeosynclinal graywacke-type sediments and interbedded volcanic rocks. Synkinematic plutonic rocks in these two foldbelts, however, are of about the same age, 1.7–1.9 b.y. (Kouvo and Tilton, 1966; Kouvo and Kulp, 1961; Wetherill and others, 1962; Welin, 1966a, b; Welin and others, 1971), suggesting that they represent different facies of the same orogenic belt. The basement gneisses east of the "Karelian" sedimentary formations are older, 2.6–2.8 b.y. (Kouvo and Tilton, 1966; Kahma, 1973). The oldest part (>3.6 b.y.) of the Fennoscandian Shield is farther northeast in the Kola Peninsula, where, according to Pavlovskiy (1971), basal conglomerate of the highly metamorphosed Kola Series rests on gabbroic and noritic rocks. Granites cutting the Kola Series have potassium-argon ages of 2.8–3.6 b.y. and uranium-lead-thorium ages of 2.8 b.y. (Gerling, Kratz, and Lobach-Zhuchenko, 1968).

A wide mineralized fault zone (Kahma, 1973) shown as the Svecokarelian fault zone of figure 3, separates the older (2.6–2.8 b.y.) Karelian block to the northeast from the Svecofennian block (U-Pb ages 1.8–1.9 b.y.) to the southwest. In central Sweden, where the Svecofennian formations continue, they are bordered by younger (1.2–1.7 b.y.) north-south-trending Gothian formations to the southwest (Lundegårdh, 1971; Hjelmqvist, 1973) and by the Paleozoic Caledonian Mountains to the west-northwest. The ages of synkine-

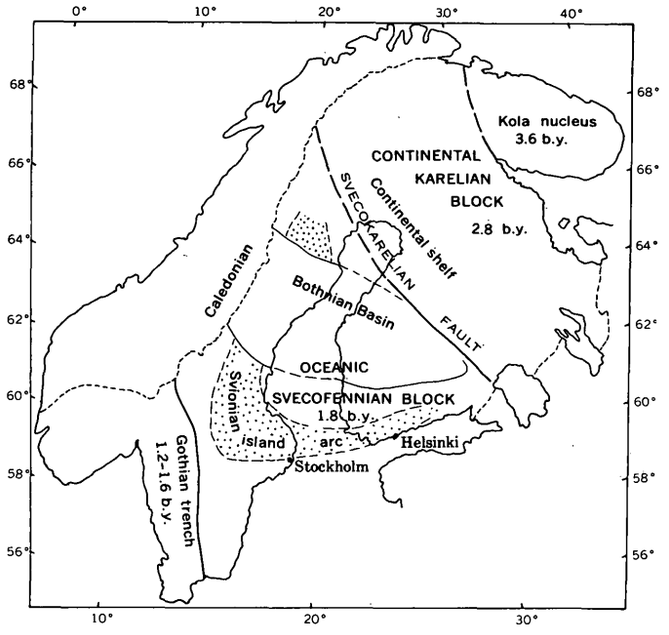

FIGURE 3.—Geotectonic elements and their radiometric ages in the Fennoscandian Shield. Svecokarelian fault zone separates the older (2.8 b.y.) continental Karelian block from the younger Svecofennian block, which was transformed from oceanic to continental during the Svecofennian orogeny (1.9–1.7 b.y. ago).

matic plutonic rocks in these tectonic blocks are generally younger westward. The exposed Svecofennian area extends for about 1000 km in an east-west direction through southern Finland and central Sweden and for more than that in the north-south direction in Sweden.

Several anticlines and synclines on east-west trending axes have been mapped in southern Finland and central Sweden. Farther north, the trends wrap around the granite complex of central Finland (fig. 4) and turn to the northwest and north in northern Sweden. Near Vassa, on the east coast of Bothnian Gulf, the trends bend around a synkinematic granite pluton, conforming with the geosynclinal structure of central Norrland in Sweden (Magnusson, 1960), west of the gulf. A low ratio between the length and width of this "geosyncline" as well as of other sedimentary basins in the Svecofennian belt, the type of folding (eye folds and flow folds being common), a diapiric rise of numerous granite masses and a profound migmatization of high grade metamorphic rocks are features common in many other Precambrian shield areas (for example Windley and Bridgewater, 1971; Anhaeusser and others, 1969). Comparison of the lithology of the Svecofennian belt in southwestern Finland with that of the northern Sierra Nevada, however, brings out many similarities between these two orogenic belts of vastly different ages.

A complete stratigraphic column of the Svecofennian belt in Finland is difficult to establish because the area is intruded by plutonic masses of various sizes to the extent that only about one-third of the ground is underlain by older metamorphic rocks (fig. 4). From detailed studies of several small but well-preserved parts of the area (Eskola, 1914; Hietanen, 1943, 1947; Neuvonen, 1954, Härme, 1954, 1960, Seitsaari, 1954; Edelman, 1960, Gaal and Rauhamäki, 1971; Laitala, 1973), its is clear that the metamorphic rocks in the Svecofennian belt originally were mainly graywacke-type sediments interbedded with argillaceous and arenaceous layers and metavolcanic rocks, constituting a sedimentary-volcanogenic succession typical of eugeosynclinal orogenic belts. The occurrences of quartzite and limestone are few and small. The metavolcanic rocks are either basaltic lavas and tuffs metamorphosed to amphibolites, or silicic and intermediate metavolcanic rocks interbedded with tuffaceous and sedimentary material and generally mapped as leptite. The leptites are particularly common in the east-west trending zone through Orijärvi and Kemiö (Eskola, 1914, 1963) in southern Finland, where they form the lowest part of the stratigraphic section (Edelman, 1960) and include andesitic, dacitic, and rhyolitic rocks. They are overlain by metasedimentary and basic metavolcanic rocks. A few discontinuous limestone layers occur in this zone. In the westernmost part of the Svecofennian belt, in central Sweden, where open

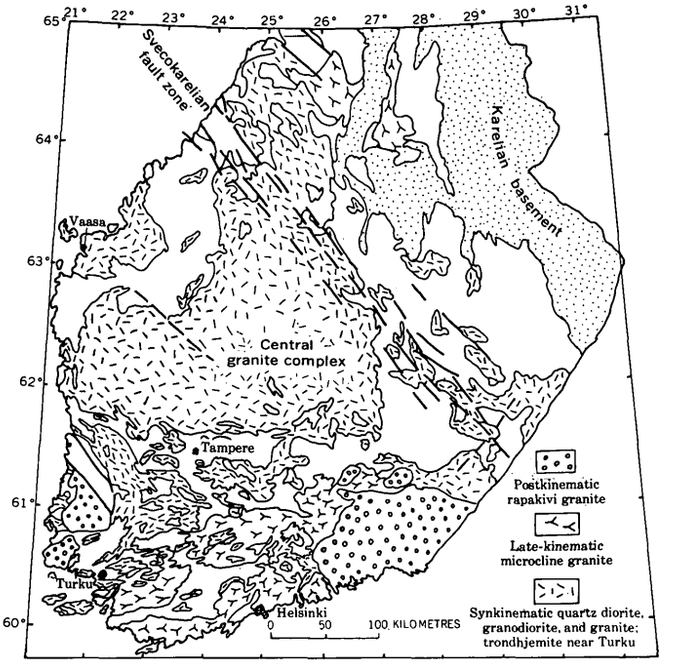

FIGURE 4.—Distribution of plutonic rocks in southern Finland. Modified from Simonen (1960a). Fault zone, here named Svecokarelian, according to Kahma (1973).

folding allows establishing a stratigraphic succession with considerable certainty (Geijer, 1963; Hjelmqvist, 1966), soda-rich volcanic rocks predominate in the lower part of the section, whereas potassium-rich rhyolites and some intermediate and mafic volcanic rocks are in the upper part. Chemically precipitated sedimentary rocks such as carbonates and quartz-banded iron ores are common in the lower part. The upper part of the leptite formation in central Sweden consists mainly of detrital material: slate and argillite in the western part and shales and subgraywacke in the eastern part.

A wide synclinal basin filled by graywacke-type metasediments interrupts the leptite belt in central Norrland, Sweden. This basin, a geosyncline according to Magnusson (1960), continues eastward to central Finland, where it has been intruded by a large granite complex. North of the basin in the Skellefteå region, Sweden, metavolcanic rocks crop out again and form there the lowest part of a stratigraphic section (Gavelin, 1955). All members of a potassium-poor island-arc type andesitic suite are represented ranging from sodarhyolite (keratophyre and quartz keratophyre by Gavelin, 1955) through dacite to andesite and basalt.

The grade of metamorphism increases generally from north to south. In Finland, the lowest grade is near Tampere, just south of the central granite complex where the graywacke-type sediments are metamorphosed to the epidote amphibolite facies. Farther south and west, these sediments were recrystallized to micaschists with cordierite and andalusite at places; the highest grade rocks, cordierite-garnet-sillimanite-biotite-potassium feldspar gneisses, are common in southernmost Finland.

The primary structures of the metasedimentary rocks, such as graded bedding, are excellently preserved in the low-grade zone near Tampere. In the high-grade zone near Turku, bedding and foliation are recognizable except where obliterated by intense migmatization. The folding on eastward-plunging axes is isoclinal or gentle with round hinges. Foliation parallel to the axial planes is vertical or dips steeply. Near the plutonic masses and in places where pegmatitic material is abundant, a second folding around steep axes is common, particularly in migmatites, in which intricate flow folding typical of all Precambrian migmatite areas prevails.

Evolution of magmas and plate tectonic model

In relation to the deformation of the Svecofennian foldbelt, two major structural groups of plutonic rocks can be distinguished, synkinematic and late kinematic. Several large masses of younger postorogenic rapakivi granite were emplaced after all deformational movement had ceased.

The earliest synkinematic plutonic rocks in southwestern Finland are trondhjemites and charnockites, both poor in potassium. They occur as long sheetlike masses parallel to the folded bedding of the cordierite-garnet gneisses and show the same structural patterns, including orientation of minerals, as their metasedimentary wall rocks (Hietanen, 1943). It is unlikely that these thin masses would have traveled through great crustal thicknesses without losing their initial heat. Farther east and northeast, the synkinematic plutonic rocks consist mainly of quartz diorite and granodiorite with some gabbroic rocks. Trondhjemitic masses, however, occur locally to the eastern border of the Svecofennian belt (Gaal and Rauhamäki, 1971).

Near Turku, granodiorite is a member of a differentiation series represented by small sheetlike or oblong masses of gabbro, quartz diorite, granodiorite, and granite. The contacts are generally concordant but at some places granodiorite cuts the veined structure of the cordierite-garnet gneiss. These contact relations and signs of only a weak deformation indicate that the granodiorite and related quartz diorite were emplaced later than the trondhjemite series (Hietanen, 1947).

Near Tampere, granite with a eutectic Q-Or-Ab composition represents the silicic end member of a normal differentiation series from gabbro through quartz diorite and granodiorite to granite (Simonen, 1960b). The individual plutonic masses are elongate in the direction of the regional trends and may have in part concordant and in part discordant contacts. Foliation and lineation are well developed near the contacts and are parallel to the steep foliation and lineation of the wall rocks. The shouldering effect of the rising magma is demonstrated by a common curvature of the structures of the wall rocks around the masses. According to Simonen (1960b), similar structures are typical of the central granite complex, especially of masses of intermediate composition, whereas many of the granite bodies show minerals in random orientation. Based on these contact relations and structures, the granites near Tampere and those in central Finland are considered late kinematic.

Large quantities of microcline granite exceptionally rich in potassium feldspar invaded southernmost Finland during the latest stages of deformation (fig. 4). These rocks occur in the broad east-west zone where the early kinematic rocks are poor in potassium. The individual masses range from a few hundred meters to 50 km or more in length, have mainly concordant

but irregular outlines, and include numerous elongate and ghostlike remnants of older rocks, still in their original position. A profound migmatization, anatexis, and potassium-feldspathization of all older rocks are genetically connected with the microcline granite. Large masses of rapakivi granite, emplaced later after the Svecofennian orogeny (age 1.6 b.y.; Kouvo and Tilton, 1966) also are exceptionally rich in potassium feldspar.

The chemistry of the charnockitic suite is identical with that of the trondhjemitic suite. The differences between the suites are strictly mineralogical and reflect the water content of the magma. The two-pyroxene–potassium-feldspar assemblage typical of the "dry" charnockites is replaced by hornblende and biotite in the "wet" trondhjemites. In the ternary Or-Ab-An and Or-Ab-Q diagrams (figs. 5 and 6), the molecular norms for both rock series plot in the same area far from the orthoclase corner. In the QFM diagram (fig. 7), the charnockites (7–10) plot with the trondhjemites close to the feldspar (F) corner. In contrast the late-kinematic microcline granite plots toward the orthoclase corner (T17 in figs. 5 and 6), as would the postkinematic rapakivi.

Simonen (1960b) has plotted the weight norms of all analyzed Svecofennian plutonic rocks in various ternary diagrams. The ternary diagram (fig. 8) modified from his Or-Ab-An diagram shows that the oldest synkinematic plutonic rocks, the trondhjemite and charnockites, are poor in normative orthoclase and that the synkinematic granodiorites have only a moderate or low orthoclase content. In contrast, the silicic end members of the late-kinematic quartz diorite-granite suite of central Finland have a composition of eutectic melts, and the youngest group, the microcline granites, are exceptionally rich in potassium.

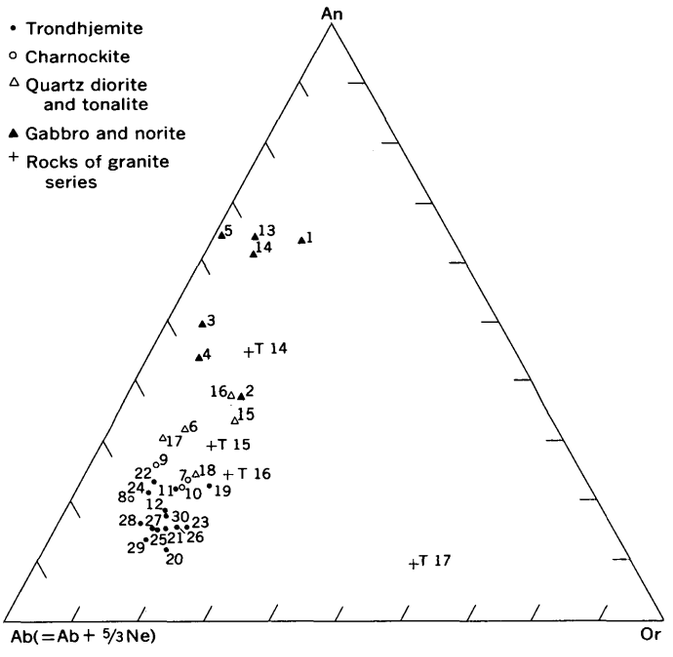

FIGURE 5.—Or-Ab-An diagram showing normative feldspar content in molecular percentages for plutonic rocks of Turku and Kalanti areas, southwestern Finland. Numbers 1–12 and T14–T17 refer to analyses in Hietanen (1947, table 1) and numbers 13–30 to analyses in Hietanen (1943, table 4).

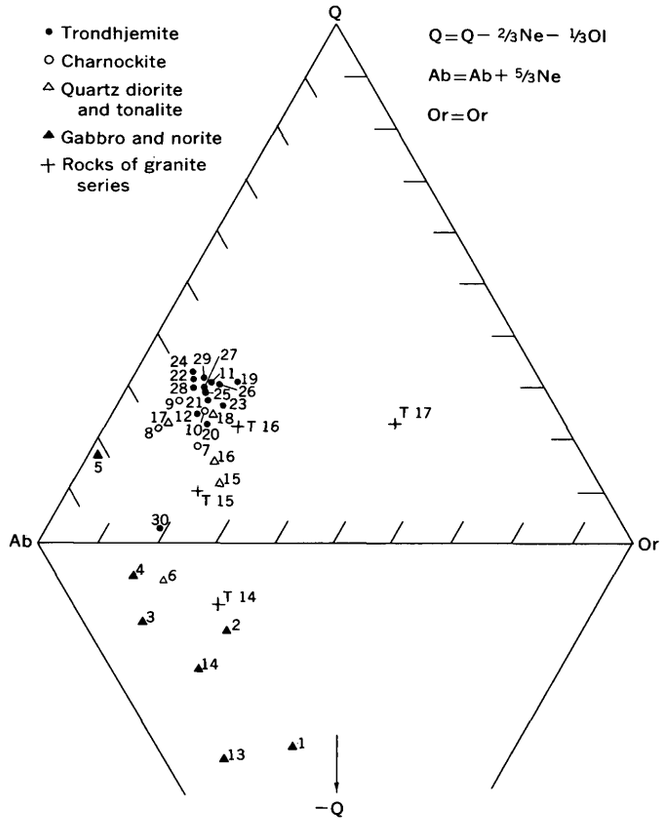

FIGURE 6.—Or-Ab-Q diagram showing normative proportions of orthoclase, albite, and quartz in molecular percentages for plutonic rocks in the Kalanti and Turku areas. Numbers refer to same analyses as in figure 5.

In summary, the potassium content of the plutonic magmas increased with decreasing age and plutonism migrated northward to central Finland, where the youngest plutonic rocks are late kinematic granites with eutectoid composition. In southernmost Finland, the zone of early potassium-poor plutonism was reinvaded during the latest phase, and these younger magmas were exceptionally rich in potassium. The increase in the potassium content of the plutonic magmas from the south to north and with time is similar to that in the Sierra Nevada from the west to east.

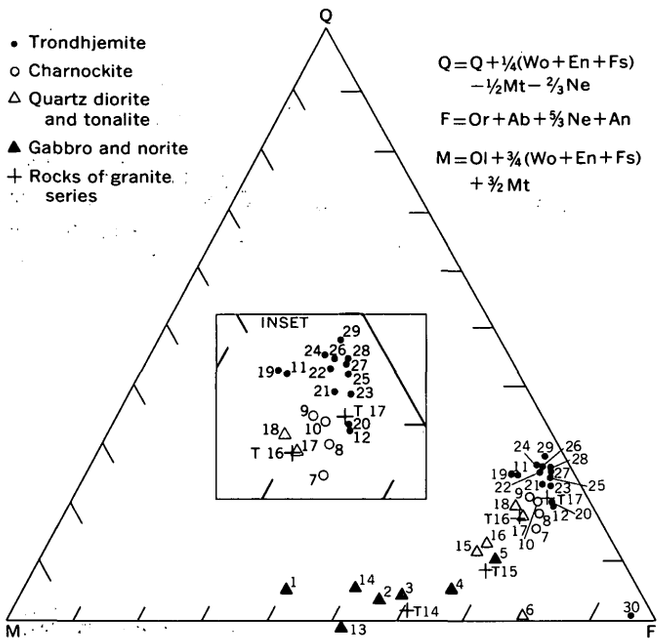

FIGURE 7.—QFM diagram showing normative proportions of quartz, feldspar and mafic constituents in molecular percentages for plutonic rocks in the Kalanti and Turku areas. Numbers refer to same analyses as in figure 5.

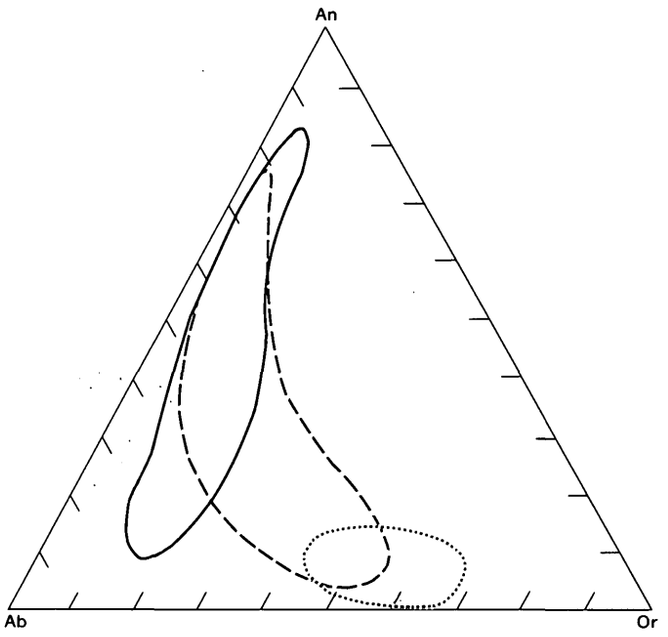

FIGURE 8.—Or-Ab-An diagram showing normative proportions of orthoclase, albite, and anorthite in weight percentages for rocks of synkinematic trondhjemite-charnockite series (solid line) and granite series (broken line). Late kinematic microcline granites (dotted line) are richer in potassium feldspar than the older granites. Modified from Simonen (1960b).

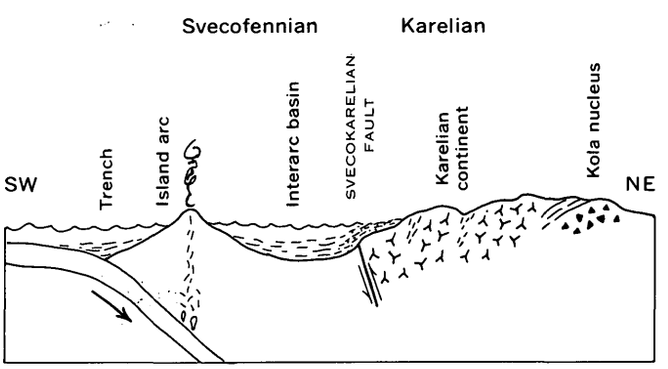

FIGURE 9.—Cross-section through figure 3 from southwest to northeast showing the possible island-arc system in the Fennoscandian Shield 2.5 to 2 b.y. ago. Deposition of quartz sand, dolomite, and pelite on the Karelian continental shelf, deposition of graywacke-type sediments in the Bothnian interarc basin, and volcanism in the Svionian island arc were coeval. The oldest nucleus is in Kola Peninsula at right and the subduction zone marked by a trench on the surface at left.

The evidence for a similar fractionation of alkalies during the Svecofennian volcanism in Finland is fragmentary and obscured by later migmatization and potassium-feldspathization. Sodium-rich and potassium-rich silicic metavolcanic rocks have been reported from areas where leptite is well preserved. In central Sweden, where the stratigraphic sequence has been established, the sodium-rich volcanic rocks are older (Geijer, 1963; Hjelmqvist, 1966). Moreover, minor rhyolitic leptites with considerable potassium-feldspar are interbedded with basaltic metavolcanic rocks near Tampere and to the southwest (Eskola, 1963; Neuvonen, 1954). These volcanogenic features, together with stratigraphic features, such as prevalence of graywacke-type metasedimentary rocks and scarcity of limestone indicate broad similarities in the evolution of the Svecofennian and western Cordilleran metamorphic belts.

The similarities in magmatic evolution suggest a possibility of similar plate-tectonic development for the western Cordilleran and Svecofennian orogenic belts. An island-arc system may have existed southwest of the Karelian continent at the time when shelf-type sediments were deposited on the continental margin (fig. 9). Volcanoes in this island arc poured out andesitic to rhyolitic lavas in which the potassium content increased with time. Graywacke-type sediments were deposited in an inter-arc basin between the continent and the island arc. In detail, the type of sedimentary and volcanogenic rocks deposited depended on the geotectonic environment and closeness of either the continent or the island-arc volcanoes.

The old familiar names of geologic units, such as Karelian, Svecofennian, Bothnian, and Svionian have lost their original meaning, which contained a con-

notation of relative ages that was later disproved by radiometric age determinations. However, the geographic connotations may be preserved, and new geotectonic meanings can now be attached to these names, as shown in figure 3. The Svecokarelian fault zone separates the oceanic Svecofennian block in the southwest from the continental Karelian block in the northeast. The Svionian island arc is shown through the leptite belt. The Bothnian Basin, in essence an interarc basin between the Karelian continent and the Svionian island arc, truncates the volcanic belt in the west, possibly indicating a zone of weakness parallel to a preexisting east-west lineament. The trench associated with the subduction zone in this plate-tectonic model could have been in southwest Sweden, where Gothian formations are separated from the Svecofennian belt by a sharp boundary.

For about 40 years the name "Karelian" has been used collectively for all the miogeosynclinal sedimentary rocks (quartzite, dolomite, pelite) deposited on the continental shelf of the Karelian continent. To avoid confusion, the name "Karelian" in this paper is reserved for the pre-Svecofennian continental block and its evolutionary period, whereas the name "Kalevian," formerly used for some of the schist and phyllite units of the shelf facies, is here proposed as a collective name for the metamorphic rocks northeast of the Svecokarelian fault zone.

The differences in the geotectonic environment and the thickness of underlying crust are likely causes for differences in tectonic features of the eastern (Kalevian) and the western (Svecofennian) foldbelts. The Kalevian shelf sediments were deposited on a continental margin that had been thickened by an earlier orogeny and by a large volume of earlier (2.8-b.y.-old) granite, whereas the Svecofennian belt was underlain by a thin oceanic crust in which basins can easily form parallel to some earlier lineament. Tuffs and graywacke-type sediments were deposited in a wide subsiding basin between the continent and the island arc, and a major fault zone developed along the boundary between the two major domains. During the Svecofennian orogeny 1.9–1.7 b.y. ago, all sediments and volcanogenic rocks were folded and intruded by plutonic magmas. The curvature of the Svecofennian trends around the granite complex of central Finland suggests that the trends were modified by diapiric emplacement of large masses of granite. This is supported by the fact that the trends northeast of the granite complex are parallel to the Svecokarelian fault zone and in northern Sweden the east-west trends turn to the north.

The emplacement of large volumes of microcline granite during the latest phase of the Svecofennian orogeny was accompanied by extensive development of migmatites or veined gneisses. The granitic plutons commonly have gradational contacts and include ghostlike remnants of wall rocks, indicating that large amounts of older rocks were digested by the magma. It has been suggested by Scandinavian geologists that these granites are products of granitization (Simonen, 1960b) or palingenesis or formed through partial melting of the metamorphic rocks, particularly those of sedimentary origin (Gavelin, 1955; Magnusson, 1960; Härme, 1962). If the granitic veins of the migmatites formed through partial melting and segregation, then large masses of granite could indeed have formed by segregation of granitic melt from downfolded metasedimentary and metavolcanic rocks at levels not much below the present erosion surface. Diapiric rise of calc-alkaline magma rich in potassium from the upper mantle into these downfolded metamorphic rocks probably initiated a large-scale melting and raised the potassium content of the newly formed magmas above that of the earlier granite.

A general increase of the Sr^{87}/Sr^{86} ratio with a decrease in age in similar granites in Sweden (Welin and others, 1971) agrees with the concept that the region of melting expanded upward to the lower part of the downfolded strata. The experimental work by Stern and Wyllie (1973a, b) indicate that granitic liquids are not obtained at mantle pressures existing in the subduction zones but rather at crustal depths less than 35 km. Depths of only about 15 km are indicated for the partial melting of the Svecofennian migmatites by mineral assemblages such as andalusite-cordierite and cordierite-garnet-sillimanite in the parent rocks (Hietanen, 1967).

COMPARISON OF THE PRESSURE-TEMPERATURE CONDITIONS FOR THE MELTING OF GRANITE

The major difference in conditions of magmatic evolution in the western Cordilleran and Svecofennian orogenic belts is a higher temperature and therefore much more extensive melting during the latest phase of plutonism at the level exposed in the Svecofennian area. It has been suggested by many investigators that this higher temperature is a function of a deeper level now exposed in the Precambrian areas such as the Svecofennian. The metamorphic mineral assemblage (andalusite-cordierite-sillimanite) found in both areas, however, indicates about the same pressure level. In the northern Sierra Nevada, cordierite and andalusite crystallized only near the contacts of the plutons, whereas the rocks farther from the plu-

tons were recrystallized under conditions transitional between the greenschist and epidote amphibolite facies. In the Svecofennian area sillimanite is common with cordierite, and hypersthene rather than hornblende crystallized locally. This indicates temperatures close to the border of the higher amphibolite and the cordierite granulite facies, which is within the region of melting of granite (Hietanen, 1967). The higher temperature can be attributed to a more extensive radioactive heat production in Precambrian time and to the fact that the crust was thin and the heat flux from the mantle therefore higher. Radioactive decay and thickening of the crust probably were the major causes for the changes in the geothermal gradient and the depth of melting with time.

REFERENCES CITED

Allen, J. C., Modreski, P. J., Haygood, Christine, and Boettcher, A. L., 1972, The role of water in the mantle of the Earth; the stability of amphiboles and micas: Internat. Geol. Cong., 24th, Montreal 1972, Proc. Sec. 2, p. 231–240.

Anhaeusser, C. R., Mason, Robert, Viljoen, M. J., and Viljoen, R. P., 1969, A reappraisal of some aspects of Precambrian Shield geology: Geol. Soc. America Bull. 80, p. 2175–2200.

Arth, J. G., and Hanson, G. N., 1972, Quartz diorites derived by partial melting of eclogite or amphibolite at mantle depths: Contr. Mineralogy and Petrology, v. 37, p. 161–174.

Baragar, W. R. A., and Goodwin, A. M., 1969, Andesites and Archean volcanism of the Canadian Shield, *in* McBirney, A. R., ed., Proceedings of the andesite conference: Oregon Dept. Geology and Mineral Industries Bull. 65, p. 121–142.

Barazangi, Muawia, Isacks, Bryan, and Oliver, Jack, 1970, Propagation of seismic waves through and beneath the lithosphere that descends under the Tonga Island arc: Geol. Soc. America Abs. with Programs, v. 2, no. 7, p. 488–489.

Bateman, P. C., and Dodge, F. C. W., 1970, Variations of major chemical constituents across the Central Sierra Nevada batholith: Geol. Soc. America Bull. 81, p. 409–420.

Boettcher, A. L., 1973, Volcanism and orogenic belts—the origin of andesites: Tectonophysics, v. 17, p. 223–240.

Burchfiel, B. C., and Davis, G. A., 1972, Structural framework and evolution of the southern part of the Cordilleran orogen, western United States: Am. Jour. Sci., v. 272, p. 97–118.

Chayes, Felix, 1969, The chemical composition of Cenozoic andesite, *in* McBirney, A. R., ed., Proceedings of the andesite conference: Oregon Dept. Geology and Mineral Industries Bull., v. 65, p. 1–12.

Christiansen, R. L., and Lipman, P. W., 1972, Cenozoic volcanism and plate-tectonic evolution of the Western United States; II, Late Cenozoic: Royal Soc. London Philos. Trans. Ser. A, v. 271, p. 249–284.

Compton, R. R., 1955, Trondhjemite batholith near Bidwell Bar, California: Geol. Soc. America Bull. 66, p. 9–44.

Daly, R. A., 1933, Igneous rocks and the depths of the earth: New York, McGraw-Hill, 598 p.

Davis, G. A., 1969, Tectonic correlations, Klamath Mountains and western Sierra Nevada, California: Geol. Soc. America Bull. 80, p. 1095–1108.

Dickinson, W. R., 1970, Relations of andesites, granites, and derivative sandstones to arc-trench tectonics: Rev. Geophysics and Space Physics, v. 8, no. 4, p. 813–860.

Dickinson, W. R., and Hatherton, T., 1967, Andesitic volcanism and seismicity around the Pacific: Science, v. 157, p. 801–803.

Edelman, Nils, 1960, The Gullkrona region, SW Finland: Finlande Comm. Géol. Bull. 187, p. 1–87.

Ernst, W. G., 1973, Blueschist metamorphism and P-T regimes in active subduction zones: Tectonophysics, v. 17, p. 255–272.

Eskola, Pentti, 1914, On the petrology of the Orijarvi region in southwestern Finland: Finlande Comm. Géol. Bull. 40, p. 1–277.

——— 1963, The Precambrian of Finland, *in* Rankama, Kalervo, ed., The geologic systems—The Precambrian 1: London, Interscience, John Wiley & Sons, Ltd., p. 145–279.

Gaal, G., and Rauhamäki, E., 1971, Petrological and structural analysis of the Haukivesi area between Varkaus and Savonlinna, Finland: Geol. Soc. Finland, Bull. 43, p. 265–337.

Gavelin, Sven, 1955, Beskrivning till berggrundskarta över Västerbottens län; 1, Ubergsområdet inom Västerbottens län: Sveriges Geol. Undersökning Ser. Ca., no. 37, p. 5–99.

Gerling, E., Kratz, K., and Lobach-Zhuchenko, S., 1968, Precambrian geochronology of the Baltic Shield: Internat. Geol. Cong., 23d Prague 1968, Proc. Sec. 4, Rept., p. 265–273.

Geijer, Per, 1963, The Precambrian of Sweden, *in* Rankama, Kalervo, ed., The geologic systems—The Precambrian 1: London, Interscience, John Wiley & Sons, Ltd., p. 81–143.

Gill, J. B., 1970, Geochemistry of Viti Levu, Fiji, and its evolution as an island arc: Contrib. Mineralogy and Petrology, v. 27, p. 179–203.

Glikson, A. Y., 1972, Early Precambrian evidence of a primitive ocean crust and island arc nuclei of sodic granite: Geol. Soc. America Bull. 83, no. 11, p. 3323–3344.

Goldschmidt, V. M., 1922, Stammestypen der Eruptivgesteine: Vidensk.-selsk. Kristiania [Oslo] Skrifter, I, Matematisk—naturvidensk. Kl., No. 10, p. 1–12.

Goodwin, A. M., 1968, Archaean protocontinental growth and early crustal history of the Canadian Shield: Internat. Geol. Cong., 23d, Prague 1968, Proc. Sec. 1, Upper Mantle, Rept., p. 69–89.

Green, D. H., 1972, Magmatic activity as the major process in chemical evolution of the earth's crust and mantle: Tectonophysics, v. 13, p. 47–71.

——— 1973, Contrasted melting relations in a pyrolite upper mantle under mid-oceanic ridge, stable crust and island arc environments: Tectonophysics, v. 17, p. 285–297.

Hanson, G. N., and Goldich, S. S., 1972, Early Precambrian rocks in the Saganaga Lake-Northern Light Lake area, Minnesota-Ontario. Part II: Petrogenesis: Geol. Soc. America Mem. 135, p. 179–192.

Härme, Maunu, 1954, Structure and stratigraphy of the Mustio area, southern Finland: Finlande comm. Géol. Bull. 166, p. 29–48.

——— 1960, The general geological map of Finland, sheet 1B, Turku: Geol. Survey Finland, 78 p.

——— 1962, An example of anatexis: Finlande Comm. Géol. Bull. 204, p. 113–125.

Hietanen, Anna, 1943, Über das Grundgebirge des Kalantigebietes im südwestlichen Finnland: Acad. Sci. Fennicae Annales, Ser. A, III, 105 p.; also in Finlande Comm. Géol. Bull. 130, p. 1–105.

——— 1947, Archean geology of the Turku District in southwestern Finland: Geol. Soc. America Bull., v. 58, no. 11, p. 1019–1084.

——— 1951, Metamorphic and igneous rocks of the Merrimac Area, Plumas National Forest, California: Geol. Soc. America Bull., v. 62, p. 565–608.

——— 1967, On the facies series in various types of metamorphism: Jour. Geology, v. 75, no. 2, p. 187–214.

——— 1973a, Origin of andesitic and granitic magmas in the northern Sierra Nevada, California: Geol. Soc. America Bull., v. 84, p. 2111–2118.

——— 1973b, Geology of the Pulga and Bucks Lake quadrangles, Butte and Plumas Counties, California: U.S. Geol. Survey Prof. Paper 731, p. 1–66.

Hjelmqvist, Sven, 1966, Beskrivning till berggrundskarta över Kopparbergs län: Sveriges Geol. Undersökning Ser. Ca., no. 40, 216 p.

——— 1973, Den Svekofennisk-karelska cykelkollisionen: Geol. Fören. Stockholm Förh., v. 95, p. 221–228.

Huang, W. L., and Wyllie, P. J., 1973, Melting relations of muscovite-granite to 35 kb as a model for fusion of metamorphosed subducted oceanic sediments: Contr. Mineralogy and Petrology, v. 42, p. 1–14.

Hurley, P. M., Bateman, P. C., Fairbairn, H. W., and Pinson, W. H., Jr., 1965, Investigation of initial Sr^{87}/Sr^{86} ratios in the Sierra Nevada plutonic province: Geol. Soc. America Bull. 76, p. 165–174.

Jakes, P., and Gill, J., 1970, Rare earth elements and the island arc tholeiitic series: Earth and Planetary Sci. Letters, v. 9, p. 17–28.

Jakes, P., and White, A. J. R., 1970, K/Rb ratios of rocks from island arcs: Geochim. et Cosmochim. Acta, v. 34, p. 849–856.

——— 1971, Composition of island arcs and continental growth: Earth and Planetary Sci. Letters, v. 12, no. 2, p. 224–230.

——— 1972, Major and trace element abundances in volcanic rocks of orogenic areas: Geol. Soc. America Bull. 83, p. 29–40.

Kahma, Aarno, 1973, The main metallogenic features of Finland: Geol. Survey Finland Bull. 265, p. 1–28.

Karig, D. E., 1971, Origin and development of marginal basins in the western Pacific: Jour. Geophys. Research, v. 76, p. 2542–2561.

Kistler, R. W., and Peterman, Z. E., 1973, Variations in Sr, Rb, K, Na, and initial Sr^{87}/Sr^{86} in Mesozoic granitic rocks and intruded wall rocks in central California: Geol. Soc. America, Bull. 84, p. 3489–3512.

Kouvo, Olavi, and Kulp, J. L., 1961, Isotopic composition of Finnish galenas: New York Acad. Sci. Annales, v. 91, p. 476–491.

Kouvo, Olavi and Tilton, G. R., 1966, Mineral ages from the Finnish Precambrian: Jour. Geology, v. 74, no. 4, p. 421–442.

Kushiro, I., 1969, The system forsterite-diopside-silica with and without water at high pressures: Am. Jour. Sci., v. 267–A (Schairer Volume), p. 269–294.

——— 1972, Effect of water on the composition of magmas formed at high pressures: Jour. Petrology, v. 13, p. 311–334.

Kushiro, I., and Yoder, H. S., Jr., 1972, Origin of calc-alkalic peraluminous andesite and dacites: Carnegie Inst. Washington Yearbook 71, p. 411–412.

Laitala, Matti, 1973, On the Precambrian bedrock and structure in the Pellinge region, South Finland: Geol. Survey Finland Bull. 264, p. 1–76.

Lipman, P. W., Prostka, H. J., and Christiansen, R. L., 1972, Cenozoic volcanism and plate tectonic evolution of the Western United States; I, Early and Middle Cenozoic: Royal Soc. London, Philos. Trans. Ser. A, v. 271, p. 217–248.

Lowder, G. G., and Carmichael, I. S. E., 1970, The volcanoes and Caldera of Talasea, New Britain—Geology and Petrology: Geol. Soc. America Bull. 81, p. 17–38.

Lundegårdh, P. H., 1971, Neue Gesichtpunkte zum schwedischen Präkambrium: Geol. Rundschau, v. 60, p. 1392–1405.

Magnusson, N. H., 1960, The Swedish Precambrian outside the Caledonian Mountain chain, *in* Description to accompany the map of the pre-Quaternary rocks of Sweden: Sveriges Geol. Undersökning Ser. Ba, no. 16, p. 5–66.

Modreski, P. J., and Boettcher, A. L., 1972, The stability of phlogopite + enstatite at high pressures—a model for micas in the interior of the Earth: Am. Jour. Sci., v. 272, p. 852–869.

Moore, J. G., 1959, The quartz diorite boundary line in the western United States: Jour. Geology, v. 67, no. 2, p. 198–210.

——— 1962, K/Na ratio of Cenozoic igneous rocks of the western United States: Geochim. et Cosmochim. Acta, v. 26, p. 101–130.

Neuvonen, K. J., 1954, Stratigraphy of the schists of the Tammela-Kalvola area, southwestern Finland: Finlande Comm. Géol. Bull. 166, p. 85–94.

Nicholls, I. A., and Ringwood, A. E., 1973, Effect of water on olivine stability in tholeiites and the production of silica-saturated magmas in the island arc environment: Jour. Geology, v. 81, p. 285–300.

Pavlovskiy, Ye. V., 1971, Early stages in development of the Earth's crust: Internat. Geol. Rev., v. 13, no. 3, p. 318–331.

Piwinskii, A. J., 1968, Experimental studies of igneous rocks series, central Sierra Nevada batholith, California: Jour. Geology, v. 76, no. 5, p. 548–570.

Scholz, C. H., Barazangi, M., and Sbar, M. L., 1971, Late Cenozoic evolution of the Great Basin, western United States, as an ensialic interarc basin: Geol. Soc. America Bull. 82, p. 2979–2990.

Seitsaari, Juhani, 1954, The Västilä area in the Tampere schist belt: Finlande Comm. Géol. Bull. 166, p. 95–106.

Simonen, Ahti, 1960a, Pre-Quaternary rocks in Finland: Finlande Comm. Géol. Bull. 191, p. 1–49.

——— 1960b, Plutonic rocks of the Svecofennides in Finnland: Finlande Comm. Géol. Bull. 189, p. 1–101.

Stern, C. R., and Wyllie, P. J., 1973a, Water-saturated and undersaturated melting relations of a granite to 35 kilobars: Earth and Planetary Sci. Letters, v. 18, p. 163–167.

——— 1973b, Melting relations of basalt-andesite-rhyolite-H_2O and a pelagic red clay at 30 kb: Contr. Mineralogy and Petrology, v. 42, p. 313–323.

Viljoen, M. J., and Viljoen, R. P., 1969a, A proposed new classification of the granitic rocks of the Barberton region, *in* Upper Mantle Project: Geol. Soc. South Africa Spec. Pub. 2, p. 153–180.

——— 1969b, The geochemical evolution of the granitic rocks of the Barberton Region, *in* Upper Mantle Project: Geol. Soc. South Africa Spec. Pub. 2, p. 189–219.

Welin, Eric, 1966a, The absolute time scale and the classification of Precambrian rocks in Sweden: Geol. Fören. Stockholm Förh., v. 88, p. 29–33.

——— 1966b, Uranium mineralizations and age relationships in the Precambrian bedrock of central and southeastern Sweden: Geol. Fören. Stockholm Förh., v. 88, p. 34–67.

Welin, Eric, Christiansson, K., and Nilsson, Ö., 1971, Rb-Sr radiometric ages of extrusive and intrusive rocks in northern Sweden, I: Sveriges Geol. Undersökning Ser. C, no. 666, Årsb. 65, p. 1–38.

Wetherill, G. W., Kouvo, Olavi, Tilton, G. R., and Gast, P. W., 1962, Age measurement on rocks from the Finnish Precambrian: Jour. Geology, v. 70, p. 74–88.

White, A. J. R., Jakes, P., and Christie, D. M., 1971, Composition of greenstones and the hypothesis of sea-floor spreading in the Archaean: Geol. Soc. Australia Spec. Pub. 3, p. 47–56.

Windley, B. F., and Bridgewater, D., 1971, The evolution of Archaean low-and high-grade terrains: Geol. Soc. Australia Spec. Pub. 3, p. 33–46.

Yoder, H. S., Jr., 1969, Calc-alkalic andesites, experimental data bearing on the origin of their assumed characteristics, *in* McBirney, A. R., ed., Proceedings of the andesite conference: Oregon Dept. Geology and Mineral Industries Bull., v. 65, p. 77–90.

——— 1973, Contemporaneous basaltic and rhyolitic magmas: Am. Mineralogist, v. 58, p. 153–171.

Jour. Research U.S. Geol. Survey
Vol. 3, No. 6, Nov.–Dec. 1975, p. 647–657

PROGRESSIVE METAMORPHISM OF SCHISTS RECOVERED FROM A DEEP DRILL HOLE NEAR FAIRBANKS, ALASKA

By ROBERT B. FORBES [1] and FLORENCE R. WEBER,
Fairbanks and College, Alaska

Abstract.—In 1965, a deep test hole drilled near Eielson Air Force Base, Fairbanks district, Alaska, penetrated 9,774 ft (2,979.1 m) into schists of the metamorphic complex of the Yukon-Tanana Upland. Cores recovered from the test hole show that the section is dominated by calc-magnesian rocks with subordinate pelitic schists. Pelitic mineral assemblages define a progressive increase in metamorphic grade with depth, from the garnet to the kyanite isograd. Diopside first appears in the calc-magnesian schists that were cored at a depth of 9,766 ft (2,976.5 m), indicating the onset of the reaction: Tremolite + 3 calcite + 2 quartz → 5 diopside + $3CO_2+H_2O$. Ubiquitous staurolite and rare andalusite occur in the kyanite-bearing pelitic schists. Andalusite appears to have crystallized under postkinematic conditions, and the staurolite is apparently of both synkinematic and postkinematic origin. Hornblende and biotite from calc-magnesian schists sampled at depths of 7,142½ ft (2,176.9 m) and 9,766 ft (2,976.5 m) gave $^{40}K/^{40}Ar$ ages of 140±8 and 57.3±1.9 m.y., respectively. The hornblende age is believed to represent the age of the latest synkinematic metamorphism, and the biotite age appears to be an anomalously young one related to the outgassing of argon from biotite at greater depth in the section. Recent experimental data on andalusite-kyanite-sillimanite and staurolite equilibria and the stability field of calcite+quartz+tremolite versus diopside in calc-magnesian rocks suggest that the rocks recovered from the 8,218- to 9,770-ft (2,504.7- to 2,977.7-m) interval were synkinematically recrystallized at crustal depths of 17 to 19 km and at temperatures of 515° to 580°C; the present thermal gradient (31.5°C/km) is similar to that which accompanied metamorphism in Jurassic time.

The core samples discussed in this paper were recovered from the Eielson deep test hole adjacent to Eielson Air Force Base (sec. 2, T. 2 S., R. 5 E., Fairbanks Meridian), approximately 26 mi (41.8 km) east-southeast of Fairbanks, Alaska (fig. 1). The hole was drilled by the Brinkerhoff Drilling Co. under contract to the Corps of Engineers, U.S. Army.

The drill site is at an altitude of 1,350 ft (411.5 m) above sea level in the low hills that define the southwest margin of the Yukon-Tanana Upland. The upland in this area is maturely dissected terrain with a relief of approximately 2,500 ft (762 m). The site is flanked by the Chena River valley to the north and the Tanana River flood plain and valley to the west. Outcrops are rare near the site, as the hills are mantled with loess derived from the Tanana River flood plain.

Several exploratory holes were drilled by the U.S. Corps of Engineers to acquire bedrock information before drilling of the deep test. Additional bedrock data were gathered from roadcuts, powerline cuts, and other excavations in the area.

The deep test was spudded in on April 26, 1965, and completed to a depth of 9,774 ft (2,979.1 m) in December of that year. Eleven 3½-in (8.9-cm) cores (recovered diameter) were taken at approximately 1,000-ft (304.8-m) intervals, and samples of the well cuttings were taken at 10-ft (3.05-m) intervals during drilling. Average recovery was about 4 ft (1.2 m) per core.

This particular drill hole offers unique opportunities for geophysical and petrologic studies because it cuts schists of the Yukon-Tanana metamorphic complex throughout its entire length, and the section penetrated by the drill hole is better exposed than any in the surrounding uplands. The edge of a quartz monzonite pluton is within 2 mi (3.2 km) of the test site, and some thermal effects on the rocks from the emplacement of this body were noted.

Geothermal and heat-flow data have been measured from the drill hole by Lachenbruch and Bunker (1971). Radioelement distribution in the hole was reported by Bunker, Bush, and Forbes (1973).

Acknowledgments.—We gratefully acknowledge the cooperation of the U.S. Army District Engineers in obtaining core samples and data from the Eileson deep test hole and the collaboration of A. H. Lachenbruch and J .H. Sass on the geophysical implications of our findings.

PETROLOGIC SETTING OF DRILL SITE

The site is in a northeast-trending belt of rocks of the greenschist facies of probable early Paleozoic age

[1] University of Alaska, Fairbanks.

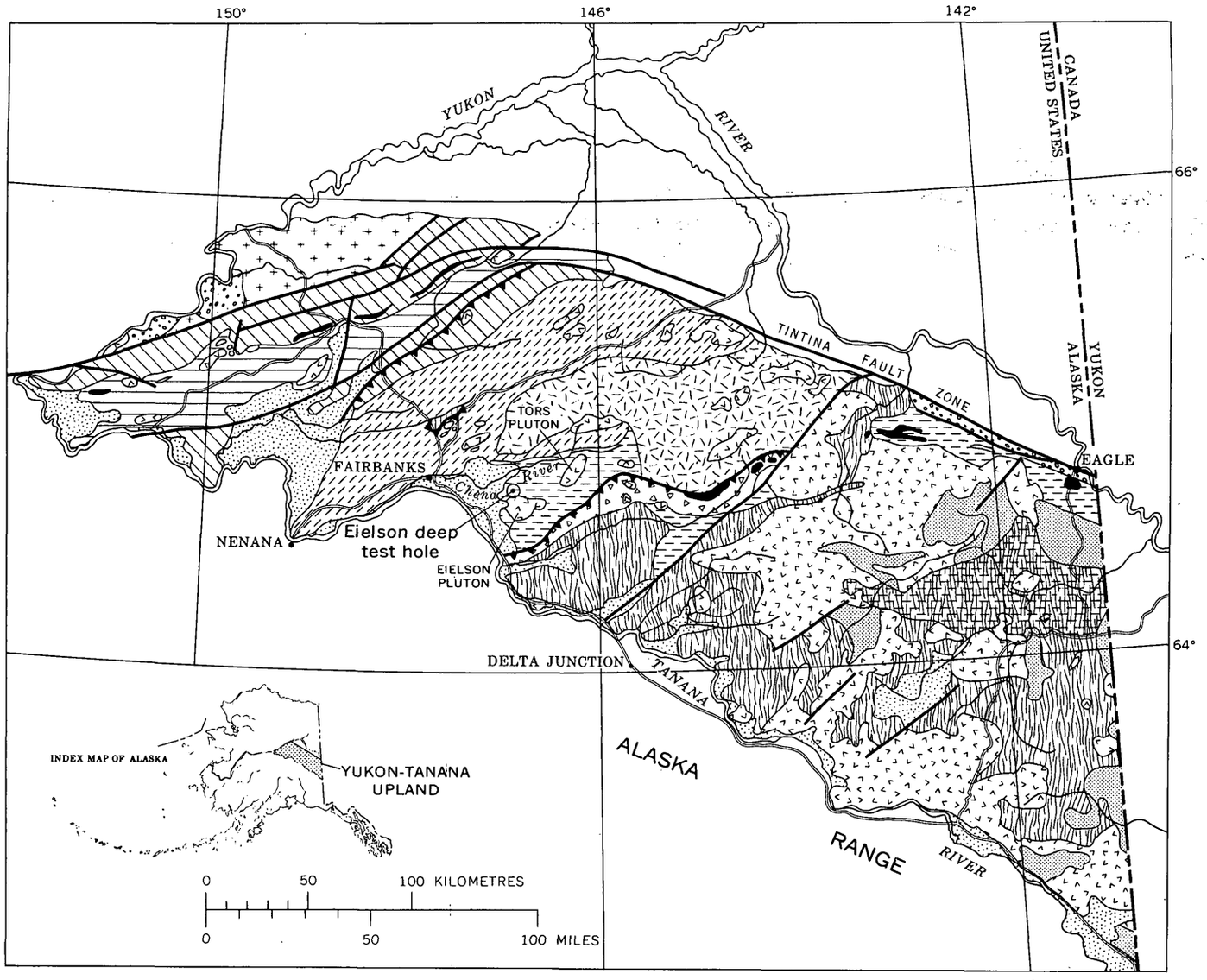

FIGURE 1.—Geologic map of the Yukon-Tanana Upland showing the location of the Eielson deep test hole. Modified by authors from Foster and others (1973) and Beikman (1974).

(fig. 1). On the basis of samples collected during geologic mapping in the surrounding area, characteristic rock types in outcrop include calc-mica schist, calc-phyllite, greenschist, phyllitic schist, slate, and fine-grained quartzites that appear to be metachert or siltstone. Where unaffected by superimposed thermal metmorphism, the mineral assemblages are characteristically those of the greenschist facies (Foster and others, 1973).

The deep test-hole site is on calc-mica schist that is typically composed of carbonate, quartz, muscovite, and minor amounts of phlogopite and albite. At some localities phlogopite is a major constituent, and the resultant rocks are more aptly described as calc-phlogopite schists. These rocks have been traced into the Fairbanks area where they form bold outcrops and steep bluffs overlooking the Tanana River.

The foliation has a northeasterly strike along the north margin of the belt but becomes highly variable in the central and south parts of the belt where the schists have been deformed and hornfelsed by the intrusion of the granitic plutons.

To the north, rocks of the greenschist facies are succeeded by schists that are transitional from greenschist to amphibolite facies. To the south, rocks of the greenschist facies are separated from terrane of the amphibolite facies by an intervening zone of cataclastic rocks. This zone is composed of mylonites that are characterized by feldspar porphyroclasts surrounded by a matrix of sericite, albite, and quartz.

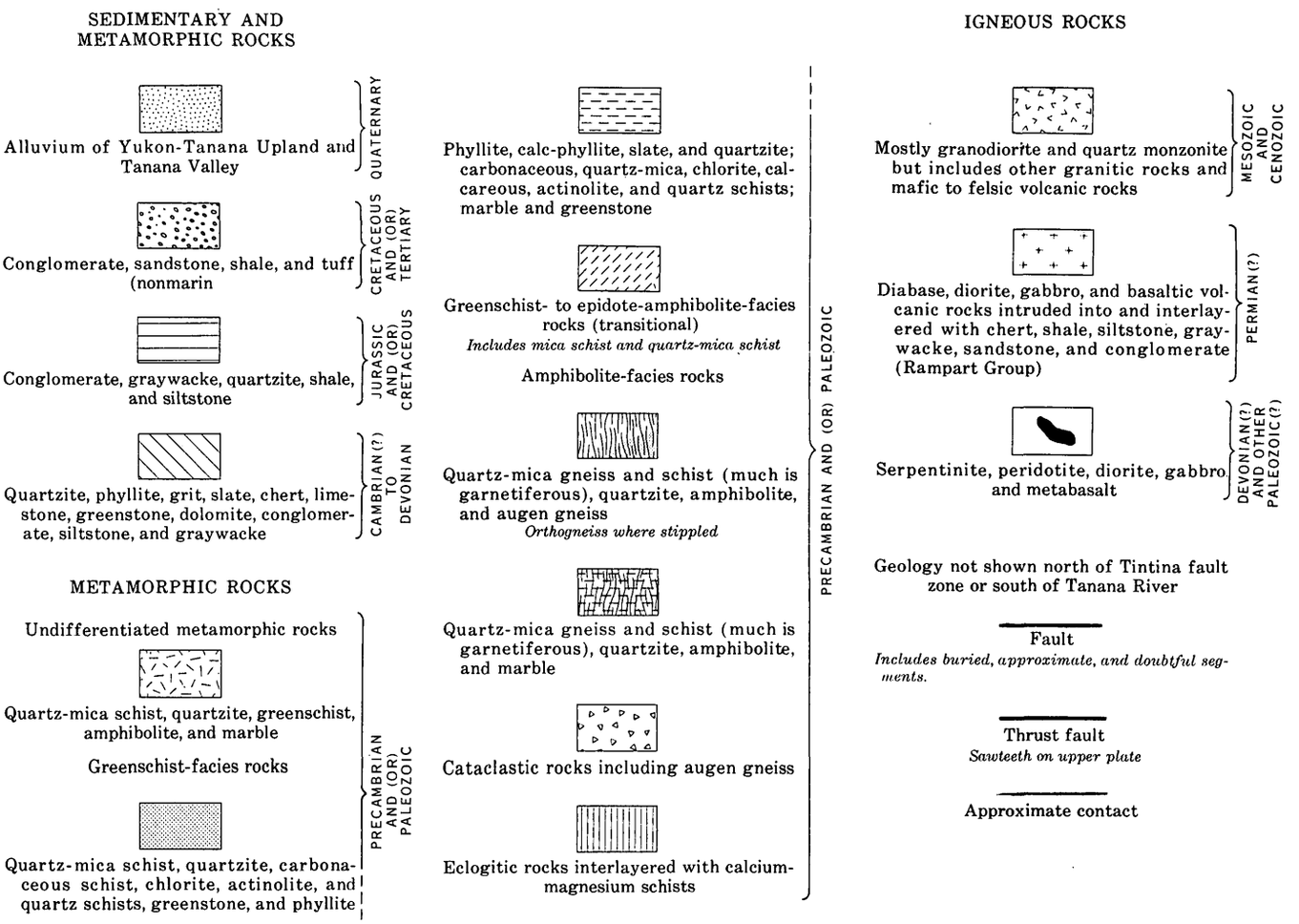

These rocks appear to be partly derived from retrograded gneisses. The tectonic significance of this zone is not yet fully understood, other than its importance as a broad zone of mechanical disruption in which cataclasis appears to postdate amphibolite-facies metamorphism and predate Mesozoic granitic intrusions.

Amphibolite-facies rock types include mica schist, garnet-mica schist, quartz-mica schist, micaceous quartzite, amphibolite, and subordinate biotite gneiss and marble. These rocks are characterized by polymetamorphic fabrics that record metamorphism to the amphibolite facies followed by a retrograde event of the greenschist facies.

Radiometric dating methods were first applied to the metamorphic complex by Wasserburg, Eberlein, and Lanphere (1963). Muscovite separated from a phyllitic schist collected near Montana Creek, in the Circle district, gave a $^{87}Rb/^{87}Sr$ age of 511 m.y. and a discordant $^{40}K/^{40}Ar$ age of 111 m.y. The parent rock, however, provided a whole-rock $^{87}Rb/^{87}Sr$ age of 1,020 m.y., the only Precambrian radiogenic age yet taken from the rocks or constituent minerals of the metamorphic complex. According to the authors, however, (oral commun., 1973) there is now considerable doubt as to whether recrystallization was adequate for complete reequilibration of the $^{87}Rb/^{87}Sr$ system in this rock, and the age determination may be related to the minimum age of the clastic mica and feldspar of the parent rock. We attach considerable importance to the discordant $^{87}Rb/^{87}Sr$ and $^{40}K/^{40}Ar$ muscovite ages, however, because they agree with two thermal events that have been detected from discordant hornblende, muscovite, and biotite $^{40}K/^{40}Ar$ ages in the Fairbanks district (Forbes and others, 1968a, b). Early Paleozoic, Jurassic, and Cretaceous synkinematic or thermal events are indicated by the $^{40}K/^{40}Ar$ ages obtained from the metamorphic complex.

Two granitic plutons are present in the greenschist-facies belt. The Eielson pluton, which is about 8 mi (12.9 km) in diameter, is east of Eielson Air Force Base. The north contact of this pluton is approximately 2 mi (3.2 km) from the well site. The elliptically shaped Tors pluton is about 20 mi (32.2 km) northeast of the site (fig. 1). Field evidence suggests it is

possible the two plutons are actually part of the same mass, which is continuous in the subsurface.

The plutons are composed of similar granitic rocks that range in composition from quartz monzonite to granite. They are composed of perthitic orthoclase, oligoclase, quartz, and biotite, with minor muscovite and hornblende; zircon, allanite, and magnetite are accessory minerals. Some of the coarse-grained granites are porphyritic, and granophyric variants occur in the chilled contact zones of the plutons. The granitic rocks are massive, and no linear or planar microfabric elements have been detected in either pluton.

Both plutons are surrounded by contact aureoles as much as 1 mi (1.6 km) wide, which include rocks that have been recrystallized under temperatures equivalent to the hornblende or pyroxene hornfels facies. In some areas contact metamorphism has been accompanied by pneumatolytic alteration that includes tourmalinization and sericitization of the wallrocks.

PETROLOGY OF ROCKS FROM DRILL HOLES

Eleven cores were retrieved from the deep hole and two from some shallow preliminary test holes. Splits of all identifiable compositional variations were taken from the cores, and thin sections were prepared from each of these. Table 1 lists the rock types sampled from the cores, their constitutent major, minor, and accessory minerals, and the facies or isograd assignment of the respective metamorphic mineral assemblages.

Preliminary Test Holes

DDH1—40 ft (12.2 m)

Calc-mica schist.—This rock is dominantly composed of carbonate, quartz, and muscovite, with minor albite, chlorite, and sphene. Trace amounts of phlogopite, apatite, zircon, and opaque minerals are present. The fabric is characterized by alternating carbonate- and mica-rich layers and a crystallization foliation that is defined by the preferred orientation of the mica. The assemblage carbonate-quartz-muscovite-chlorite is typical of the greenschist facies in calc-magnesian rocks. The bulk composition of this rock is suitable for the crystallization of tremolite, garnet, diopside, and wollastonite, and the absence of these phases indicates that pressure-temperature conditions were below those of the amphibolite facies.

DDH2—521 ft (158.8 m)

Calc-mica schist.—The mineralogy of this rock is basically the same as that of core DDH1 described above.

Eielson Deep Test Hole

EDT1—1,032, 1,034, and 1,035¼ ft (314.5, 315.1, and 315.5 m)

Calc-mica schist.—These rocks have a mineralogy similar to those described from the 40- and 521-ft (12.2- and 158.8-m) levels; they are composed chiefly of carbonate, quartz, and muscovite, with chlorite as a major constituent in one sample (1,034 ft; 315.1 m). Minor and accessory minerals include chlorite, phlogopite, albite, tourmaline, and opaque minerals. The absence of amphibole in these rocks indicates that pressure-temperature conditions were below those associated with the tremolite isograd during crystallization.

EDT2—2,010 ft (612.6 m)

Calc-phlogopite schist.—This rock is composed of the assemblage carbonate-quartz-muscovite-chlorite-phlogopite, with sphene, apatite, albite, zircon, and opaque minerals as accessories. Much of the phlogopite is apparently of postkinematic origin. Some grains have grown across the earlier schistosity, late phlogopite has partly replaced some chlorite grains, and a vein of phlogopite has filled a fissure that cuts through schistosity and compositional layering. However, the presence of phlogopite in calc-mica schists from higher in the section indicates that phlogopite is also a stable phase in the synkinematic assemblage. The crystallization of phlogopite, without the appearance of either tremolite or diopside, implies that these rocks were thermally overprinted in the outer part of the contact aureole under conditions of the albite-epidote hornfels facies.

EDT3—2,341 ft (713.5 m)

Quartz-biotite-clinozoisite schist.—The definitive assemblage in this rock is quartz-clinozoisite-phlogopite-albite. There are also trace amounts of muscovite, sphene, apatite, and opaque minerals. Postkinematic phlogopite is also present, in addition to earlier phlogopite that appears to have been in equilibrium with the other phases in the synkinematic assemblage. This assemblage has been frequently described from the biotite zone in progressively metamorphosed belts and coincident with the upper part of the greenschist facies.

EDT3—2,343½ ft (714.3 m)

Calc-mica schist.—This rock is a compositional variation taken from the same core as the rock described above. It is composed of the essential phases

TABLE 1.—*Petrographic data for analyzed cores from drill holes near Fairbanks, Alaska*

Core	Depth (ft)	Rock type	Constituent minerals			Metamorphic facies or isograd
			Major (>10 percent)	Minor (2–10 percent)	Accessory (<2 percent)	
DDH1	40	Calc-mica schist	Carbonate, muscovite, quartz,	Sphene, plagioclase (albite), chlorite.	Phlogopite, opaques, zircon, apatite.	Greenschist.
DDH2	521	do	do	Chlorite, sphene, plagioclase (albite).	Phlogopite, apatite, opaques.	Do.
EDT1	1,032 1,034 1,035¼	do	do	Chlorite	Opaques, plagioclase (albite), sphene, apatite, tourmaline.	Do.
EDT2	2,010	Calc-mica-phlogopite schist.	Carbonate, muscovite, quartz. phlogopite.	Chlorite, sphene	Tourmaline, plagioclase (albite), opaques, zircon(?), apatite.	Do.
EDT3	2,341	Phlogopite-clinozoisite schist.	Phlogopite, quartz, epidote (clinozoisite).	Plagioclase (albite), muscovite.	Sphene, apatite, opaques.	Do.
	2,343½	Calc-mica schist	Carbonate, muscovite, quartz, phlogopite.		Opaques, sphene	Do.
	2,345	Clinozoisite-carbonate-mica schist.	Carbonate, muscovite, quartz, phlogopite, epidote (clinozoisite).		Tourmaline, opaques, albite, sphene.	Do.
EDT4	3,193	Calc-greenschist	Amphibole (actinolite), biotite. carbonate, epidote (clinozoisite).	Chlorite, quartz	Plagioclase (albite), opaques sphene.	Do.
	3,195½	do	Chlorite, phlogopite, actinolite, carbonate.	Quartz	Sphene, plagioclase (albite), epidote.	Do.
EDT5	4,065	Garnet-bearing quartz-mica schist (hornfels?).	Quartz, muscovite, garnet.	Plagioclase, chlorite.	Tourmaline, carbonate.	Albite-epidote-hornfels(?).
	4,066	Garnet-tourmaline rocks (hornfels?).	Garnet, tourmaline, quartz, plagioclase (albite-oligoclase).	Chlorite, muscovite	Opaques	Do.
	4,067¼	Garnet-mica schist (hornfels?).	Quartz, muscovite	Tourmaline, chlorite.	Opaques, plagioclase (albite-oligoclase).	Albite-epidote.
						Possible garnet isograd.
EDT6	5,011	Garnet-mica schist	Muscovite, plagioclase (oligoclase), garnet, quartz.	Biotite, plagioclase (oligoclase).	Opaques, chlorite	Albite-epidote.
	5,013	do				
EDT7	6,141	Biotite-bearing amphibolite.	Hornblende, biotite.	Plagioclase (oligoclase), quartz, opaques.	Apatite, sphene	Do.
	6,142	Garnet-mica schist	Biotite, muscovite, quartz.	Plagioclase (albite-oligoclase), garnet.	Epidote, opaques	Do.
	6,143	Biotite-amphibolite	Hornblende, biotite.	Plagioclase (oligoclase), quartz, sphene.	Apatite	Do.
EDT8	7,140	Epidote-bearing quartz-mica schist.	Biotite, muscovite, plagioclase (oligoclase), quartz.	Epidote (clinozoisite).	Opaques, apatite	Do.

TABLE 1.—*Petrographic data for analyzed cores from drill holes near Fairbanks, Alaska*—Continued

Core	Depth (ft)	Rock type	Constituent minerals			Metamorphic facies or isograd
			Major (>10 percent)	Minor (2–10 percent)	Accessory (<2 percent)	
EDT8—Con.	7,140¼	Garnet-mica schist.	Muscovite, biotite, garnet, quartz, plagioclase (albite–oligoclase).		Epidote, opaques, apatite.	Do.
	7,142½	Biotite-hornblende schist.	Hornblende, biotite.	Quartz	Sphene, opaques, plagioclase.	Do.
	7,144	----do	Hornblende, biotite.	Sphene, plagioclase (oligoclase), quartz, garnet.	Opaques, epidote, chlorite.	Do.
						Kyanite and staurolite isograds.
EDT9	8,216	Kyanite-staurolite schist.	Muscovite, garnet, kyanite, quartz.	Staurolite, plagioclase (oligoclase), biotite.	Opaques, chlorite	Amphibolite facies.
	8,217	----do	Biotite, muscovite, garnet, staurolite, quartz.	Plagioclase (albite-oligoclase), tourmaline, kyanite.	----do	Do.
	8,218	----do	Biotite, muscovite, garnet, plagioclase (oligoclase), quartz.	Tourmaline, kyanite, staurolite.	----do	Do.
	8,218¼	Andalusite-bearing kyanite-staurolite schist.	Biotite, muscovite, garnet, kyanite, quartz.	Staurolite andalusite, plagioclase (oligoclase).	----do	Do.
EDT10	9,196	Biotite-epidote schist.	Biotite, epidote, quartz.	Sphene, plagioclase (oligoclase).	Opaques, apatite	Do.
	9,198	Quartz-mica schist.	Muscovite, quartz	Chlorite, plagioclase (oligoclase), biotite.	Apatite, opaques, allanite.	Do.
EDT11	9,766	Diopside-bearing actinolite-carbonate-mica schist.	Carbonate, phlogopite, quartz, plagioclase (oligoclase).	Actinolite, K-feldspar, diopside.	Sphene, zoisite	First evidence of reaction tremolite +3 calcite +2 quartz →5 diopside +3 CO_2 +H_2O.
	9,767	----do	Carbonate, phlogopite, actinolite, quartz, plagioclase (albite-oligoclase).	Muscovite	Sphene, opaques	Amphibolite facies.
	9,770	Actinolite-bearing calc-mica schist.	Phlogopite, muscovite, quartz, plagioclase (oligoclase).	Carbonate, actinolite.	Sphene, zoisite, opaques.	Do.

carbonate-quartz-phlogopite-muscovite. Apatite and opaque minerals are present as accessories.

EDT3—2,345 ft (714.7 m)

Clinozoisite-carbonate-mica schist.—This rock represents a third compositional variation taken from the same core; it is composed of the diagnostic assemblage carbonate-clinozoisite-muscovite-phlogopite-quartz, with accessory amounts of tourmaline, albite, sphene, and opaque minerals. This assemblage is also stable in the biotite zone (upper greenschist facies).

EDT4—3,193 ft (973.2 m)

Calc-greenschist.—This assemblage consists of actinolite-carbonate-clinozoisite-phlogopite-quartz. Minor phases include sphene, apatite, albite, chlorite, and opaque minerals. This assemblage signals the tremolite isograd, with the first appearance of amphibole with coexistent carbonate, quartz, and chlorite. Although two generations of phlogopite appear to be present, there is no evidence that the appearance of actinolite in the assemblage is related to a superimposed thermal event. The presence of amphibole as a major phase

with coexistent quartz, carbonate, and chlorite suggests metastable equilibrium at the tremolite isograd, as defined by the reaction: Calcite + quartz + chlorite →tremolite.

EDT4—3,195½ ft (973.9 m)

Calc-greenschist.—The composition of this rock is defined by actinolite-chlorite-carbonate-phlogopite-quartz, with minor albite and accessory clinozoisite, sphene, and opaque minerals.

EDT5—4,065 ft (1,239 m)

Garnet-bearing quartz-mica schist.—The rock is dominated by the assemblage quartz-muscovite-garnet. Minor and accessory minerals include albite, chlorite, tourmaline, carbonate, and opaque minerals. The quartz fabric has been annealed in this rock, and the garnet occurs as skeletal growths along intergranular zones between quartz grains, where it has recrystallized from argillaceous cement. Reticulated garnet growths such as these are usually disrupted during synkinematic metamorphism, and the garnet is clearly of late or postkinematic origin.

EDT5—4,066 ft (1,239.3 m)

Garnet-tourmaline rock.—The fabric is dominated by large garnets surrounded by a matrix of quartz, plagioclase (albite-oligoclase), and tourmaline (schorlite). The plagioclase is partly replaced by sericite or carbonate. Accessories include chlorite, muscovite, and opaque minerals. Some garnet grains do not display any evidence of synkinematic growth but appear to have undergone late growth under static thermal conditions. The tourmaline composes over 25 volume percent of the rock and is concentrated in zones that coincide with boundary surfaces between compositional layers in the schist. The hornfelsic texture, abnormally high tourmaline content, and matrix alteration in this rock suggest pneumatolytic alteration.

EDT5—4,067¼ ft (1,239.6 m)

Garnet-mica schist.—The rock is composed of the assemblage garnet-quartz-muscovite with accessory tourmaline, chlorite, plagioclase, and opaque minerals. This rock is similar to the preceding specimen, but without the copious tourmaline.

EDT6—5,011 ft (1,527.3 m)

Garnet-mica schist.—The assemblage consists of garnet-muscovite-biotite-quartz-oligoclase. Trace chlorite and opaque minerals are also present. This assemblage is diagnostic of the garnet (almandine) zone. The garnet porphyyroblasts are of synkinematic origin, as interpreted from folded inclusion trains within the garnet grains. Because some of the garnet grains in the rocks from core EDT5 appear to have undergone postkinematic growth and garnet-bearing pelitic schists have been collected from outcrops in the nearby areas, these assemblages cannot be used to define the garnet isograd.

EDT6—5,013 ft (1,527.9 m)

Garnet-mica schist.—The rock is composed of the assemblage biotite-muscovite-quartz-garnet-albite-oligoclase with accessory tourmaline, apatite, and opaque minerals. This rock is similar to the rock sampled at 5,011 ft (1,527.3 m).

EDT7—6,141 ft (1,871.7 m)

Biotite-bearing amphibolite. — Hornblende-biotite-quartz-oligoclase dominate the mode, accompanied by trace sphene, apatite, and opaque minerals. Hornblende exceeds 85 percent of this rock, and the bulk composition is that of a basic igneous rock. Plagioclase has developed incipient twinning, but many grains show decalcification and annealing effects from retrograde metamorphism.

EDT7—6,142 ft (1,872 m)

Garnet-mica schist.—The composition of this rock is dominated by the assemblage garnet-muscovite-biotite-quartz-oligoclase. Accessories include epidote and opaque minerals.

EDT7—6,143 ft (1,872.3 m)

Biotite-bearing amphibolite.—The mineralogy and bulk composition of this rock are similar to that described at the 6,141-ft (1,871.7-m) level.

EDT8—7,140 ft (2,176.2 m)

Quartz-mica schist.—This rock is composed of the assemblage muscovite-biotite-quartz-oligoclase. Accessories include clinozoisite, apatite, and opaque minerals. Garnet does not occur even though the composition seems to be aluminous. Biotite rosettes appear to cut across the earlier mica foliation, suggesting post-kinematic recrystallization.

EDT8—7,140¼ ft (2,176.2 m)

Garnet-mica schist. — Garnet-muscovite-biotite-quartz-oligoclase is the facies assemblage in this rock, accompanied by accessory apatite, epidote, and opaque minerals. Biotite rosettes appear to transect the earlier foliation, as described above. Large plagioclase grains

show retrograde effects, including exsolution and the obliteration of twinning.

EDT8—7,142½ ft (2,177 m)

Biotite-bearing amphibolite.—Although this massive amphibolite is composed of about 95 percent hornblende, it contains the assemblage hornblende-biotite-quartz-plagioclase. Accessories include sphene and opaque minerals. Hornblende separated from this rock gave a $^{40}K/^{40}Ar$ age of 140±8 m.y.

EDT8—7,144 ft (2,177.4 m)

Biotite-bearing amphibolite.—This rock is very similar to the amphibolite described above, but sphene is more abundant in this variant.

EDT9—8,216 ft (2,504.1 m)

Kyanite-staurolite-mica schist.—This rock contains the diagnostic assemblage kyanite-staurolite-garnet-muscovite-biotite-quartz-plagioclase. Trace constituents include chlorite and opaque minerals. This and the subsequent kyanite-staurolite and kyanite-staurolite-andalusite-bearing rocks that were examined from this core document a rather complex petrogenetic history. Coarse-grained kyanite is cut by a later foliation defined by second-generation kyanite and muscovite. Staurolite appears to have crystallized under both synkinematic and postkinematic conditions. The first appearance of both staurolite and kyanite in aluminous pelitic schists indicates that pressure-temperature conditions were transitional between the staurolite and kyanite zones of Barrovian metamorphism. This assemblage is also considered to be diagnostic of the amphibolite facies on the basis of the critical reactions: Chlorite + muscovite→staurolite + biotite + quartz, and muscovite + quartz→K-feldspar + kyanite + H_2O.

EDT9—8,217 ft (2,504.4 m)

Kyanite-staurolite-mica schist.—The mineralogy and fabric of this rock are very similar to those described for the 8,216-ft (2,504.1-m) interval. Postkinematic staurolite is more abundant than at 8,216 ft (2,504.1 m).

EDT9—8,218 ft (2,504.7 m)

Kyanite-staurolite-mica schist.—This rock is similar to those at 8,217 and 8,216 ft (2,504.4 and 2,504.1 m).

EDT9—8,218¼ ft (2,504.8 m)

Andalusite-bearing kyanite-staurolite-mica schist.—This rock is similar to the previously described kyanite-staurolite rocks, but it also contains andalusite and associated biotite aggregates that are clearly of postkinematic origin.

EDT10—9,196 ft (2,802.8 m)

Biotite-epidote schist.—The rock is dominated by the assemblage biotite-epidote-quartz-oligoclase. Accessory constituents include sphene, apatite, muscovite, and opaque minerals.

EDT10—9,198 ft (2,803.4 m)

Quartz-mica schist.—The assemblage muscovite-biotite-quartz-oligoclase composes most of the rock. Trace amounts of chlorite, allanite, apatite, and opaque minerals are present.

EDT11—9,766 ft (2,976.5 m)

Diopside-bearing actinolite-carbonate-mica schist.—This rock is composed of the assemblage diopside-actinolite-carbonate-phlogopite-quartz-plagioclase, and accessory sphene, clinozoisite, and K-feldspar. This rock is very similar to those described from core EDT4, except for incipient diopside. The pressure-temperature parameters affecting these rocks should be those of the kyanite zone in the amphibolite facies. The first appearance of diopside in this assemblage with increasing depth in the section reinforces the apparent downhole increase in metamorphic grade. Biotite separated from this rock gave a $^{40}K/^{40}Ar$ age of 57.3±1.9 m.y. The discordance between this age and that determined for the hornblende taken from the 7,142½-ft (2,177-m) level (140±8 m.y.) suggests that thermal overprinting or differential argon diffusion is responsible for the apparent younger age of the biotite. Implications of these discordant mineral ages are discussed in more detail later.

EDT11—9,767 ft (2,976.8 m)

Diopside-bearing actinolite-carbonate-mica schist.—The mineralogy of this rock is similar to that at the 9,766-ft (2,976.5-m) level.

EDT11—9,770 ft (2,977.8 m)

Actinolite-bearing calc-mica schist.—The mineral composition of this rock is similar to that at the 9,766-ft (2,976.5-m) and 9,767-ft (2,976.8-m) level, but diopside is absent.

CONCLUSIONS

Parentage of the Crystalline Schists

Rock types recovered from the drill hole can be subdivided into the following compositional groups.

Quartzose	*Pelitic*	*Calc-magnesian (with carbonate)*	*Calc-magnesian (without carbonate)*
Quartz-mica schist.	Garnet-quartz-mica schist.	Calc-mica schist; diopside-bearing actinolite-carbonate-mica schist.	Phlogopite-clinozoisite schist.
	Garnet-kyanite-staurolite schist.	Carbonate-clinozoisite-mica schist.	Biotite amphibolite.
	Garnet-andalusite-kyanite-staurolite schist.	Calc-green-schist.	Biotite-hornblende schist.
			Biotite-epidote schist.
			Quartz-clinozoisite schist.

The above rock types appear to be of sedimentary parentage, except for the carbonate-free and quartz-poor biotite amphibolites that are more likely derived from the recrystallization of basic igneous rocks. The cores were taken from widely spaced intervals in the drill hole, so lithologic extrapolations must be made with caution. On the basis of intervening chip samples and the drilling logs, however, approximately the top 3,195 ft (974m) of the section is composed chiefly of calc-mica schist and calc-greenschists that represent recrystallized impure (argillaceous) dolomitic limestones and marls. From 4,065 to 9,198 ft (1,239 to 2,803.4 m), the section includes both calc-magnesian and pelitic schists and rare layers of micaceous quartzite. The deepest core (EDT11) is composed of diopside-bearing actinolite-carbonate-mica schists that are compositionally similar to the actinolite-carbonate-mica schists in the cores taken from the 3,193- to 3,195½-ft (973.2- to 973.9-m) interval.

Metamorphic Facies and Reactions

The metamorphic mineral assemblages in the section cut by the drill hole indicate that metamorphic grade increases with depth. This increase in grade represents the transition from upper greenschist to amphibolite facies. Calc-mica schists taken from cores above the 2,345-ft (714.7-m) level, with bulk compositions suitable for the development of tremolite or actinolite, do not contain this phase. Actinolite was observed in calc-magnesian schists at the 3,193-ft (973.2-m) level. Epidote, which should also be a stable phase in these rocks, is first seen in assemblages in cores taken at 2,341 ft (713.5 m). Phlogopite, which is present in trace or minor quantities in calc-mica schists in the upper part of the section, increases in model percent with depth in compositionally suitable rocks. Both synkinematic and postkinematic phlogopite fabrics were detected in the cores, however, so this mineral is of questionable value as a synkinematic metamorphic index mineral.

Upper pressure-temperature limits can be assigned to the calc-magnesian assemblages in the deepest part of the section on the basis of the first appearance and continuance of green hornblende and accompanying sphene in both carbonate-bearing and carbonate-free assemblages and the appearance of incipient diopside without wollastonite in rocks containing the reactive assemblage amphibole + quartz + carbonate. Rutile does not appear in any of these assemblages, and sphene appears to be the stable titanium-bearing phase throughout the section.

On the basis of experimental data summarized by Turner (1968) and Winkler (1967), tremolite should appear in compositionally suitable systems at temperatures between 400° to 480°C, when $P_{H_2O} = P_{CO_2}$ at 500 to 1,400 bars, through the reaction: 5 dolomite + 8 quartz + $H_2O \rightarrow$ tremolite + 3 calcite + $7CO_2$. In the same pressure range, we could expect tremolite to become unstable at temperatures ranging between 490° and 580°C in the presence of coexistent calcite and quartz, which encourages the reaction: Tremolite + 3 calcite + 2 quartz $\rightarrow$ 5 diopside + $3CO_2$ + H_2O.

Mineral assemblages in pelitic rocks reinforce the evidence for the transition from greenschist to amphibolite facies indicated by the calc-magnesian assemblages. The transition includes a progressive increase in metamorphic grade through the garnet, staurolite, and kyanite isograds. Rocks exposed at the surface may actually be in the biotite zone because the garnets that occur in nearby pelitic schists may be related to thermal metamorphism from the Eielson pluton.

Problems associated with the recognition of possible superimposed thermal metamorphism include the difficulty of determining whether the rocks in the upper part of the hole are within the biotite or the garnet zone; and the uncertainty that surrounds the paragenesis of the andalusite and the staurolite in the core from the 8,218¼-foot (2,504.7-m) level. Microfabric relations appear to support strongly the development of kyanite and first-generation staurolite as coexistent stable phases during synkinematic metamorphism. Chloritoid does not appear in the pelitic schists of lower metamorphic grade, and staurolite was more likely derived from chlorite + muscovite through the reaction:

Chlorite + muscovite $\rightarrow$ staurolite + biotite + quartz + H_2O, rather than

23 Chloritoid + 7 quartz
$\rightarrow$ 2 staurolite + 5 almandine + $19H_2O$.

Although experimental data do not establish an

upper pressure limit for the stability field of staurolite, the data of Garlick and Epstein (1967), Richardson (1968), and Richardson, Gilbert, and Bell (1969) when plotted on a pressure-temperature diagram (fig. 2) show that Barrovian schists that carry the assemblage kyanite-staurolite-quartz-biotite were crystallized at pressures no less than 4.5 kbar, at a minimum temperature of 515°C. The appearance of diopside in the calc-magnesian assemblages that are stratigraphically below the kyanite-bearing rocks indicates that kyanite-staurolite equilibrium must have been obtained in the upper part of the pressure-temperature stability field for this mineral pair. At a fluid pressure of 4.5 kbar, the diopside reaction should proceed at a temperature of 580°C in compositionally suitable rocks. On the basis of the diopside reaction in the calc-magnesian rocks in the bottom of the hole, we conclude that maximum temperatures of crystallization were no less than 580°C.

Radiogenic Age Determinations

Hornblende separated from biotite-hornblende schist from the 7,142½-ft (2,177-m) level gave a $^{40}K/^{40}Ar$ age of 140±8 m.y., which is thought to be related to the latest synkinematic metamorphic event in the region. Biotite from a diopside-bearing actinolite-carbonate-mica schist from a core taken from 9,766 feet (2,976.5 m) was dated at 57.3±1.9 m.y. Initially, the age discordance was attributed to thermal overprinting accompanying the emplacement of the nearby Eielson pluton. Subsequently, however, biotite from the Eielson pluton gave a $^{40}K/^{40}Ar$ age of 67.8±2 m.y., and fission-track and $^{40}K/^{40}Ar$ mineral age data have revealed a systematic downhole decrease in the apparent age of discordant biotite-hornblende pairs. This effect is believed to be related to the steep thermal gradient in the section, and the rate at which the argon-blocking isotherms moved through the successive rock units.

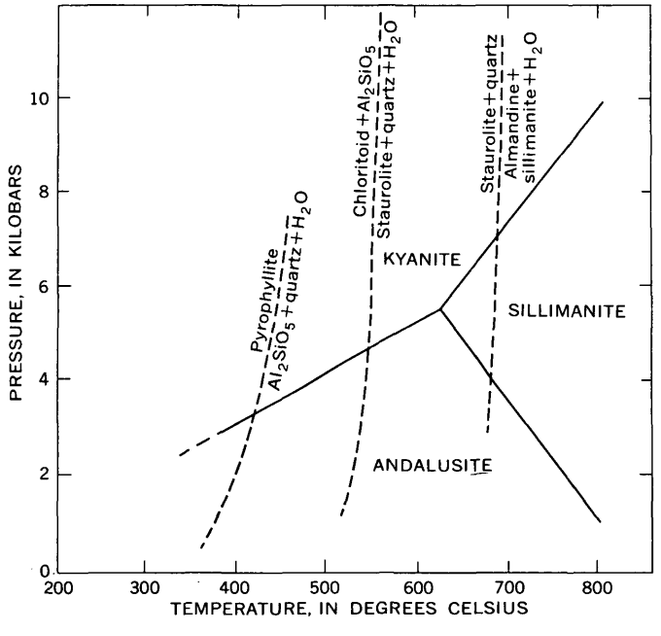

FIGURE 2.—Composite pressure-temperature diagram showing equilibria relations of kyanite, sillimanite, andalusite, and staurolite from the data of Garlick and Epstein (1967), Richardson (1968), and Richardson, Gilbert, and Bell (1969).

Geothermal Gradients and Depth of Tectonic Burial

The kyanite-staurolite-bearing assemblages are located at a depth of 8,216 feet (approx 2.5 km) as intersected by the drill hole. Kyanite-bearing rocks have rarely been detected in outcrops in the Yukon-Tanana Upland. The presence of kyanite-bearing rocks in the subsurface and the rarity of such rocks in surface exposures suggest that epeirogenic uplift has proceeded rather slowly since the last major synkinematic thermal event in Jurassic time.

There has been considerable discussion concerning the thermal gradients that accompany Barrovian metamorphism. 30°C/km is considered a normal gradient. A 30°C/km gradient curve intersects the kyanite field at a very low angle when plotted on the pressure-temperature diagram for the Al_2SiO_5 system as derived by Richardson, Gilbert, and Bell (1969).

If a 30°C/km gradient is used, temperatures of 515° to 580°C could have existed at depths of 17 to 19 km. This depth range correlates with hydrostatic pressures of 4.8 to 5.3 kbar, a pressure range that is compatible with minimum pressures indicated by the pressure-temperature diagram for the stable association of staurolite + kyanite.

Geothermal data obtained from the drill hole by A. J. Lachenbruch and J. H. Sass (oral commun., 1970) about 6 mo after its completion, included the bottom-hole temperature of 94.75°C and a linear temperature-depth curve that defined a thermal gradient of approximately 31.5°C/km. This gradient is very close to the 30°C/km gradient proposed for crustal sections undergoing synkinematic metamorphism of the Barrovian type and in excellent agreement with parameters defined by the metamorphic mineral assemblages and reactions previously discussed.

On the basis of a 31.5°C/km geothermal gradient, the temperature at 17 km would be approximately 535°C. This temperature is within the 515°–580°C range assigned to the constituent mineral assemblages in the rocks from the 8,216- to 9,770-ft (2,504.1- to 2,977.8-m) interval.

Few data are available on the behavior of geothermal gradients during various orogenic cycles. It is possible that certain geothermal gradients may be unique to a particular type of metamorphic process or belt (for example, Barrovian, blueschist facies, Buchan). The decay rates of thermal gradients after the end of a synkinematic event are not well known. In this area, however, it appears that the geothermal gradient, as measured in the Eielson drill hole, may have changed little since Jurassic time.

REFERENCES CITED

Beikman, H. M., 1974, Preliminary geologic map of the southeast quadrant of Alaska: U.S. Geol. Survey Misc. Field Studies Map MF–612.

Bunker, C. M., Bush, C. A., and Forbes, R. B., 1973, Radioelement distribution in the basement complex of the Yukon-Tanana Upland, Eielson deep test hole, Alaska: U.S. Geol. Survey Jour. Research, v. 1, no. 6, p. 659–664.

Forbes, R. B., Pilkington, H. D., and Hawkins, D. B., 1968a, Gold gradients and anomalies in the Pedro Dome-Cleary Summit area, Fairbanks district, Alaska: U.S. Geol. Survey open-file rept., 43 p.

Forbes, R. B., Swainbank, R. C., and Burrell, D. C., 1968b, Structural setting and petrology of eclogite-bearing terrane near Fairbanks, Alaska [abs.]: Am. Geophys. Union Trans., v. 49, no. 1, p. 345.

Foster, H. L., Weber, F. R., Forbes, R. B., and Brabb, E. E., 1973, Regional geology of Yukon-Tanana Upland, Alaska, *in* Arctic geology: Am. Assoc. Petroleum Geologists Mem. 19, p. 388–395.

Garlick, G. D., and Epstein, Samuel, 1967, Oxygen isotope ratios in coexisting minerals of regionally metamorphosed rocks: Geochim. et Cosmochim. Acta, v. 31, no. 2, p. 181–214.

Lachenbruch, A. H., and Bunker, G. M., 1971, Vertical gradients of heat production in the continental crust—[Pt.] 2, Some estimates from borehole data: Jour. Geophys. Research, v. 76, p. 3852–3860.

Richardson, S. W., 1968, Staurolite stability in a part of the system Fe–Al–Si–O–H: Jour. Petrology, v. 9, no. 3, p. 467–488.

Richardson, S. W., Gilbert, M. C., and Bell, P. M., 1969, Experimental determination of kyanite-andalusite and andalusite-sillimanite-equilibria; the aluminum silicate triple point: Am. Jour. Sci., v. 267, no. 3, p. 259–272.

Turner, F. J., 1968, Metamorphic petrology [2d ed.]: New York, McGraw-Hill, 403 p.

Wasserburg, J. G., Eberlein, G. D., and Lanphere, M. A., 1963, Age of the Birch Creek Schist and some batholithic intrusions in Alaska: Geol. Soc. America Spec. Paper 73, p. 258–259.

Winkler, H. G. F., 1967, Petrogenesis of metamorphic rocks [2d ed.]: New York, Springer-Verlag, 237 p.

Jour. Research U.S. Geol. Survey
Vol. 3, No. 6, Nov.-Dec. 1975, p. 659–663

PHOSPHATE FERTILIZER MATERIALS IN COLOMBIA—IMPORTS, USES, AND DOMESTIC SUPPLIES

By JAMES B. CATHCART, Denver, Colo.

Work done in cooperation with the Instituto Nacional de Investigaciones Geológico-Mineras, Colombia, under the auspices of the Government of Colombia and the Agency for International Development, U.S. Department of State

Abstract.—The distribution of potentially economic phosphate deposits and the locations of major users of phosphate products in Colombia are some of the economic factors that indicate the capability of the deposits to supply domestic demands. Much research is required to determine the types of processing plants needed and to outline changes from standard procedures, but there is little doubt that with proper planning a phosphate chemical industry could be developed that would supply domestic demands for the forseeable future.

Potentially minable phosphate rock deposits in Colombia are known in the Cordillera Oriental from Neiva in the southwest to Cúcuta in the northeast (fig. 1). The deposits are in two facies; that nearest the craton is sandy and contains little or no calcite, whereas that to the west is characterized by abundant calcite. Data on tonnage and chemical characteristics of the phosphate rock are derived from geologic mapping and sampling of outcrops or samples taken from shallow trenches, except for the Conejera area (loc. C, fig. 1) where exploratory drilling has been done.

Deposits of sandy phosphate rock have been examined in some detail at Sardinata (loc. A, fig. 1), and at Conejera (loc. C, fig. 1). Deposits of phosphate rock near Yaguará-Llanoverde (loc. D) have been mapped and sampled, in part. The deposits of calcareous phosphate rock at Azufrada-Conchal-Vanegas (loc. B) have been mapped and sampled by trenching at the outcrop. Other areas have been mapped; additional detailed mapping is needed in intervening areas and additional drilling is needed to determine the chemical characteristics, thickness, and tonnage. For this report, only areas A, B, C, and D (fig. 1) will be considered.

SARDINATA AREA

The Sardinata area (loc. A, fig. 1) was originally mapped by geologists of the Instituto Nacional de Investigaciones Geológico-Mineras (INGEOMINAS) (Cathcart and Zambrano O., 1967; Zambrano O., 1971); later detailed trenching and sampling by Empresa Colombiana de Minas (ECOMINAS) (Abozaglo

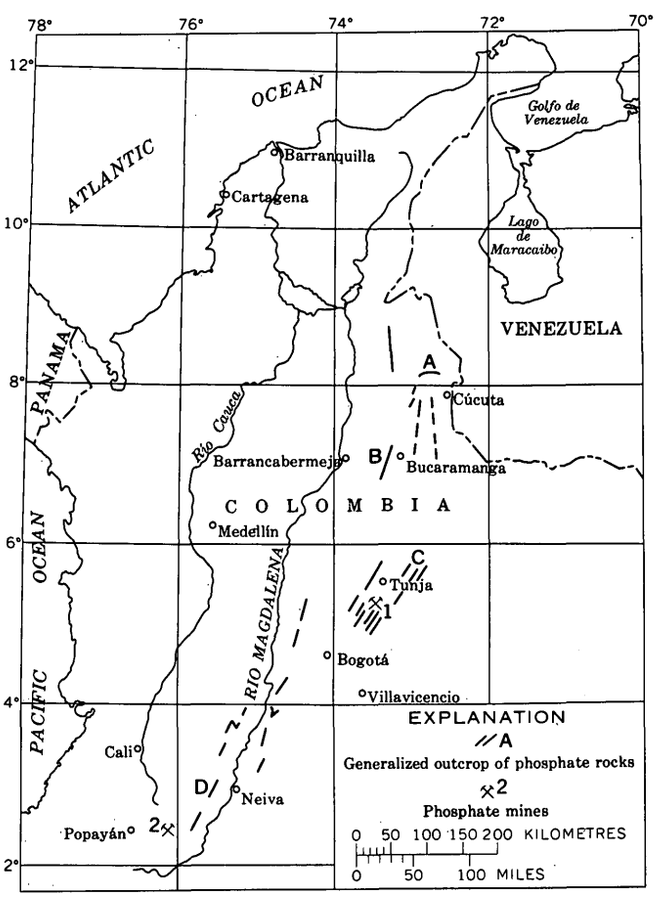

FIGURE 1.—Index map of part of Colombia showing approximate location of outcrops of phosphate rock (A, Sardinata area; B, Azufrada-Conchal-Vanegas area; C, Conejera area; D, Yaguará-Llanoverde area) and of phosphate mines (1, La Cascajera; 2, La Juanita).

M., 1973) was done in the area amenable to open-pit mining. This part of the deposit is flat or dips gently to the north, and overburden is very thin (from 0.5 to 5 m). The phosphate bed ranges in thickness from 0.5 to 3.5 m and is weathered and poorly consolidated. Stripping ratios are excellent and mining can be done cheaply by means of simple earthmoving equipment. Measured reserves of strippable rock are about 9 million tons; recovery should be high, perhaps as much as 90 percent.

Chemical data (table 1) show that all the P_2O_5, CaO, CO_2, and F can be assigned to the apatite mineral and that no calcite is present. X-ray diffraction patterns of samples from the phosphate bed at Sardinata show that the rock consists of carbonate fluorapatite and quartz as major mineral phases and feldspar, organic material, and a clay mineral in minor or trace amounts. The clay mineral is either illite or a mixed-layer clay, probably chlorite-montmorillonite. Trace amounts of an iron oxide are also present. Although all samples are weathered, only a few samples (the most thoroughly weathered) contain trace amounts of the aluminum phosphate mineral, wavellite, and the clay mineral, kaolinite.

TABLE 1.—*Partial chemical composition, in percentage, of selected phosphate samples, Colombia*

	A	B	C	D
P_2O_5	28.18	21.6	20.1	23.8
CaO	41.37	40.3	28.3	31.7
CO_2	2.71	8.5	1.16	1.55
F	3.15	2.4	2.21	2.28
Al_2O_3	1.86	1.9	1.57	----
Fe_2O_3	.87	.56	.92	----
Acid insoluble	16.55	19.6	44.0	31.75
Ratios:				
$CaO:P_2O_5$	1.47	1.87	1.41	1.33
$F:P_2O_5$	.112	.111	.110	.095
$CO:P_2O_5$	.096	.394	.058	.065

A. Sardinata area: Average of many samples; analyses by Empressa Colombiana de Minas (ECOMINAS).
B. Azufrada-Conchal-Vanegas area: Average of 44 samples; analyses by Instituto Nacional de Investigaciones Geológico-Mineras (INGEOMINAS) (Pedro Mojica G., unpub. data, 1969) except analyses of F and CO_2 by Instituto Fomento Industrial (IFI) (Lasman and others, 1968).
C. Conejera area: Average of 25 samples; analyses by INGEOMINAS and U.S. Geological Survey (USGS) (J. B. Cathcart and Francisco Zambrano O., unpub. data, 1973).
D. Yaguará-Llanoverde area: Average of 11 samples; analyses by USGS and INGEOMINAS.

If this rock is to be used in a chemical plant for making phosphoric acid or other phosphate chemicals, the only deleterious material is organic, which can be removed by calcining.

The average content of acid-insoluble material in the rock is about 16 percent (table 1) of silica which present as quartz, but is very fine grained, chertlike material. When the rock is ground the silica forms sharp angular fragments that could cause excess wear, by abrasion, in pumps, pipelines, and filters. Scrubbing and screening after grinding may ease the problem. Grinding, scrubbing, screening, and calcining tests are currently being made.

Sardinata is the only area known in Colombia where phosphate rock can be mined by open-pit methods. Reserves are adequate for mining at a rate of a few hundred thousand tons per year, P_2O_5 content is fairly high, and the mining area is about 100 km (airline) from the Magdalena River. Phosphate rock at the Magdalena River can be transported north to Barranquilla and Cartagena and south to Barrancabermeja where the major fertilizer plants of the country are located.

AZUFRADA-CONCHAL-VANEGAS AREA

The Azufrada-Conchal-Vanegas area (loc. B, fig. 1) has been mapped and sampled by geologists of INGEOMINAS (Pedro Mojica G., unpub. data, 1969) and Instituto Fomento Industrial (IFI) (Lasman and others, 1968). The phosphate rock is folded and faulted; much is in beds that are nearly vertical, and the only data available are from trenches and outcrops.

The main phosphate bed ranges from 1 to 2 m in thickness and probably averages about 1.5 m. Total reserves are not known, but Lasman, Cuevas B., and Peña (1968) have shown indicated reserves of about 1 million tons in a strike length of only 4 km in the Azufrada area, and Pedro Mojica G. (unpub. data, 1969) showed inferred reserves of about 3.5 million tons of possible mineable material in the Azufrada-Conchal area. Inferred mineable reserves in the Azufrada-Conchal-Vanegas area total about 1.5 million tons; the total resource is about 6 million tons. Reserves are computed only to a depth of 100 m below the surface, and possible minable reserves are that part of the rock that is above entry level. Almost all mining would have to be underground, although Mojica G. (unpub. data, 1969) indicated that about 0.8 million tons may be minable by open-pit methods. Drilling is necessary to prove reserves and to determine the best mining sites.

X-ray data show that the rock contains apatite, quartz, and calcite as major mineral phases, dolomite, pyrite, glauconite (in some samples) and the clay minerals, illite, and a mixed-layer clay, probably chlorite-montmorillonite as traces.

Thin sections show that the rock is composed of phosphate pellets, rod-shaped grains, phosphatized foraminifers, and some silt-sized quartz grains, cemented by fine-grained calcite. Calcite-filled veinlets that cut the pellets as well as the cement are common.

The location of the Azufrada-Conchal-Vanegas area is excellent with regard to a future chemical plant at

Barrancabermeja, and estimated reserves are adequate for this plant's potential demand. However, mining costs probably will be high, and if the rock is to be used for chemical processing, calcite must be removed. Calcining at elevated temperatures followed by rapid quenching and wet screening will eliminate calcite; froth flotation may be used to remove calcite from the phosphate rock as it is for similar rock mined in Israel (Hoffman and Mariacher, 1961). Both processes are expensive.

CONEJERA AREA

The Conjera area (loc. C, fig. 1) has been mapped and sampled on a detailed scale by geologists of INGEOMINAS (Zambrano O. and Mojica G., 1973), and the west flank of the syncline has been drilled. Drilling and sampling on the west flank of the syncline have established a measured reserve of 12 million tons and indicated and inferred reserves of about 40 million tons. The structure is synclinal; dips on the west flank are 20°–30°. The bed is 2–4 m thick and probably averages about 2.5 m. Mining would have to be underground, but a slightly inclined adit could be driven below the synclinal axis so all mined material could be moved by gravity. A good unpaved road connects the mine to the railroad at Sogamoso, only a few kilometres away.

Chemical analyses of outcrop and core samples are similar; average data are shown in table 1. The $CaO:P_2O_5$ ratio is low, indicating that the rock contains no calcite. X-ray and thin-section data confirm this. Apatite and quartz are the only major mineral phases present, but the rock also contains trace amounts of iron oxide (pyrite at depth), orthoclase, organic material, and kaolinite. Surface samples contain wavellite and crandallite, and certain core samples also contain traces of wavellite. Thin sections show that many of the phosphate pellets are phosphatized foraminifers, thus the rock originally contained calcite. The silica content is high (44 percent acid insoluble, table 1). Silica is present as silt-sized detrital quartz grains, as partial replacement of foraminifers, as fine silt inclusions in some of the phosphate pellets, and as very fine grained cement. Much of the silica forms sharp angular fragments on grinding.

Silica may cause problems in processing, as at Sardinata, but preliminary tests in the laboratory indicate that the rock can be used to make acceptable superphosphate and that good quality phosphoric acid can be produced. The ratio of silica to apatite in the rock is close to the ratio needed to make elemental phosphorus by electric furnace methods. Research on processing methods is needed.

Flotation tests made on ground and deslimed phosphate rock from Conejera using reagents standard for Florida, U.S., phosphate rock were not successful, probably because most of the silica is present as chertlike material rather than as rounded quartz sand. Different reagents or different amounts of the standard reagents probably would produce acceptable results.

Conejera is close to the agricultural area of the Sabana and could supply phosphate rock to the Llanos. Measured and inferred reserves are large enough to supply domestic demands for many years. The rock is somewhat lowgrade, but has no deleterious chemical characteristics. Problems of exploitation include transportation to a chemical plant and high silica content. The rock may be usable for direct application in acid soils.

YAGUARÁ-LLANOVERDE AREA

Geologic mapping of Yaguará-Llanoverde (loc. D, fig. 1) by geologists of INGEOMINAS has been going on for about 2 yr. Only grab samples at the outcrop have been taken. Trenching is planned, and drilling should be done to determine the chemical character of the phosphate rock in the subsurface.

The most promising locality is the Llanoverde syncline. The phosphate bed here ranges in thickness from about 0.8 to almost 2.0 m and probably averages about 1.2 m. The area of the Llanoverde syncline is about 15 km²; dips are 25°–40° on the east flank and are less steep (5°–10°) on the west flank. Structural complications such as faulting and cross folding are not extreme.

Reserves have not been measured, but a bed 1 m thick underlying 1 km² represents about 2 million tons of phosphate rock; as much as 30 million tons may be present in the 15 km² area. Drilling is needed to prove thickness and structure.

Chemical analyses of outcrop samples by INGEOMINAS and the U.S. Geological Survey show an average of about 23 percent P_2O_5 and show a distinct deficiency of CaO in the samples (table 1), indicating that the samples are leached. X-ray data show apatite and quartz as major mineral phases, and kaolinite, feldspar, the aluminum phosphate mineral wavellite, and the iron phosphate mineral cacoxenite as trace mineral phases.

Thin sections show that the phosphate is present as structureless pellets, phosphatized bone fragments, a few phosphatized foraminifers, and some rod-shaped grains. Silica is present as silt-sized quartz grains and very fine grained cement. Secondary iron and aluminum phosphate minerals are present in the groundmass and around the phosphate pellets.

The phosphatized foraminifers indicate that calcite may be present in the rock in the subsurface. Drilling, therefore, is necessary to determine the chemical character of the rock, which must be established before plans for utilization can be made.

The Llanoverde area is in the southern part of the country and could be a source of phosphate rock for agricultural demands in the upper Magdalena Valley and the Cauca Valley. Inferred reserves are large, but must be be proved; chemical data are available only for leached surface samples. Mining will have to be by underground methods, but more data are needed to determine the location of the actual mining area. If a phosphate chemical plant is ever built in the southern part of the country, a mine here might be possible.

A summary of tonnage data for the four localities discussed is given in table 2.

TABLE 2.—*Summary of phosphate-rock tonnage data for selected localities*

Locality	Tonnage	
	Measured	Inferred
A. Sardinata	9×10^6	------
B. Azufrada-Conchal-Vanegas	1×10^6	5×10^6
C. Conejera	12×10^6	40×10^6
D. Yaguará-Llanoverde	------	30×10^6

PHOSPHATE FERTILIZER PRODUCTS

Announcements in December 1973 of dramatic price increases in phosphate rock (Morocco high grade as much as US$45 per ton; Florida low-grade as much as US$21 per ton) point to the possibility of mining and processing domestic Colombia phosphate rock and delivering the products to areas of use within Colombia at prices that would be competitive or cheaper than imported materials. The following tables contain data on imports to Colombia (table 3) and the producers and amounts of fertilizer materials (mixed goods) produced from the imported material (table 4). Both tables show equivalent tons of P_2O_5 and the amount of phosphate rock of 20 and 28 percent P_2O_5 needed to make the phosphate parts of the mixed fertilizers. Almost 200,000 tons per year of 28-percent P_2O_5 phosphate rock or 300,000 tons per year of 20 percent rock would have to be produced to meet the demands for fertilizer products.

The principal users of the imported phosphate products in 1972 were Abocol in Cartagena, Monómeros in Barranquilla, and Caja Agraria in Bogotá and Cali.

A mine at Sardinata could easily supply the raw materials for Abocol and Monómeros (about 130,000 tons in 1972) by moving phosphate rock to the Magdalena River (perhaps by pipeline) and then to Barranquilla and Cartagena. In addition, if the 29,000 equivalent tons per year used by Caja Agraria (table 4) could be processed at the Ferticol plant at Barrancabermeja, this amount of phosphate rock could easily be moved and shipped on the Magdalena River.

Chemical plants, of course, would have to be built to make phosphoric acid, ordinary superphosphate, and, perhaps, triple superphosphate. A possible example is discussed below.

The nitrogen plant at Barrancabermeja makes urea and ammonium nitrate, which is used by Caja Agraria

TABLE 3.—*Tonnages of phosphate products imported in 1972 and the equivalent phosphate rock needed to produce the products*

Product	Tonnage				Remarks
	Imported in 1972 [1]	P_2O_5 equivalent (rounded)	28-percent P_2O_5 phosphate rock [2]	20-percent P_2O_5 phosphate rock [2]	
Ammonium phosphate	33,232	15,000	54,000	75,000	46 percent P_2O_5 in product.
Phosphoric acid	20,768	11,000	39,000	55,000	54 percent P_2O_5 acid.
Triple superphosphate	19,900	9,000	32,000	45,000	46 percent P_2O_5.
Phosphate rock	37,188	12,000	43,000	60,000	32 percent P_2O_5.
Mixed goods (for example 10–30–10, 10–20–20) [3]	27,150	7,000	25,000	35,000	Average 26 percent P_2O_5.
Total	-----	54,000	193,000	270,000	----------

[1] After Perdomo and Sánchez (1973).
[2] Tons of phosphate rock needed to make the tons of product if grade of the phosphate rock is 28 percent (Sardinata) or 20 percent (other deposits.) Figures rounded.
[3] 10–30–10 is amount, in percent, of available plant nutrient in the order of N (nitrogen), P, (P_2O_5), and K (K_2O). This is standard fertilizer notation.

TABLE 4.—*Principal producers of fertilizer mixed goods, and tonnages of 1972 production and of equivalent phosphate rock needed to supply the P_2O_5 for the products*

	1972 production		Equivalent phosphate rock [1]	
	Mixed goods [2]	[3] P_2O_5	28 percent	20 percent
Abocol	137,400	26,000	93,000	130,000
Monómeros	56,570	11,000	39,000	55,000
Caja Agraria	40,480	8,000	29,000	40,000
Others	49,460	9,000	32,000	45,000
Total	283,910	54,000	193,000	270,000

[1] Tonnage of phosphate rock needed to make tonnage of product if 28 percent or 20 percent P_2O_5 phosphate rock is used.
[2] From Perdomo V. and Sánchez (1973).
[3] Tonnage of P_2O_5 equivalent used in making the totals for mixed goods, using an average of 19 percent P_2O_5 in the products.

at several places in the country. It would be possible to move phosphate rock to this plant from Sardinata. Nitric acid can be used to make phosphoric acid and other phosphate fertilizer products. The plant at Barrancabermeja has additional land, excess power, and trained personnel, and additional natural gas is available, so nitric acid capacity can be increased. Making mixed fertilizers here for delivery to other areas in the country might be economical.

The calcareous phosphate rock at Azufrada (loc. B, fig. 1) is particularly intriguing because of its proximity to Barrancabermeja. Shipping costs for delivery of phosphate rock should be very low, and reserves are adequate for the present demand of 40,000 tons per year (table 4).

REFERENCES CITED

Abozaglo M., Jacob, 1973, Estudios exploratorios del yacimiento de fosfatos de Sardinata (Depto. Norte de Santander): Empresa Colombiana de Minas (ECOMINAS), 13 p.

Cathcart, J. B., and Zambrano O., Francisco, 1967, Roca fosfática en Colombia: Colombia Servicio Geol. Nac. Bol. Geol., v. 15, nos. 1–3, p. 65–162. (English abs.).

Hoffman, I., and Mariacher, B. C., 1961, Beneficiation of Israeli phosphate ore: Mining Eng., v. 13, p. 472–474.

Lasman, Noach, Cuevas B., Jairo, and Peña, Guillermo, 1968, Yacimiento de roca fosfórica en "La Azufrada" (Santander): Bogotá, Inst. Fomento Industrial, Dept. Minería, 23 p.

Perdomo V., Regulo, and Sánchez, I. P., 1973, Producción, importación y consumo de abonos en Colombia 1971–72: Medellín, Colombia, Soc. Colombiana Ciencia del Suelo, 12 p. (Gráficas presentadas en la conferencia dictada el 25 de Junio de 1973).

Zambrano O., Francisco, 1971, Roca fosfórica de Sardinata: Inst. Nac. Inv. Geol.-Mineras, Geología Económica, Informe no. 1572.

Zambrano O., Francisco, and Mojica G., Pedro, 1973, Roca fosfórica en el alto de la Conejera y zonas aledañas a Pesca: Columbia Inst. Nac. Inv. Geol.-Mineras (INGEOMINAS), Inf. no. 1570, 122 p.

Jour. Research U.S. Geol. Survey
Vol. 3, No. 6, Nov.–Dec. 1975, p. 665–669

DESCRIPTION OF THE GEOELECTRIC SECTION, RATTLESNAKE HILLS UNIT 1 WELL, WASHINGTON

By DALLAS B. JACKSON, Denver, Colo.

Abstract.—A complex 64-in. normal log from the 3,249-m-deep Rattlesnake Hills well was digitized and reduced to a form resembling a simple resistance log. The simplified form of the log made it possible to recognize three major geoelectric intervals in the well that were not apparent on the original log. The apparent resistivity values from each geoelectric interval are grouped into a frequency-distribution table, where midpoints of the class interval are corrected for the effects of hole diameter and mud resistivity. Using corrected class-interval midpoint resistivities, first-approximation values are calculated for five geoelectric parameters: total transverse resistance, total longitudinal conductance, average longitudinal resistivity, average transverse resistivity, and the coefficient of anisotropy. Comparison of anisotropies, resistivity variations, and resistivity-frequency polygon shapes indicates quantitative differences among the three geoelectric intervals.

The Columbia Plateaus physiographic province, which covers more than 130,000 km² in southeastern Washington, northeastern Oregon, and western Idaho, consists of nearly horizontal basalt flows with some interflow tuffs and lacustrine deposits. The basalt flows issued from fissures and flowed out over the area forming layers 30 to 150 m thick; many flows have been traced 200 km without their edges being located (King, 1959). Most of the information on the thickness and lithology of the rocks has been gained from exposures in canyons incised as deep as 1,800 m into the plateau surface.

In 1958, a Standard Oil Co. of California petroleum exploration well, Rattlesnake Hills unit 1, sec. 15, T. 11 N., R. 24 E., was drilled in the Rattlesnake Hills between the towns of Yakima and Pasco in south-central Washington (fig. 1). The well bottomed at 3,249 m without penetrating the base of the basaltic rocks. A complex electrical resistivity log was run in the well by the Schlumberger Well Surveying Corp. and furnished to the U.S. Geological Survey by the Rocky Mountain Well Log Service, Denver, Colo. The log was digitized, reduced to a simplified transverse resistance log, and analyzed in terms of its geoelectric parameters. The reduction of the digitized electric log from this well to a simplified transverse resistance log, and the examination of the geoelectric parameters suggest that the volcanic rocks penetrated by the well can be subdivided into three geoelectric intervals whose boundaries are at 1,265 and 2,100 m. These boundaries nearly coincide with major breaks in the geologic-geoelectric section of the Rattlesnake Hills well identified by Raymond and Tillson (1968) at 1,500- and 2,100-m depths. Raymond and Tillson postulated that the 1,500-m depth marks the base of the Columbia River Group.

GEOELECTRIC PARAMETERS

Five geoelectric parameters that describe the average electrical properties of a sequence of layered rocks of thickness H may be computed from digitized electric logs (Keller, 1966; Zohdy, 1965). These parameters for a column of rock 1 m² in cross section consist of the following:

1. Total transverse resistance, T, is the total resistance perpendicular to the bedding planes of a column

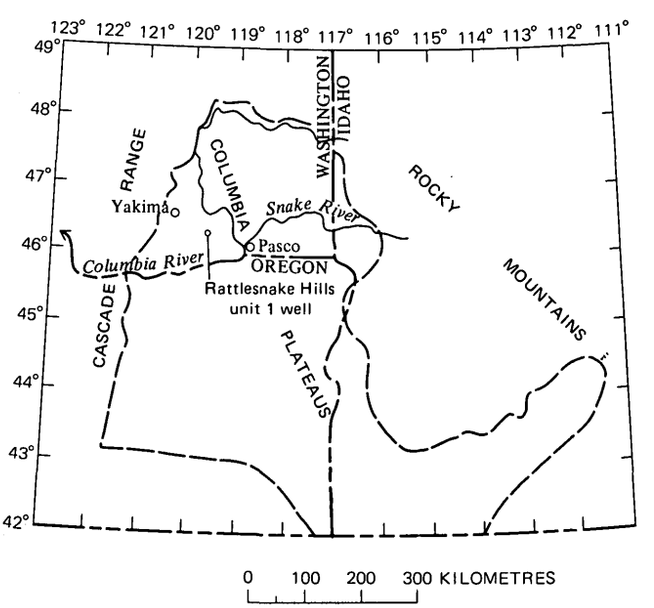

FIGURE 1.—Index map showing the location of Rattlesnake Hills unit 1 well.

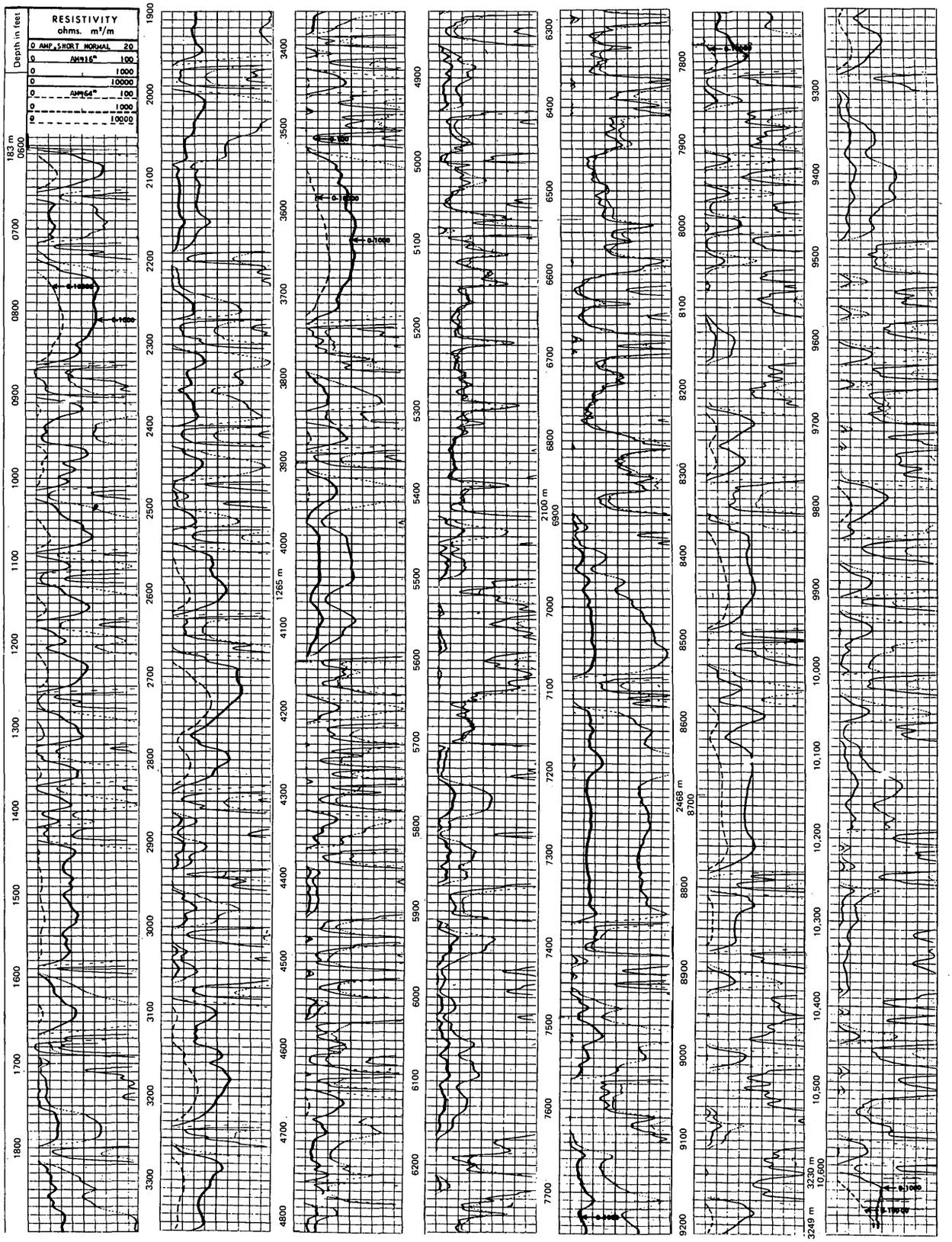

FIGURE 2.—Resistivity log of Rattlesnake Hills unit 1 well, Benton County, Wash. 183–2,468 m, R_m 7.0 ohm-m at 47°F, R_m 2.3 ohm-m at 149°F, *BHT*; 2,468–3,249 m, R_m 7.0 ohm-m at 70°F and 2.0 ohm-m at 225°F. R_m is the mud resistivity and *BHT* is the bottom hole temperature.

of rock measured in ohm-metres squared.

$$T=\sum_{i=1}^{n}\rho_i h_i, \quad (1)$$

where ρ_i is the resistivity in ohm-metres, h_i is the thickness in metres of the ith layer, and n is the total number of layers.

2. Total longitudinal conductance, S, is the sum of the conductances horizontally through the column of layers of rock measured in mhos,

$$S=\sum_{i=1}^{n}\frac{h_i}{\rho_i}. \quad (2)$$

3. Average longitudinal resistivity, ρ_L, is the average resistivity for current flow parallel to the layers measured in ohm-metres.

$$\rho_L=H/S. \quad (3)$$

4. Average transverse resistivity, ρ_{tr}, is the average resistivity for current flow transverse to the layers measured in ohm-metres,

$$\rho_{tr}=T/H. \quad (4)$$

5. Coefficient of anisotropy, λ is dimensionless and is 1 for an isotropic medium,

$$\lambda=\sqrt{\rho_{tr}/\rho_L}. \quad (5)$$

GEOELECTRIC PARAMETERS OF RATTLESNAKE HILLS UNIT 1 WELL

As is evident from figure 2, a resistivity log of the Rattlesnake Hills well, extreme resistivity variations make it very difficult to separate the log objectively into discrete major sections. A comparison of the electric log to descriptions of 19 sidewall cores in the well furnished by D. D. Hastings, Standard Oil Co. of California, indicates that most of these resistivity variations are caused by porous tuffaceous beds intercalated with the higher resistivity basalt flow material of relatively low porosity. To reduce the complexity of the log and to accentuate the major trends, a simple numerical filtering technique was used; the 64-in. normal log was digitized at 1.52-m (5-ft) intervals and the total transverse resistance, T, was computed for the sum of each 30.48 m (100 ft). The values of T are plotted on a logarithmic scale versus the values of depth on a linear scale (fig. 3*A*). A plot of 30.48-m sums taken at 1.52-m samplings, of apparent resistivity, would have exactly the same shape as the plot in figure 3*A*. However, the curve would be shifted to the left by log 1.52 m because

$$T_{30.48\ \mathrm{m}}=1.52\ \mathrm{m}\sum_{1}^{20}\rho_n$$

or

$$\log T=\log 1.52\ \mathrm{m}+\log\sum_{1}^{20}\rho_n,$$

where 1.52 is the sampling interval in metres.

Although trends are more apparent in figure 3*A* than on the original electric log, further filtering is

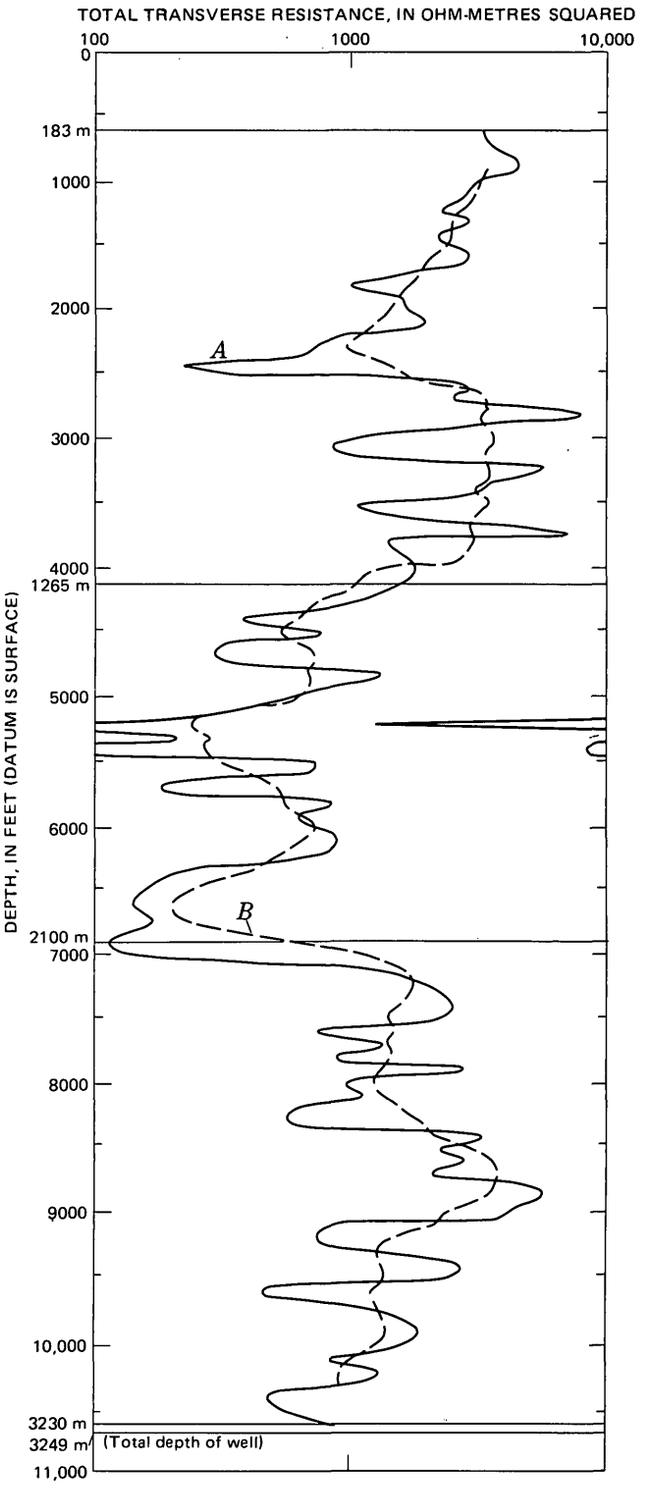

FIGURE 3.—Sums (A) of total transverse resistances at 30.48-m intervals versus depth, and simplified transverse resistance log B, showing running mean over 150-m intervals computed for the curve of A.

desirable to emphasize the major resistivity units. Because the short-interval variations occur in cycles of about 150 m a running arithmetic mean over 150-m intervals computed for the data of figure 3*A* simplifies the curve to that shown in figure 3*B*.

From the simplified representation of the electric log (fig. 3*B*) three major subdivisions, whose boundaries are at approximately 1,265 m and 2,100 m depth, can be recognized.

Calculation of the geoelectric parameters, equations 1 through 5, of the three major intervals in the well, is facilitated by constructing a frequency distribution table of the resistivities in each geoelectric interval. (A frequency distribution table is a tabulation of the number of occurrences of a parameter in class intervals over the range that the parameter covers.) After the resistivities have been separated into classes, each class midpoint is departure corrected for the effects of the hole diameter and the mean mud resistivity (Pirson, 1963) of the geoelectric section being examined (table 1). (Values of mud resistivities are shown in fig. 2 caption.) The geoelectric parameters for each depth interval are then calculated using the values of the class midpoints rather than departure correcting and calculating T and S values for each digitized point of the sampled interval.

The geoelectric parameters calculated for the three intervals of the Rattlesnake Hills unit 1 well are shown in table 2. Distinct differences are apparent. The values of T and S are related directly to the thicknesses of the sections they represent; thus, they cannot be compared directly. However, the average values of ρ_L, ρ_{tr}, and λ are independent of the thickness of the sampled interval and may be compared directly from section to section or correlated from well to well. For purposes of correlation, only the values of ρ_L and λ, or ρ_{tr} and λ, need be considered. Comparing anisotropies and longitudinal resistivities among the three intervals of the Rattlesnake Hills well (table 2) makes it apparent that the central interval, from 1,265 to 2,100 m, differs markedly from the other two.

The data from the frequency distributions, table 1, are plotted at class midpoints for each of the three geoelectric intervals in figure 4. The abscissa gives

TABLE 1.—*Apparent resistivity frequency distributions at the class midpoints and the corresponding departure-corrected class-midpoint values for the three geoelectric intervals*

Apparent resistivity classes (ohm-m)	Class midpoints (ohm-m)	Resistivities (706 points) in geoelectric interval 183–1,265 m		Resistivities (550 points) in geoelectric interval 1,265–2,100 m		Resisitivities (740 points) in geoelectric interval 2,100–3,230 m	
		Frequency distribution (percent)	Corrected resistivity (ohm-m)	Frequency distribution (percent)	Corrected resistivity (ohm-m)	Frequency distribution (percent)	Corrected resistivity (ohm-m)
13.3– 17.8	15.4	----	----	1.6	13.9	----	----
17.8– 23.7	20.5	0.4	18.6	4.3	18.1	0.5	17.5
23.7– 31.6	27.3	0.4	24.5	8.2	23.5	0.8	22.8
31.6– 32	36.4	1.9	31.6	16.5	30.6	1.0	29.5
42 – 56	48.7	3.7	41.0	14.5	39.6	4.9	37.8
56 – 75	64.9	3.7	53.0	7.5	50.8	3.5	48.0
75 – 100	86.6	5.5	68.7	6.7	65.0	13.3	61.5
100 – 133	115	1.8	87.5	6.1	87.5	8.5	79.5
133 – 178	154	5.4	112	5.5	107	6.1	104
178 – 237	205	4.5	144	6.5	139	6.2	135
237 – 316	273	6.3	186	6.9	180	4.8	178
316 – 422	364	5.2	242	7.1	237	6.7	236
422 – 562	487	9.0	317	4.3	315	7.1	320
562 – 750	649	9.9	418	2.9	425	10.3	442
750 – 1,000	866	9.0	563	1.2	583	8.4	622
1,000 – 1,330	1,150	9.9	793	----	----	4.5	881
1,330 – 1,780	1,540	7.3	1,080	----	----	4.6	1,290
1,780 – 2,370	2,050	6.2	1,530	----	----	6.1	1,950
2,370 – 3,160	2,730	5.9	2,180	----	----	2.4	2,870
3,160 – 4,220	3,640	2.7	3,210	----	----	----	----
4,220 – 5,620	4,870	0.7	4,970	----	----	----	----
5,620 – 7,500	6,490	----	----	----	----	----	----
7,500 –10,000	8,660	----	----	----	----	----	----

TABLE 2.—*Geoelectric parameters of Rattlesnake Hills unit 1 well, Benton County, Wash.*

Geoelectric interval (m)	Total transverse resistance, T (ohm-m^2)	Total longitudinal conductance, S (mhos)	Average longitudinal resistivity, ρ_L (ohm-m)	Average transverse resistivity, ρ_{tr} (ohm-m)	Anisotropy (ohms)
183–1,265	966,000	5.24	206	893	2.08
1,265–2,100	117,000	13.5	57.6	150	1.61
2,100–3,230	754,000	7.35	162	634	1.98

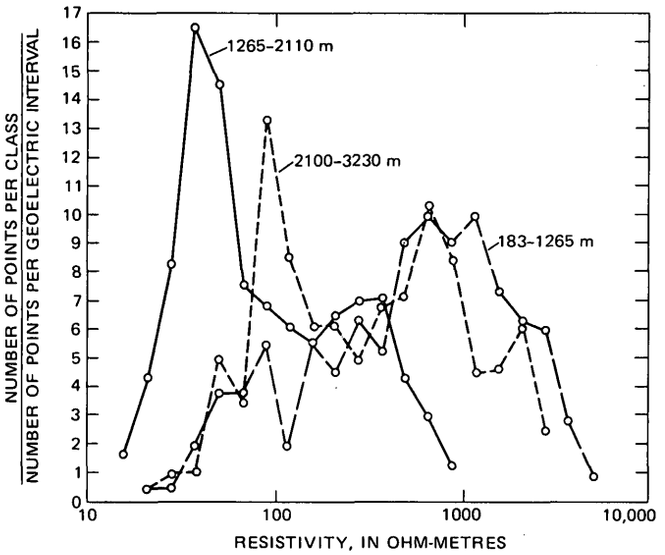

FIGURE 4.—Frequency polygons of resistivity classes versus number of occurrences of resistivities per class normalized to total points per geoelectric interval.

values for departure-corrected resistivity, from 10 to 10,000 ohm-m; the ordinate gives normalized values of the frequency of resistivity value occurrences at the class-interval midpoints. The resistivity classes begin at 10 ohm-m; each successive class bound is $\sqrt[8]{10}$ times greater than the preceding class bound. This interval of $\sqrt[8]{10}$ gives eight equally spaced logarithmic classes per decade.

In figure 5, which can also be thought of as a resistivity modal analysis, two curves have similar shape and a third is substantially different. The solid curve, which is sharply skewed to the left and does not contain resistivities above 1,000 ohm-m, is from the center interval of the well; it confirms the conclusion, reached by comparing the geoelectric parameters ρ_{tr} and λ, that the center interval differs from the other intervals.

The normalized frequency polygons also are useful for comparing sections which might be lithologically similar, but saturated with solutions of differing salinity (as could happen from one area to another), or from vertical separation of the same section, by thrust faulting. In this event, the comparison of one average resistivity and anisotropy is not sufficient for correlation since identical sections saturated with different solutions will have identical anisotropies but different average longitudinal and transverse resistivities. That is, from the well known Archie's Law, relationship $R_0 = a\frac{R_w}{\phi_m}$ (Keller and Frischknecht, 1966), where R_0 is the rock resistivity, R_w is the formation water resistivity, ϕ is the porosity, and a and m are constants, to a first approximation the resistivity of a rock will vary directly with changes in the resistivity of the formation water. Accordingly, both average longitudinal and transverse resistivities will vary in proportion to the ratio R_{w2}/R_{w1}, but the anisotropy will remain constant. Thus, when two similar lithologic sections are saturated with different formation waters, the basic shapes of the frequency polygons of both sections will be similar; however, the curves will be separated laterally on the abscissa, provided that a logarithmic resistivity scale is used.

CONCLUSIONS

Evidence from the electric resistivity log of the Rattlesnake Hills unit 1 well shows that:

1. A simplified transverse resistance log indicates three major geoelectric intervals.
2. Comparison of average resistivities and anisotropies indicates that each interval is distinctive.
3. The shape of frequency polygons definitely indicates upper and lower geoelectric intervals, separated by a central geoelectric interval; the central interval lacks the high resistivity of the upper and lower intervals.

Significant lithologic differences probably exist between the major adjacent geoelectric intervals.

Similar treatment of additional borehole data may enable correlation of major geoelectric intervals over such large areas as the Columbia River Plateaus (where most of the exposed rocks are widespread flood-type basalts). Even though correlation of individual flows may not be possible, thick sequences of flows and interbeds could be correlated.

REFERENCES CITED

Keller, G. V., 1966, Statistical studies of electrical well logs, *in* Seventh annual logging symposium: Soc. Prof. Well Log Analysts, p. AA1–19.

Keller, G. V., and Frischknecht, F. C., 1966, Electrical methods in geophysical prospecting: New York, Pergamon Press, 519 p.

King, P. B., 1959, The evolution of North America: Princeton Univ. Press, 190 p.

Pirson, S. J., 1963, Handbook of well log analysis: Englewood Cliffs, N.J., Prentice-Hall, Inc., 326 p.

Raymond, J. R., and Tillson, D. D., 1968, Evaluation of a thick basalt sequence in south central Washington: U.S. Atomic Energy Comm. Research and Devel. Rept., BNWL–776, 126 p.

Zohdy, A. A. R., 1965, The auxiliary point method of electrical sounding interpretation, and its relationship to the Dar Zarrouk parameters: Geophysics, v. 30, no. 4, p. 644–660.

Jour. Research U.S. Geol. Survey
Vol. 3, No. 6, Nov.–Dec. 1975, p. 671–689

STRUCTURE AND PALEOZOIC STRATIGRAPHY OF A COMPLEX OF THRUST PLATES IN THE FISH CREEK RESERVOIR AREA, SOUTH-CENTRAL IDAHO

By BETTY SKIPP and WAYNE E. HALL

Denver, Colo., Menlo Park, Calif.

Abstract.—Permian, Pennsylvanian, Mississippian, Devonian, and Silurian marine rocks of diverse facies are brought together in a complex of six thrust sheets in the Fish Creek Reservoir area on the north edge of the Snake River Plain, Idaho. The lowest structural element, the parautochthon, is made of more than 450 m (1,500 ft) of folded and faulted Devonian miogeosynclinal carbonate rocks present in a 6.5-km^2 (2.5-mi^2) window. Along the east margin of the window, a sliver of continental margin transitional carbonate rocks of Early Devonian and Late Silurian age assigned to the Roberts Mountains Formation is thrust over the miogeosynclinal rocks. The window of middle Paleozoic rocks is overridden along the Fish Creek thrust fault by the flysch facies of the Copper Basin Formation, a turbidite–submarine-fan sequence more than 1,000 m (3,300 ft) thick, of Mississippian age. About 4.8 km (3 mi) southwest of the window, about 100 m (300 ft) of deepwater siliceous oceanic facies clastic rocks are exposed, which are assigned with question to the Milligen(?) Formation of Devonian age. These clastic rocks are interpreted to be thrust over the Copper Basin Formation. The highest structural elements are sequences more than 610 m (2,000 ft) thick of interbedded sandy and conglomeratic limestones, quartzites, and conglomerates and interbedded siltstones and argillites of the Wood River Formation of Middle Pennsylvanian to Early Permian age. The Wood River Formation is in thrust contact with the Milligen(?) Formation in the southwest part of the mapped area and with Copper Basin Formation along the west side of Fish Creek Reservoir. All the thrust sheets have moved eastward. The minimum distance moved is estimated from sedimentation models and facies reconstructions to range from perhaps several kilometres for the allochthon of the Roberts Mountains Formation to 48 km (30 mi) for the Milligen(?) Formation allochthon. The principal period of thrusting was post-Early Permian (post-Wood River Formation) and pre-Eocene (pre-Challis Volcanics) and is of probable Sevier age. Middle Paleozoic rocks of the Milligen and Roberts Mountains Formations, however, also may have been involved in an earlier period of thrusting of latest Devonian to earliest Mississippian age related to the Antler orogeny. The thrust sheets were deformed into a northwest-trending dome in late Mesozoic time and were broken by basin-range faults during the Tertiary.

Fish Creek Reservoir is on the north edge of the Snake River Plain, 8 km (5 mi) north of U.S. Highway 93A between the town of Carey and the Craters of the Moon National Monument in Blaine County, south-central Idaho (fig. 1). Three facies of Devonian rocks (shelf, shelf margin, and ocean basin), flysch deposits of the Mississippian Copper Basin Formation (lower part), and continental basin deposits of the Pennsylvanian and Permian Wood River Formation were brought together by a complex of thrust faults in an area of 65 km^2 (25 mi^2) in the vicinity of the reservoir. The six structural units in the area, in ascending order, are the parautochthon (1) which consists of the Devonian shelf carbonates of the Fish Creek Reservoir window, and the following five allochthonous plates: (2) small patches of the transitional facies continental margin deposits of the Roberts Mountains Formation of Late Silurian and Early Devonian age, (3) the turbidite–submarine-fan sequence of the Copper Basin Formation of Mississippian age, (4) deepwater transitional siliceous oceanic clastics of the Devonian Milligen(?) Formation, (5) calcareous siltstones and argillites of the Permian part of the Wood River Formation, and (6) clastic limestones, quartzites, and conglomerates of the Pennsylvanian part of the Wood River Formation (fig. 2). Some of the allochthonous plates are absent locally.

The stratigraphy of each structural unit is described, but the Devonian and Silurian rocks of the Fish Creek Reservoir window, inasmuch as they are dealt with in detail in a companion paper by Skipp and Sandberg (1975), are only briefly mentioned here. The Permian, Pennsylvanian, and Mississippian rocks of the upper plates are discussed in detail, and the overlying Cenozoic volcanic rocks are briefly described.

All Paleozoic rocks in the area, with the possible exception of the miogeosynclinal Devonian rocks, are allochthonous, having moved generally eastward or northeastward on a complex of thrust faults that are both folded and faulted. The direction and amount of translation of the thrust faults in the Fish Creek area

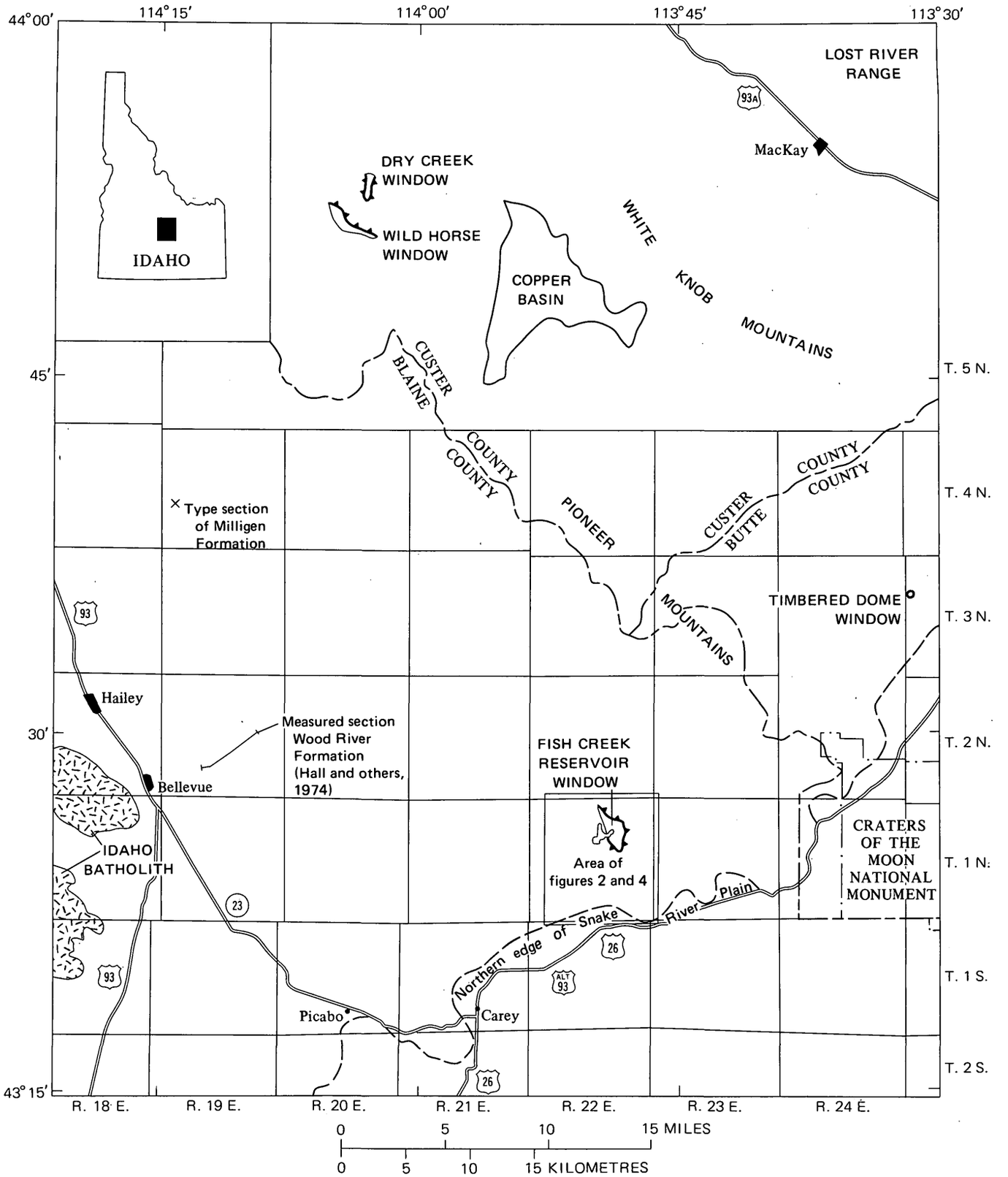

FIGURE 1.—Index map of central Idaho showing location of Fish Creek Reservoir window and map area.

can be estimated only from very generalized facies reconstructions and sedimentation models. No autochthonous Paleozoic rocks with which the rocks in the Fish Creek area can be correlated are exposed to the west. The Wood River and Milligen Formations in the Hailey-Bellevue area are allochthonous, and the area

west of these exposures is underlain by the Idaho batholith (W. E. Hall, unpub. data, 1974; fig. 1).

Discussions of the structure of the parautochthon and overlying thrust plates accompany the stratigraphic descriptions. These are followed by a brief review of ages of thrusting and descriptions of structural features.

PARAUTOCHTHON

Stratigraphy

The lowest structural unit consists of about 457 m (1,500 ft) of miogeosynclinal shelf carbonate rocks of Middle and Late Devonian age that are exposed on the north and east sides of Fish Creek Reservoir (figs. 2, 3).

The Carey Dolomite of Early and Middle Devonian age (Skipp and Sandberg, 1975) is the oldest formation of the shelf sequence exposed in the window. It consists of 148 m (485 ft) or more of light- to medium-gray, mostly clean, finely crystalline laminated dolomite which was deposited in a dominantly intertidal to supratidal marine environment. The Carey Dolomite is overlain disconformably by the Jefferson Formation of Middle and Late Devonian age. The Jefferson consists of about 245 m (800 ft) of dolomite, dolomite conglomerate, and minor sandstone deposited in a fluctuating subtidal to intertidal marine environment. The Jefferson Formation is overlain, locally conformably but regionally unconformably, by the Picabo Formation of Late Devonian age (Skipp and Sandberg, 1975). The Picabo consists of 58 m (190 ft) or more of gray fine-grained quartzose and calcareous sandstone, light-gray to pale-yellowish-brown sandy dolomite conglomerate, and minor gray fine-grained dolomite. All the dolomite clasts in the conglomerate probably were derived from beds coextensive with the underlying Jefferson Formation and Carey Dolomite. The well-bedded sandstones and conglomerates of the Picabo were deposited in a relatively shallow subtidal marine environment beyond the reach of major shore currents. Westward-dipping imbrication of many pebbles indicates at least local eastward-flowing currents and a possible western source for the dolomite clasts of the Picabo Formation. Thus, Devonian miogeosynclinal rocks probably extended west of the Fish Creek Reservoir area, perhaps 8–16 km (5–10 mi). The conglomerates of the Picabo probably are associated with an early phase of the Antler orogeny to the west (Skipp and Sandberg, 1975).

Structure

The rocks of the parautochthon are both folded and faulted (figs. 2, 3). A series of steep faults of relatively small displacement trend east, southeast, and north and apparently are confined to the rocks of the parautochthon and the Roberts Mountains Formation beneath the Fish Creek thrust. Fracture cleavage trending N. 70° E. is present in the Carey Dolomite beneath the Fish Creek thrust in the northeast corner of the window (fig. 4), and tectonic breccias were noted in several places in the Carey Dolomite and Jefferson Formation. Beds in the parautochthon are gently inclined to vertical, and have an average dip of about 35°.

Much of the folding is probably the result of doming that postdates thrusting (see fig. 5 and "Folds" section), but the presence of both discordant northeast-trending fracture cleavage and normal faulting, which apparently is confined to the window, suggests an earlier period of folding and possible detachment of the rocks of the parautochthon itself. Such a zone of detachment is postulated on the cross sections (fig. 5). Eastward movement of these rocks over any great distance is unlikely, as this area is one of the westernmost exposures of Middle Devonian miogeosynclinal rocks in Idaho (Skipp and Sandberg, 1972, 1975).

ALLOCHTHON OF THE ROBERTS MOUNTAINS FORMATION

Stratigraphy

The Roberts Mountains Formation in the Fish Creek area is a sequence more than 200 m (660 ft) thick of Upper Silurian and Lower Devonian medium-gray fossiliferous reef limestone, platy calcareous and dolomitic siltstone, and limestone phenoplast conglomerate exposed in an area of less than 1.3 km^2 (0.5 mi^2) on the east side of the window (fig. 3). The rock types are similar to those of the type Roberts Mountains Formation in Nevada, described by Winterer and Murphy (1960), where the facies have been interpreted to represent the edge of the middle Paleozoic continental shelf (Berry and Boucot, 1970; Johnson and others, 1973). Because the Devonian Picabo Formation of the miogeosynclinal sequence contains clasts of dolomite that may have been derived from western continental shelf sequences as much as 8–16 km (5–10 mi) distant, the site of deposition of the Roberts Mountains Formation is postulated to have been at least that far west of the Fish Creek Reservoir area.

Structure

The Roberts Mountains Formation is thrust over the Carey Dolomite and Jefferson Formation, both part of the parautochthon. The thrust contact with the Carey Dolomite is shown in figure 6. The top of the Roberts Mountains Formation is cut out by the Fish Creek thrust at the base of the Copper Basin Formation.

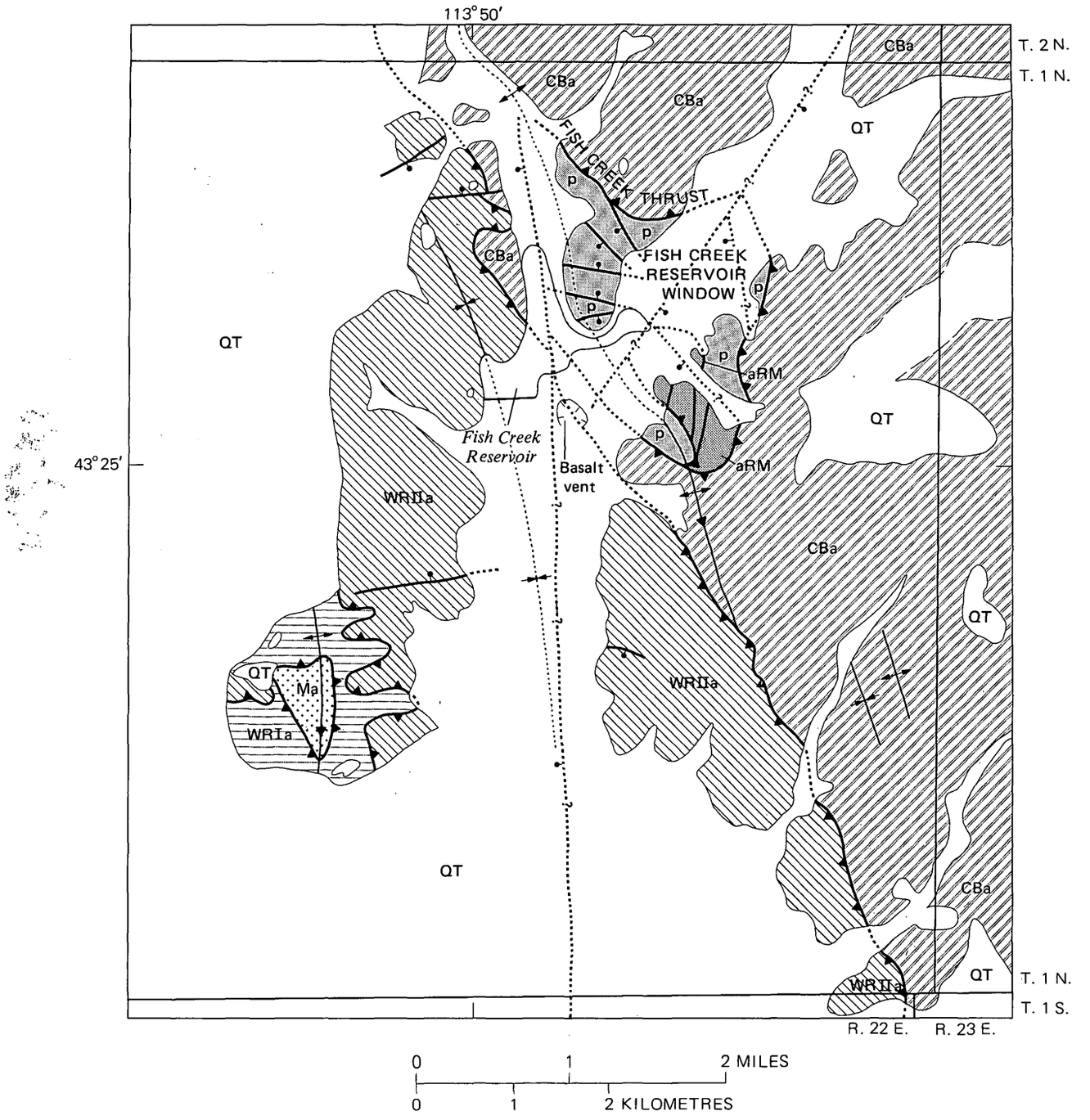

FIGURE 2.—Structure map of the Fish Creek Reservoir area.

The rocks of the Roberts Mountains Formation are both folded and faulted, and are more complexly deformed than the underlying Carey Dolomite. Within the small area of outcrop in the southeast corner of the window, the beds dip from 15° N. to 55° SE. (fig. 4). Some north-trending vertical beds are present but not shown. The underlying Carey is folded into a symmetrical north-northwest-trending anticline with limbs dipping not more than 40°.

The Roberts Mountains Formation, therefore, has been thrust from its western depositional site on the Devonian continental edge to its present position above younger Devonian continental shelf miogeosynclinal rocks. The distance involved is estimated to have been at least 8–16 km (5–10 mi). However, in the Wildhorse window to the northwest (fig. 1), Dover and Ross (1975) considered the Roberts Mountains Formation possibly autochthonous.

EXPLANATION FOR FIGURE 2

QT — Quaternary and Tertiary undivided

WRIIa — Wood River II allochthon

WRIa — Wood River I allochthon

Mâ — Milligen(?) allochthon

CBa — Copper Basin allochthon

aRM — Allochton of the Roberts Mountains Formation

p — Parautochthon

—?— Thrust fault – Sawteeth on upper plate. Dotted where covered; queried where inferred

Steep fault – Bar and ball on downthrown side. Dotted where covered; queried where inferred

Crestline of anticline – Showing direction of plunge and direction of dip of limbs. Dotted where concealed

Troughline of syncline – Showing direction of dip of limbs. Dotted where concealed

COPPER BASIN ALLOCHTHON

Stratigraphy

The Copper Basin Formation was the name given by Ross (1962) to a thick sequence of clastic rocks exposed in the upper part of Star Hope Creek at the southern edge of Copper Basin (fig. 1). The formation was raised to group rank and subdivided into six formations, five with new names, by Paull, Wolbrink, Volkmann, and Grover (1972). In ascending order, the six formations are the Milligen Formation, Drummond Mine Limestone, Scorpion Mountain Formation, Muldoon Canyon Formation, Brockie Lake Conglomerate, and Iron Bog Creek Formation. Type sections for the formations were designated in the central Pioneer Mountains west and south of Copper Basin (fig. 1; Paull and others, 1972, p. 1374).

The term Milligen Formation as used by Paull, Wolbrink, Volkmann, and Grover (1972) refers to rocks which correlate in part with Lower Mississippian beds previously given this name in the Pioneer Mountains and Lost River Range (Ross, 1934; Sandberg and others, 1967; Sandberg and Mapel, 1967); these rocks termed Milligen Formation do not correlate with the Devonian Milligen Formation of the type locality in the Wood River area, with which dark-gray siliceous argillites in the southwest corner of the map area (fig. 4) are tentatively correlated. (See Sandberg and others, 1975.) In its type locality, the Copper Basin Group of Paull, Wolbrink, Volkmann, and Grover (1972) consists of more than 5,500 m (18,000 ft) of argillite, sandstone, conglomerate, and limestone. Neither the base nor the top of the group is exposed, and stratigraphic relations are speculative.

In the Fish Creek Reservoir area, we have not subdivided the Copper Basin into the formations of Paull, Wolbrink, Volkmann, and Grover (1972), but have called this sequence the lower part of the Copper Basin Formation in the sense of Ross (1962). Probable correlation of these rocks with parts of the Milligen Formation, Drummond Mine Limestone, and Scorpion Mountain Formation of Paull, Wolbrink, Volkmann, and Grover (1972) is indicated. The sequence ranges in thickness from 0 to more than 1,200 m (4,000 ft) in the Fish Creek area.

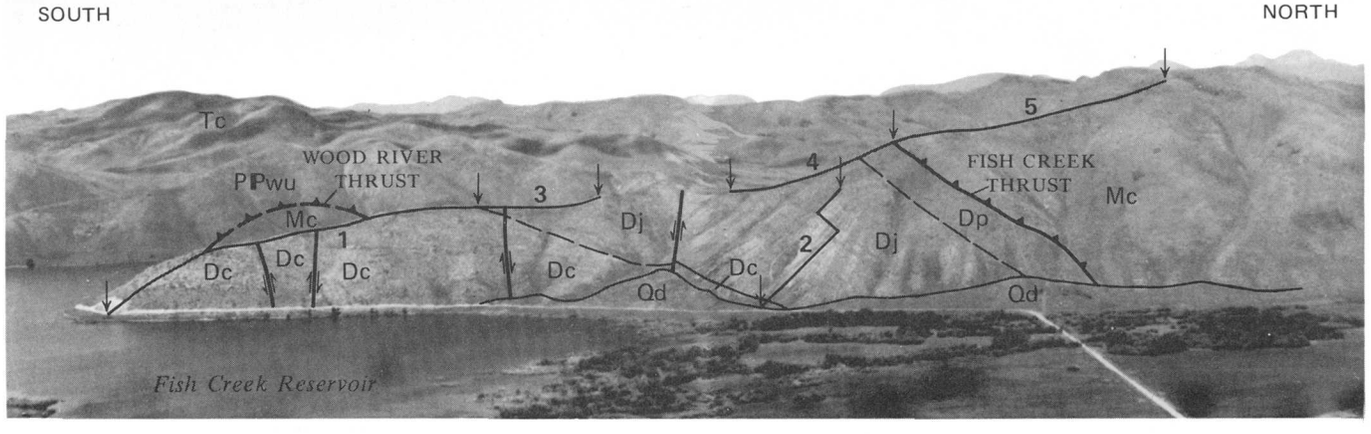

FIGURE 3.—View of east side of promontory at north end of Fish Creek Reservoir showing location of measured sections 1 through 5, distribution of some map units, the trace of the Fish Creek thrust, and a segment of the trace of the Wood River thrust between the Wood River and Copper Basin Formations. Arrows denote ends of measured sections. (See also Skipp and Sandberg, 1975.) Dc, Carey Dolomite; Dj, Jefferson Formation; Dp, Picabo Formation; Mc, Copper Basin Formation; PPwu, upper part of Wood River Formation; Tc, Challis Volcanics; Qd, colluvial, alluvial, and lake deposits.

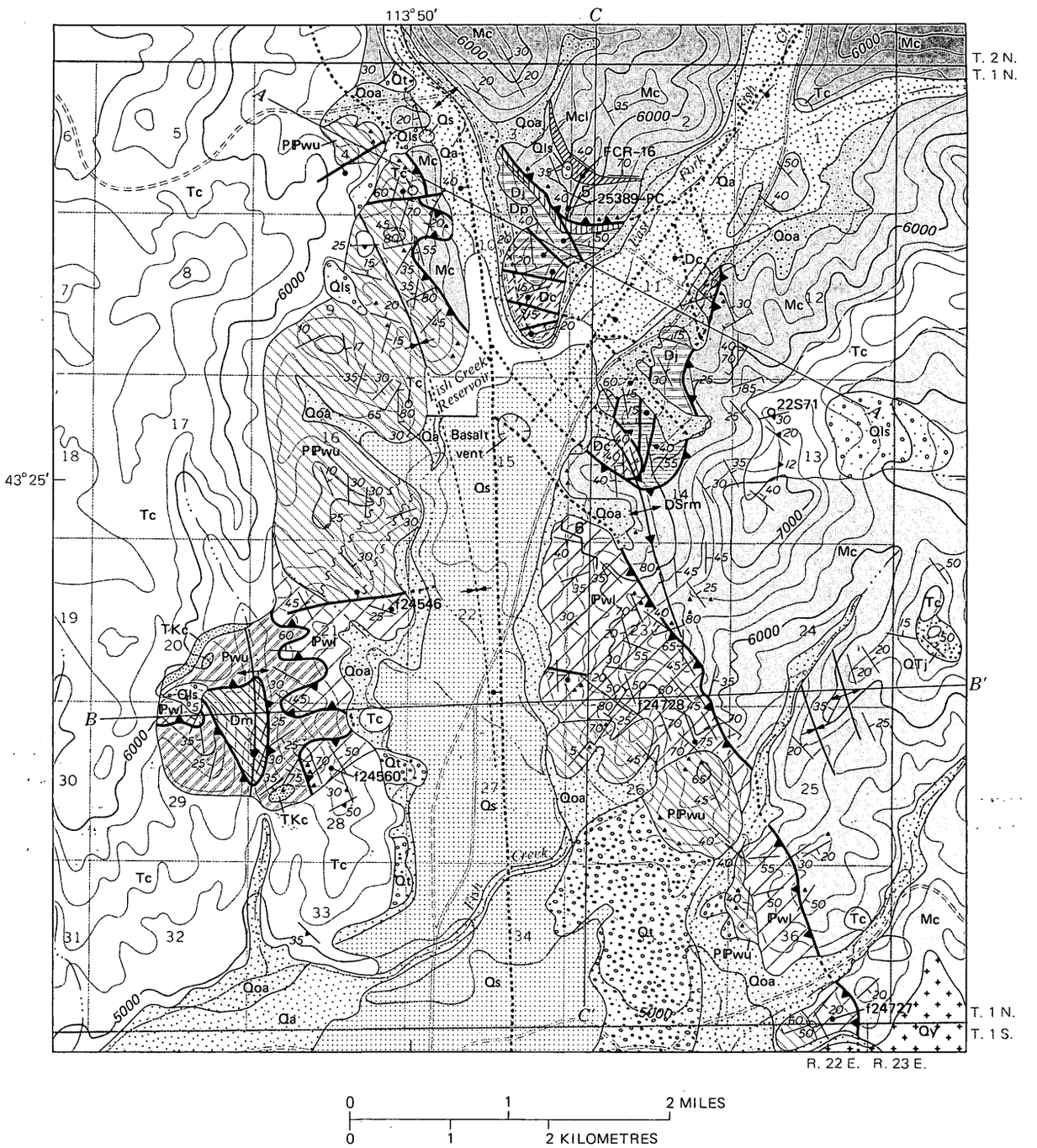

FIGURE 4.—Geologic map of Fish Creek Reservoir area, Blaine County, Idaho. Sections shown in figure 5. Base from U.S. Geological Survey Idaho Falls topographic quadrangle, scale 1:250,000, 1955; location of section lines approximate.

Description of units shown in figure 4

Alluvium (Quaternary): Sand and gravel; in some places forms thin cover over basalt; at Fish Creek Reservoir includes lake deposits.

Landslide deposits (Quaternary): Largely the result of failure of incompetent tuff beds in Challis Volcanics.

Younger basalt (Quaternary): Fresh black basalt; undissected. Contemporaneous with flows associated with the Great Rift zone.

Snake River Group (Quaternary): Dark-gray dictytaxitic basalt extruded from vent just southeast of dam. Basalt is dissected to a depth of about 10 m (33 ft) at dam.

Older alluvium and colluvium (Quaternary): Sand and gravel composed largely of Paleozoic detritus; covered by basalt in the Fish Creek drainage; includes some young alluvium and colluvium along present drainages.

Terrace deposits (Quaternary): Gravels about 10 m (33 ft) above present streams on extensive surfaces inclined toward the plain; gravels near mouth of Fish Creek contain abundant Challis detritus; whereas adjacent older alluvium does not.

Jasperoid (Quaternary or Tertiary): Secondarily silicified upper Paleozoic limestone and argillite.

Challis Volcanics (Eocene): Gray, black, and brown, reddish-brown-weathering, largely rhyolitic welded

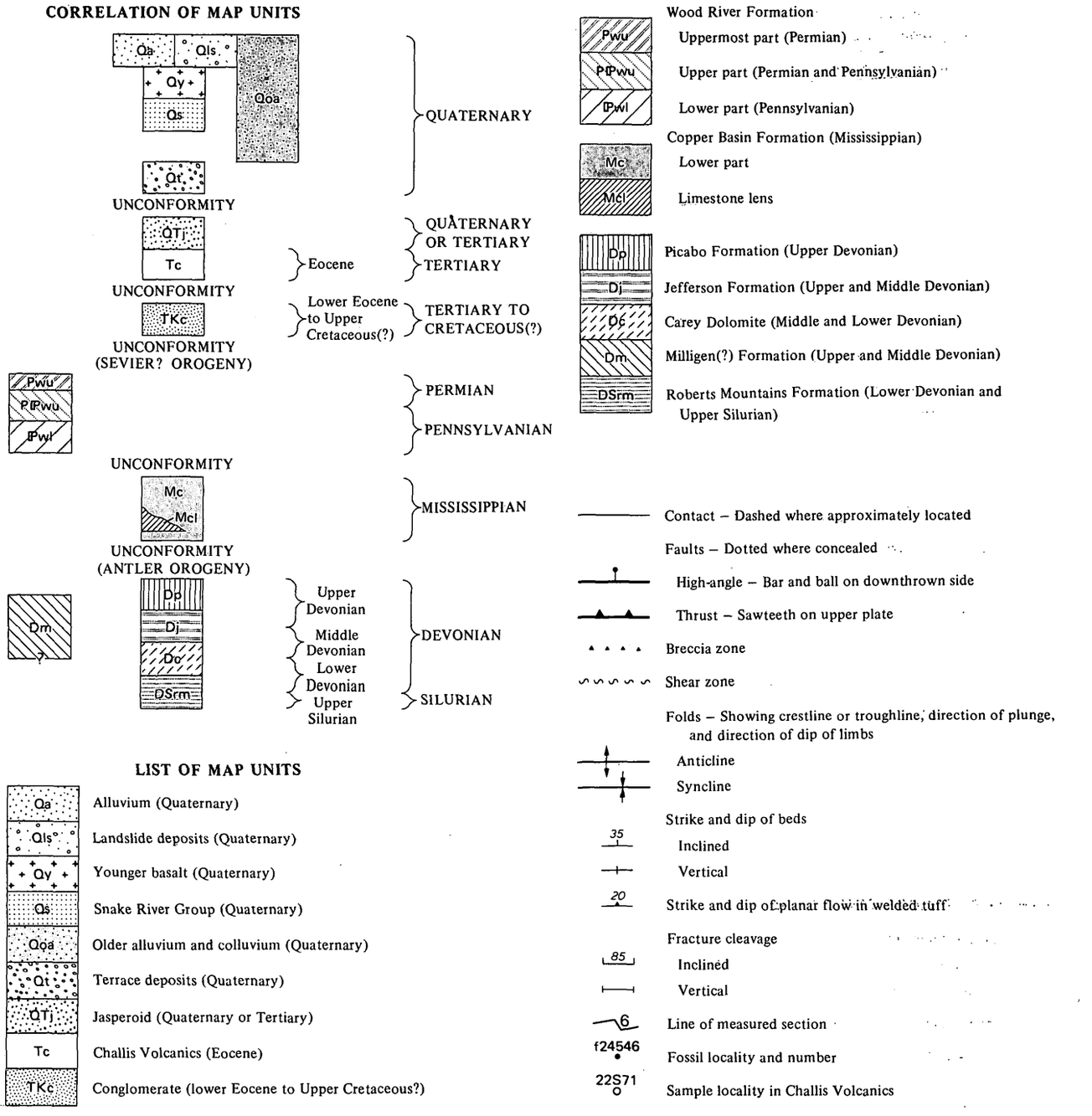

Description of units shown in figure 4—Continued

and nonwelded ash-flow tuffs, vitrophyres, some air-fall tuff, and minor lava flows. Forms ledges.

Conglomerate (lower Eocene to Upper Cretaceous?): Pebble to boulder conglomerate consisting of rounded clasts of locally derived Paleozoic quartzite, argillite, conglomerate, and limestone. 0–6 m (0–20 ft) thick. Erosional remnant of pre-Challis alluvial fan; brecciated locally; forms slope and resistant ledges.

Wood River Formation:

Uppermost part (Permian): Medium-gray limy siltstone, varicolored and laminated in places, brown-weathering dolomitic siltstone, dark-gray argillite, light-brown fine-grained quartzite, and minor gray silty thin-bedded limestone. About 180 m (600 ft) thick. Top and base faulted; forms steep slopes.

Upper part (Permian and Pennsylvanian): Very light gray to medium-dark-gray fine-grained siliceous sandstone and minor granule to pebble conglomerate and sandy limestone, medium- to thick-bedded, locally laminated, brecciated in places; conglomerate clasts are dominantly chert and quartzite. Several hundred metres thick. Top eroded; base of upper part gradational with lower part; forms ledges and steep slopes.

Lower part (Pennsylvanian): Medium-gray to medium-dark-gray sandy and conglomeratic limestone and calcareous sandstone, locally graded and laminated, medium-bedded; conglomerate clasts, granule to pebble size, are chert, quartzite, limestone, and argillite; interbedded with minor pale-red-purple calcareous siltstone and shale and siliceous sandstone; weathers gray, light brown, and reddish brown. More than 207 m (680 ft) thick. Top gradational; base faulted; forms ledges and steep slopes.

Copper Basin Formation (Mississippian):

Lower part: Very light gray to medium-dark-gray interbedded quartzite, granule to cobble conglomerate, argillite, and limestone (see limestone lens). Quartzite is fine grained to conglomeratic, noncalcareous, laminated and graded in places, medium bedded; conglomerate clasts are chert, quartzite, and argillite; quartzite and conglomerate weather gray and moderate brown, but argillite weathers mostly light gray. More than 900 m (3,000 ft) thick. Top eroded; base faulted; forms ledges and cliffs.

Description of units shown in figure 4—Continued

Limestone lens: Interbedded dark-gray to pale-red and moderate-yellowish-brown fine-grained silty and sandy laminated limestone and gray to light-brown calcareous quartzose sandstone, thin-bedded. 0 to about 34 m (0–110 ft) thick. Forms slope.

Picabo Formation (Upper Devonian): Interbedded medium-light-gray to pale-yellowish-brown fine-grained laminated dolomitic quartzose sandstone and thick-bedded sandy dolomite conglomerate; dolomite clasts rounded and as much as 125 mm in diameter. More than 57 m (189+ ft) thick. Top faulted; forms ledges and steep slopes.

Jefferson Formation (Upper and Middle Devonian): Light-gray to grayish-black and pale-yellowish-brown finely to coarsely crystalline dolomite, sandy and silty in places, locally laminated; interbedded with minor dolomite breccia, sandy dolomite conglomerate, and quartzose sandstone near the base. About 244 m (802 ft) thick. Forms ledges and steep slopes.

Carey Dolomite (Middle and Lower Devonian): Light-gray to medium-dark-gray finely crystalline to aphanitic dolomite, laminated; sand and silt rare; some dolomite granule to pebble conglomerate; medium bedded. More than 148 m (485+ ft) thick. Base not exposed; forms steplike ledges.

Milligen(?) Formation (Upper and Middle Devonian): Dark-gray siliceous argillite, fine-grained quartzite, and black chert, medium-bedded, sheared; fracture cleavage present in places. More than 90 m (300+ ft) thick. Top faulted; base not exposed; forms steep slopes with scattered ledges.

Roberts Mountains Formation (Lower Devonian and Upper Silurian): Medium-gray to medium-dark-gray fossiliferous medium-bedded limestone and phenoplast conglomerate interbedded with gray, grayish-orange, and grayish-red platy calcareous siltstone and silty limestone. More than 140 m (450+ ft) thick. Top faulted; base faulted; forms ridge.

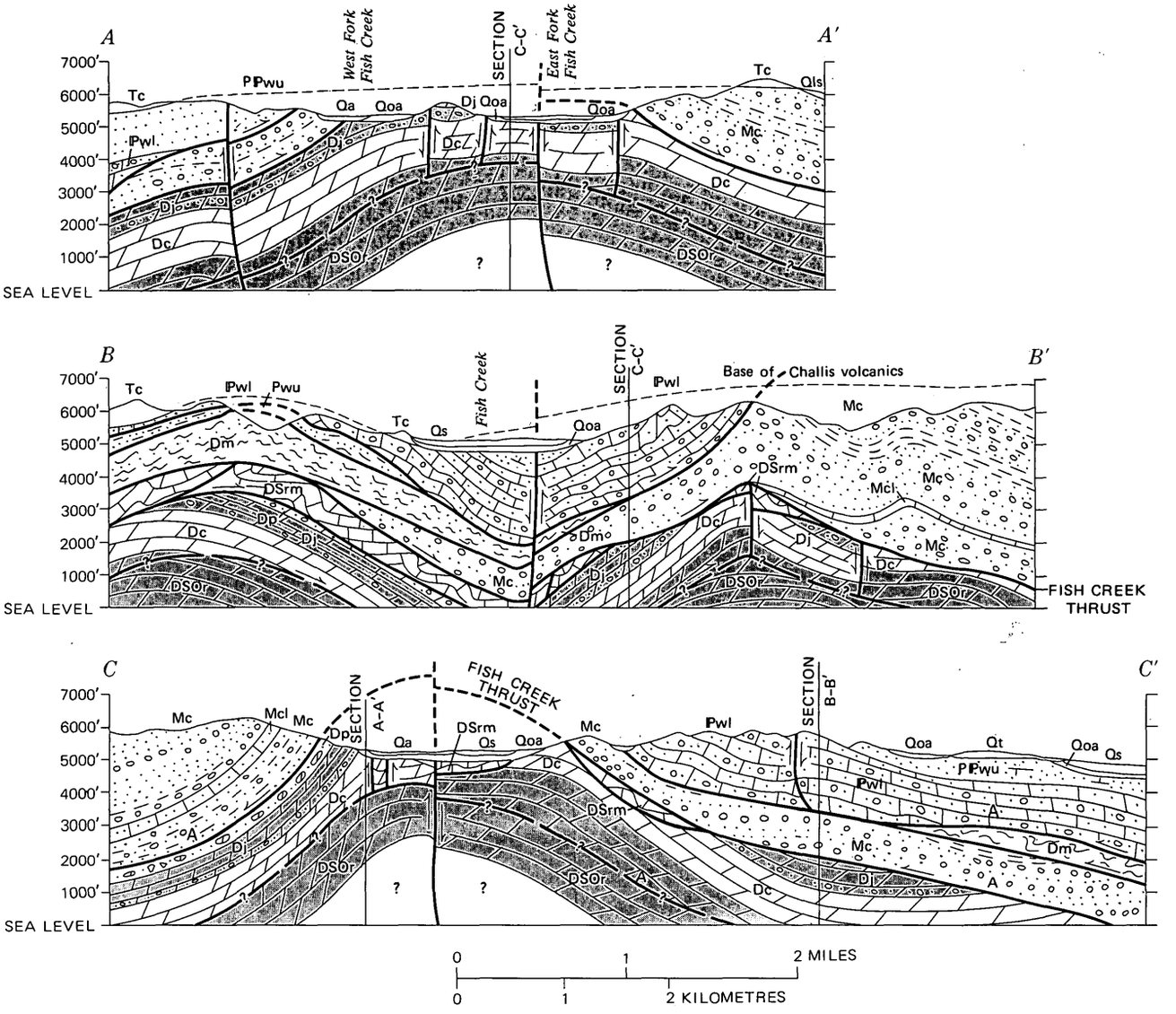

FIGURE 5.—Cross sections, Fish Creek Reservoir area, Blaine County, Idaho. Lines of sections and correlation and ages of units shown in figure 4. Qa, alluvium; Qls, landslide deposits; Qoa, older alluvium and colluvium; Qs, Snake River Group; Qt, terrace deposits; Tc, Challis Volcanics. Wood River Formation: Pwu uppermost part; PPwu, upper part; Pwl, lower part. Copper Basin Formation: Mc, lower part; Mcl, limestone lens; Dp, Picabo Formation; Dj, Jefferson Formation; Dc, Carey Dolomite; Dm, Milligen(?) Formation; DSrm, Roberts Mountains Formation; DSOr, Devonian, Silurian, and Ordovician rocks undivided. Arrows indicate relative direction of movement on faults; A, movement away from observer.

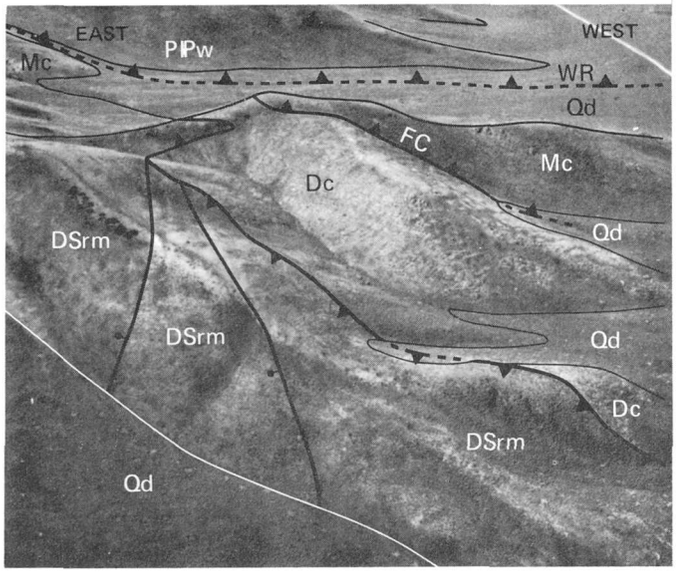

FIGURE 6.—Oblique aerial photograph, looking south, of southwest corner of Fish Creek Reservoir window, showing trace of Fish Creek thrust (FC) between the Copper Basin Formation (Mc) and Carey Dolomite (Dc), and trace of the thrust which brings Roberts Mountains Formation (DSrm) over Carey Dolomite. Wood River Formation (PPw) exposed on hills in background. Wood River Thrust (WR), which separates Wood River and Copper Basin Formations, is buried beneath Quaternary alluvial and colluvial deposits (Qd).

The Copper Basin Formation is a complex sequence of turbidites, interturbidites, and submarine fan deposits that Poole (1974) recognized and assigned to the flysch deposits of the Carboniferous Antler foreland basin.

Lithology and thickness

In the Fish Creek area, quartzite, chert, and quartzite conglomerate constitute the major lithologies of the Copper Basin Formation, which also contains lesser amounts of argillite and minor silty and sandy limestone.

A partial section (figs. 3 and 4, measured section 5) of the formation, 372 m (1,230 ft) thick, was measured on the ridge above the thrust fault contact with the Upper Devonian Picabo Formation (fig. 7). About 50 percent of the section is exposed, consisting of more quartzite than argillite in beds generally 0.3–0.9 m (1–3 ft) thick. The quartzite is light gray to medium dark gray and weathers gray and brown. It is fine grained to conglomeratic, laminated and graded in places; load casts and scour-and-fill structures are common. Laminations are the result of alternating concentrations of dark chert and light quartz grains. Within 1 m (3 ft) of the thrust contact with the Picabo Formation, the laminated quartzites are iron stained and brecciated and weather moderate brown. Chert-granule conglomerate beds are present in several positions (fig. 7). The chert is medium gray, grayish black, and some yellowish brown; granules are subangular to subrounded. The matrix consists of rounded quartz sand grains. The conglomerates are moderately well sorted, and some beds are graded. Poorly exposed interbedded argillite and siltstone are mostly light gray, but some are grayish black, brown, and pale red. Weathered surfaces are light colored. The argillite and siltstone are generally thin bedded, and some are laminated. Meandering trails identical to those shown by Ketner (1970, p. D20, fig. 3) from Mississippian turbidites in northern Nevada that belong to Seilacher's (1964) *Nereites* facies are common on argillite bedding surfaces. Flattened coiled ammonoid impressions are also present, and yellow-brown-weathering impressions of stems or twigs are found in both the argillites and quartzites.

Approximately 34 m (110 ft) of fine-grained, silty and sandy limestone and minor interbedded calcareous sandstone and quartzite is poorly exposed below a cliff of massive conglomerate at the top of the measured section (fig. 7). The limestone is dark gray, pale red, and yellowish brown and weathers dark yellow orange and pale yellowish brown. The limestone contains meandering trails and calcareous sponge spicules. A 1.5-m (5-ft) bed of fine-grained medium-gray to light-brown calcareous quartzose sandstone and dark-gray laminated quartzite is 6 m (20 ft) above the base of the unit. Limestone float from this unit contained conodonts (collection FCR–15) and coiled imprints of ammonoids. The massive conglomerate directly above the limestone is gray and noncalcareous, and weathers reddish brown. Clasts are rounded pebbles of black, olive-gray, and yellowish-gray chert as much as 5 cm (2 in) in diameter, and black angular fragments of argillite. Holes in the conglomerate probably resulted from solution of carbonate fragments.

In the eastern part of the map area (fig. 4), more than 900 m (3,000 ft) of Copper Basin Formation crops out stratigraphically above the limestone lens of the measured section. Quartzite and lesser amounts of interbedded conglomerate, breccia, and argillite compose this interval. The quartzites are very light to medium light gray and weather yellowish gray to moderate yellow brown. Bedding ranges from medium to massive and outcrops form ledges. Well-developed fracture cleavage makes bedding difficult to ascertain in many places. The quartzites are made up of quartz, chert, and lithic fragments in a cryptocrystalline quartz matrix.

Massive chert- and quartzite-pebble conglomerates

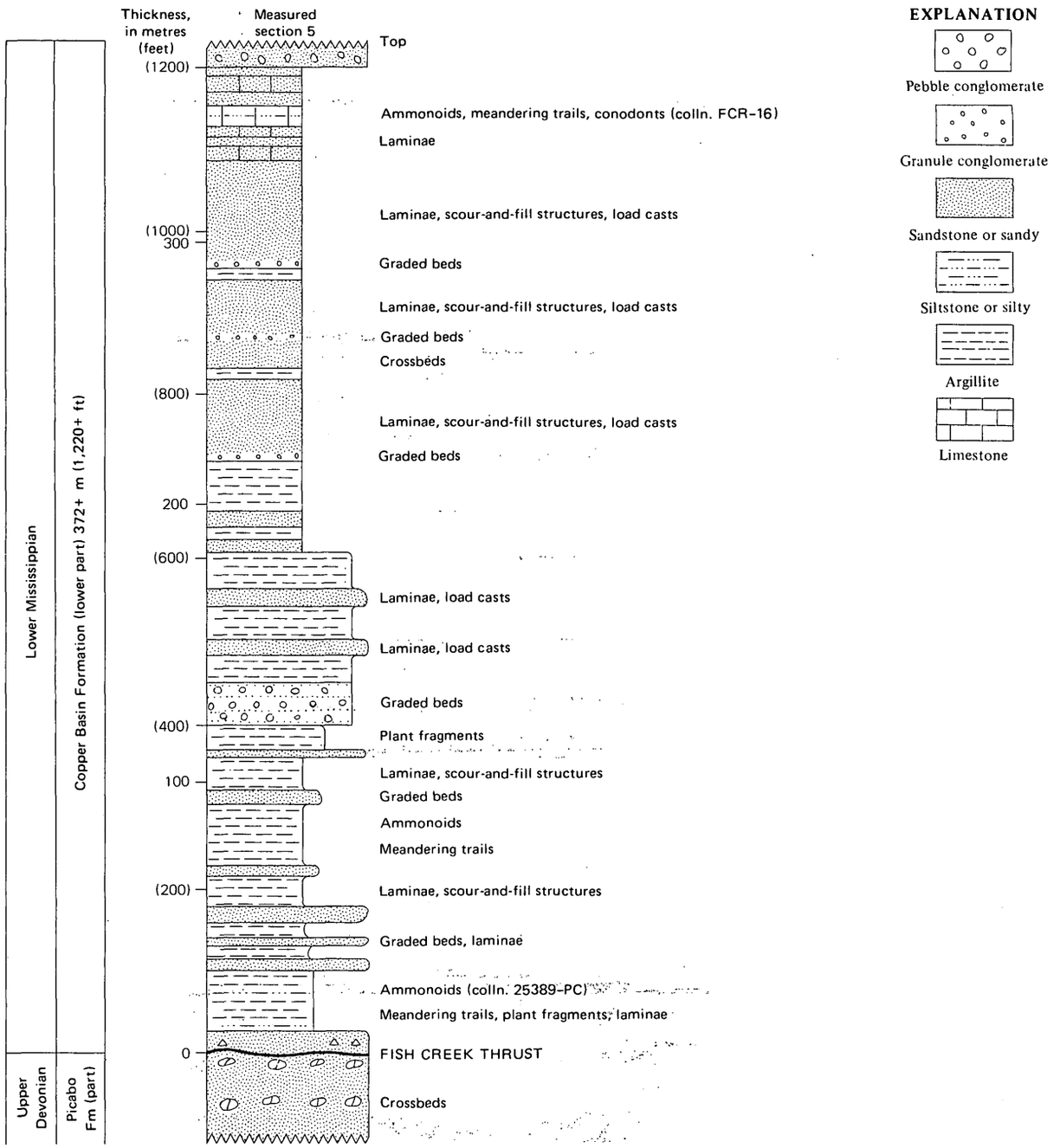

FIGURE 7.—Measured section 5 (see figs. 3, 4) of lower part of Copper Basin Formation in NE¼ sec. 10 and along the line between SW¼ sec. 2 and the SE¼ sec. 3 (approx.) T. 1 N., R. 22 E., Blaine County, Idaho.

form ledges with the quartzites. Many of the conglomerates are brecciated. Quartzite clasts as much as 15 cm (6 in) in diameter were noted in places. Paull, Wolbrink, Volkmann, and Grover (1972, p. 1390) noted quartzite clasts as much as 35 cm (14 in) in diameter at similar stratigraphic levels in their type Scorpion Mountain Formation at Copper Basin about 40 km (25 mi) to the north.

The massive quartzites and conglomerates, the graded and laminated quartzites, the granule conglomerates, the impure limestones, and the spicular limestones and argillites with abundant meandering trails together make up a complex sequence of turbidites, both proximal and distal, and interturbidites composing flysch deposits of the Antler foreland basin (Poole, 1974). The Copper Basin Formation in the Fish Creek area is generally finer grained than that in the Copper Basin area. Graded and laminated

quartzites and granule conglomerates, which make up much of the sequence, probably are turbidites generally farther from the source than the massive conglomerates and quartzites described by Paull, Wolbrink, Volkmann, and Grover (1972) to the north.

The formation has a minimum thickness of approximately 1,200 m (4,000 ft) east of the Fish Creek Reservoir window. It has been thinned tectonically and by erosion which predated the Fish Creek thrust (see discussion of structure of Wood River II allochthon) to less than 300 m (1,000 ft) on the south and west sides of the window between the Fish Creek thrust and the overlying Wood River allochthon (figs. 3, 6). This thinning is projected westward to a zero edge on cross section *B–B′* (fig. 5).

Age and correlation

Recent paleontologic and stratigraphic evidence indicates that the Copper Basin Formation is probably entirely of Mississippian age. Locally, some latest Devonian rocks may be present at the base, and the possibility remains that some Lower Pennsylvanian beds are present at the top.

The Copper Basin Formation, when described and named, was recognized to be in large part of Mississippian age (Ross, 1960, 1962; Nelson and Ross, 1969b), but was assigned an Early Mississippian to Early Permian age range. Doubt was cast on the Permian age designation by Nelson and Ross (1969a) when they noted that "no paleontologic or stratigraphic evidence has been found to indicate that any of the * * * formation is younger than Pennsylvanian." Paull, Wolbrink, Volkmann, and Grover (1972) assigned an Early(?) Mississippian to Middle(?) Pennsylvanian age range to the Copper Basin Group, but emphasized the sparsity of fossils.

Recent faunal evidence—conodonts determined by C. A. Sandberg and calcareous Foraminifera determined by Betty Skipp from samples collected by R. A. Paull (Geology Dept., University of Wisconsin at Milwaukee) and Skipp, and ammonoids identified by Mackenzie Gordon, Jr., from samples collected by W. E. Hall and Paull—suggests that the Copper Basin ranges in age from Early to Late Mississippian. Calcareous Foraminifera and conodonts of Early Mississippian (Kinderhookian) age were identified from beds just northeast of the Fish Creek area that were correlated by Paull with his Drummond Mine Limestone. A conodont fauna (colln. FCR–15, fig. 7) recovered from float of the limestone lens in the measured section about 304 m (1,100 ft) stratigraphically above the Fish Creek thrust is of Early Mississippian (Kinderhookian) age. The fauna includes *Siphonodella isosticha* (Cooper) and is very similar to faunas described by Sandberg from rocks elsewhere assigned by Paull (oral commun., 1973) to the Drummond Mine Limestone. Coiled imprints from the limestone in this measured section were collected by R. A. Paull and identified by Mackenzie Gordon, Jr., and J. T. Dutro, Jr. (written commun., 1972) as "prolecanitacean ammonoid, indet.," which ranges through the Mississippian into the mid-Permian.

At Fish Creek Reservoir more than 304 m (1,100 ft) of flysch clastics are present below this *Siphonodella*-bearing limestone. Ammonoids (colln., 25389–PC) recovered by W. E. Hall from argillite just above the basal thrust contact near measured section 5 (fig. 6) were identified by Mackenzie Gordon, Jr. (written commun., 1974) as *Imitoceras*(?) sp., indet, and prolecanitid, gen. and sp. indet. He stated:

> The age range is probably Late Devonian to Early Mississippian. The supposed prolecanitid is no help because similar shapes are present among the clymeniids of the Late Devonian. Nevertheless, in the western United States, I would expect to find these two shapes together more often in the Early Mississippian.

Calcareous Foraminifera of Late Mississippian (early Chesterian) age representing foraminiferal zones 16s–17 of Mamet (Mamet and Skipp, 1970) are present in samples collected by R. A. Paull from near the eroded top of the Copper Basin Formation on the southern edge of Copper Basin (fig. 1). Faunal zones 17 and 18 of Late Mississippian (late Chesterian) age have been recognized in limestones interbedded with conglomerate lenses, thought to be eastward-pointing tongues of the Copper Basin Formation and assigned to the White Knob Limestone north and east of Copper Basin (Skipp and Mamet, 1970; Skipp, unpub. data, 1974).

To date, no definite Pennsylvanian faunas have been recovered, either from rocks assigned to the Copper Basin Formation or from limestones associated with lenses of clastic material that might correlate with the Copper Basin Formation in the Copper Basin area. A conglomerate bed associated with probable Pennsylvanian limestones is reported by Paull, Wolbrink, Volkmann, and Grover (1972, p. 1397) near Timbered Dome (fig. 1). Stratigraphic evidence from the Fish Creek area (see discussion of structure of Wood River II allochthon) indicates that by Middle Pennsylvanian time the Copper Basin Formation was emergent locally.

Structure

The Copper Basin allochthon overrides the parautochthon and the allochthon of the Roberts Moun-

tain Formation on the Fish Creek thrust fault, and is in turn overridden by the Wood River II allochthon on another folded and faulted thrust. The Copper Basin allochthon is more than 1,200 m (4,000 ft) thick on the east side of the Fish Creek Reservoir area but is less than 300 m (1,000 ft) thick on the west and south sides, where it forms a thin slice between the Devonian miogeosynclinal rocks and the Wood River and Milligen allochthons (cross section *B–B′*, fig. 5). Most of this thinning is tectonic, but some may be the result of Middle and Late Pennsylvanian erosion. (See discussion of structure of Wood River II allochthon.)

Quartzites in the Copper Basin Formation near either the sole thrust or the overlying thrust display a well-developed fracture cleavage and contain local zones of tectonic breccia (fig. 4). The fracture cleavage strikes N. 30°–70° E., generally parallel to the direction of thrusting. In the vicinity of the north-northwest-trending anticlinal axis, the fracture cleavage is cut by a northwest-trending axial plane cleavage. The axial plane cleavage is restricted to the crest of the anticline, whereas the northeast-striking fracture cleavage in the Wood River-Fish Creek area everywhere is related to thrust faults.

The amount of displacement of the Fish Creek thrust fault is speculated to be relatively small, possibly several kilometres. The stratigraphic displacement on the north side of the window appears to be very small, and the contact between the Upper Devonian Picabo Formation and the Copper Basin Formation may be very close to the original depositional contact. On the east side of the window, however, the lower 304 m (1,000 ft) of the Copper Basin Formation of the measured section is cut out. Conglomerates and quartzites like those above the conodont-bearing limestone unit of measured section 5 rest directly on Devonian dolomites. The Copper Basin Formation was deposited in a trench east of the Antler highland. The trench probably was located largely within the Devonian continental margin. The Devonian Milligen Formation is a likely source for some of the dark argillite and quartzite clasts of the Copper Basin Formation. In this paper, we postulate that the Devonian continental margin was at least 16 km (10 mi) west of the Fish Creek Reservoir area.

MILLIGEN(?) ALLOCHTHON

Stratigraphy

Rocks questionably correlative with the lower part of the Milligen Formation of Devonian age (Sandberg and others, 1975) are present in the southwest corner of the Fish Creek map area (fig. 3) beneath rocks assigned to the Wood River Formation. The Milligen(?) Formation is made up of a minimum of 90 m (300 ft) of unfossiliferous dark-gray siliceous argillite, fine-grained quartzite, and black chert, in beds 0.3–1.2 m (1–4 ft) thick. The sequence is mineralized and contains lenses, veinlets, and irregular masses of quartz. Most of the siliceous argillite, although sheared, is competent and does not display cleavage. Some thin less-competent interbeds, however, have a well-developed fracture cleavage. The base of the Milligen(?) is not exposed. The top is a sheared and iron-stained zone, 1.0–1.3 m (3–4 ft) thick, with lenses and veinlets of white quartz. The contact with overlying less deformed varicolored calcareous and dolomitic siltstone, gray argillite, and light-brown fine-grained quartzite assigned to the Wood River Formation is a thrust fault.

The type Milligen Formation is considered to be a transitional, not eugeosynclinal, deepwater oceanic sequence deposited at the toe of or not far west of the continental slope. If the outcrop southwest of the Fish Creek Reservoir window is indeed the Milligen, then Devonian deepwater clastic rocks have been thrust into proximity to shallow-water continental-shelf carbonate rocks of the same age in the report area.

Structure

The Milligen(?) allochthon is interpreted to have been thrust eastward over the Copper Basin allochthon, and to have been overridden in turn by both Wood River allochthons (fig. 5, cross section *B–B′*). Geologic relations in the Fish Creek Reservoir window indicate that the Milligen(?) Formation probably is also thrust over the Jefferson Formation, perhaps with slices of Roberts Mountains and Copper Basin Formations (cross section *A–A′* and *B–B′*, fig. 5) intervening. If one conservatively estimates the Milligen(?) depositional site to be 8 km (5 mi) west of the Devonian continental slope—which is itself at least 8 km (5 mi) wide—the Milligen(?) Formation must have been transported eastward at least 32 km (20 mi); 48 km (30 mi) may be a more realistic minimum estimate.

The Milligen Formation of the type locality has a pervasive shear cleavage at an angle of 45° to 60° to bedding (Sandberg and others, 1975). This cleavage is present, though not well developed, in the Milligen(?) of the Fish Creek Reservoir area, but it is absent nearly everywhere in the other Paleozoic formations of the area. The pervasive shear cleavage probably indicates deformation of the Milligen Formation prior to deposition of the overlying Copper Basin and Wood River Formations. The possible age

range of the deformation is latest Devonian to earliest Mississippian, the same as that of the Roberts Mountains thrust system in Nevada (Roberts and others, 1958, p. 2817; Smith and Ketner, 1968; Nolan, 1974), which Roberts and Thomasson (1964, p. D3) have extended into the Wood River area. In Nevada, emplacement of eugeosynclinal assemblages over eastern carbonate assemblages may have required movements of about 145 km (90 mi) along the Roberts Mountains thrust (Roberts and others, 1958, p. 2851). In Idaho, the juxtaposition of transitional and eastern carbonate (miogeosynclinal) assemblages east of the batholith would have required much less movement.

The Milligen(?) allochthon also has undergone eastward thrusting of post-Antler age. The Milligen and Wood River Formations crop out together for a distance of more than 80 km (50 mi) northwest from Fish Creek Reservoir, as shown in part by the map patterns of Umpleby, Westgate, and Ross (1930, pl. 1). The two formations do not occur separately at any place, and, though a thrust fault separates the two, this regional pattern of coexistence suggests that the two thrust sheets moved together during the latest period of thrusting.

WOOD RIVER I ALLOCHTHON

Stratigraphy

Siltstones and argillites which are thrust over the Milligen(?) Formation in the southwest part of the map area of figure 3 tentatively are assigned, on the basis of lithologic similarity, to a part of the Wood River Formation which lies stratigraphically above the seven units described by Hall, Batchelder, and Douglass (1974) in the type locality of the Wood River Formation. In the type locality, beds in this stratigraphic position are gradational with beds of the underlying unit 7, and are presumed to be of the same age—Early Permian or Leonardian(?) (Hall and others, 1974, p. 92).

In the Fish Creek area, this part of the Wood River Formation consists of approximately 180 m (600 ft) of thin-bedded gray limy siltstone, brown-weathering dolomitic siltstone, gray soft argillite, some light-brown fine-grained quartzite, and minor gray fine-grained impure limestone and grayish-orange dolomite. Some of the siltstones are banded in shades of green, grayish purple, and red. Worm tracks with concentric concave infilling patterns are present.

Structure

The siltstones of the Wood River Formation are folded into open folds with limbs dipping an average of 35° and some as much as 75° (fig. 3). Individual siltstone beds have well-developed cleavage which is mostly parallel to, but in some places across, the bedding. Cleavage is best developed in the softer beds.

Folds in the siltstone and argillite beds are truncated above by a thrust fault which brings brecciated limestone and sandy limestone of the Wood River II allochthon over them. (See also discussion of structure of Wood River II allochthon.)

WOOD RIVER II ALLOCHTHON

Stratigraphy

The Permian and Pennsylvanian Wood River Formation in the type locality is divided by Hall, Batchelder, and Douglass (1974) into seven units with a total stratigraphic thickness of about 3,000 m (9,800 ft). These seven units, which exclude the lithologies of the Wood River I allochthon, consist principally of gray fine-grained calcareous sandstone, limestone, and sandy limestone, and have a chert-quartzite pebble conglomerate at their base.

The Wood River Formation of the Wood River II allochthon at Fish Creek correlates with units 1 through 6(?) of the type locality, and is divided into two parts. The upper part consists mostly of quartzitic noncalcareous sandstone and conglomerate with minor sandy limestone, and the lower part consists of sandy and conglomeratic limestone and calcareous sandstone. The contact between the two parts is gradational through 4.6 m (15 ft) just northwest of fossil locality f24546 on the west side of Fish Creek (fig. 3). Elsewhere the contact appears to be abrupt, and on the east side of Fish Creek there is a suggestion of faulting or differential movement at the contact.

The distribution of chert-quartz-quartzite conglomerates within the Wood River II allochthon suggests a local eastern or southeastern source for these beds, probably an emergent Copper Basin terrane.

Lithology and thickness of lower part

A partial section of the lower part, 207+ m (680+ ft) thick, was measured just southwest of the sole thrust on the east side of Fish Creek (fig. 4, measured section 6, and figs. 6, 8). Limestones in the section are medium gray to medium dark gray and contain much fine quartz sand. They grade into limy sandstone and most are laminated. Conglomeratic beds are common in the lower and middle parts of the measured section where they form as much as 40 percent of the interval. Conglomerate fragments are angular to subrounded clasts of varicolored (black, gray, yellow) chert, light-

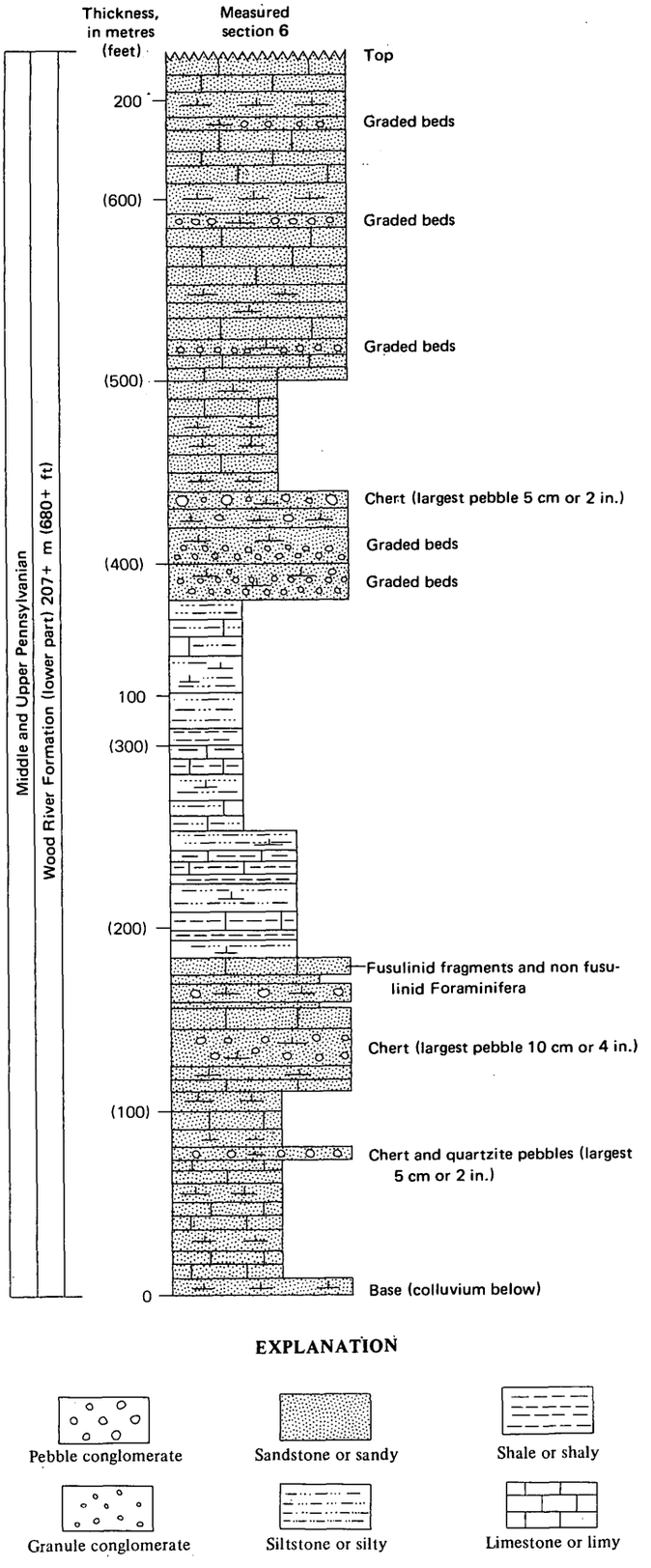

FIGURE 8.—Measured section 6 (see fig. 4) of lower part of Wood River Formation in NW¼ sec 23 and NE¼ sec. 15 (approx.), T. 1 N., R. 22 E., Blaine County, Idaho.

gray quartzite, spicular limestone, and minor dark-gray and yellow argillite. Fragments are as large as 10 cm (4 in) across but most are much smaller, ranging in size from granules to small pebbles. The conglomerates, many with disrupted frameworks, are most commonly the lowest part of a graded sequence of 0.3- to 0.6-m (1 to 2-ft)-thick beds. The sand is uniformly fine to very fine and is composed principally of quartz with accessory feldspar, zircon, sericite, and hornblende. The graded conglomerates and laminated sandstones are probably turbidity-current deposits laid down in water of moderate depth. A distinctive unit, about 61 m (200 ft) thick in the middle part of the sequence, is a slope-forming series of pale-red to pale-reddish-purple calcareous siltstones and shales and noncalcareous shales.

Conglomerates and siltstones are present in the lower part on both sides of Fish Creek. Calcareous sandstones and conglomerates are brecciated near the sole thrust above Wood River I allochthon on the west side.

Lithology and thickness of upper part

The upper part of the Wood River Formation in the Fish Creek area is more than 600 m (2,000 ft) thick and consists of very light gray to medium-dark-gray and brown fine-grained siliceous sandstone interbedded with minor granule to pebble conglomerate and sandy limestone or calcareous sandstone. The sequence is medium to thick bedded. The uniform grain size of much of the sequence makes determination of bedding difficult in many places. A few of the sandstones are laminated and many of them are brecciated. The breccia fragments are recemented by sand of the same size and composition as that of the fragments and are stratabound, indicating that brecciation was a sedimentary feature contemporaneous with deposition.

Petrographic study by John Batchelder (written commun., 1974) of the fine-grained beds in the upper part on the west side of Fish Creek indicates that these beds consist almost entirely of subrounded quartz, with accessory chert, sericite, zircon, amphibole, and altered feldspar; grain size ranges from 0.04 to 0.4 mm.

The conglomerate beds in the upper part of the Wood River Formation are found only on the east side of Fish Creek in the southeastern part of the map area (fig. 4). In this area approximately 150 m (500 ft) of interbedded granule to pebble conglomerate and fine- to coarse-grained siliceous sandstone and siltstone extends above the contact with the lower part of the formation. A few limy sandstones and a distinctive

light-greenish-gray platy siltstone are also present. The granule conglomerates and sandstones are graded, laminated, and convoluted. Pebble conglomerate is rare, but a few fragments as much as 2.5 cm (1 in) in diameter were noted. The clasts in the conglomerates are largely chert, quartz, and quartzite in a siliceous or sericitic matrix. These beds are typical proximal turbidites as described by Bouma and Hollister (1973, p. 79–118).

Age and correlation

The Wood River Formation of Wood River II allochthon correlates with units 1, 2, 3, 4, 5, and 6(?) of Middle Pennsylvanian to Early Permian age of the type Wood River. Fossils are rare in the formation at Fish Creek, but echinoderm and bivalve debris, a few poorly preserved gastropods, bryozoa, corals, and rare detrital fusulinids and other Foraminifera are present in the lower unit. Fusulinids from four localities were determined by R. C. Douglass to be of Middle and Late Pennsylvanian age. Sample locality f24560 (fig. 3) near the thrust fault contact with Wood River I allochthon contains rare abraded partly rounded fragments of fusulinids that strongly suggest *Fusulinella* sp. and *Wedekindella* sp., which indicate that the age of the enclosing rock is Middle Pennsylvanian (Des Moinesian) or younger (R. C. Douglass, written commun., 1973). These beds are tentatively correlated with unit 2 of the type locality. Three other collections, f24546, f24727, and f24728, from near the top of the lower part on both sides of the reservoir (fig. 3) contain *Triticites* sp., *Pseudofusulinella* sp., and *Staffella* sp., which indicate a Late Pennsylvanian age (R. C. Douglass, written commun., 1972, 1974). The latter faunal association was reported (Hall and others, 1974, p. 92) from unit 4 of the stratigraphic section of the type Wood River Formation east of Bellevue (fig. 1). The Late Pennsylvanian fusulinids in the Fish Creek area were found either in limy granule conglomerates or in fine-grained beds associated with conglomerates. The fine-grained calcareous sandstones and sandy limestones interbedded with these conglomerates in the Fish Creek area resemble in color, grain size, and mineralogy those of unit 4 in the type locality. The grayish-red limy siltstone 91–151 m (300–495 ft) above the base of the measured section (fig. 8) is identical to lithologies in unit 3 of the type locality.

Thus, although the lower part of the Wood River Formation in the Fish Creek area contains conglomerates found only in unit 1 of the type locality farther west, similarities in fine-grained lithologies and included faunas suggest correlation with units 2, 3, and 4 of the type locality. Unit 1 (Hailey Conglomerate Member) was recognized with certainty in only one place—just west of Fish Creek Reservoir where a large boudin of conglomerate is caught up on the sole of the thrust and is overlain by the upper siliceous part (unit 5) of the Wood River Formation.

Fossils were not found in the upper part in the Fish Creek area. However, the mineralogy, grain size, and texture of the fine-grained beds is very similar to unit 5 of the type locality. Unit 5 is Late Pennsylvanian in age (Hall and others, 1974). It is likely that some of the sandstone sequence at the top of the upper part at Fish Creek may correlate with the lower part of unit 6 of the type locality.

Middle and Upper Pennsylvanian turbidite conglomerates in the Wood River Formation of this area had an eastern or, perhaps, southeastern local source. Clasts are identical to those that make up the Mississippian Copper Basin Formation, and probably they were derived from an emergent Copper Basin terrane to the east. The mineralogy of the bulk of the sandstones of the Wood River, however, suggests that they were derived from a cratonic igneous or low-grade-metamorphic terrane, rather than from the siliceous clastics and limestone of the Copper Basin Formation (Hall and others, 1974, p. 94).

Structure

A well-exposed thrust, the trace of which trends about N. 20° W. through the area of figures 2 and 4, brings the Wood River Formation over the Copper Basin allochthon. In the southwest corner of the map area, Wood River II allochthon is thrust over the Wood River I allochthon (cross section *B–B′*, fig. 5). Outcrops of the Wood River Formation in the Fish Creek areas are the easternmost known and may represent the distal ends of both the Wood River I and Wood River II allochthons. The same is true for the Milligen(?) Formation. Conglomeratic facies of both the lower and upper parts of the Wood River Formation in the southeastern part of the map area (fig. 3) override quartzites and conglomerates of the Copper Basin Formation, which probably constituted a former local eastern source area.

Both the Wood River I and II allochthons are deformed into broad folds that predate thrusting. These folds are truncated by the sole thrusts which themselves are both folded and faulted (cross section *B–B′*; fig. 5). Quartzites near the thrusts are brecciated and broken by a northeast-striking fracture cleavage.

The Wood River II allochthon has a maximum thickness of 825 m (2,700 ft) (section *C–C′*, fig. 5).

Unit 1 (Hall and others, 1974) of the Wood River Formation, which is present only as a boudin caught in the thrust fault along the west side of the reservoir, is overlain by the upper siliceous part (unit 5) of the Wood River Formation. At this locality, then, the lower 610 m (2,000 ft) or more of the Wood River Formation has been cut out by the thrusting. Elsewhere, beds of the lower part correlated with units 2, 3, 4, and 5 are in thrust contact with the Copper Basin Formation (fig. 4).

The Wood River Formation was deposited west of the Copper Basin Formation. When deposition started, in Middle Pennsylvanian time, the Copper Basin trough already was filled with coarse clastic flysch sediments and was locally emergent. The Wood River basal conglomerate was deposited farther west on the Milligen Formation in the subsiding Wood River basin. The Wood River Formation subsequently was thrust eastward over the Milligen in a series of imbricate slices, possibly cutting out as much as 3,000 m (9,800 ft) of the Wood River I allochthon in the Fish Creek area. The Wood River was then, in part, carried piggyback upon the Milligen Formation as they both were thrust over the Copper Basin Formation. The eastward translation of the Wood River Formation must exceed, but not necessarily by much, the several kilometres estimated for translation of the Copper Basin Formation. An eastward displacement of 16–24 km (10–15 mi) seems likely.

CHALLIS VOLCANICS

Challis Volcanics of early Tertiary (Eocene) age lie unconformably on the eroded surfaces of the Copper Basin and Wood River allochthons (fig. 3). In the report area, the Challis is composed largely of rhyolitic glassy fragmental rocks, vitrophyres, welded and nonwelded tuffs, and minor flows. An electron microprobe analysis by G. A. Desborough (written commun., 1971) of the fine-grained matrix of a partly crystallized welded tuff from sample locality 22S71 (fig. 4) gave the following results in weight percent:

SiO_2	77.5	Na_2O	3
Al_2O_3	12.3	TiO_2	.2
MgO	.1	MnO	.01
FeO*	1.6	K_2O	5.7
CaO	.5	Total	100.91

* All Fe calculated as FeO.

Feldspar phenocrysts and lithic fragments form less than 3 percent of the tuff; thus the microprobe analysis closely approximates the bulk chemical composition.

The base of the Challis in the report area is preserved at altitudes generally ranging from 2,130 m (5,200 ft) to 2,740 m (7,200 ft). Relief of about 610 m (2,000 ft) must have existed on the prevolcanic surface on both sides of the valley on a subdued topography somewhat like that being exhumed today. The post-Challis north-south normal fault, which is inferred along Fish Creek valley to explain facies differences in the Wood River Formation, may have enhanced apparent relief between the two sides of the valley. Axelrod (1968, p. 727) proposed local maximums of as much as 610 m (2,000 ft) of relief on the pre-Challis surface.

An Eocene age for the Challis Volcanics is indicated by radiometric dates reported by D. I. Axelrod (1966), R. L. Armstrong (written commun., 1971), and J. D. Obradovich (written commun., 1974).

SNAKE RIVER GROUP

Basalt of the Snake River Group occupies the valley below Fish Creek Reservoir. The vent for the main flow in the valley is just southeast of the Fish Creek Reservoir dam. The basalt is dark gray on fresh surfaces and consists of small sparse phenocrysts of labradorite in an intersertaldictytaxitic groundmass of plagioclase, clinopyroxene, orthopyroxene, olivine and opaque minerals, and a small amount of clear glass.

AGES OF THRUSTING

All Paleozoic rocks of the Fish Creek Reservoir area may be allochthonous, having moved generally eastward or northeastward on a complex of thrust faults that are both folded and faulted. The youngest rocks involved in thrusting in the Fish Creek area are Leonardian (Early Permian) strata of the upper Wood River Formation; the oldest rocks not involved in the thrusts are alluvial conglomerates exposed beneath the Eocene Challis Volcanics (fig. 4). A Sevier age for the main period of thrusting seems likely. Middle Paleozoic rocks of the Milligen(?) and Roberts Mountains Formations may have been involved in earlier thrusting of latest Devonian to earliest Mississippian age that was related to the Antler orogeny described in north-central Nevada (Roberts and others, 1958; Smith and Ketner, 1968; Nolan, 1974). Extension of this system into south-central Idaho was hypothesized earlier by Churkin (1962) and Roberts and Thomasson (1964, p. D3).

FOLDS

Folds of at least two ages are present in the Fish Creek area. Prior to thrusting, the Paleozoic rocks were folded into broad open folds such as those of the

Wood River and Copper Basin Formations in the southeast part of the map area (figs. 4, 6). These folds were truncated by the thrusts between the Wood River and Copper Basin Formations (fig. 3). A later stage of deformation, the very pronounced doming of the Fish Creek window and overlying thrust sheets, followed. (See cross sections, fig. 5.) This doming succeeded the thrusting but preceded deposition of the Challis (Eocene) (cross section *A–A′*, fig. 5). All the Paleozoic rocks have been involved. The arching can be recognized as postthrusting in age because the Wood River and Copper Basin allochthons do not have the abundant drag folds in incompetent beds that would be expected if the thrusts rode over an original highland. The Challis has not been domed and must postdate this uplift (cross section *A–A′*, fig. 5). Thus, the arching is postthrusting and pre-Eocene in age and is probably a late Mesozoic feature. Structures in southern Idaho involving domal uplifts of about the same age and in approximately the same structural setting have been described by Armstrong (1968, p. 1295).

STEEPLY DIPPING FAULTS

Steeply dipping faults of two ages also are present in the Fish Creek Reservoir area. Some steep faults are confined to a single allochthon and are tear faults that formed at the time of thrusting. They are shown in the Wood River allochthon in section *C–C′* and in the parautochthon in the Carey Dolomite in cross section *B–B′*. They all have small displacements.

Tertiary normal faults that cut Eocene Challis Volcanics and trend generally northward are common in the Pioneer Mountains to the north. Such a normal fault is inferred beneath the Quaternary Snake River basalts to account for the offset of Wood River facies and the crosscutting north-south trend of Fish Creek valley (fig. 3). The symmetrical distribution of Quaternary deposits on both sides of the valley indicates that the fault, if present, has not moved during Quaternary time.

SUMMARY AND CONCLUSIONS

Within the 6.5 km² (2.5 mi²) of the Fish Creek Reservoir window, 450 m (1,500 ft) of folded and faulted Devonian miogeosynclinal carbonate rocks assigned to the Carey Dolomite, Jefferson Formation, and Picabo Formation are exposed. Along the east edge of the window about 140 m (460 ft) of coralline limestone, limestone phenoplast conglomerate, and limy siltstone of earliest Devonian and latest Silurian age, assigned to the Roberts Mountains Formation, is thrust over the Carey Dolomite and Jefferson Formation. The rocks of the Roberts Mountains Formation are interpreted to be a continental margin transitional facies that has been thrust eastward over the shelf carbonate sequence. The window of middle Paleozoic rocks is overridden along the Fish Creek thrust fault by quartzite, conglomerate, argillite, and minor limestone of the lower part of the Mississippian Copper Basin Formation described by Ross (1962) and Paull, Wolbrink, Volkmann, and Grover, 1972).

West and south of the window, sandy and conglomeratic limestone, calcareous sandstone, and quartzitic sandstone of the Wood River Formation (Permian and Pennsylvanian) are thrust over the Copper Basin Formation. In the southwest corner of the map area (fig. 4), siltstone and argillite of the Wood River Formation rest in thrust contact on the Milligen(?) Formation. The Milligen(?) Formation of the Fish Creek area is tentatively correlated with the Milligen of the Hailey-Bellevue area, which is a deepwater siliceous oceanic sequence deposited in Devonian time just west of the toe of the continental slope. In the Fish Creek area, the Milligen(?) overrides Devonian shelf carbonates of the same age. Probable tectonic transport of at least 48 km (30 mi) is indicated for the Milligen(?) Formation.

The following geologic history for the region can be inferred from the geologic relations described in the Fish Creek area and from other published reports.

During much of Silurian and Devonian time, shallow shelf seas covered the area and may have extended westward another 16–32 km (10–20 mi) at this latitude. Intertidal and shallow subtidal deposits accumulated to a thickness of at least 450 m (1,500 ft), probably to much more. Simultaneously, continental-margin-reef and reef-flank facies were deposited on the edge of the shelf, and deepwater oceanic deposits were laid down west of the continental slope, perhaps near the present eastern edge of the batholith.

In Late Devonian time, a highland emerged at or near the continental margin and miogeosynclinal detritus was shed to the east. Latest Devonian to earliest Mississippian thrusting from west to east may have accompanied the rise of the highland, and western transitional facies rocks of Silurian and Devonian age may have been thrust over miogeosynclinal facies.

In latest Devonian(?) and Mississippian time, the Antler orogenic belt (Churkin, 1962; Roberts and Thomasson, 1964; Roberts and others, 1965) shed large quantities of early Paleozoic eugeosynclinal and transitional detritus eastward to make up the more than 5,500 m (18,000 ft) of the Copper Basin Formation. The Copper Basin Formation accumulated, largely

west of the Fish Creek area but probably mostly within the middle Paleozoic continental margin, in the narrow, rapidly subsiding, Copper Basin trough (Muldoon trough of Thomasson, 1959). Flysch or clastic wedge sedimentation and basin filling continued into at least latest Mississippian time as indicated by Copper Basin-like conglomerate lenses of the White Knob Limestone (Skipp, 1961; Skipp and Mamet, 1970).

In Early Pennsylvanian time, shelf limestone with interbedded craton-derived sandstones spread westward, perhaps overlapping the Copper Basin flysch deposits. In Middle and Late Pennsylvanian time, subsidence of the Wood River basin took place on the site of the former Antler highland, and more than 2,750 m (9,000 ft) of calcareous sandstone, sandy limestone, and conglomerate of cratonic origin (Hall and others, 1974) filled the depression. Conglomerate locally was shed westward into the eastern part of the Wood River basin from an emergent Copper Basin terrane.

Sometime after Wood River deposition, but before extrusion of the Challis Volcanics, extensive thrusting from the west or southwest took place, and the Wood River and Milligen(?) Formations and upper Paleozoic flysch facies and middle Paleozoic miogeosynclinal and transitional facies were telescoped along a series of thrusts. Thrusting is believed to be, at least in part, a result of detachment and gravity sliding of the Wood River allochthons during the emplacement of the Cretaceous Idaho batholith 40 km (25 mi) to the west. After thrusting, but before Eocene time, the Paleozoic rocks in the Fish Creek area were uplifted into a northwest-trending dome.

Mesozoic tectonic activity in this part of Idaho provided much of the detritus for the thick Cretaceous molasse deposits which accumulated to the east and west (Axelrod, 1968, p. 729). Mesozoic sedimentation in the immediate area has not been reported; however, it may be present in the alluvial conglomerate at the base of the Challis Volcanics (fig. 4), which lies unconformably on the pre-Challis surface.

Explosive volcanic activity followed in early Tertiary time and the Challis Volcanics poured out over and probably covered the entire region, which had a relief of at least 610 m (2,000 ft) by the end of Eocene time. Challis volcanism was followed by late Tertiary basin-range faulting with vertical displacements of as much as several hundred metres in the Fish Creek area. Drainages were localized along some of the faults, and the broad valleys thus formed were later partly filled by Quaternary Snake River basalt. Downcutting of this basalt is now underway.

REFERENCES CITED

Armstrong, R. L., 1968, Mantled gneiss domes in the Albion Range, southern Idaho: Geol. Soc. America Bull., v. 70, p. 1295–1314.

Axelrod, D. I., 1966, Potassium-argon ages of some western Tertiary floras: Am. Jour. Sci., v. 264, p. 497–506.

——— 1968, Tertiary floras and topographic history of the Snake River Basin, Idaho: Geol. Soc. America Bull., v. 79, p. 713–734.

Berry, W. B. N., and Boucot, A. J., eds., 1970, Correlation of the North American Silurian rocks: Geol. Soc. America Spec. Paper 102, 289 p.

Bouma, A. H., and Hollister, C. D., 1973, Deep ocean basin sedimentation, *in* Middleton, G. V. and Bouma, A. H., chm., Turbidites and deep-water sedimentation—Lecture notes for a short course: Los Angeles, Soc. Econ. Paleontologists and Mineralogists, Pacific section, p. 79–118.

Churkin, Michael, Jr., 1962, Facies across Paleozoic miogeosynclinal margin of central Idaho: Am. Assoc. Petroleum Geologists Bull., v. 46, no. 5, p. 569–591.

Dover, J. H., and Ross, R. J., Jr., 1975, Ordovician and Middle Silurian rocks of the Wildhorse window, northeastern Pioneer Mountains, central Idaho: U.S. Geol. Survey Jour. Research, v. 3, no. 4, p. 431–436.

Hall, W. E., Batchelder, John, and Douglass, R. C., 1974, Stratigraphic section of the Wood River Formation, Blaine County, Idaho: U.S. Geol. Survey Jour. Research, v. 2, no. 1, p. 89–95.

Johnson, J. G., Boucot, A. J., and Murphy, M. A., 1973, Pridolian and early Gedinnian age brachiopods from the Roberts Mountains Formation of central Nevada: California Univ. Pubs. Geol. Sci., v. 100, 75 p.

Ketner, K. B., 1970, Limestone turbidite of Kinderhook age and its tectonic significance, Elko County, Nevada, *in* Geological Survey research 1970: U.S. Geol. Survey Prof. Paper 700–D, p. D18–D22.

Mamet, B. L., and Skipp, Betty, 1970, Lower Carboniferous calcareous foraminifera—Preliminary zonation and stratigraphic implications for the Mississippian of North America: Internat. Cong. on Stratigraphy and Carboniferous Geology, 6th, Sheffield 1967, Compte Rendu, v. 3, p. 1129–1146.

Nelson, W. H., and Ross, C. P., 1969a, Geologic map of the Mackay quadrangle, south-central Idaho: U.S. Geol. Survey Misc. Geol. Inv. Map I–580.

——— 1969b, Geology of the Mackay 30-minute quadrangle, Idaho: U.S. Geol. Survey open-file rept., 161 p.

Nolan, T. B., 1974, Stratigraphic evidence on the age of the Roberts Mountains thrust, Eureka and White Pine Counties, Nevada: U.S. Geol. Survey Jour. Research, v. 2, no. 4, p. 411–416.

Paull, R. A., Wolbrink, M. A., Volkmann, R. G., and Grover, R. L., 1972, Stratigraphy of the Copper Basin Group, Pioneer Mountains, south-central Idaho: Am. Assoc. Petroleum Geologists Bull., v. 56, p. 1370–1401.

Poole, F. G., 1974, Flysch deposits of Antler foreland basin, western United States, *in* Dickenson, W. R., ed., Tectonics and sedimentation, a symposium: Soc. Econ. Paleontologists and Mineralogists Spec. Pub. 22, p. 58–82.

Roberts, R. J., Crittenden, M. D., Jr., Tooker, E. W., Morris, H. T., Hose, R. K., and Cheney, T. M., 1965, Pennsylvanian and Permian basins in northwestern Utah, northeastern Nevada and south-central Idaho: Am. Assoc. Petroleum

Geologists Bull., v. 49, no. 11, p. 1926–1956.

Roberts, R. J., Hotz, P. E., Gilluly, James, and Ferguson, H. G., 1958, Paleozoic rocks of north-central Nevada: Am. Assoc. Petroleum Geologists Bull., v. 42, no. 12, p. 2813–2857.

Roberts, R. J., and Thomasson, M. R., 1964, Comparison of late Paleozoic depositional history of northern Nevada and central Idaho, *in* Short papers in geology and hydrology: U.S. Geol. Survey Prof. Paper 475–D, p. D1–D6.

Ross, C. P., 1934, Correlation and interpretation of Paleozoic stratigraphy in south-central Idaho: Geol. Soc. America Bull., v. 45, no. 5, p. 937–1000.

——— 1960, Diverse interfingering Carboniferous strata in the Mackay quadrangle, Idaho, *in* Short papers in the geological sciences: U.S. Geol. Survey Prof. Paper 400–B, p. B232–B233.

——— 1962, Upper Paleozoic rocks in central Idaho: Am. Assoc. Petroleum Geologists Bull., v. 46, no. 3, p. 384–387.

Sandberg, C. A., Hall, W. E., Batchelder, J. N., and Axelsen, Claus, 1975, Stratigraphy, conodont dating, and paleotectonic interpretation of the type Milligen Formation (Devonian), Wood River area, Idaho: U.S. Geol. Survey Jour. Research, v. 3, no. 6.

Sandberg, C. A., and Mapel, W. J., 1967, Devonian of the Northern Rocky Mountains and Plains *in* Oswald, D. H., ed., Internat. symposium on the Devonian System, Calgary, Alberta, Sept. 1967 [Proc.], V. 1: Calgary, Alberta Soc. Petroleum Geologists, p. 843–877 [1968].

Sandberg, C. A., Mapel, W. J., and Huddle, J. W., 1967, Age and regional significance of basal part of Milligen Formation, Lost River Range, Idaho *in* Geologic Survey research 1967: U.S. Geol. Survey Prof. Paper 575–C, p. C127–C131.

Seilacher, Adolph, 1964, Biogenic sedimentary structures, *in* Imbrie, John, and Newell, Norman, eds., Approaches to paleoecology: New York, John Wiley and Sons, p. 296–316.

Skipp, B. A. L., 1961, Interpretation of sedimentary features in Brazer Limestone (Mississippian) near Mackay, Custer County, Idaho: Am. Assoc. Petroleum Geologists Bull., v. 45, no. 3, p. 376–389.

Skipp, Betty, and Mamet, B. L., 1970, Stratigraphic micropaleontology of the type locality of the White Knob Limestone (Mississippian), Custer County, Idaho, *in* Geological Survey research 1970: U.S. Geol. Survey Prof. Paper 700–B, p. B118–B123.

Skipp, Betty, and Sandberg, C. A., 1972, Window of Silurian and Devonian miogeosynclinal and transitional rocks, west of Craters of the Moon National Monument, central Idaho: Geol. Soc. America Abs. with Programs, v. 4, no. 6, p. 411.

——— 1975, Silurian and Devonian miogeosynclinal and transitional rocks of the Fish Creek Reservoir window, central Idaho: U.S. Geol. Survey Jour. Research, v. 3, no. 6.

Smith, J. F., Jr., and Ketner, K. B., 1968, Devonian and Mississippian rocks and the date of the Roberts Mountains thrust in the Carlin-Pinon Range area, Nevada: U.S. Geol. Survey Bull. 1251–I, 18 p.

Thomasson, M. R., 1959, Late Paleozoic stratigraphy of paleotectonics of central and eastern Idaho: Wisconsin Univ. Ph. D. thesis, 288 p.

Umpleby, J. B., Westgate, L. G., and Ross, C. P., 1930, Geology and ore deposits of the Wood River region, Idaho, *with a description of* The Minnie Moore and near-by mines, by D. F. Hewitt: U.S. Geol. Survey Bull. 814, 250 p.

Winterer, E. L., and Murphy, M. A., 1960, Silurian reef complex and associated facies, central Nevada: Jour. Geology, v. 68, no. 2, p. 117–139.

Jour. Research U.S. Geol. Survey
Vol. 3, No. 6, Nov.–Dec. 1975, p. 691–706

SILURIAN AND DEVONIAN MIOGEOSYNCLINAL AND TRANSITIONAL ROCKS OF THE FISH CREEK RESERVOIR WINDOW, CENTRAL IDAHO

By BETTY SKIPP and CHARLES A. SANDBERG, Denver, Colo.

Abstract.—Documentation of Devonian continental-shelf shallow-water carbonate rocks in the core of the Fish Creek Reservoir window shifts the known westernmost limit of the Devonian miogeosyncline 50 km (30 mi) southwest across the structural grain from the well-known miogeosynclinal sequence in the Lost River Range. The miogeosynclinal carbonate sequence in the window has a minimum thickness of 450 m (1,500 ft). It comprises the upper Lower Devonian (Emsian) and lower Middle Devonian (Eifelian) Carey Dolomite (new), the upper Middle Devonian (Givetian) and Upper Devonian Jefferson Formation, and the Upper Devonian Picabo Formation (new). Conodont faunas precisely date the Carey. The Picabo Formation, composed of interbedded sandy dolomite-pebble conglomerate and dolomitic quartzose sandstone, is unlike any previously described formation of Late Devonian or Early Mississippian age in central Idaho. It resembles parts of the Stansbury, Beirdneau, Leatham, and Victoria Formations, which reflect areas of local Late Devonian uplift and erosion of older shelf rocks in northern Utah and southeastern Idaho. Transitional (continental-slope) rocks of the Roberts Mountains Formation representing reef and off-reef facies are thrust over the Devonian shelf sequence within the Fish Creek Reservoir window. The Roberts Mountains Formation here is precisely dated as latest Silurian (Pridolian, *costeinhornensis* Zone) through earliest Devonian (Lochkovian) by a sequence of conodont faunas. The easternmost known exposures of possible Devonian siliceous facies rocks assigned to the Milligen(?) Formation are present less than 4.8 km (3 mi) southwest of the shelf sequence. Structural relations and paleotectonic reconstructions suggest that they have a minimum eastward translation of 32 km (20 mi). The Devonian continent–ocean basin interface, along which the Antler orogenic belt developed at this latitude, probably was located near the east edge of the present Idaho batholith.

Fish Creek Reservoir lies along the north edge of the Snake River Plain between the town of Carey, 16 km (10 mi) to the southwest, and the Craters of the Moon National Monument, 16 km (10 mi) to the east. (See fig. 1 in Skipp and Hall, 1975.)

In a reconnaissance geologic map, Ross (1963, map 6) outlined the extent of Carboniferous, Tertiary, and Quaternary rocks in the Fish Creek area. Although Ross did not show any older rocks in the vicinity of the Fish Creek Reservoir, Thomasson (1959, p. 184) earlier had reported about 230 m (750 ft) of Devonian carbonate rocks in approximately the same location as some of our measured sections.

Our mapping and study of the Fish Creek Reservoir area, which was prompted by Thomasson's report, was initiated late in 1970, and we immediately confirmed the presence of a relatively thick sequence of Devonian dolomite, sandstone, and conglomerate, a large part of which was identical to the lower part of the miogeosynclinal Jefferson Formation in the Lost River Range. Rocks beneath the Jefferson Formation, which we at first lithologically correlated with the Silurian Laketown Dolomite (Skipp and Sandberg, 1972), proved to be Middle Devonian on the basis of contained conodont faunas, and a new formation, the Carey Dolomite, was recognized. Rocks above the Jefferson on the northeast side of the reservoir represent an unconformably overlying newly recognized formation, the Picabo, of Late Devonian age. In addition, we found a transitional continental-slope sequence of the Roberts Mountains Formation (Devonian and Silurian) in thrust contact with the shelf rocks on the east side of the reservoir, and recognized that both sequences occupy a window through the Mississippian Copper Basin Formation.

Further work south of the reservoir disclosed the easternmost known exposures of a unit that may be the allochthonous Milligen Formation (Devonian).

The Fish Creek Reservoir window comprises about 6.5 km^2 (2.5 mi^2) on the northeast and east sides of the reservoir. It lies 32–40 km (20–25 mi) east of the Idaho batholith (see fig. 1 in Skipp and Hall, 1975) and 50 km (30 mi) southwest of and across the structural grain from the Lost River Range in which Silurian and Devonian miogeosynclinal rocks have been recognized (Umpleby, 1917; Ross, 1934, 1937, 1947; Sloss, 1954; Sandberg and Mapel, 1967; Mapel and Sandberg, 1968).

Three other windows—the Wildhorse, Dry Creek, and Timbered Dome windows—containing Silurian and Devonian rocks are now recognized in the central and southern Pioneer Mountains (Skipp and Hall, 1975, fig. 1). In the Wildhorse and Dry Creek windows, 55 km (34 mi) northwest of Fish Creek Reservoir, lower Paleozoic miogeosynclinal and transi-

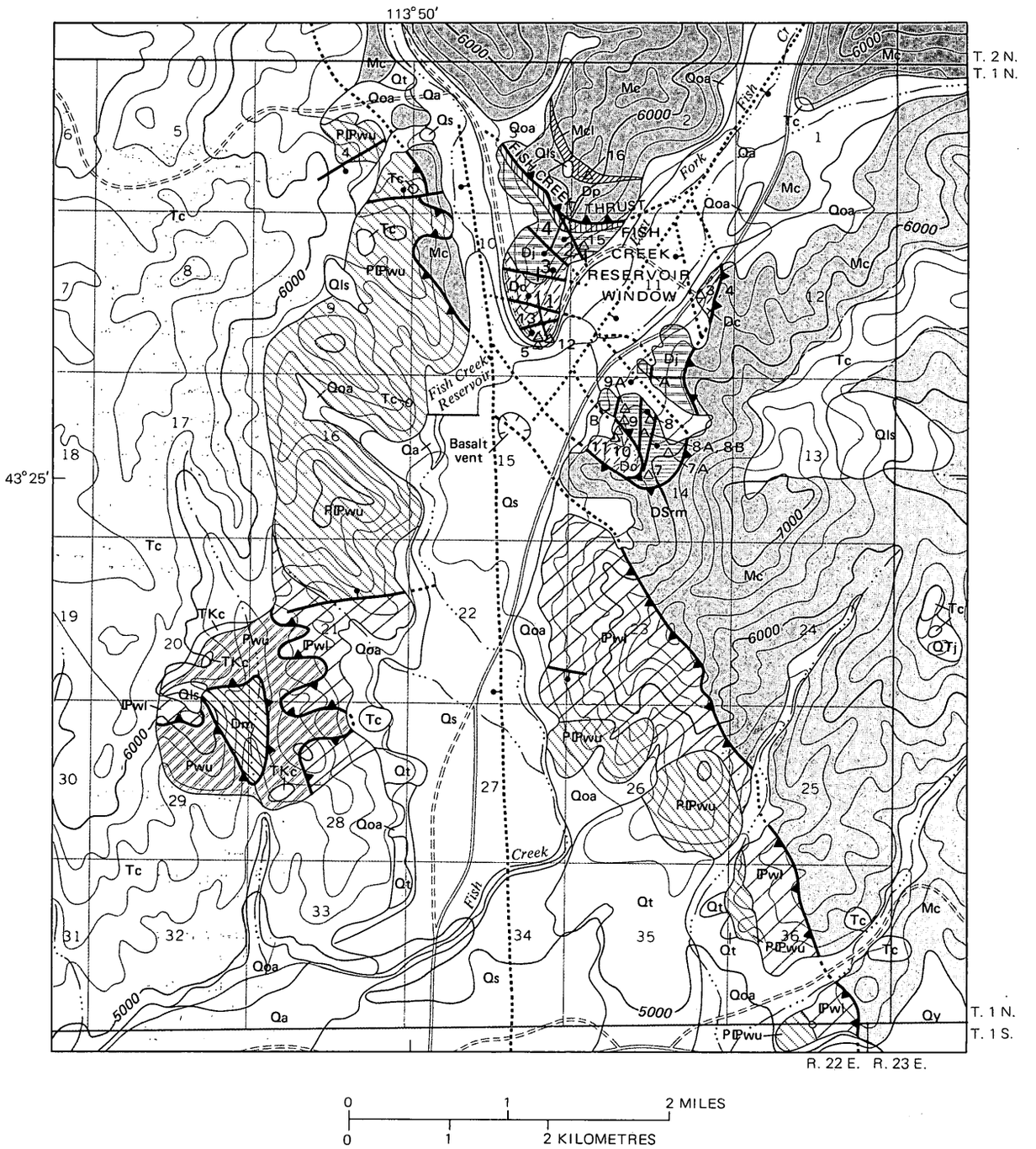

FIGURE 1.—Geologic map of Fish Creek Reservoir area (modified from Skipp and Hall, 1975, fig. 3) showing locations of lines of measured sections and fossil localities. Numbered fossil localities have a prefix FCR– (also see fig. 3). Locality 8784–SD is designated by A; locality 8786–SD by B; locality 8785–SD is very close to FCR–8A. Location of section lines in T. 1 N., R. 22 E. (unsurveyed), approximate.

tional rocks have been described recently by Paull and Rothwell (1973) and Dover and Ross (1975). At Timbered Dome window (Skipp and Hall, 1975, fig. 1; Skipp, 1961, p. C239–C240), a section at least 100 m (328 ft) thick, of shallow-water sparsely fossiliferous dolomite with minor interbedded quartzite was measured by Sandberg and E. J. Biller. These rocks, which are assignable to the lower part of the Carey Dolomite, contain Early Devonian (probably Emsian) conodonts that are slightly older than the Eifelian conodonts recovered from the upper part of the Carey exposed at Fish Creek Reservoir. At Timbered Dome

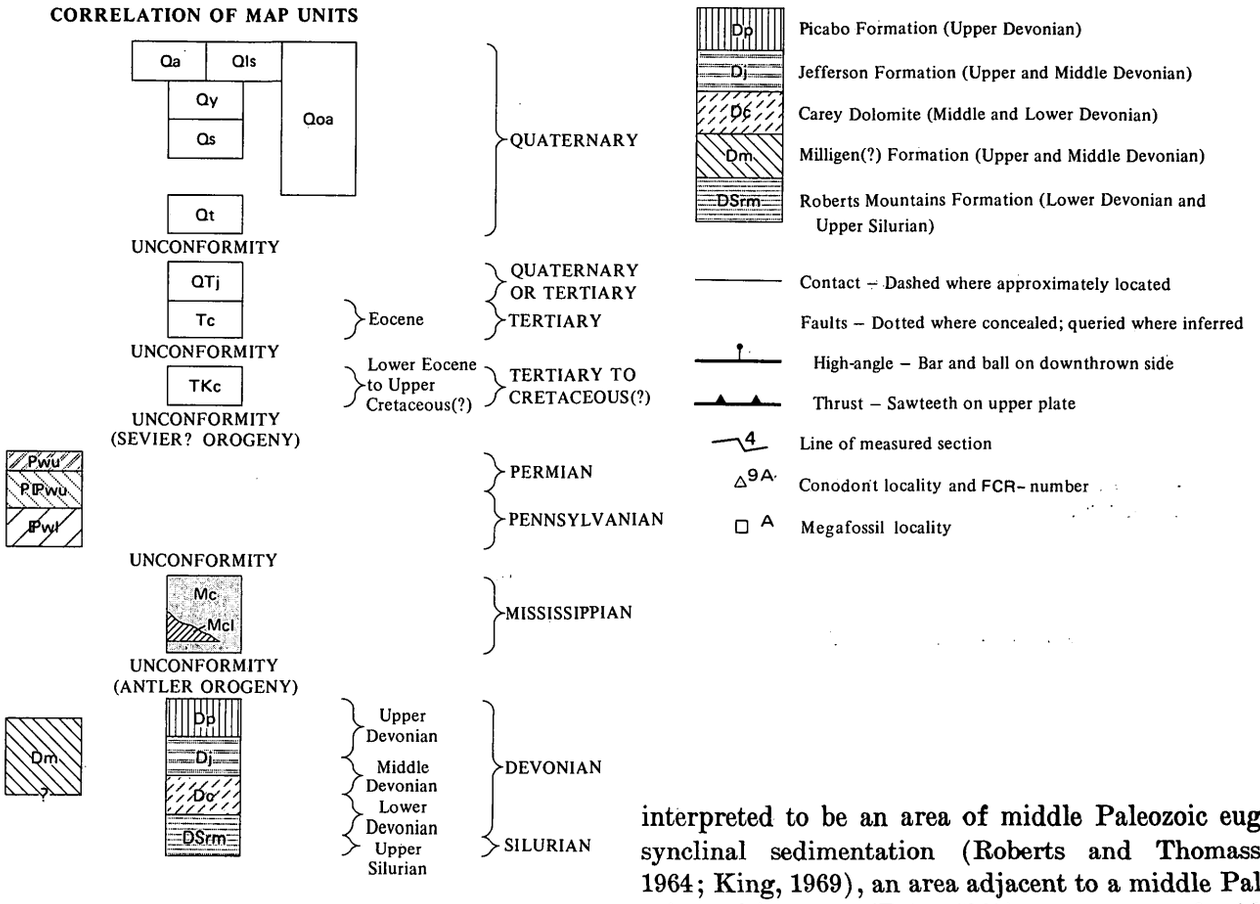

LIST OF MAP UNITS

Qa	Alluvium (Quaternary)
Qls	Landslide deposits (Quaternary)
Qy	Younger basalt (Quaternary)
Qs	Snake River Group (Quaternary)
Qoa	Older alluvium and colluvium (Quaternary)
Qt	Terrace deposits (Quaternary)
QTj	Jasperoid (Quaternary or Tertiary)
Tc	Challis Volcanics (Eocene)
TKc	Conglomerate (lower Eocene to Upper Cretaceous?)
	Wood River Formation
Pwu	Uppermost part (Permian)
PIPwu	Upper part (Permian and Pennsylvanian)
PIPwl	Lower part (Pennsylvanian)
	Copper Basin Formation (Mississippian)
Mc	Lower part
Mcl	Limestone lens

the Carey is unconformably overlain by quartzite of the Copper Basin Formation.

The area containing the windows has been variously interpreted to be an area of middle Paleozoic eugeosynclinal sedimentation (Roberts and Thomasson, 1964; King, 1969), an area adjacent to a middle Paleozoic positive area (Ross, 1962), or an area of middle Paleozoic miogeosynclinal sedimentation (Sloss and Moritz, 1951; Scholten, 1957; Thomasson, 1959; Churkin, 1962; and Mapel and Sandberg, 1968). The third interpretation is now known to be most correct. The presence of allochthonous Devonian transitional continental-slope and continental-rise rocks indicates, however, that the Devonian continental edge was not far west of the Fish Creek Reservoir area and perhaps was just east of the present Idaho batholith.

STRATIGRAPHY

Middle and Upper Devonian miogeosynclinal dolomite and sandstone about 450 m (1,500 ft) thick are exposed in an area of about 5.2 km² (2 mi²) of the Fish Creek Reservoir window (fig. 1). The sequence (fig. 2) comprises the Middle Devonian (Eifelian) part of the Carey Dolomite (new), the Middle and Upper Devonian Jefferson Formation, and the Upper Devonian Picabo Formation (new). The Carey Dolomite, of which only the upper 148 m (485 ft) is exposed, consists mostly of light-gray finely crystalline laminated dolomite. The Jefferson Formation, about 245 m (804 ft) thick, disconformably overlies the Carey Dolomite and consists mostly of light-gray,

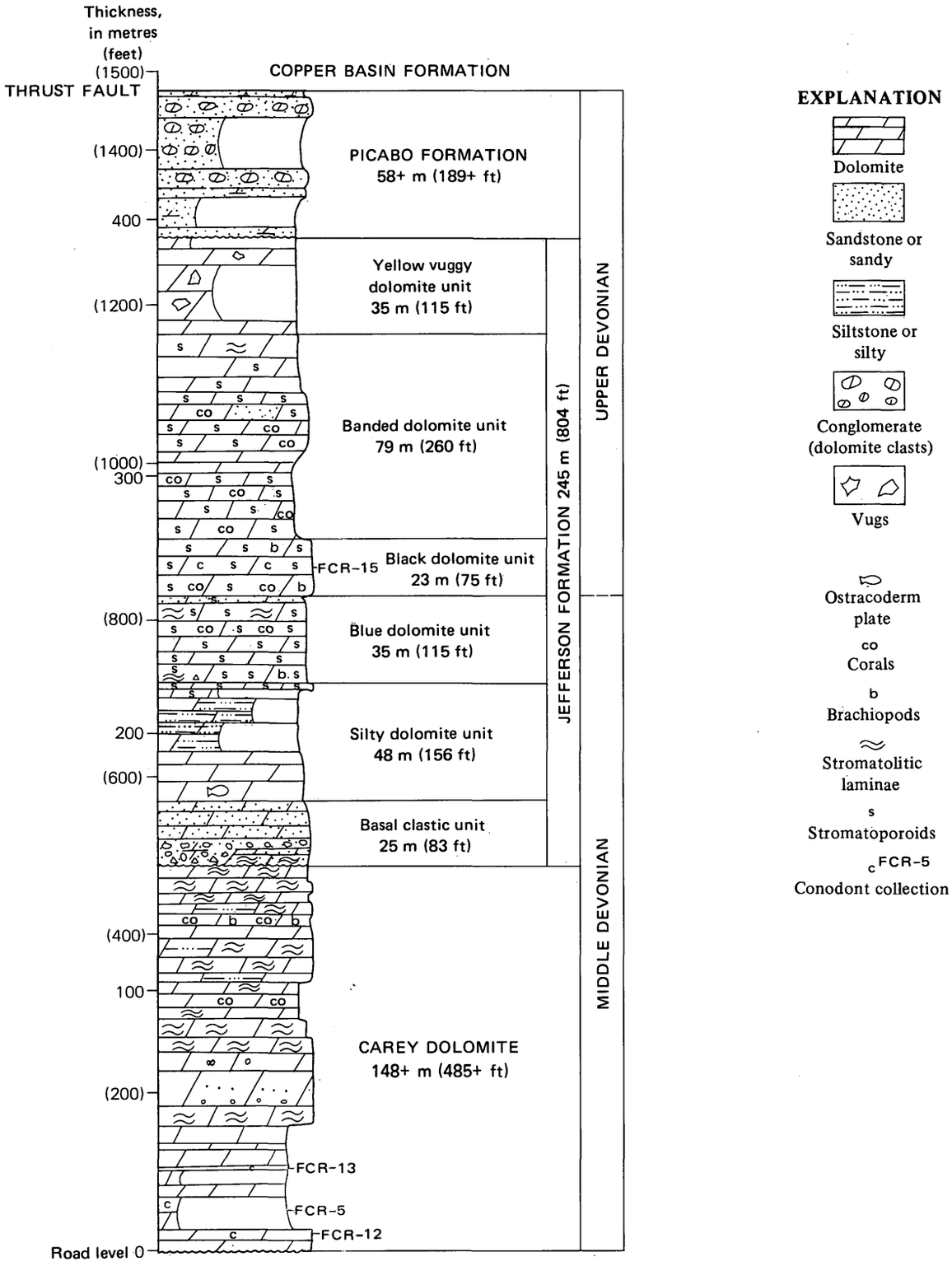

FIGURE 2.—Composite columnar section of Devonian miogeosynclinal rocks in Fish Creek Reservoir area.

grayish-black, and yellowish-brown dolomite, which is finely to coarsely crystalline, sandy, and silty. Stromatoporoids, especially *Amphipora*, are abundant in the Jefferson. Recrystallized corals and brachiopods are abundant in the Jefferson but less common in the Carey. Conodonts were recovered from most samples of both formations.

The Picabo Formation, which has a minimum

thickness of 58 m (189 ft), unconformably overlies the Jefferson Formation and consists of dolomitic quartzose sandstone and sandy dolomite-pebble conglomerate. Larger clasts in the conglomerate appear to be composed almost entirely of fragments of the underlying Jefferson Formation and Carey Dolomite. Although nonfossiliferous, the Picabo is interpreted as Late Devonian on the basis of regional correlations.

Upper Silurian and Lower Devonian transitional fossiliferous limestones and siltstones of the Roberts Mountains Formation are thrust over the shelf (miogeosynclinal) sequence in the southeastern part of the window in an isolated exposure of less than 1.3 km² (0.5 mi²).

All four formations are truncated by the Fish Creek thrust.

Devonian Miogeosynclinal Rocks

Carey Dolomite

Rocks assigned to the Carey Dolomite are exposed on the northeast and east sides of the reservoir in two small areas, which together make up less than 1.3 km² (0.5 mi²). The wide alluvial valley of the East Fork of Fish Creek, which separates the two outcrops, has been partly filled with basalt of the Snake River Group (fig. 1). However, the rocks in both outcrops have identical attitudes, indicating that they are part of the same structural block. In the southeast corner of the Fish Creek Reservoir window, the westward-dipping Carey Dolomite is truncated by quartzite of the Copper Basin Formation lying on the Fish Creek thrust. The formation is named after the town of Carey, 16 km (10 mi) southwest of the reservoir, near the junction of Idaho Highway 23 and U.S. Highway Alternate 93.

The faulted, incomplete type section of the Carey Dolomite (measured section 1, in fig. 1), at least 148 m (485 ft) thick, was measured across the outcrop that forms a peninsula on the northeast side of Fish Creek Reservoir. (See fig. 4 in Skipp and Hall, 1975). The following measured section begins in gently dipping beds just above road level and ends on the ridgetop at the contact with a thick sedimentary conglomerate and breccia, which was later further brecciated by faulting, at the base of the overlying Jefferson Formation.

MEASURED SECTION 1.—*Type section of Carey Dolomite*

[Located in sec. 10 (unsurveyed), T. 1 N., R. 22 E., Blaine County, Idaho]

	Thickness in metres	(feet)
Jefferson Formation:		
Breccia and conglomerate	5.2	(17)
Normal fault separates Carey Dolomite and Jefferson Formation (measured sec. 3) on top of ridge.		
Carey Dolomite:		
Upper unit:		
n. Dolomite, medium-dark-gray to medium-gray, aphanitic to finely crystalline, slightly silty, laminated, medium-bedded. Weathers yellowish gray to light gray; forms steplike outcrop. Basal bed contains fragments of corals and brachiopods	22.9	(75)
m. Dolomite, medium-dark-gray to medium-gray, aphanitic to finely crystalline, slightly silty, medium-bedded. Weathers light olive gray and light brownish gray; partly covered	19.8	(65)
l. Dolomite, algal(?), medium-light-gray to medium-gray, very fine grained to aphanitic, slightly silty, medium-bedded. Weathers light gray to very light olive gray	1.8	(6)
Total upper unit	44.5	(146)
Lower unit:		
k. Dolomite, light-gray, thick-bedded, with three interbeds of medium-dark-gray dolomite. Contains corals and algal-mat structures. Weathers light gray and light olive gray	15.3	(50)
j. Dolomite, light-gray, sugary, finely crystalline, thick-bedded. Contains wavy laminae with birdseye porosity and algal-mat structures	7.0	(23)
i. Dolomite, light-gray, finely crystalline, medium-bedded. Medium-dark-gray bed at base. Thin porous algal-mat dolomite 0.9 m (3 ft) above base. Stylolitic contacts common. Rough light-gray weathering surfaces	4.9	(16)
Normal fault, south side down, trends east, dips 70° S; about 7.6 m (25 ft) vertical displacement.		
h. Dolomite, light-gray to medium-light-gray, finely crystalline, slightly sandy. Weathers light gray to light olive gray; thick bedded to massive; forms cliffs	6.1	(20)
g. Dolomite, light-gray to light-olive-gray, mostly finely crystalline. Some quartz sand streaks in middle part; sparse coarse dolomite sand and granule- to pebble-conglomerate in lower part. Weathers light gray to light olive gray; thick bedded to massive; forms cliffs	14.3	(47)

	Thickness in metres	(feet)
Carey Dolomite—Continued		
Lower unit—Continued		
f. Dolomite, light-gray, finely crystalline, slightly sandy in part. Thick-bedded to massive, cross-beds and thin laminae common; forms lower part of cliff	7.0	(23)
e. Dolomite, light-gray to very light gray, finely crystalline. Weathers light gray; thick bedded to massive: forms steep rubbly slope	6.7	(22)
d. Dolomite, medium-gray to medium-dark-gray and some dark-gray, finely crystalline. Conodont collection FCR–13 from beds correlative with lower 3 m (10 ft). Weathers medium dark gray and light olive gray; thin bedded to massive; forms steep slope	9.1	(30)
c. Partly covered; talus of large angular blocks of black and gray dolomite. Upper 1.5 m (5 ft) is well-exposed light-gray thick-bedded dolomite. Conodont collection FCR–5 from beds correlative with unit c west of line of section	11.3	(37)
b. Covered; colluvium at least 3 m (10 ft) thick forms steep unstable slope above cliff; includes fault zone which separates rocks of units a and c	14.0	(46)
a. Dolomite, light-gray to greenish-gray, medium to coarsely crystalline. Conodont collection FCR–12 from 2 m (6 ft) above the the base. Weathers to light-olive-gray smooth surface; massive; forms small cliff above road	7.6+	(25+)
Total lower unit	103.3+	(339+)
Total measured Carey Dolomite	147.8+	(485+)
Measured section ends at road level; beds below covered by colluvium and lake sediments.		

The Carey Dolomite is predominantly light-gray to medium-dark-gray dolomite that weathers light gray, yellowish gray, and olive gray. It is finely crystalline to aphanitic, has birdseye porosity, and contains common algal-mat laminae and mudchip conglomerates. Quartz sand and silt grains are rare in the dolomite, occurring either as floating grains or as sandy and silty streaks. Minor dolomite sand and granule- to pebble-conglomerate are also present. Stylolitic contacts between beds are common. Beds are commonly 0.3–0.9 m (1–3 ft) thick and some are as much as 3 m (10 ft) thick. Much of the formation is exposed in a series of steplike ledges that produce a talus made up of large rectangular blocks.

Recrystallized corals and brachiopods occur in the uppermost unit (n), and corals and crinoid ossicles are scattered through some of the lower units. The abundant laminae formed by algal mats of blue-green algae suggest that deposition was largely in an intertidal and supratidal marine environment. Some shallow subtidal deposition is indicated by the brachiopod, coral, and conodont faunas.

Seven conodont collections that clearly establish the age of the part of the Carey Dolomite exposed at Fish Creek Reservoir as Eifelian (early Middle Devonian) were made from crinoidal streaks in units a, c, and d in the lower 31 m (100 ft) of the measured section and at two localities on the east side of the reservoir (fig. 3).

The conodont collections, which are listed in table 1, may be divided into two discrete faunas—a polygnathid-pandorinellinid fauna and an icriodid fauna—that may be facies controlled.

Conodont collections FCR–5, 13, and 11, from sparsely crinoidal dolomite or finely to medium crystalline dolomitized encrinite, contain a fauna characterized by the joint occurrence of the platform elements *Icriodus* cf. *I. angustus* (sensu Orr, 1971, pl. 2, figs. 7–9) and *I. corniger* Wittekindt (sensu Carls and Gandl, 1969, pl. 17, fig. 21). Polygnathid and pandorinellinid platform elements are almost completely excluded from this fauna. Conodont collections FCR–3, 4, and 10, on the other hand, are from very coarsely crystalline dolomitized encrinite containing crinoid ossicles as much as 15 mm (0.6 in) in diameter. These collections contain a fauna dominated by polygnathid and pandorinellinid elements notably *Polygnathus perbonus* n. subsp. D Perry, Klapper, and Lenz; *P.* cf. *P. dobrogensis* Mirauta; and *Pandorinellina exigua* n. subsp., without any icriodids.

Both faunas are clearly Eifelian in age, and most likely middle to early Eifelian, but zonal names have not yet been given to Eifelian conodont faunas in North America (Klapper and others, 1971). In Europe, the Eifelian zone to which these faunas most likely would be assigned is the *Spathognathodus bidentatus* or the *Icriodus corniger* Zone (Ziegler, 1971). The polygnathid-pandorinellinid fauna is nearly identical to that in the Eifelian part of the type Salmontrout Limestone of Alaska (H. R. Lane, oral commun., Jan. 15, 1974). Both this fauna and the icriodid fauna contain two-hole crinoid ossicles, which are common in rocks adjacent to the Lower-Middle Devonian boundary in the Western United States.

The exclusive character of the two coeval faunas

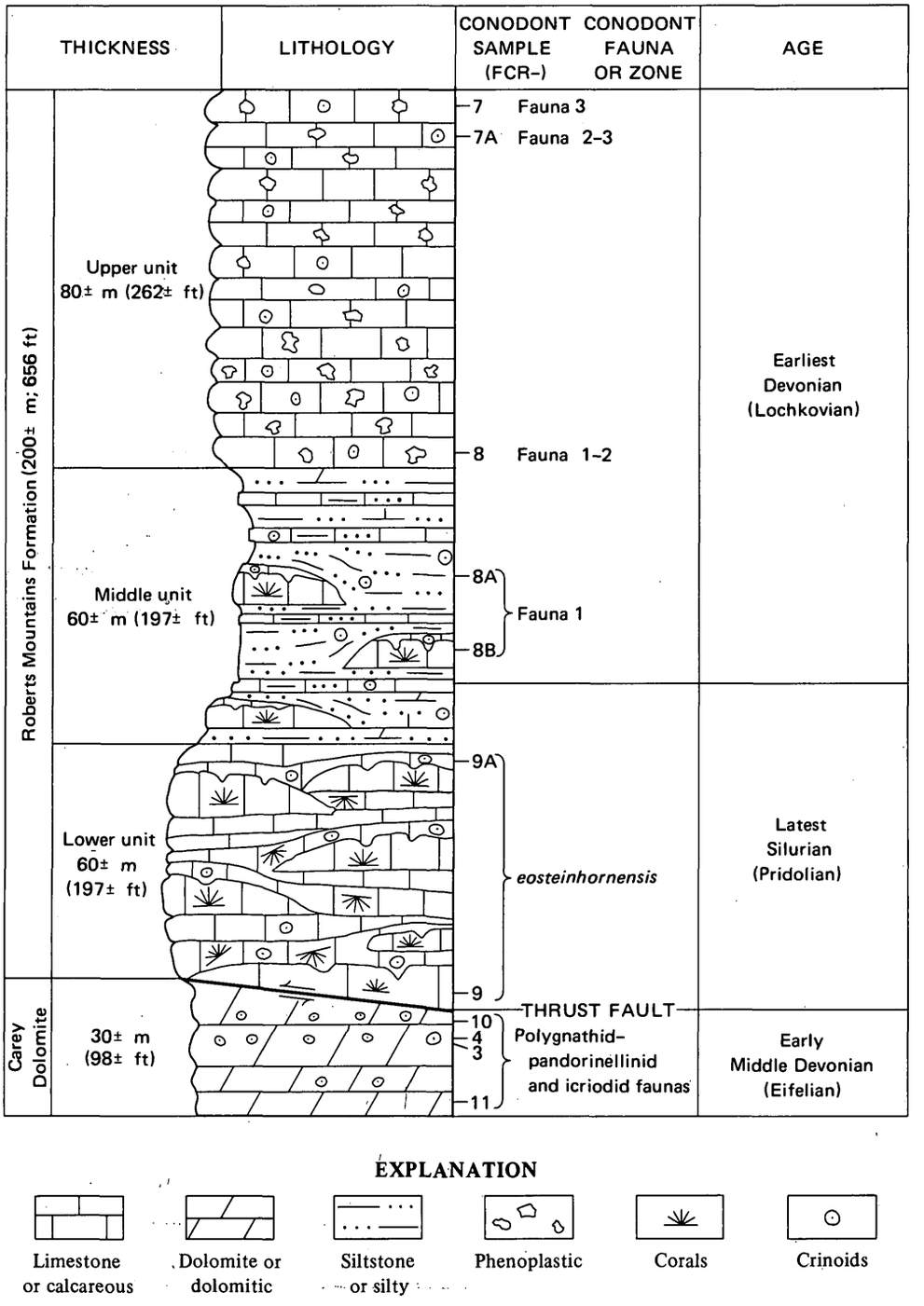

FIGURE 3.—Diagrammatic (partly restored) section showing conodont zonation of faulted sequence along ridge on east side of Fish Creek Reservoir in NW¼ sec. 14 (unsurveyed), T. 1 N., R. 22 E. Numbered faunas are modified from Klapper and others (1971, p. 288, fig. 1). Samples FCR-3, 4 are projected into section from outcrop in NE¼ sec. 11, about 1.4 km (0.9 mi) to northeast.

might be attributed to current sorting and winnowing, but, in view of the different grain sizes of the host rocks, it is more likely that the faunas were controlled by different depositional and (or) ecological facies. The polygnathid-pandorinellinid facies also contains large numbers of belodellids such as occur abundantly in Lower and Middle Devonian reef facies in Nevada. The belodellids are thin-walled, sheathlike

TABLE 1.—*Eifelian (early Middle Devonian) conodont faunas from Carey Dolomite, Fish Creek Reservoir window, central Idaho*

[Arranged in relative stratigraphic succession from left to right. Collecting localities shown in fig. 1]

	Number of specimens from collection FCR–						
	12	5	13	11	3	4	10
Icriodus cf. *I. angustus* Stewart and Sweet (sensu Orr, 1971, pl. 2, figs. 7–9)	--	20	11	24	---	---	---
I. corniger Wittekindt (sensu Carls and Gandl, 1969, pl. 17, fig. 21)	--	5	8	12	---	---	---
Pandorinellina exigua n. subsp	2 (?)	1 (?)	--	--	12	11	26
Polygnathus perbonus n. subsp. D Perry, Klapper, and Lenz	21 (?)	--	--	--	12	6	---
P. cf. *P. dobrogensis* Mirauta	--	--	--	--	8	4	2
P. costatus costatus Klapper	--	1 (?)	--	--	---	---	2
P. angustipennatus Bischoff and Ziegler	--	--	--	--	---	---	5
P. intermedius (Bultynck)	--	--	--	--	---	---	2
Ozarkodina denckmanni Ziegler	4	--	--	--	1	3	---
O. n. sp. A Uyeno	--	--	--	--	---	2	5
"Spathognathodus" n. sp	--	1	--	--	---	---	---
Belodella devonica (Stauffer)	3	4	--	2	12	21	490
B. sp	5	--	--	--	13	10	---
Neopanderodus sp. and *Panderodus* sp	22	--	--	--	141	76	208
Ramiform elements	7	4	3	--	26	31	46
Simple cones	--	1	1	1	---	---	1
Total specimens	64	37	23	39	225	164	787
Specimens per kilogram	20	13	7	56	69	66	168

forms, which normally would not be sorted together with the thicker, heavier polygnathids and pandorinellinids. Consequently, the polygnathid-pandorinellinid facies is believed to represent reef or bioherm talus. The icriodid facies probably represents normal shallow-water subtidal deposition such as might occur between influxes of reef or bioherm talus.

The seventh and lowest collection FCR–12, is from a highly altered, medium to coarsely crystalline dolomite situated only about 25 m (82 ft) from a basalt flow of the Snake River Group. Alteration of the dolomite is attributable either to its proximity to the flow or to a dike at depth. The conodonts are badly etched and intruded by crystals of limonite (after pyrite pyritohedrons) and dolomite. Exact determinations of the conodonts and of the original rock type are difficult, but, clearly, collection FCR–12 should belong to the polygnathid-pandorinellinid facies.

Sparse conodont faunas, including a new species of *Icriodus*, from the Carey Dolomite at Timbered Dome window indicate that the formation extends below the base of the Middle Devonian and includes beds of late Early Devonian (probably Emsian) age in its lower part.

Jefferson Formation

The Middle Devonian (Givetian) to Upper Devonian (Famennian) Jefferson Formation, largely dolomite, is subdivided into six stratigraphic units which have a total thickness of about 245 m (804 ft). Three partial sections (measured secs. 2, 3 and 4, fig. 1) on the north side of the reservoir were measured and composited to provide the following stratigraphic summary:

	Thickness in metres (feet)	
Yellow vuggy dolomite unit	35	(115)
Banded dolomite unit	79	(260)
Black dolomite unit	23	(75)
Blue dolomite unit	35	(115)
Silty dolomite unit	48	(156)
Basal clastic unit	25	(83)
Total Jefferson Formation	245	(804)

The basal contact of the Jefferson Formation with the underlying Carey Dolomite is not exposed, but the two formations are separated by only 0.9 m (3 ft) of cover at the base of measured section 2. The contact is presumed to be disconformable on the basis of the abrupt change in rock types across the short covered interval and the presence of reworked fragments and pebbles of Carey Dolomite in the basal clastic unit of the Jefferson.

The basal clastic unit is 25 m (83 ft) thick in section 2 and 35 m (115 ft) thick in section 3. The lower 4.5 m (15 ft) is medium-gray dolomite breccia and sandy dolomite conglomerate, which weather light gray to light olive gray. Poorly sorted dolomite fragments in the breccia are as much as 0.6 m (2 ft) in diameter, perhaps larger, and they are angular to well rounded. The larger fragments are laminated algal dolomite. Along strike the breccias merge with undisturbed laminated beds and interbedded rounded dolomite pebble- and cobble-conglomerate. Rounded dolomite fragments are as large as 12.7 cm (5 in) in diameter and resemble Carey Dolomite. Beds above the lower 4.5 m (15 ft) are sandy, generally laminated, dolomite and dolomitic sandstone, which is commonly crossbedded, and have minor dolomite granule-to pebble-conglomerate. Blue-green algae were important carbonate sediment binders throughout deposition of this unit. Near the top, small stromatolitic mounds 2.5–5 mm (0.1–0.2 in) in length and 12–25 mm (0.5–1 in) in height are present, indications of primary porosity are common, and penecontemporaneous slump structures occur locally within the laminated beds. These highest beds of the basal clastic unit were laid down in a dominantly tidal flat environment much like that represented by the upper part of the underlying Carey Dolomite. Brackish water channels with

terrigenous sources intermittently cut across the tidal flats and deposited thin sheets and lenses of sand and conglomerate. The dolomite fragments appear to have been locally derived, whereas the sand had a more distant origin.

The silty dolomite unit ranges in thickness from 20 m (66 ft) in measured section 2 to 48 m (156 ft) in measured section 3. A breccia zone representing a near-bedding-plane fault is present at the top of the unit in measured section 2, so the greater thickness is used in the composite section (fig. 2). Medium-gray to medium-dark-gray finely crystalline silty dolomite, much of it laminated and some with small-scale festoon crossbedding, and minor dolomitic quartz siltstone make up most of the unit. Silt is not present in all the dolomite beds. The unit characteristically weathers light olive gray or light gray. Molds of brachiopods and corals filled with secondary dolomite are common in some beds. Small stromatoporoids, *Amphipora*, are extremely abundant in thin beds scattered through the middle and upper parts of the unit. An ostracoderm fish plate was identified about 4.5 m (15 ft) above the base of the unit. Part of this unit was deposited in a tidal-flat environment. The presence of bony fish, corals, brachiopods, and stromatoporoids, however, suggests shallow subtidal deposition for other parts. The silt indicates a less active or more distant terrigenous source for this unit than for the underlying unit.

The blue dolomite unit ranges in thickness from 35 m (115 ft) in section 2 to 44 m (145 ft) in section 3 and is made up of alternating beds, 0.6–3 m (2–10 ft) thick, of medium-gray to medium-dark-gray finely crystalline dolomite. Medium-gray beds weather light olive gray and medium-dark-gray beds weather medium dark gray. Beds of algal laminae about 0.6 m (2 ft) thick are common. A few thin sedimentary breccia beds, in which breccia fragments are generally less than 12 mm (0.5 in) across, are present near the base. Large recrystallized stromatoporoids as much as 7.6 cm (3 in) across are abundant in several zones as thick as 3 m (10 ft) throughout the unit. Brachiopods and small rugose corals, also recrystallized, commonly are associated with the stromatoporoids.

Most of the blue dolomite unit was deposited under shallow subtidal conditions that fostered the growth of thick stromatoporoid banks. For relatively short periods of time, however, subtidal conditions alternated with intertidal conditions to allow formation of thin zones of algal laminae.

The black dolomite unit forms a conspicuous ledge, 23 m (75 ft) thick (fig. 2). The dolomite is predominantly grayish black and finely crystalline. It weathers grayish black, although a white caliche coating characterizes the outcrop. Minor light-gray and medium-dark-gray dolomite is present in beds 0.3–1.5 m (1–5 ft) thick. Algal laminae were not seen. Abundant recrystallized stromatoporoids including *Amphipora*, brachiopods, and corals weather out medium gray or brownish gray on the grayish-black surfaces. This unit, which comprises a series of stromatoporoid banks, was deposited entirely under shallow subtidal conditions. Conodont collection FCR–15 from the upper part of the unit in measured section 2 yielded a sparse, poorly preserved conodont fauna composed mainly of polygnathids with a few ramiform elements. The polygnathids are mainly *Polygnathus xylus* Stauffer but include a few specimens of a new species that has a platform weakly ornamented along the margins as in *P. decorosus* or *P. dubius* but with a short, very high free blade and a slitlike pit. This new species is unlike any known Middle Devonian species but resembles in evolutionary development some Late Devonian (Frasnian or younger) species. Consequently, the Middle-Upper Devonian boundary is tentatively placed at the base of the black dolomite unit, although it may be somewhat lower or higher.

The banded dolomite unit, approximately 79 m (260 ft) thick, was measured in section 2, where it forms a long yellowish slope above the prominent ledge of the black dolomite unit. The banded dolomite unit contains a great variety of dolomite types and colors. The lower 35 m (115 ft) is medium-bedded to massive, fossiliferous, partly calcitic dolomite, ranging in color from pale yellowish brown to medium dark gray and in texture from finely to medium crystalline. Coarsely crystalline pale-yellowish-brown calcite spar commonly fills fossil molds. Large stromatoporoids, as much as 7.6 cm (3 in) across, and corals are the major biota.

The upper part of the banded dolomite unit contains light-brownish-gray to grayish-black mottled, finely to coarsely crystalline dolomite in beds 0.3–3 m (1–10 ft) thick. The coarsely crystalline beds have been altered diagenetically. Laminated beds are present, and commonly they are sandy and silty. Recrystallized stromatoporoids and corals are abundant. The grayish-black beds are identical to those in the black dolomite unit below and indicate a similar shallow subtidal depositional environment. Associated thin laminated beds, however, indicate fluctuating subtidal to intertidal deposition.

The yellow vuggy dolomite unit, about 35 m (115 ft) thick, is poorly exposed in both measured sections 2 and 4 (fig. 1), where it forms a pale-yellowish-brown slope. The dolomite is pale yellowish brown, grayish

orange, light gray, and medium gray, and it weathers dark yellowish orange to pale yellowish brown and, in part, medium gray. Medium-gray beds exposed in the lower 15.2 m (50 ft) are laminated and fine grained. The rest of the unit appears to be medium to coarsely crystalline with very coarse spar in numerous vugs and cavities. Bedding is mostly massive; a 6-m (20-ft)-thick bed is present near the top of the unit. The contact of the yellow vuggy unit with the overlying sandstones is covered.

Picabo Formation

The Picabo Formation of Late Devonian age is named for a small community, Picabo, about 24 km (15 mi) southwest of Fish Creek Reservoir. The following type section is present in measured section 4 (fig. 1), where the Picabo has a minimum thickness of 58 m (189 ft).

MEASURED SECTION 4.—*Type section of Picabo Formation*

[Located in the NE¼ sec. 10 (unsurveyed), T. 1 N., R. 22 E., Blaine County, Idaho]

	Thickness in metres	(feet)
Copper Basin Formation:		
Iron-stained laminated quartzite and light-gray argillite.		
Thrust fault.		
Picabo Formation:		
Sandstone, calcareous, light-gray to pale-red, very fine to fine-grained; thin bedded; in part laminated. Weathers pale yellowish brown	1.5+	(5+)
Dolomite conglomerate and dolomitic sandstone, interbedded, medium-light-gray to pale-yellowish-brown, sandy; weathers mostly pale yellowish brown. Upper 7.6 m (25 ft) forms ledge composed of 60 percent conglomerate and 40 percent sandstone. Rounded pebbles, as much as 10 cm (4 in) in diameter, are light-gray to grayish-black dolomite. Matrix is fine- to medium-grained dolomitic sandstone. Interbedded dolomitic sandstone in beds 0.9–1.5 m (3-5 ft) thick is medium light gray, fine grained, and quartzose. Laminae formed by quartz sand concentrations common; load casts common; crossbedding rare. Middle part covered; float is laminated dolomitic sandstone. Lower part is 6-(20-ft)-thick massive bed of sandy dolomite conglomerate as described above; forms moderately steep slope	36.6	(120)
Quartzitic sandstone and dolomite. Interval largely covered but float is medium-light-gray fine-grained laminated quartzitic sandstone weathering medium gray. Upper 3 m (10 ft) is quartzitic, medium-light-gray, calcareous, laminated, fine-grained sandstone weathering light olive gray; interbedded with laminated sandy light-gray and light-yellowish-gray dolomite. Basal 3.0 m (10 ft) is interbedded pale-red, calcareous, fine-grained sandstone and medium-gray fine-grained quartzitic sandstone, forming moderately steep slope	19.5	(64)
Total measured Picabo Formation	57.6+	(189+)
Jefferson Formation:		
Covered interval	3.0	(10)
Dolomite, grayish-orange to moderate-brown, finely to coarsely crystalline, weathers dark yellowish orange	6.1+	(20+)

The base of the Picabo Formation is covered, but the attitude of higher beds appears to be concordant with that of the Jefferson Formation. Regional evidence, however, suggests that the base of the Picabo overlies an unconformity (Sandberg and others, 1975). The top of the formation is cut off by the Fish Creek thrust fault, which brings rocks of the Copper Basin Formation over the Picabo and other Devonian miogeosynclinal formations. Only about a quarter of the Picabo is exposed and the rest is covered by talus. The bottom 19.5 m (64 ft) and top 1.5 m (5 ft) or more are predominantly dolomitic sandstone, not unlike some clastic interbeds in the Jefferson of the Lost River Range. The lithology of conglomerate interbeds in the middle part of the Picabo, however, does not resemble any part of the Jefferson in that area.

The middle 36.5 m (120 ft) of the Picabo Formation constitutes a distinctive polymict conglomerate-sandstone unit (fig. 4) unlike any previously described in miogeosynclinal rocks at this stratigraphic level in central Idaho. However, the conglomerate resembles parts of the Devonian Stansbury, Beirdneau, and Victoria Formations as well as the lower part of the Devonian and Mississippian Leatham Formation in northern Utah and southeastern Idaho. The conglomerate of the Picabo is medium light gray to pale yellowish brown and weathers mostly pale yellowish brown. Pebbles appear to be entirely dolomite and are bimodal. The larger pebbles are well rounded, subtabular, and as much as 12.5 cm (5 in) in diameter. The smaller pebbles average about 6 mm (0.25 in) in diameter and are commonly subrounded. The dolomite that makes up the pebbles ranges in color from light gray to grayish black and in texture from aphanitic to coarsely crystalline. All the pebbles can be matched lithologically with beds in the underlying Jefferson Formation and Carey Dolomite.

Imbrication of the pebbles is indicative of locally eastward-flowing currents. Long axes of the larger

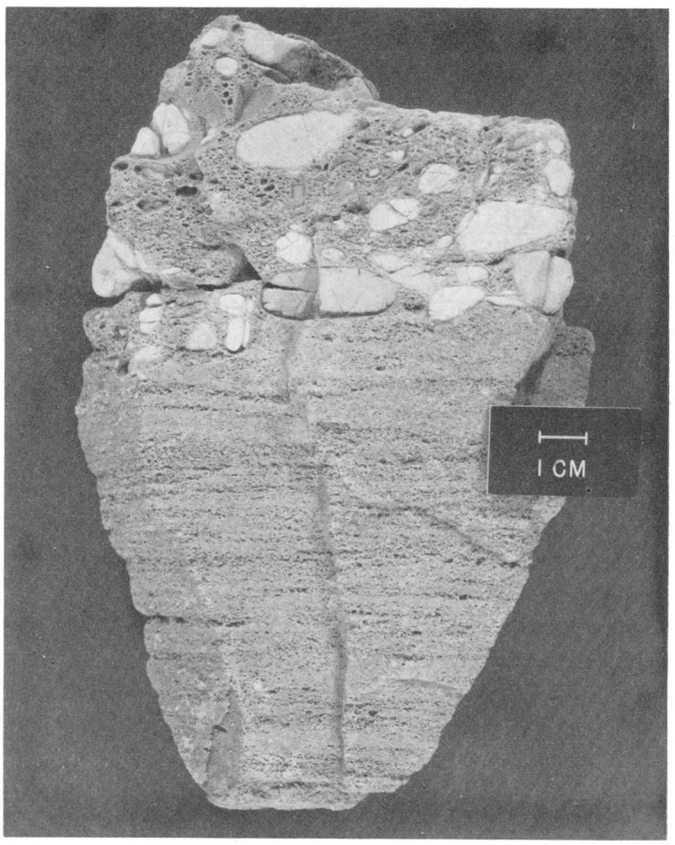

FIGURE 4.—Weathered slab from Picabo Formation showing interbedding of fine-grained dolomitic quartz sandstone with sandy dolomite conglomerate composed of large rounded tabular dolomite pebbles. Pebbles are lithologically identical to beds in underlying Jefferson Formation and Carey Dolomite.

pebbles are oriented subparallel to bedding. Many pebbles show a low-angle, westward-dipping imbrication, and a few are inclined as much as 60° to the west.

The polymict conglomerates apparently had more than one source. The larger dolomite fragments must have had a nearby, unstable source. The rounded pebbles probably are marine gravels related to a transgressing beach. The smaller angular pebbles are similarly derived but were carried farther out from the source as seas deepened across the area. Sand makes up more of the volume of the exposed sequence than do the dolomite fragments and probably was derived from a different and more distant source terrane than that which produced the dolomite clasts. Lack of crossbedding suggests final deposition beyond major shore currents.

The conglomerate in the Picabo Formation provides evidence of local Late Devonian uplift of the shelf sequence in or near the Fish Creek Reservoir area. Probably this local uplift was associated with an early phase of Antler orogeny to the west. Similar local Late Devonian uplift is well documented in northern Utah in the vicinity of the Stansbury uplift (Rigby, 1958; Morris and Lovering, 1961; Roberts and others, 1958; Poole and others, 1967, p. 879). More recently another local uplift has been recognized in east-central Idaho in the southern Beaverhead Mountains (Sandberg and others, 1975). There, at Long Canyon, a Late Devonian unconformity on the Jefferson Formation is overlain by the Sappington Member of the Three Forks Formation (Sandberg and others, 1972, fig. 2 and p. 194). The Sappington is mostly very late Devonian in age, but locally, as at the type locality, it may include lowermost Mississippian beds at the top (Sandberg and others, 1972). Although the Picabo is nonfossiliferous, it is presumed to be very late Devonian in age because it occupies the same stratigraphic position as sandstone lag beds at the base of the Sappington. If fossil evidence were found, the Picabo likewise might be demonstrated to range into the lowermost Mississippian.

Transitional Rocks

Roberts Mountains Formation

A sequence of Upper Silurian and Lower Devonian fossiliferous reef limestone, platy calcareous and dolomitic siltstone, and limestone phenoplast conglomerate is exposed in an area of less than 1.3 km^2 (0.5 mi^2) on the east side of the Fish Creek Reservoir window (fig. 1). This sequence of transitional rocks lies in thrust contact on both the miogeosynclinal Carey Dolomite and Jefferson Formation within the window, and is overridden by quartzite, argillite, and conglomerate of the Copper Basin Formation lying on the Fish Creek thrust.

The sequence of Upper Silurian and Lower Devonian transitional rocks, which is precisely dated by a sequence of conodont zones (fig. 3), is here assigned to the Roberts Mountains Formation on the basis of similar age, lithologic character, and paleotectonic setting to the type Roberts Mountains Formation. The Roberts Mountains was originally defined in central Nevada by Merriam (1940, p. 11, 12). A sequence of Middle Silurian chert and silty slabby limestone in the Wildhorse window to the northwest has also been equated to the Roberts Mountains Formation by Dover and Ross (1975). That sequence, which is at least 40 m (130 ft) thick, is older than any part of the Roberts Mountains exposed in the Fish Creek window and must represent a lower part of the formation.

The Roberts Mountains Formation, about 200 m (656 ft) thick in the Fish Creek Reservoir window,

comprises three lithologically distinct units, as shown in figure 3. The lower and upper units, the outcrops of which are separated by several normal faults, have been measured. The thickness of the middle unit, which, because of faulting and folding, is not totally exposed at any one locality, has been estimated from field observations. The conodont evidence demonstrates that the faulted exposures represent a nearly continuous stratigraphic succession.

The lower unit, about 60 m (197 ft) thick, is predominantly medium-gray, medium- to coarse-grained coralline patch-reef limestone. A sample from one of the lowest beds of reef limestone yielded conodont collection FCR–9 (fig. 3). The largest individual coral colonies, as much as 3 m (10 ft) long and 1 m (3 ft) high, are *Favosites*. Smaller coral heads of *Favosites* and other genera, about 0.3 m (1 ft) in diameter, are as commonly found overturned as they are found in growth position, suggesting that they have been rolled by current or wave action. Interbedded with the reef limestones and commonly infiltrating their irregular tops are thin beds of medium-dark-gray, coarse to very coarse encrinite. One of these encrinite beds was sampled for conodonts and yielded collection FCR–9A (fig. 3).

The middle unit, estimated to be 60 m (197 ft) thick, is gradational with the underlying unit. The lower part contains a few lenticular beds of reef limestone similar to those in the lower unit. The beds of reef limestone in this unit are also overlain by darker, coarser encrinite, which fills irregularities in their upper surfaces, as shown in figure 5. The bed in figure 5 with the painted sample designation FCR–8A yielded an important condont collection. Laterally and vertically the coral reef limestones give way to platy, yellowish-brown silty limestone and calcareous siltstone that commonly are irregularly dolomitized and weather dark yellowish orange and light brown. These platy beds contain abundant reef talus, especially adjacent to abrupt terminations of reefs.

The upper unit, about 80 m (262 ft) thick, is dominantly a fossiliferous phenoplast conglomerate or intraformational sedimentary limestone breccia. It crops out along the ridge crest and is truncated toward the south by the Copper Basin Formation above the Fish Creek thrust. The phenoplast conglomerate consists of subangular to subrounded fragments, as much as 25 cm (10 in) in diameter, of medium-gray-weathering bioclastic limestone and encrinite in a yellowish-orange-weathering fossiliferous lime-mud matrix (fig. 6).

Fossils are common in all three units and the biota includes, in addition to the ubiquitous pelmatozoan ossicles, such diverse groups as colonial tabulate corals, finely branching colonial corals, solitary rugose corals, gastropods, tentaculitids, trilobites, brachiopods, primitive calcareous foraminifers, calcareous blue-green algae, and conodonts. The age assignment is based largely on the precise conodont zonation, and is supported by determinations of corals and brachiopods.

FIGURE 5.—Outcrop of lower (Upper Silurian) part of Roberts Mountains Formation showing irregularly surfaced reef limestone overlain and infiltrated by darker encrinite, on which is painted "FCR–8A" that designates conodont collection.

The age of the Roberts Mountains Formation in the Fish Creek Reservoir window is latest Silurian (Pridolian) to earliest Devonian (Lochkovian) based on seven conodont collections representing a nearly complete succession from the *eosteinhornensis* Zone to Fauna 3 of Klapper and others (1971, p. 288 and fig. 1). The dating of individual collections is discussed below and is shown by figure 3.

Conodont collections FCR–9 and 9A are from reef limestone and encrinite, respectively, in the lower unit. They contain all the elements of the multielement species *Ozarkodina eosteinhornensis* (Walliser) as well as fragments of several characteristically Late Silurian species, including *O.* cf. *O. gaertneri* and a late morphotype of *O. confluens* (Branson and Mehl). These collections are assigned to the latest Silurian *eosteinhornensis* Zone.

Conodont collections FCR–8B and 8A from the lower part of the middle unit contain a fauna characterized by the joint occurrence of the multielement species *Icriodus woschmidti* Ziegler and *Ozarkodina remscheidensis* (Ziegler). This association, which

FIGURE 6.—Phenoplast conglomerate in upper (Lower Devonian) part of Roberts Mountains Formation. Subangular to subrounded fragments of crinoidal limestone are set in penecontemporaneous fossiliferous lime-mud matrix. Conodont collections FCR–7 and 7A are from this conglomerate, which is interpreted to be a reef-flank deposit.

characterizes Fauna 1 of Klapper and others (1971), marks the base of the Devonian in North America. Consequently, the Silurian-Devonian boundary probably is located in the basal part of the middle unit below collection FCR–8B and above collection FCR–9A near the top of the lower unit (fig. 3).

Three conodont collections were made from the phenoplast conglomerate of the upper unit. The lowest collection, FCR–8, contains fragmentary *Icriodus woschmidti* and *Ozarkodina remscheidensis* together with abundant *O.* n. sp. E Klapper and Murphy (1975, pl. 7, figs. 6, 9, 10), which characterizes Faunas 1, 2 in the upper part of the type Roberts Mountains Formation (G. Klapper, oral commun., Feb. 2, 1973). Sample FCR–7A, which is poorly preserved and fragmentary, contains as its most important constituents *O. remscheidensis*, *O. excavata excavata* (Branson and Mehl), and *O. stygia* (Flajs). This collection is assigned a faunal designation between those of collections FCR–8 below and FCR–7 above. Collection FCR–7 from the highest exposed beds of the upper unit contains *O. excavata excavata* and *O. stygia* together with *O.* n. sp. D Klapper (*in* Lenz and Pedder, 1972, p. 15, 21), which according to Klapper (oral commun., Feb. 2, 1973) is widespread in Fauna 3 of Klapper and others (1971) between Nevada and the Canadian Arctic in western North America.

Corals from the lower and middle units of the Roberts Mountains Formation at fossil localities 8784–SD and 8785–SD (fig. 1) include *Favosites* sp., *Aulopora* sp., *Asthenophyllum*? sp., and *Cladopora* sp. (W. A. Oliver, Jr., written commun., Dec. 15, 1971). Megafossils from the same bed as conodont collection FCR–9 were identified by W. A. Oliver, Jr. (written commun., June 17, 1974), as amphiporoid and massive stromatoporoids, as coral genera, *Alveolites*, *Cladopora*, *Favosites*, *Thamnopora*, and *Neomphyma*?, and as an unnamed genus and species of coral that are described in manuscript by C. W. Merriam from rocks of Late Silurian age. Oliver dated the fauna as Late Silurian. The bed that yielded conodont sample FCR–8 contains *Stylopleura* sp. cf. *S. berthiaumi* Merriam, which is compatible with the Early Devonian age determination based on conodonts (W. A. Oliver, written commun., June 17, 1974).

Silicified brachiopods from the lower unit at fossil localities 8784–SD and 8786–SD (fig. 1) include species of *Cyrtina*, *Howellella*, *Atrypa*, *Isorthis*?, *Glassia*?, and perhaps *Salopina* and *Rhipidomelloides*, all of which support a probable Silurian age (J. T. Dutro, Jr., written commun., Nov. 19, 1971). Silicified brachiopods from the upper unit at the same location as conodont collection FCR–7A include many specimens of *Strophochonetes*, which indicates a general Late Silurian to earliest Devonian age, and a single specimen of *Resserella* (J. T. Dutro, Jr., written commun., May 17, 1974).

Unilocular calcareous foraminifers and blue-green calcareous algae were found in collections 8784–SD and 8785–SD. The foraminifers include ?*Bisphaera* and ?*Cribrosphaeroides*. These forms have not been reported from rocks older than Devonian. Clasts of blue-green algae, *Girvanella*, *Renalcis*, and *Sphaerocodium*, were found in samples associated with the reef limestones. These primitive plants are common in both Silurian and Devonian rocks.

Brachiopods collected by David Budge (identified by J. T. Dutro, Jr., written commun., June 18, 1973)

from the middle unit just north of conodont collection FCR–9A compose an Early Devonian assemblage similar to that in the Lower Devonian part of the Roberts Mountains Formation of Nevada. The assemblage includes *Skenidiodes* sp., *Aesopum* sp., *Salopina* sp., *Leptaena* sp., *Iridostrophia*? sp., *Resserella* sp., *Gypidula*? sp., and *Cryptatrypa*? sp.

The rock types in the Roberts Mountains Formation of the Fish Creek Reservoir window—coral reef limestones, laminated siltstones, and phenoplast conglomerates—are identical to those of the type Roberts Mountains described by Winterer and Murphy (1960), who interpreted them to be reef-flank, offreef, and basin deposits which were laid down in deeper water than age-equivalent dolomites to the east. Several authors (Berry and Boucot, 1970; Johnson and others, 1973) have interpreted the laterally gradational contact between the Roberts Mountains Formation and age-equivalent shelf dolomites in Nevada to represent the edge of the lower and middle Paleozoic continental shelf. East of the Fish Creek Reservoir area in the Lost River Range, shelf equivalents of the Roberts Mountains Formation are absent, inasmuch as an unconformity there separates the Beartooth Butte Formation of Early Devonian (Siegenian) age from the Laketown Dolomite which is of older Silurian age than the lower unit of the Roberts Mountains Formation.

Milligen(?) Formation

Rocks questionably correlative with the lower part of the Milligen Formation of Devonian age (Sandberg and others, 1975) cover an area of about 0.8 km^2 (0.3 mi^2), 4.8 km (3 mi) southwest of the Fish Creek Reservoir window (fig. 1). Steep slopes with scattered ledges of dark-gray siliceous argillite and fine-grained quartzite and black chert make up the outcrop, which represents an incomplete stratigraphic thickness of roughly 90 m (295 ft). Bedding ranges from 0.3 to 1.2 m (1–4 ft) in thickness. The Milligen(?) sequence is mineralized and contains lenses, veinlets, and irregular masses of quartz. Most of the siliceous argillite, although sheared, is too competent to display cleavage. Some thin, less competent interbeds, however, do have well-developed fracture cleavage. The base of the Milligen(?) is not exposed. The top is a sheared and iron-stained zone, 1.0–1.3 m (3–4 ft) thick, with lenses and veinlets of white quartz. The contact with overlying less deformed varicolored calcareous and dolomitic siltstone, gray argillite, and light-brown fine-grained quartzite assigned to the Wood River Formation is interpreted to be a thrust fault.

The type Milligen Formation is considered to be a transitional, not eugeosynclinal, deepwater oceanic sequence deposited at the toe of or not far west of the continental slope. Turbidites and debris flows interbedded with the argillites and quartzites that compose most of the formation appear to have had an eastern continental origin (Sandberg and others, 1975). If the outcrop southwest of the Fish Creek Reservoir window is indeed the Milligen, then deepwater clastic rocks have been thrust into proximity to shallow-water continental-shelf carbonate rocks of the same age in the report area.

CONCLUSIONS

Two Devonian facies—shallow-water continental-shelf (miogeosynclinal) carbonate rocks and continental-shelf edge transitional carbonate rocks—are brought together in the Fish Creek Reservoir window. The shelf-facies rocks, 450 m (1,500 ft) thick, comprise the Lower and Middle Devonian Carey Dolomite (new), the Middle and Upper Devonian Jefferson Formation, and the upper Devonian Picabo Formation (new). The Middle Devonian age of the exposed part of the Carey Dolomite is based on two conodont faunas representing slightly different shallow-water facies. The Picabo Formation consists of dolomitic quartzose sandstone and sandy dolomite-pebble conglomerate containing clasts derived from the underlying Carey Dolomite and Jefferson Formation. It evidences a local Late Devonian uplift of shelf rocks associated with the true Antler orogeny farther west.

Small patches of transitional facies rocks assigned to the Roberts Mountains Formation are thrust over the shelf sequence in the eastern part of the Fish Creek Reservoir window. The Roberts Mountains in the Fish Creek area is precisely dated as latest Silurian (Pridolian) to earliest Devonian (Lochkovian) by a sequence of conodont faunas. It has an estimated thickness of about 200 m (656 ft) and consists of reef limestone, limy siltstone, and limestone phenoplast conglomerate.

About 4.8 km (3 mi) southwest of the window, a third Devonian facies—deepwater oceanic clastic rocks—may be represented by the rocks questionably assigned to the Milligen Formation.

The presence of Devonian shelf rocks in the window extends the limit of the Devonian miogeosyncline at least 50 km (30 mi) farther west at lat 43° 15′ N. in Idaho. Telescoping of the transitional Roberts Mountains and Milligen(?) Formations suggests that the continental margin was not much farther west than the Fish Creek area, perhaps near the east edge of the Idaho batholith (long. 114° 30′ W.).

REFERENCES CITED

Berry, W. B. N., and Boucot, A. J., eds., 1970, Correlation of the North American Silurian rocks: Geol. Soc. America Spec. Paper 102, 289 p.

Carls, Peter, and Gandl, Josef, 1969, Stratigraphie und Conodonten des Unter-Devons der Östlichen Iberischen Ketten (NE-Spanien): Neues Jahrb. Geologie u. Paläontologie Abh., v. 132, no. 2, p. 155–218, pls. 15–20.

Churkin, Michael, Jr., 1962, Facies across Paleozoic miogeosynclinal margin of central Idaho: Am. Assoc. Petroleum Geologists Bull., v. 46, no. 5, p. 569–591.

Dover, J. H., and Ross, R. J., Jr., 1975, Ordovician and Middle Silurian rocks of the Wildhorse window, northeastern Pioneer Mountains, central Idaho: U.S. Geol. Survey Jour. Research v. 3, no. 4, p. 431–436.

Johnson, J. G., Boucot, A. J., and Murphy, M. A., 1973, Pridolian and Early Gedinnian age brachiopods from the Roberts Mountains Formation of central Nevada: California Univ. Pubs. Geol. Sci., v. 100, 75 p.

King, P. B., compiler, 1969, Tectonic map of North America: U.S. Geol. Survey, scale 1:5,000,000.

Klapper, Gilbert, and Murphy, M. A., 1975, Silurian-Lower Devonian conodont sequence in the Roberts Mountains Formation of central Nevada: California Univ. Pubs. Geol. Sci., v. 111, 62 p., 12 pls.

Klapper, Gilbert, Sandberg, C. A., Collinson, Charles, Huddle, J. W., Orr, R. W., Rickard, L. V., Schumacher, Dietmar, Seddon, George, and Uyeno, T. T., 1971, North American Devonian conodont biostratigraphy, *in* Sweet, W. C., and Bergström, S. M., eds., Symposium on conodont biostratigraphy: Geol. Soc. America Mem. 127, p. 285–316, 6 figs.

Lenz, A. C., and Pedder, A. E. H., 1972, Lower and Middle Paleozoic sediments and paleontology of Royal Creek and Peel River, Yukon, and Powell Creek, N.W.T.: Internat. Geol. Cong., 24th, Montreal 1972, Field Excursion A–14 Guidebook, 43 p.

Mapel, W. J., and Sandberg, C. A., 1968, Devonian paleotectonics in east-central Idaho and southwestern Montana, *in* Geological Survey research 1968: U.S. Geol. Survey Prof. Paper 600–D, p. D115–D125.

Merriam, C. W., 1940, Devonian stratigraphy and paleontology of the Roberts Mountains region, Nevada: Geol. Soc. American Spec. Paper 25, 114 p.

Morris, H. T., and Lovering, T. S., 1961, Stratigraphy of the East Tintic Mountains, Utah, *with a section on* Quaternary deposits, by H. D. Goode: U.S. Geol. Survey Prof. Paper 361, 145 p. [1962].

Orr, R. W., 1971, Conodonts from Middle Devonian strata of the Michigan Basin: Indiana Geol. Survey Bull. 45, 110 p., 6 pls.

Paull, R. A., and Rothwell, B. G., 1973, Miogeosynclinal and transitional Silurian and Devonian rocks, central Pioneer Mountains, south-central Idaho: Geol. Soc. America Abs. with Programs, v. 5, no. 6, p. 500–501.

Poole, F. G., Baars, D. L., Drewes, Harald, Hayes, P. T., Ketner, K. B., McKee, E. D., Teichert, C., and Williams, J. S., 1967, Devonian of the southwestern United States, *in* Oswald, D. H., ed., Internat. symposium on the Devonian System, Calgary. Alberta, Sept. 1967 [Proc.], v. 1: Calgary, Alberta Soc. Petroleum Geologists, p. 879–912.

Rigby, J. K., ed., 1958, Geology of the Stansbury Mountains, Tooele County, Utah: Utah Geol. Soc. Guidebook to the Geology of Utah 13, 134 p.

Roberts, R. J., Hotz, P. E., Gilluly, James, and Ferguson, H. G., 1958, Paleozoic rocks of north-central Nevada: Am. Assoc. Petroleum Geologists Bull., v. 42, no. 12, p. 2813–2857.

Roberts, R. J., and Thomasson, M. R., 1964, Comparison of the late Paleozoic depositional history of northern Nevada and central Idaho, *in* Short papers in geology and hydrology: U.S. Geol. Survey Prof. Paper 475–D, p. D1–D6.

Ross, C. P., 1934, Correlation and interpretation of Paleozoic stratigraphy in south-central Idaho: Geol. Soc. America Bull., v. 45, no. 5, p. 937–1000.

——— 1937, Geology and ore deposits of the Bayhorse region, Custer County, Idaho: U.S. Geol. Survey Bull. 877, 161 p.

——— 1947, Geology of the Borah Peak quadrangle, Idaho: Geol. Soc. America Bull., v. 58, no. 12, p. 1085–1160.

——— 1962, Paleozoic seas of central Idaho: Geol. Soc. America Bull., v. 73, no. 6, p. 769–793.

——— 1963, Geology along U.S. Highway 93 in Idaho: Idaho Bur. Mines and Geology Pamph. 130, 98 p., 7 maps.

Sandberg, C. A., Hall, W. E., Batchelder, J. N., and Axelsen, Claus, 1975, Stratigraphy, conodont dating, and paleotectonic interpretation of the type Milligen Formation (Devonian), Wood River area, Idaho: U.S. Geol. Survey Jour. Research, v. 3, no. 6, p. 707–720.

Sandberg, C. A., and Mapel, W. J., 1967, Devonian of the Northern Rocky Mountains and Plains, *in* Oswald, D. H., ed., Internat. symposium on the Devonian System, Calgary, Alberta, Sept. 1967 [Proc.], v. 1: Calgary, Alberta Soc. Petroleum Geologists, p. 843–877.

Sandberg, C. A., Streel, Maurice, and Scott, R. A., 1972, Comparison between conodont zonation and spore assemblages at the Devonian-Carboniferous boundary in the western and central United States and in Europe: Cong. Internat. de Stratigraphie et de Géologie du Carbonifère, 7th, Krefeld 1971, Compte rendu, v. 1, p. 179–203, 4 pls.

Scholten, Robert, 1957, Paleozoic evolution of the geosynclinal margin north of the Snake River Plain, Idaho-Montana: Geol. Soc. America Bull., v. 68, no. 2, p. 151–170.

Skipp, B. A. L., 1961, Stratigraphic distribution of endothyrid Foraminifera in Carboniferous rocks of the Mackay quadrangle, Idaho, *in* Short papers in the geologic and hydrologic sciences: U.S. Geol. Survey Prof. Paper 424–C, p. C239–C244.

Skipp, Betty, and Hall, W. E., 1975, Structure and Paleozoic stratigraphy of a complex of thrust plates in the Fish Creek Reservoir area, south-central Idaho: U.S. Geol. Survey Jour. Research, v. 3, no. 6, p. 671–689.

Skipp, Betty, and Sandberg, C. A., 1972. Window of Silurian and Devonian miogeosynclinal and transitional rocks, west of Craters of the Moon National Monument, central Idaho: Geol. Soc. America Abs. with Programs, v. 4, no. 6, p. 411.

Sloss, L. L., 1954, Lemhi arch, a mid-Paleozoic positive element in south-central Idaho: Geol. Soc. America Bull., v. 65, no. 4, p. 365–368.

Sloss, L. L., and Moritz, C. A., 1951, Paleozoic stratigraphy of southwestern Montana: Am. Assoc. Petroleum Geologists Bull., v. 35, no. 10, p. 2135–2169.

Thomasson, M. R., 1959, Late Paleozoic stratigraphy and paleotectonics of central and eastern Idaho: Wisconsin Univ. Ph. D. thesis, 288 p.

Umpleby, J. B., 1917, Geology and ore deposits of the Mackay region, Idaho: U.S. Geol. Survey Prof. Paper 97, 129 p.

Winterer, E. L., and Murphy, M. A., 1960, Silurian reef complex and associated facies, central Nevada: Jour. Geology, v. 68, no. 2, p. 117–139.

Ziegler, Willi, 1971, Conodont stratigraphy of the European Devonian, *in* Sweet, W. C., and Bergström, S. M., eds., Symposium on conodont biostratigraphy: Geol. Soc. America Mem. 127, p. 227–284, 6 charts.

Jour. Research U.S. Geol. Survey
Vol. 3, No. 6, Nov.–Dec. 1975, p. 707–720

STRATIGRAPHY, CONODONT DATING, AND PALEOTECTONIC INTERPRETATION OF THE TYPE MILLIGEN FORMATION (DEVONIAN), WOOD RIVER AREA, IDAHO

By CHARLES A. SANDBERG; WAYNE E. HALL, JOHN N. BATCHELDER; and CLAUS AXELSEN;[1] Denver, Colo.; Menlo Park, Calif.; Denver, Colo.

Abstract.—The Milligen Formation at and near its type locality in the Wood River area is considerably older than and unrelated to rocks of Early Mississippian age called Milligen Formation in the Lost River Range and other ranges of east-central Idaho. Conodont faunas were found in limestones of a thin upper member of the sparsely fossiliferous marine Milligen Formation in its principal reference section at Milligen Gulch, at Fisher Canyon, and near Bellevue, Idaho. The faunas include indigenous conodonts here assigned to the early Late Devonian (early Frasnian) Lower and Middle *Polygnathus asymmetricus* Zones, and reworked conodonts derived from several Middle and Early Devonian conodont zones. An underlying much thicker argillite member of the Milligen contains fewer limestones, but a thin encrinite interbed near the middle of the member yielded early Middle Devonian (Eifelian) conodonts. This lower member probably represents most of Middle and Early Devonian time. Although its base is nowhere exposed in the Wood River area, the Milligen is inferred to have been deposited on the Silurian Trail Creek Formation, which crops out just to the east in the Pioneer Mountains. The age of the Milligen is therefore wholly Devonian and the highest fossiliferous beds are no younger than early Late Devonian. Reworked Middle and Early Devonian conodonts in limestone turbidites of the upper member of the Milligen Formation are identical to conodonts found in shelf (miogeosynclinal) carbonate rocks farther east. A postulated eastern source for the turbidites is supported by new data on the distribution, thickness, and tectonic facies of Devonian rocks that suggest the presence of a Late Devonian ridge on the continental shelf east of the Milligen depositional area. The Milligen Formation was intensely folded and was emergent during most of the Mississippian time when it formed part of the Antler Highlands, which shed flysch sediments eastward into the Copper basin. The Wood River Formation of Pennsylvanian and Permian age was then deposited over a subdued topography on the Milligen Formation. The Hailey Conglomerate Member at the base of the Wood River filled many irregularities in the surface. This depositional contact later was largely destroyed and the contact between the Milligen and Wood River is now a regional thrust fault at most places.

Dark-gray fine-grained argillaceous rocks of supposed Mississippian and Devonian(?) age in the Wood River area were named the Milligen Formation by Umpleby, Westgate, and Ross (1930, p. 25). The type locality is Milligen Gulch (formerly Milligen Creek), about 10 km (6.2 mi) southeast of Ketchum, Idaho, and the principal reference section is here considered to be the poor exposures extending from creek level to the divide east of the creek. Only one fossil locality has been described previously from the Milligen Formation of the Wood River area. A collection of badly broken, rolled corals, stromatoporoids, and crinoids, to which Edwin Kirk tentatively assigned a Devonian age, was reported from the divide east of Milligen Gulch by Umpleby, Westgate, and Ross (1930, p. 28). However, Ross (1934, p. 972; 1962, p. 384) considered these fossils to be reworked and discounted their value for dating the Milligen, which he considered to be of Mississippian age. We interpret the supposedly reworked fossils to have come from a turbidite bed or a possible debris-flow deposit in the upper part of the Milligen and to represent the true Devonian age of the formation.

The name Milligen Formation was extended by Ross (1934) to include dark-gray argillite in the Lost River Range and in mountain ranges to the east in Idaho on the basis of its similar lithologic character and stratigraphic position to the Milligen in the Wood River area. Most later workers accepted Ross' correlation, and the term Milligen Formation became commonly used for the westward-thickening wedge of argillite that overlies the Upper Devonian Trident Member of the Three Forks Formation. The base of this supposed Milligen Formation in the Lost River Range was dated as Early Mississippian (Kinderhookian) on the basis of conodonts assigned to the Lower *Siphonodella crenulata* Zone by Sandberg, Mapel, and Huddle (1967), and slightly higher beds were assigned to the overlying Kinderhookian zone, the Upper *S. crenulata* Zone, by Sandberg (in Macqueen and Sandberg, 1970, p. 51). The presence of a heretofore unreported conodont fauna containing the form-species *Hindeodella segaformis* Bischoff now dates the upper part of the Lost River Range Milligen as Osagean. Thus, the Milligen of Ross (1934) in the Lost River Range is entirely Early Mississippian

[1] Bobcat Oil Company.

(Kinderhookian and Osagean). Dover (1969, p. 28, 29) recognized the problem of correlation of the type Milligen Formation in the Wood River area with that in eastern Idaho, where continuity of outcrop with the type area cannot be established. He proposed restricting the Milligen Formation to the broad northwest-trending belt that extends through Milligen Gulch.

In the absence of contradictory paleontologic data in the type locality, an Early Mississipian age assignment was advocated by Sandberg, Mapel, and Huddle (1967) for all rocks called Milligen Formation in Idaho. Usage of Milligen Formation in this sense has become almost universal in recent years with acceptance by subsequent workers (for instance, Mamet and others, 1971; Paull and others, 1972). Our present study demonstrates, however, that although an Early Mississippian assignment is valid for most of the rocks heretofore called Milligen east of the Wood River area, it is invalid for the Milligen in the Wood River area. Furthermore, some of the rocks previously included in the basal part of the Milligen in the Beaverhead Mountains (Sandberg and others, 1972, p. 194) and the southern Lemhi Range are actually the Devonian part of the Sappington Member of the Three Forks Formation.

This report describes the stratigraphy of the Milligen Formation at its type locality and elsewhere in the Wood River area, dates the formation as Early, Middle, and Late Devonian, and divides it into informal upper and lower members. The upper member is dated as very early Late Devonian on the basis of conodont faunas. The thicker lower member is dated as Middle and Early Devonian. Although at present only Middle Devonian conodonts have been found in the lower member, these represent very early Middle Devonian time and occur so far above the base of the member that Lower Devonian beds most likely are present in the lower part. The eastern provenance of sediments and the paleotectonic setting of the type Milligen are interpreted from turbidites and possible debris-flow deposits and from the structural and facies relations of the Milligen to other known Devonian rocks in Idaho north of the Snake River River Plain and east of the Idaho batholith.

Sources of data and acknowledgments.—W. E. Hall and J. N. Batchelder, who mapped the Wood River area in the vicinity of Bellevue and Hailey, Idaho, are largely responsible for the lithologic descriptions and the stratigraphic section. C. A. Sandberg determined and dated the conodont faunas and interpreted the regional paleotectonics on the basis of an almost total revision, presented here, of his previously published Devonian isopach maps (Sandberg and Mapel, 1967, fig. 5; Mapel and Sandberg, 1968, fig. 1). Claus Axelsen discovered the initial conodont fauna from the Milligen Formation as a result of fieldwork in 1971 for his M.S. thesis at Oregon State University on Pennsylvanian stratigraphy. All four authors bear joint responsibility for the conclusions.

We thank our colleagues J. W. Huddle and F. G. Poole for their help in reviewing this paper. Poole visited us in the field in July and August 1973 and contributed significantly to our interpretations of the depositional environment and tectonic setting of the Milligen Formation. We are also grateful to Dr. Gilbert Klapper, University of Iowa, for his review of this paper.

STRATIGRAPHY

The Milligen Formation crops out discontinuously in a belt, 50 km (31 mi) long and as much as 11 km (6.8 mi) wide, trending north-northwest within Blaine County, Idaho, and extending from just south of Bellevue to the southern part of the Boulder Mountains (Umpleby, Westgate, and Ross, 1930, pl. 1). Figure 1 is a geologic map of the southern part of this belt. Most exposures in the belt are on the east sides of the valleys of the Big Wood and North Fork Big Wood Rivers, except between Bellevue and Hailey (fig. 1), where the Milligen abuts the east side of the Idaho batholith.

Most of the thin beds in the Milligen Formation have a poorly to moderately well developed cleavage at an angle of about 60° to the original bedding. The float has a distinctive crinkly surface and phyllitic sheen that help distinguish the Milligen from similar lithologies in other formations.

The Milligen Formation consists predominantly of interbedded dark-gray siliceous argillite and fine-grained quartzite, with some interbedded siltstone, siltite, and micritic silty limestone and minor interbedded dolomite, chert, and granule conglomerate. The Milligen is divisible into two members—a thick argillite lower member at least 900 m (3,000 ft) thick and a thin limestone upper member as much as 300 m (1,000 ft) thick.

The lower member is mainly interbedded dark-gray carbonaceous argillite and fine-grained quartzite that weather to dark-gray and brownish-gray slabby float and dark-gray soil. The argillite consists of poorly to moderately sorted 10-μm grains of quartz with some 2- to 5-μm grains of sericite, many of which show a preferred orientation. Quartz, carbonate, feldspar, tremolite, carbonaceous matter, limonite, and hematite are minor constituents of the argillite. The quartzites generally consist of poorly sorted sand composed

mainly of 50- to 150-μm subangular grains of quartz, which commonly show a weak preferred orientation. The quartzites in the lower member have appreciable amounts of carbonate, chert, and sericite, and a few conodont fragments. A few thin interbeds of micritic silty limestone and rare very thin beds of encrinite are also present in the lower member.

The upper member is generally much less argillitic and more heterogeneous in lithologic character. It contains abundant medium-dark-gray micritic sandy to silty limestone interbedded with quartzite, siltite, argillite, siltstone, dolomitic sandstone, and granule-conglomerate that weather light gray, pinkish gray, brownish gray, and reddish brown. The sandy limestone and dolomitic sandstone in the upper member generally contain subrounded to subangular quartz grains, which average 150 μm in diameter. Moderately to poorly sorted chert, argillite, feldspar, and phosphorite are other common constituents of these beds. Beds of limestone characteristically have veins and veinlets filled with white and black calcite. Siltite and quartzite in the upper member are poorly sorted, argillaceous, and contain constituents similar to those of the sandy limestone. Some siltite is finely laminated and some is thinly crossbedded.

The top 75 m (246 ft) of the upper member on a ridge east of Uncle Johns Gulch and south of Corral Creek, 6.5 km (4.0 mi) north of the Milligen principal reference section, is a dark-yellowish-orange-weathering medium-dark-gray banded dolomitic siltstone with thin interbeds of argillite. This distinctive lithologic unit is just north of the map area (fig. 1) and has not been seen anywhere to the south.

The maximum deposited thickness of the Milligen Formation is unknown. The base is not exposed in the map area as the formation either extends below the bottom of all drainages or is in fault contact with underlying rocks. The Milligen is presumed to have been deposited on the Silurian Trail Creek Formation, which crops out in the Pioneer Mountains just east of the map area. Whether a normal depositional contact is still preserved in the Wood River area or whether the base of the Milligen Formation is now everywhere a regional thrust fault is not known. Although the upper contact of the Milligen with the Wood River Formation of Pennsylvanian and Permian age is a regional thrust fault at all observed exposures (fig. 1), originally the Hailey Conglomerate Member (Middle Pennsylvanian) at the base of the Wood River was deposited unconformably on the Milligen. Four partial sections of the Milligen, all poorly exposed and in part tightly folded, were measured. On the basis of these partial stratigraphic sections and of measurements from structural cross sections, the maximum thickness of the formation is estimated to be at least 1,200 m (4,000 ft).

The following generalized stratigraphic section is here considered to be the principal reference section of the Milligen Formation.

Principal reference section of Milligen Formation

[Measured on east side of Milligen Gulch between ridge crest and creek bottom, in N½NW¼ sec. 19, T. 4 N., R. 19 E., Blaine County, Idaho, Hyndman Peak 7½-minute quadrangle]

	Thickness in metres	(feet)
Upper member:		
Limestone granule- and pebble-conglomerate, fossil-fragmental, sandy, silty, medium-dark-gray- and yellowish-gray-mottled. Contains some limestone pebbles as much as 15 mm (0.6 in.) in diameter and broken silicified fragments of *Alveolites*, brachiopods, and crinoids. Conodont sample C–58 (Ca:Mg molal ratio, 30.96; percent carbonate, 65.52) yields fauna assigned to upper part of Middle *Polygnathus asymmetricus* Zone. Conglomerate is interbedded with fossil-fragmental silty calcarenite and calcareous siltstone. Weathers medium gray and yellowish orange; forms rubbly ledges on ridge crest	2+	(6+)
Limestone, argillaceous, sandy, silty, medium-gray. Weathers yellowish gray; forms slopes	26	(86)
Limestone granule- and pebble-conglomerate, fossil-fragmental, sandy, silty, medium-dark-gray- and yellowish-gray-mottled. Contains phosphorite nodules and some silicified horn corals, *Alveolites*, and crinoids. Conodont sample C–189 (Ca:Mg molal ratio, 61.92; percent carbonate, 64.45) yields fauna assigned to lower part of Middle *P. asymmetricus* Zone. Weathers medium gray and yellowish orange; forms rubbly ledges on ridge crest 60 m (197 ft) north of sample locality C–58	2	(6)
Total exposed upper member	30+	(98+)
Concealed contact.		
Lower member:		
Argillite, carbonaceous, siliceous, dark-gray and grayish-black; thin interbeds of medium-gray fine-grained quartzite. Weakly resistant and poorly exposed; weathers to dark-gray and brownish-gray slabby float and dark-gray soil	370+	(1,214+)
Total exposed lower member	370+	(1,214+)
Total exposed Milligen Formation	400+	(1,312+)

A partial section of the Milligen Formation, which yielded two productive conodont samples, was measured on the ridge that trends northeast from the east side of Bellevue on the south side of Slaughterhouse Creek (fig. 1), in the SE¼SW¼ sec. 30, T. 2 N., R.

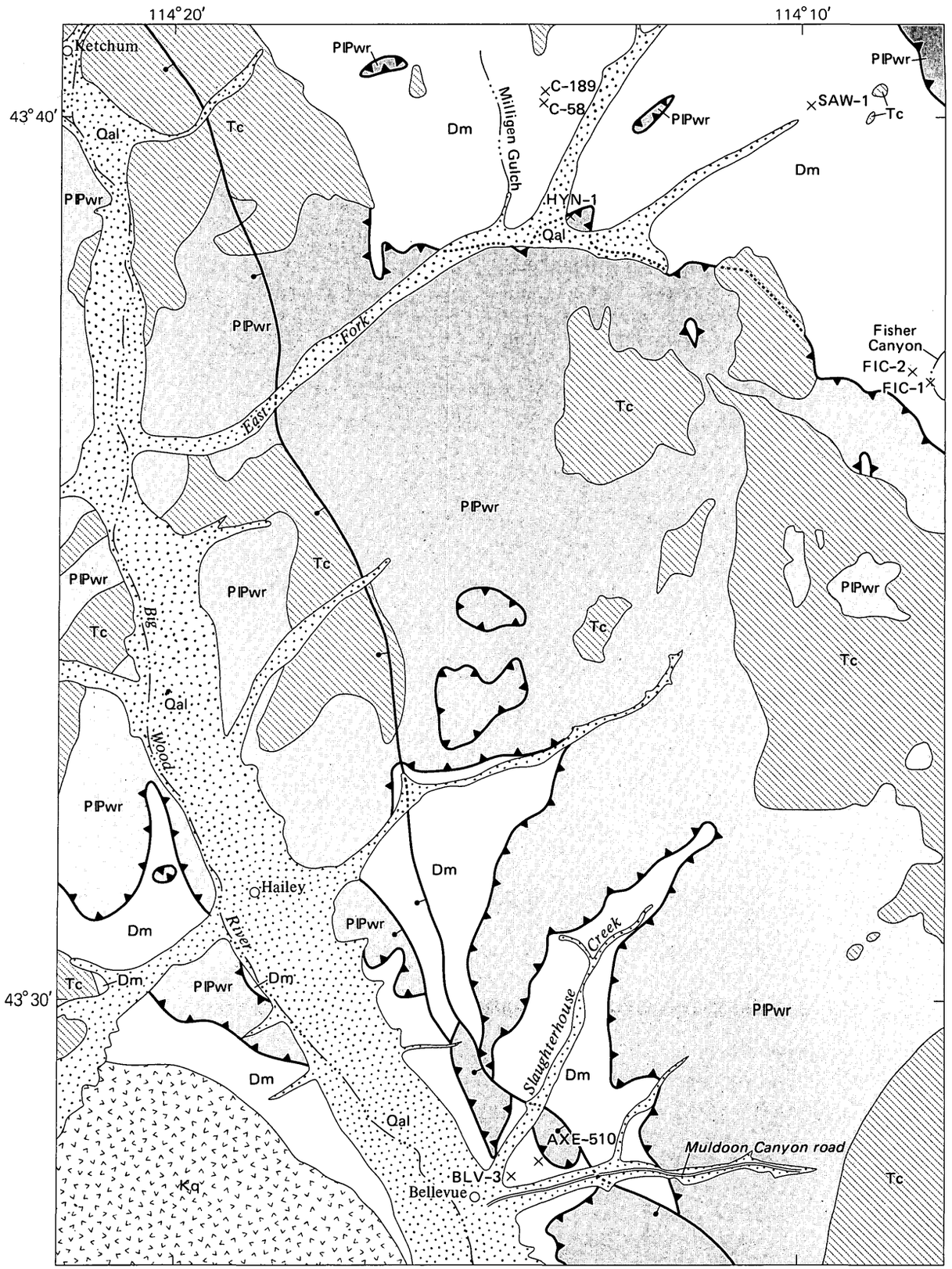

FIGURE 1.—Geologic map, Wood River area, Blaine County, Idaho. Geology by W. E. Hall and J. N. Batchelder, 1969–74.

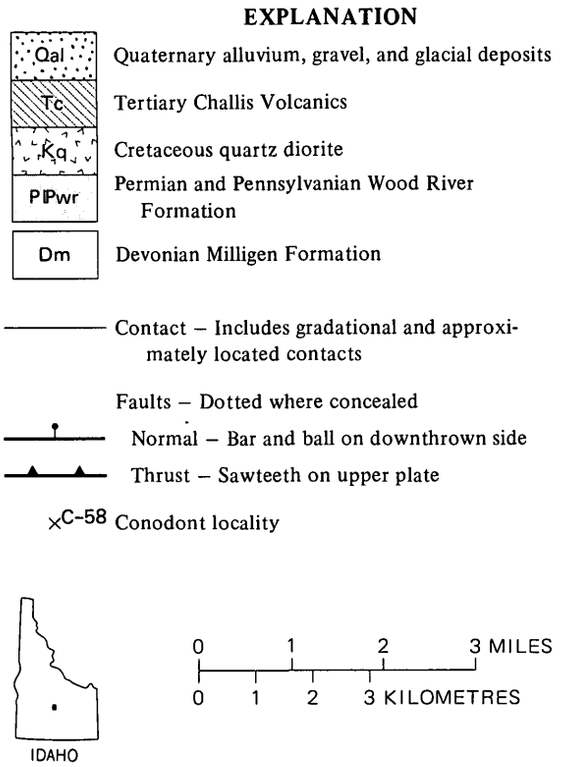

19 E., Blaine County. There the strata are tightly folded and probably form an anticline. The upper member is present at the bottom of the ridge and also just below the base of the Wood River Formation. These two outcrops are separated by nearly vertical beds of the lower member. A conodont sample (AXE–510) from just below the Wood River and another sample (BLV–3) from near the bottom of the ridge are believed to have come from almost precisely the same bed within the upper member. Both samples yielded a fauna assigned to the Lower *Polygnathus asymmetricus* Zone.

Two other partial sections were measured. One is on the ridge trending northeast from the Muldoon Canyon road, 4 km (2.5 mi) east of Bellevue (fig. 1). There the lower member is at least 700 m (2,300 ft) thick. and the fault-capped upper member is about 43 m (141 ft) thick. The other section is on the west side of Fisher Canyon along the east edge of the map area (fig. 1). Approximately 600 m (2,000 ft) of the upper member was measured at Fisher Canyon, but conodont dating (samples FIC–1 and FIC–2) demonstrates that lithologically similar limestone beds near the base and top of the section are identical and that consequently the thickness of the member must be doubled by a recumbent isoclinal fold.

CONODONT DATING AND AGE CORRELATION

Lower member of Milligen Formation

The lower member of the Milligen Formation contains fewer and thinner limestone interbeds than does the upper member. Most of these interbeds are relatively deepwater micritic silty limestones that yield only a few specimens of *Belodella* sp., which is nondiagnostic and ranges from Upper Silurian through Upper Devonian (Famennian) rocks in Idaho and Nevada. However, a very thin coarse encrinite was found near the middle of the lower member at Sawmill Gulch on the East Fork of the Wood River, about 6 km (3.7 mi) east of the principal reference section, in the SE¼NW¼NW¼ sec. 23, T. 4 N., R. 19 E., Blaine County, Idaho. Conodont sample SAW–1 from this bed yielded about 2,000 specimens including the following indigenous platform elements, which are considered diagnostic of an Eifelian (early Middle Devonian) age (number of specimens counted shown in parentheses):

Icriodus cf. *I. angustus* Stewart and Sweet (sensu Orr, 1971, pl. 2, figs. 7–9)	(10)
I. corniger Wittekindt (sensu Carls and Gandl, 1969, pl. 17, fig. 2)	(200+)
Pandorinellina exigua n. subsp.	(2)
Polygnathus angusticostatus Wittekindt	(5)
P. angustipennatus Bischoff and Ziegler	(9)
P. costatus costatus Klapper	(17)
P. costatus patulus Klapper	(5)
P. cf. *P. dobrogensis* Mirauta	(200+)
P. linguiformis linguiformis Hinde	(80+)
P. perbonus n. subsp. D Perry, Klapper, and Lenz	(200+)
P. trigonicus Bischoff and Ziegler	(4)

Sample SAW–1 also yielded several hundred indigenous ramiform elements and simple cones as well as some reworked Early Devonian conodonts. Inasmuch as this sample represents very early Middle Devonian time, at least part of the approximately 300 m (1,000 ft) of paleontologically undated underlying beds of the lower member must represent Early Devonian time. For this reason the lower member is considered Early and Middle Devonian in age.

Upper member of Milligen Formation

Six productive conodont samples, which yielded three distinct faunas having closely similar very early Late Devonian (very early Frasnian) ages, were obtained from the upper member of the Milligen Formation at three measured sections. The samples from the Bellevue section (sample AXE–510 collected by Axelsen and sample BLV–3 collected by Sandberg), the Fisher Canyon section (samples FIC–1 and FIC–2 collected by Sandberg, Hall, and F. G. Poole), and the principal reference section (samples C–189 and C–58 col-

lected by Hall and Batchelder) are located on figure 1, and their faunas are listed in table 1.

TABLE 1.—*Early Late Devonian (Frasnian) conodont faunas from upper limestone member of Milligen Formation, Idaho*

	Polygnathus asymmetricus Zones					
	Lower				Middle	
					Lower part	Upper part
Sample No.	AXE–510	BLV–3	FIC–1	FIC–2	C–189	C–58
Conodonts						
Ancyrodella gigas Youngquist	--	--	---	1?	3	3
A. rotundiloba alata Glenister and Klapper	3	2	50	12	-	--
A. rotundiloba rotundiloba (Bryant)	--	3	3	--	-	--
Belodella devonica (Stauffer)	--	--	4	4	-	7
Icriodus symmetricus Branson and Mehl	4	2	142	18	2	10
Nothognathella klapperi Uyeno	--	--	47	15	-	--
Palmatolepis punctata (Hinde)	--	--	---	--	-	11
Polygnathus ancyrognathoideus Ziegler	--	--	---	1	-	--
P. angustidiscus Youngquist	2	--	3	6	-	--
P. asymmetricus asymmetricus Bischoff and Ziegler	1	9	152	15	2	17
P. asymmetricus ovalis Ziegler and Klapper	13	5	86	34	6	12
P. cristatus Hinde	--	1	18	1	-	--
P. dengleri Bischoff and Ziegler	2	--	39	11	-	--
P. dubius Hinde	6	8	31	17	4	11
P. ordinatus Bryant	--	2	---	1	-	--
P. pennatus Hinde	--	--	---	--	2	1
P. cf. *P. rhenanus* Klapper, Philip, and Jackson	--	--	1	--	3	2
P. n. sp. (ex *P. varcus* group)	--	--	6	--	-	--
P.? variabilis Bischoff and Ziegler	3	1	---	--	-	5
P. xylus Stauffer	--	4	101	22	8	9
Schmidtognathus cf. *S. pietzneri* Ziegler	--	--	37	--	1	--
"Spathognathodus" sannemanni Bischoff and Ziegler	--	--	---	--	1	--
"S." gradatus (Youngquist)	2	--	103	2	-	--

Common to all six conodont samples are *Polygnathus asymmetricus asymmetricus* Bischoff and Ziegler, the index species for the Lowermost, Lower, Middle, and Upper *Polygnathus asymmetricus* Zones, as well as *P. asymmetricus ovalis* Ziegler and Klapper, *P. dubius* Hinde, and *Icriodus symmetricus* Branson and Mehl. The presence of *Ancyrodella rotundiloba alata* Glenister and Klapper and (or) *A. rotundiloba rotundiloba* (Bryant) in samples AXE–510, BLV–3, and FIC–1 precludes their assignment to the Lowermost *P. asymmetricus* Zone and permits assignment to either the Lower or Middle *P. asymmetricus* Zone. However, the absence of *Ancyrodella gigas* Youngquist and of *Palmatolepis punctata* (Hinde) from these faunas restricts their assignment to the Lower *P. asymmetricus* Zone. This zonal assignment is confirmed for samples AXE–510 and FIC–1 by the presence of *Polygnathus dengleri* Bischoff and Ziegler, which ranges only as high as the top of that zone. Sample FIC–2 likewise has an association of *P. dengleri* with *A. rotundiloba alata* and is thus assigned to the Lower *P. asymmetricus* Zone. However, the presence of a single juvenile specimen of an *Ancryodella* that is questionably referred to *A. gigas* suggests that this sample might be from very close to the boundary with the Middle *P. asymmetricus* Zone. The questionable specimen possibly could be *A. rugosa* Branson and Mehl, juveniles of which are difficult to distinguish from juveniles of *A. gigas*. If so, no conflict of established ranges would be involved and sample FIC–2 could be from any part of the Lower *P. asymmetricus* Zone.

Conodont samples C–189 and C–58 are assigned to the Middle *Polygnathus asymmetricus* Zone. In Europe, the lower boundary of this zone was defined by Ziegler (1962, 1971) solely on the basis of the first occurrence of *Palmatolepis punctata*, although the first occurrence of *Ancryodella gigas* is at the same level (Ziegler, 1971, chart 6). In North America, however, the first occurrence of *A. gigas* is slightly below that of *P. punctata* (Klapper and others, 1971, p. 301 and fig. 3). This order of occurrence is matched in the principal reference section of the Milligen Formation where *A. gigas* is present alone in sample C–189 but occurs with *P. punctata* 26 m (85 ft) higher in sample C–58. Thus, the Middle *Polygnathus asymmetricus* Zone in North America may be divided on the basis of this order of occurrence into a lower part without *P. punctata*, represented by sample C–189, and an upper part with *P. punctata*, represented by sample C–58.

The conodont zonation dates the upper member of the Milligen Formation as very early Late Devonian (very early Frasnian). In terms of conodont zones, the base of the Frasnian in Europe was placed by Ziegler (1971, p. 259–262) either at the base of the Lowermost *Polygnathus asymmetricus* Zone or possibly at the base of the underlying upper part of the *Schmidtognathus hermanni–Polygnathus cristatus* Zone. However, current discussions among European biostratigraphers studying the stratotypes of the Givetian (Middle Devonian) and Frasnian (Late Devonian) Stages in northern France and southern Belgium indicate a convergence of opinion toward raising the present boundary between these two stages (Paul Sartenaer, oral commun., Sept. 30, 1972). The Subcommission on Devonian Stratigraphy of the International Stratigraphic Commission is now considering a proposal, which, if accepted by the International Geological Congress, would entirely restore to the Middle Devonian the controversial Assise de Fromelennes in northern France. By this proposal, the base

of the Frasnian would become the base of the overlying Zone des Monstres, which, in terms of conodont zonation, coincides with the base of the Lower *Polygnathus asymmetricus* Zone (Tsien, 1972, table 2). Thus, even if the Middle Devonian-Late Devonian boundary is raised, the oldest recovered conodont zone in the upper member of the Milligen still would be assigned to the Late Devonian.

The upper member of the Milligen Formation is presumed to be entirely Frasnian in the Wood River area because no younger Devonian faunas have been found there and because new stratigraphic evidence from the Pioneer Mountains to the east suggests the existence of a westward-extending regional unconformity above Frasnian rocks. The only reported conodonts from the Milligen outside the map area support an early Frasnian age. The following fragmentary conodont collection (with number of specimens identified in parentheses) was obtained by J. W. Huddle (written commun., April 4, 1972) from a sample submitted by C. M. Tschanz from the north side of Trail Creek (USGS loc. 8928–SD) in sec. 22, T. 5 N., R. 18 E., Blaine County, about 7 km (4.3 mi) north of Ketchum:

Ancyrodella sp.	(2)
Polygnathus asymmetricus Bischoff and Ziegler	(3)
P. aff. *P. dengleri*? Bischoff and Ziegler	(1)

This fauna clearly falls within one of the four *Polygnathus asymmetricus* Zones.

The only younger Devonian (post-Frasnian) conodont fauna close to the Wood River area is from a grab sample, collected by R. A. Paull (Geology Dept., University of Wisconsin at Milwaukee) from the North Fork Big Lost River, about 43 km (26.7 mi) due north of Hailey. This fauna is assigned to the much younger very late Devonian (very late Famennian) Upper *Polygnathus styriacus* Zone and is the same age as faunas obtained from the lower unit of the Sappington Member of the Three Forks Formation, which overlies a regional unconformity in the southern Beaverhead Mountains (Sandberg and others, 1972) and southern Lemhi Range, Idaho, and in western Montana. The sample is from a nodular argillaceous limestone similar to those limestones found interbedded in argillites of Silurian to Pennsylvanian age in this area. Because of structural complexities, however, the source bed of this conodont sample and its relation to the Milligen Formation are unknown.

Because of the revised age of the Milligen Formation, previous interpretations of Devonian regional stratigraphy and paleotectonics must be modified significantly. Consequently, it is important to relate as accurately as possible the stratigraphic position of the top of the Milligen Formation in the Wood River area to the Devonian miogeosynclinal and cratonic sequences in adjacent regions on the east and south. This has been accomplished largely by conodont biostratigraphy.

The upper member of the Milligen correlates with the upper part of the lower third of the Middle and Upper Devonian (Givetian to Famennian) miogeosynclinal Jefferson Formation of the Lost River Range. At Hawley Mountain (fig. 2), the Jefferson is about 928 m (3,045 ft) thick. There, late Frasnian conodont faunas assigned to the *Palmatolepis gigas* Zone were found as low as 455 m (1,490 ft) above the base of the formation, and the top of a dark dolomite unit, which in other sections contains a Middle Devonian stringocephalid brachiopod fauna, is 171 m (560 ft) above the base. Allowing for the probable presence of the *Ancyrognathus triangularis* Zone, which intervenes between the *Polygnathus asymmetricus* Zones and the *P. gigas* Zone, the Lower and Middle *P. asymmetricus* Zones of the upper member of the Milligen must correlate with a position in the Jefferson just above the dark dolomite and probably within the 171- to 268-m (560- to 880-ft) interval above the base of the Jefferson. This interval is informal unit B of the Jefferson in the section described by Mapel and Shropshire (1973).

Correlated with the cratonic Upper Devonian sequence in the Logan area of southwestern Montana, 120 km (74.6 mi) northeast of Dillon (fig. 1), the upper member of the Milligen Formation is older than the type Jefferson Formation but about the same age as the underlying Maywood Formation. At Milligan Canyon, Mont. (not to be confused with Milligen Gulch, Idaho), the Maywood contains a diversified early Late Devonian biota, including conodonts (Sandberg and McMannis, 1964). The conodonts are assignable to the *Pandorinellina insita* Fauna (formerly *Spathognathodus insitus* Fauna of Klapper and others, 1971), which is believed to be the shallow-water biofacies equivalent of all or most of the four deeper water *Polygnathus asymmetricus* Zones. The *Pandorinellina insita* (Stauffer) in this fauna generally has a widely flared basal cavity and at least three small denticles anterior to the main offset denticle in the anterior part of the blade. It is similar to specimens from the Middle *P. asymmetricus* Zone in the Snyder Creek Shale of Missouri. In a sample of the Maywood Formation from Crane School, 37 km (23 mi) northeast of Milligan Canyon, R. W. Orr identified "*Spathognathodus*" *sannemanni adventus* Pollock for J. H. Meyers (written commun., Jan. 30, 1971). This

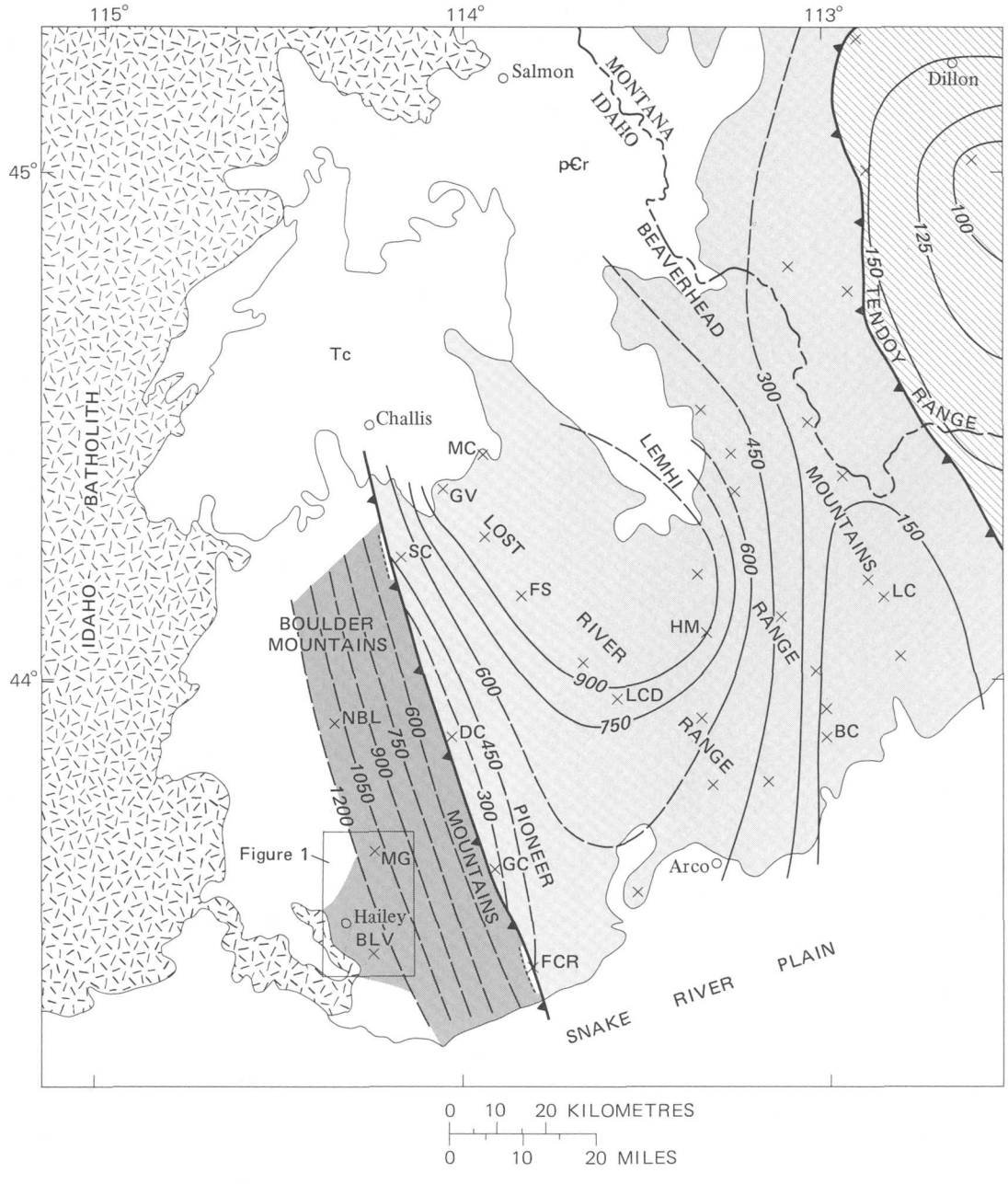

EXPLANATION

Devonian facies

- Deeper water transitional rocks – Argillite and quartzite
- Shallower water transitional rocks – Limestone, siltstone, and quartzite
- Shelf carbonate rocks
- Cratonic carbonate rocks

—150— Isopachs – Dashed where approximately located. Interval 150 and 25 m

Thrust fault – Sawteeth on upper plate

× Measured section or partial section of Devonian rocks

FIGURE 2.—Partly restored isopach and tectonic facies map of Devonian System north of Snake River Plain, Idaho and southwestern Montana. Tc, Tertiary Challis Volcanics (omitted in and west of Lost River Range, where patches cover at least half the surface area); p€r, Precambrian sedimentary and metamorphic rocks. Measured sections mentioned in text; BC, Black Canyon; BLV, Bellevue; DC, Dry Canyon; FCR, Fish Creek Reservoir; FS, Freighter Spring; GC, Garfield Canyon; GV, Grandview Canyon; HM, Hawley Mountain; LC, Long Canyon; LCD, Lower Cedar Creek; MC, Meadow Creek; MG, Milligen Gulch; NBL, North Fork Big Lost River; SC Spar Canyon.

subspecies is reported by Pollock (1968, p. 439) to occur in Alberta in the Moberly and Mildred Members of the Waterways Formation, which Uyeno (1967) places in the Middle *P. asymmetricus* Zone. Thus, two independent lines of evidence suggest that the *Pandorinellina insita* Fauna of the Maywood Formation is equivalent to the Middle *P. asymmetricus* Zone. Consequently the youngest faunas from the upper member of the Milligen are approximately the same age as faunas from the Maywood Formation in the Logan area.

Correlated with the miogeosynclinal Devonian sequence in extreme northern Utah, the upper member of the Milligen Formation represents a stratigraphic position extending upward an unknown interval from about 50–60 m (164–197 ft) above the base of the Samaria Limestone Member of Williams (1973) of the Middle and Upper Devonian Hyrum Formation. At Portage Canyon in the Blue Spring Hills, Utah, just south of the Idaho State line, faunas dominated by *Icriodus eslaensis* Adrichem Boogaert and assigned to the late Middle Devonian *Polygnathus varcus* Zone occur in the basal 17 m (56 ft) of the Hyrum, a Middle or Late Devonian fauna with a descendant of *I. eslaensis* occurs at 42 m (138 ft) above the base, and the *Pandorinellina insita* Fauna occurs from 47 to 58 m (154–190 ft) above the base. The collection at 47 m (154 ft) contains mostly a primitive form of *P. insita* with a single large offset anterior denticle, but three higher collections are dominated by typical forms with one or more smaller denticles anterior to the main offset denticle. These four collections are considered to be equivalent to parts of the Lowermost and Lower *Polygnathus asymmetricus* Zones.

Wood River Formation

A single sparse conodont collection (HYN–1), which supports algal and foraminiferal evidence for a Pennsylvanian age for the basal part of the Wood River Formation, was obtained from a very coarse encrinite in the lower part of the thrust plate that overlies the Milligen Formation, just east of its type locality (fig. 1). The collection comprises four specimens of *Idiognathodus* sp.

PALEOTECTONIC INTERPRETATION

The Milligen Formation is interpreted to have been deposited in relatively deep water in a continental-rise environment (F. G. Poole, oral commun., July 27, 1973). Most of the fine-grained sediments probably had an eastern provenance. The dominant lithologies in the lower member—dark-gray argillite and fine-grained quartzite with minor micritic silty limestone—are similar to those of transitional and siliceous assemblage rocks in the Great Basin of Nevada, according to F. G. Poole (oral commun., July 27, 1973). The lower member contains a few fine-grained quartzitic and encrinitic turbidites and some possible debris-flow deposits. The lithologically heterogeneous upper member, however, contains limestone-granule and limestone-pebble conglomerates and coarse encrinites that are interpreted to have been deposited by turbidite currents and, possibly, by debris flows. Conglomerates such as those capping the divide east of Milligen Gulch contain indigenous early Late Devonian (early Frasnian) relatively deepwater conodont faunas in the matrix, a shallow-water megafauna comprising brachiopods, *Alveolites*, and horn corals of the same age, and some older conodonts reworked from Middle and Lower Devonian sediments. Interpretation of the provenance of these varied organic constituents requires an eastern source for the sediments. This interpretation is supported by regional paleotectonic considerations, which are discussed later.

The early Late Devonian (early Frasnian) megafauna in the conglomerates consists mostly of rolled, badly broken fossils. Hence, they must have been moved from their original area of growth and deposition. As the megafauna consists largely of brachiopods and corals, it is interpreted to be of shallow-water origin. The similarity of the rolled brachiopods and corals to those in the middle part of the Jefferson Formation suggests that the most likely provenance of the megafauna would have been miogeosynclinal (continental shelf) sediments that formed the Jefferson in the area of the present Pioneer Mountains, east of the Wood River area. The Jefferson is widespread at depth in the Pioneer Mountains and is exposed in windows through the Mississippian Copper Basin Formation, such as those at Fish Creek Reservoir (fig. 2; Skipp and Sandberg, 1975) and at Dry Canyon (fig. 2).

The conglomerates in the upper member of the Milligen Formation contain, in addition to indigenous early Late Devonian (early Frasnian) conodont faunas listed in table 1, a few reworked Early Devonian conodonts including *Icriodus huddlei huddlei* Klapper and Zeigler; *Polygnathus perbonus* (Philip); *Ozarkodina remscheidensis* (Zeigler); *O. steinhornensis* (Ziegler); and *O.* n. sp. D Klapper. They also contain many more reworked Middle to Early Devonian conodonts including *Icriodus* cf. *I. angustus* Stewart and Sweet (sensu Orr, 1971); *I. corniger* Wittekindt; *Pandorinellina exigua* n. subsp.; *Polygnathus* cf. *P. dobrogensis* Mirauta; and *P. perbonus* n. subsp. D Perry, Klapper, and Lenz. These same

conodonts are found east of the Wood River area at the Fish Creek Reservoir window (fig. 2; Skipp and Sandberg, 1975) in the Carey Dolomite of late Early Devonian (Emsian) and early Middle Devonian (Eifelian) age, which underlies the Jefferson Formation. The conodonts are indigenous to beds of shallow-water sparsely crinoidal dolomite and fine to very coarse grained dolomitized encrinite. The Carey has also been recognized to the north at Garfield Canyon, Spar Canyon, and Meadow Creek, and it is probably concealed beneath Tertiary Challis Volcanics just north of Grandview Canyon (fig. 2). Thus, the Carey Dolomite was widely distributed east of the Wood River area at a time when the turbidites and possible debris-flow deposits of the upper member were being emplaced. The sediments of the Carey are therefore considered the most likely source of the reworked Middle to Early Devonian conodonts.

Further support for a major eastern sediment source of the Milligen Formation is provided by the coarse encrinite bed in the lower member at Sawmill Gulch. Conodont sample SAW–1 from this bed yielded a fauna containing elements of both the polygnathid-pandorinellinid and the icriodid biofacies faunas of the same age that occur separately in the lower Middle Devonian part of the Carey Dolomite in the Fish Creek Reservoir window (Skipp and Sandberg, 1975). The mixing of these faunas in an encrinite that is so much coarser than other rocks in the lower member suggests that this encrinite is a coarse turbidite or a debris-flow deposit derived from the depositional area of the Carey Dolomite on the east.

Devonian transitional rocks deposited in shallower water than the Milligen Formation have been recognized recently (Skipp and Sandberg, 1975) at the Fish Creek Reservoir window (fig. 2). They are assigned to the Roberts Mountains Formation of Silurian and Early Devonian age. At Fish Creek Reservoir, the Roberts Mountains comprises three units: a lower coralline patch-reef limestone of latest Silurian (Pridolian) age, a middle silty dolomitic limestone and calcareous siltstone, and an upper limestone phenoplast conglomerate. The two higher units, which are dated by conodonts as earliest Devonian (Lochkovian), are interpreted to have been deposited on the upper part of the continental slope. Westward they might intertongue with the basal part of the lower member of the Milligen, although such intertonguing has not been observed. The Roberts Mountains has also been identified at Spar Canyon (fig. 2), where it consists of interbedded siltstone, fine-grained quartzite, encrinite, and limestone phenoplast conglomerate. To date, however, only Late Silurian conodonts have been recovered at that locality. Shallower water transitional facies equivalents of the Middle and Upper Devonian parts of the Milligen have not been recognized.

The present location and inferred thickness of the transitional rocks of the Milligen and Robert Mountains Formations and their relation to Devonian shelf (miogeosynclinal) and cratonic carbonate rocks to the east is shown by a partly restored isopach and tectonic facies map (fig. 2). The Devonian shelf carbonate rocks in Idaho comprise, in ascending order, the marginal marine part of the Beartooth Butte Formation of Early Devonian (Siegenian) age, the Carey Dolomite of Early Devonian (Emsian) and Middle Devonian (Eifelian) age, the Jefferson Formation of Middle Devonian (Givetian) to Late Devonian (early Famennian) age, and the Trident Member of the Three Forks Formation of Late Devonian (late Famennian) age. The cratonic carbonate rocks in southwestern Montana comprise, in ascending order, the principally Frasnian Maywood and Jefferson Formations and the Famennian Logan Gulch and Trident Members of the Three Forks Formation. Excluded from the isopach map are discontinuous sinkhole and nonmarine and estuarine channel-fill deposits of the Lower Devonian Beartooth Butte Formation, estuarine channel-fill deposits equivalent to the Carey Dolomite, and the Upper Devonian and lowermost Mississippian Sappington Member of the Three Forks.

The isopach map (fig. 2) represents an almost total revision and westward extension of previously published isopach maps of this region (Sandberg and Mapel, 1967, fig. 5; Mapel and Sandberg, 1968, fig. 1). Only in southwestern Montana are thicknesses and structural relations unchanged from previous interpretations. There shelf carbonate rocks were moved eastward by a miogeosynclinal-margin thrust-fault system trending northwestward along the Tendoy Range, so that they abut severely thinned cratonic rocks at the west end of the eastward-trending ancestral Yellowstone Park uplift. Farther west, the isopachs of shelf carbonate rocks that show the shape of the miogeosynclinal basin and location of ancestral uplifts or ridges have been completely changed on the basis of new data, and inferred form isopachs for the Milligen Formation have been added.

The revised isopach-tectonic facies map reveals three new major structural or stratigraphic features that bear significantly on interpretation of the paleotectonics and provenance of the Milligen Formation. These features are (1) the thinning of shelf carbonates on a north-trending ancestral ridge in the southern Beaverhead Mountains; (2) the westward thinning of

shelf carbonates onto a similarly north-trending inferred ancestral ridge in the Pioneer Mountains; and (3) the subsequent eastward thrusting of the Milligen and Roberts Mountains Formations across the crest of the former ridge in the Pioneer Mountains during the Antler orogeny, possibly on a northward extension from Nevada of the Roberts Mountains thrust system.

1. The first new feature, the Southern Beaverhead Mountains uplift, is an ancestral uplift that trends northward through Long Canyon (fig. 2). The uplift is represented by an area of extremely thin Jefferson Formation—only the upper part of the lower member and the overlying Birdbear Member—that rests on a ridge formed mainly by the Precambrian Z Wilbert Formation and locally capped by a thin wedge of Ordovician Kinnikinic Quartzite. At Long Canyon, the Birdbear is unconformably overlain by the Sappington Member of the Three Forks Formation (Sandberg and others, 1972, p. 194 and sec. 13 on fig. 2). The lower two members of the Three Forks—the Logan Gulch and Trident—have been truncated beneath the pre-Sappington unconformity.

   The ancestral Southern Beaverhead Mountains uplift is a newly recognized feature that differs in trend, location, and origin from other inferred ancestral uplifts in this region that were discussed by previous workers (Sloss, 1954; Scholten, 1957; Scholten and Hait, 1962; Mapel and Sandberg, 1968). On the basis of an unusually thin Devonian section at Black Canyon (fig. 2), the Lemhi arch was proposed by Sloss (1954). The thinning in this area at the south end of the Lemhi Range is explained, however, partly by thrust faulting (Mapel and Sandberg, 1968) and partly by thinning on the west flank toward the crest of the Southern Beaverhead Mountains uplift. At Black Canyon, after correcting for the fault repetition, the Jefferson Formation is still considerably thicker than at Long Canyon and the overlying Trident Member of the Three Forks Formation is present beneath the Sappington Member, whereas it is absent at Long Canyon. The Tendoy dome of Scholten (1957) was largely refuted by Mapel and Sandberg (1968), who attributed the supposed uplift to a combination of thinning by previously unrecognized faulting in the Beaverhead Mountains and Tendoy Range and thinning over the west end of the intracratonic ancestral Yellowstone Park uplift. On figure 2, the so-called Tendoy dome would extend from the area of the 100-m isopach of cratonic carbonate rocks and across the miogeosynclinal-margin thrust-fault system to about 7 km (4.3 mi) east of Long Canyon. The area of thinning associated with the Southern Beaverhead Mountains uplift was nearly correctly located by Mapel and Sandberg (1968, fig. 1), but they attributed the thinning largely to faulting. At a subsequent field conference in July 1969, Mapel and Sandberg and Robert Scholten (of Pennsylvania State University) jointly gathered new data that support the existence of unconformities in addition to faults bounding the Jefferson Formation in the Beaverhead Mountains. This collaboration permitted the melding of previously divergent concepts into the joint recognition of the Southern Beaverhead Mountains uplift.

   Recognition of the uplift is important to understanding the regional paleotectonics of the Milligen in that it confirms the existence of an ancestral ridge on the former continental shelf. It also suggests a northward trend that might be paralleled by other inferred ridges to the west, closer to the Milligen depositional area.

2. A second ancestral ridge with a dominantly northward trend is recognized in the Pioneer Mountains on the basis of recent fieldwork by Sandberg with Betty Skipp at Fish Creek Reservoir, with R. A. Paull at Dry Canyon, and with W. H. Hays at Spar Canyon (fig. 2). At Fish Creek Reservoir, the exposed miogeosynclinal Devonian sequence, comprising the Carey Dolomite and Jefferson Formation, is about 450 m (1,500 ft) thick (Skipp and Sandberg, 1975). There the Three Forks Formation is absent and the Jefferson is unconformably overlain by the Picabo Formation of very late Devonian age. The Picabo comprises dolomitic sandstone and sandy dolomite-pebble conglomerate and is at least 58 m (189 ft) thick.

   At Dry Canyon, the Three Forks Formation is likewise absent, and the Frasnian part of the Jefferson Formation is at least 90 m (295 ft) thick and is overlain by at least 6 m (20 ft) of calcareous quartz sandstone that probably is equivalent to the Picabo Formation.

   North of the Snake River Plain, the Devonian System attains its maximum thickness—in excess of 900 m (3,000 ft)—in the Lost River Range. There the Trident Member of the Three Forks Formation averages 82 m (269 ft) in thickness at Freighter Spring and Lower Cedar Creek (fig. 2; Sartenaer and Sandberg, 1974).

Just to the west of the Lost River Range, at Grandview Canyon (fig. 2), is one of the thickest and most complete Devonian sections in Idaho. Only the Carey Dolomite, lying between the Jefferson Formation exposed in the canyon and the Beartooth Butte Formation exposed on low knobs to the north, is covered by Tertiary Challis Volcanics. At Grandview Canyon, all units of the Jefferson are present, and the Birdbear Member at the top is capped by the Trident, only 43 m (141 ft) thick.

Directly west of Grandview Canyon, Devonian rocks are concealed beneath Challis Volcanics, but a short distance farther west, in the vicinity of Spar Canyon, they crop out (fig. 2). In that area, currently being mapped by W. H. Hays, no higher unit of the Jefferson Formation has been recognized above the dark dolomite unit that is present within the lower third of the formation at Grandview Canyon and in the Lost River Range. Moreover, the Three Forks Formation has not been mapped anywhere near Spar Canyon and only two possible traces of it have been observed. W. H. Hays (oral commun., Aug. 27, 1970) found a patch of yellowish-weathering soil that may have been derived from the Three Forks in a possible narrow graben within the Jefferson east of Spar Canyon, and Ross (1937) reported some Three Forks fossils in Little Bradshaw Basin, 4.5 km (2.8 mi) north of Spar Canyon. Considered independently, the absence of the higher part of the Jefferson and of the Three Forks in the Spar Canyon area could be attributed to fortuitous pre-Challis erosion. However, in consideration of the westward thinning of the Three Forks from 82 m (269 ft) in the Lost River Range to only 42 m (141 ft) at Grandview Canyon and the absence of the Three Forks and thinness of the Jefferson farther south at Dry Canyon and Fish Creek Reservoir, the data from the Spar Canyon area would seem to fit a consistent regional pattern. This pattern is one of abrupt westward thinning of the total Devonian sequence from the Lost River Range into the Pioneer Mountains (fig. 2). Thinning by removal of beds from the top of the sequence would be even more strongly reflected by the isopachs between Grandview and Spar Canyons fig. 2) were it not compensated for by abrupt westward thickening in the same area of both the Carey Dolomite of Early and early Middle Devonian (Eifelian) age and the Beartooth Butte Formation of Early Devonian age at the base of the sequence.

By comparing the westward thinning of Devonian rocks beneath a probable very late Devonian unconformity in the Pioneer Mountains to similar erosional thinning over the Southern Beaverhead Mountains uplift, the second northward-trending positive feature can be postulated in the Pioneer Mountains. This ancestral uplift or ridge separated shelf deposits of the Jefferson Formation, Carey Dolomite, and Beartooth Butte Formation on the east from transitional deposits of the Roberts Mountains and Milligen Formations on the west.

The very late Devonian unconformity probably extended westward over the ridge and across the top of the Milligen Formation, as the highest beds of the Milligen on the west side of the ridge are about the same age as the highest beds of the Jefferson on the east side. No younger Devonian beds are known in this area except for the bed that yielded a very late Devonian conodont fauna at North Fork Big Lost River (fig. 2). This fauna is the same age as that in the basal part of the Sappington Member above the post-Jefferson unconformity on the Southern Beaverhead Mountains uplift at Long Canyon. This unconformity overlain by lag beds containing conodont faunas of closely similar very late Devonian ages is widespread in western North America. It extends south from Alberta (Macqueen and Sandberg, 1970) for at least 1,900 km (1,178 mi) through Montana (Sandberg and Klapper, 1967; Sandberg and others, 1972) and northern Utah (Sandberg and Gutschick, 1969) to southern Nevada (Sandberg and Poole, 1970; Sandberg and Ziegler, 1973).

3. The westernmost outcrops of Devonian shelf carbonate rocks lie along a line trending N. 20° W. and passing through or near measured sections at Fish Creek Reservoir and Spar Canyon (fig. 2). Along this same line are found the easternmost exposures of Silurian and Devonian shallow water transitional rocks. The juxtaposition of a thick wedge of westward-thickening Devonian transitional rocks to the ridge of westward-thinning Devonian shelf carbonate rocks (fig. 2) demonstrates that following very late Devonian erosion the Roberts Mountains and Milligen Formations were thrust eastward across the same ridge that earlier had contributed sediments to the Milligen Formation. This thrust is inferred to be a northward extension from

Nevada of the Roberts Mountains thrust system and to have been emplaced during the Antler orogeny. It has been observed at two localities—Fish Creek Reservoir and Spar Canyon. At Fish Creek Reservoir, transitional rocks of latest Silurian to very early Devonian age (in terms of conodont zonation, Silurian *Ozarkodina eosteinhornensis* Zone through Early Devonian Fauna 3 of Klapper and others, 1971) are thrust over the Carey Dolomite of Early and early Middle Devonian (Eifelian) age within a window in a younger Laramide or Sevier thrust plate. In the lower part of Spar Canyon, transitional rocks, presumably of Late Silurian to Early Devonian age but which thus far have yielded only Late Silurian conodonts, are found in large recumbent isoclinal folds in thrust contact over relatively undeformed Silurian shelf carbonate rocks.

CONCLUSIONS

The data presented herein permit the following conclusions to be made concerning the age, correlation, and depositional and tectonic history of the Milligen Formation.

1. The type Milligen Formation in the Wood River area is entirely Devonian in age. Its upper member contains conodont faunas assigned to the Lower and Middle *Polygnathus asymmetricus* Zones, which are indicative of a very early Late Devonian (early Frasnian) age. Its lower member contains a Middle Devonian (Eifelian) conodont fauna near the middle and nonfossiliferous beds of presumed Early Devonian age near the base.
2. The Milligen Formation is a relatively deepwater transitional sequence that was deposited in a continental-rise environment (F. G. Poole, oral commun., July 27, 1973). It contains sparse turbidites and possible debris-flow deposits, the reworked organic constituents of which require an eastern provenance.
3. The Milligen Formation in the Wood River area is older than and completely unrelated to the argillite of Early Mississippian (Kinderhookian and Osagean) age that has been called Milligen Formation in the Lost River Range and other ranges to the east in Idaho. The argillite of east-central Idaho constitutes part of the western-derived Mississippian flysch related to the Antler orogeny (Poole, 1974). Consequently, the name Milligen should not be used in east-central Idaho and extreme western Montana.
4. The source of turbidites and possible debris-flow deposits in the Milligen Formation was partly consolidated shallow-water Devonian sediments on an inferred ancestral ridge in the area of the present Pioneer Mountains. This ridge separated Devonian shelf carbonate deposits on the east from Devonian transitional deposits on the west.
5. In very late Devonian time, both the then-consolidated relatively deep water transitional rocks and the shallow-water shelf carbonate rocks adjacent to the ancestral ridge were deeply eroded. The resulting unconformity is part of an extensive interregional unconformity that is recognized from Alberta to southern Nevada.
6. During and after the final phase of very late Devonian erosion, the Milligen was intensely folded and moved eastward during the Antler orogeny by a northward extension from Nevada of the Roberts Mountains thrust system.
7. After its eastward emplacement across the former ancestral ridge, the Milligen Formation constituted a part of the Antler Highlands, which shed flysch sediments eastward into a rapidly subsiding basin to form the thick Mississippian Copper Basin Formation in the area of the present Pioneer Mountains.
8. The Antler Highlands in Idaho was eroded to an area of subdued topography that became the site for deposition of Wood River sediments during Pennsylvanian and Early Permian time. There is no record of sedimentation on the Milligen Formation in the interval between Late Devonian and Middle Pennsylvanian (Des Moinesian) time when the basal conglomerate member of the Wood River Formation was deposited.
9. Eastward thrusting of the Wood River and Milligen Formations during the Laramide or Sevier orogeny later destroyed most of the original depositional contact between these two formations.

REFERENCES CITED

Carls, Peter, and Gandl, Josef, 1969. Stratigraphie and Conodonten des Unter-Devons der Östlichen Iberischen Ketten (NE-Spanien) : Neues Jahrb. Geologie u. Paläontologie Abh., v. 132, no. 2, p. 155–218, pls. 15–20.

Dover, J. H., 1969, Bedrock geology of the Pioneer Mountains, Blaine and Custer Counties, central Idaho: Idaho Bur. Mines and Geology Pamph. 142, 61 p.

Klapper, Gilbert, Sandberg, C. A., Collinson, Charles, Huddle, J. W., Orr, R. W., Rickard, L. V., Schumacher, Dietmar, Seddon, George, and Uyeno, T. T., 1971, North American Devonian conodont biostratigraphy, *in* Sweet, W. C., and Bergström, S. M., eds., Symposium on condodont biostratigraphy: Geol. Soc. America Mem. 127, p. 285–316, 6 figs.

Macqueen, R. W., and Sandberg, C. A., 1970, Stratigraphy, age, and interregional correlation of the Exshaw Formation,

Alberta Rocky Mountains: Canadian Petroleum Geology Bull., v. 18, no. 1, p. 32–66.

Mamet, B. L., Skipp, Betty, Sando, W. J., and Mapel, W. J., 1971, Biostratigraphy of Upper Mississippian and associated Carboniferous rocks in south-central Idaho: Am. Assoc. Petroleum Geologists Bull., v. 55, no. 1, p. 20–33.

Mapel, W. J., and Sandberg, C. A., 1968, Devonian paleotectonics in east-central Idaho and southwestern Montana, *in* Geological Survey research 1968: U.S. Geol. Survey Prof. Paper 600–D, p. D115–D125.

Mapel, W. J., and Shropshire, K. L., 1973, Preliminary geologic map and section of the Hawley Mountain quadrangle, Custer, Butte, and Lemhi Counties, Idaho: U.S. Geol. Survey Misc. Field Studies Map MF–546.

Orr, R. W., 1971, Conodonts from Middle Devonian strata of the Michigan Basin: Indiana Geol. Survey Bull. 45, 110 p., 6 pls.

Paull, R. A., Wolbrink, M. A., Volkmann, R. G., and Grover, R. L., 1972, Stratigraphy of Copper Basin Group, Pioneer Mountains, south-central Idaho: Am. Assoc. Petroleum Geologists Bull., v. 56, no. 8, p. 1370–1401.

Pollock, C. A., 1968, Lower Upper Devonian conodonts from Alberta, Canada: Jour. Paleontology, v. 42, no. 2, p. 415–443, pls. 61–64.

Poole, F. G., 1974, Flysch deposits of Antler foreland basin, western United States, *in* Dickinson, W. R., ed., Tectonics and sedimentation: Soc. Econ. Paleontologists and Mineralogists Spec. Pub., no. 22, p. 58–82.

Ross, C. P., 1934, Correlation and interpretation of Paleozoic stratigraphy in south-central Idaho: Geol. Soc. America Bull., v. 45, no. 5, p. 937–1000.

——— 1937, Geology and ore deposits of the Bayhorse region, Custer County, Idaho: U.S. Geol. Survey Bull. 877, 161 p. [1938].

——— 1962, Upper Paleozoic rocks in central Idaho: Am. Assoc. Petroleum Geologists Bull., v. 46, no. 3, p. 384–387.

Sandberg, C. A., and Gutschick, R. C., 1969, Stratigraphy and conodont zonation of type Leatham Formation (Devonian and Mississippian), Bear River Range, Utah: Geol. Soc. America Abs. with Programs 1969, pt. 5, p. 70–71.

Sandberg, C. A., and Klapper, Gilbert, 1967, Stratigraphy, age, and paleotectonic significance of the Cottonwood Canyon Member of the Madison Limestone in Wyoming and Montana: U.S. Geol. Survey Bull. 1251–B, 70 p.

Sandberg, C. A., and Mapel, W. J., 1967. Devonian of the Northern Rocky Mountains and Plains, *in* Oswald, D. H., ed., Internat. Symposium on the Devonian System, Calgary, Alberta, Sept. 1967 [proc.], v. 1: Calgary, Alberta Soc. Petroleum Geologists, p. 843–877.

Sandberg, C. A., Mapel, W. J., and Huddle, J. W., 1967, Age and regional significance of basal part of Milligen Formation, Lost River Range, Idaho, *in* Geological Survey research 1967: U.S. Geol. Survey Prof. Paper 575–C, p. C127–C131.

Sandberg, C. A., and McMannis, W. J., 1964, Occurrence and paleogeographic significance of the Maywood Formation of Late Devonian age in the Gallatin Range, southwestern Montana, *in* Geological Survey research 1964: U.S. Geol. Survey Prof. Paper 501–C, p. C50–C54.

Sandberg, C. A., and Poole, F. G., 1970, Conodont biostratigraphy and age of West Range Limestone and Pilot Shale at Bactrian Mountain, Pahranagat Range, Nevada: Geol. Soc. America Abs. with Programs, v. 2, no. 2, p. 139.

Sandberg, C. A., Streel, Maurice, and Scott, R. A., 1972, Comparison between conodont zonation and spore assemblages at the Devonian-Carboniferous boundary in the western and central United States and in Europe: Cong. Internat. de Stratigraphie et de Géologie du Carbonifère, 7th, Krefeld, 1971, Compte rendu, v. 1, p. 179–203, 4 pls.

Sandberg, C. A., and Ziegler, Willi, 1973, Refinement of standard Upper Devonian conodont zonation based on sections in Nevada and West Germany: Geologica et Palaeontologica, v. 7, p. 97–121, 5 pls.

Sartenaer, Paul, and Sandberg, C. A., 1974, New North American species of Upper Famennian rhynchonellid genus *Megalopterorhynchus* from Lost River Range, Idaho: Jour. Paleontology, v. 48, no. 4, p. 756–765.

Scholten, Robert, 1957, Paleozoic evolution of the geosynclinal margin north of the Snake River Plain, Idaho- Montana: Geol. Soc. America Bull., v. 68, no. 2, p. 151–170.

Scholten, Robert, and Hait, M. H., Jr., 1962, Devonian System from shelf edge to geosyncline, southwestern Montana-central Idaho, *in* The Devonian System of Montana and adjacent areas, Billings Geol. Soc. Guidebook, 13th Ann. Field Conf.: p. 13–22.

Skipp, Betty, and Sandberg, C. A., 1975, Silurian and Devonian miogeosynclinal and transitional rocks of the Fish Creek Reservoir window, central Idaho: U.S. Geol. Survey Jour. Research, v. 3, no. 6, p. 691–706 .

Sloss, L. L., 1954, Lemhi arch, a mid-Paleozoic positive element in south-central Idaho: Geol. Soc. America Bull., v. 65, no. 4, p. 365–368.

Tsien, H. H., 1972, Middle Devonian and Frasnian stratigraphy of Belgium: Belgique Service Géol. Doc. 7, 25 p.

Umpleby, J. B., Westgate, L. G., and Ross, C. P., 1930, Geology and ore deposits of the Wood River region, Idaho: U.S. Geol. Survey Bull. 814, 250 p.

Uyeno, T. T., 1967, Conodont zonation, Waterways Formation (Upper Devonian), northeastern and central Alberta: Canada Geol. Survey Paper 67–30, 21 p., 2 pls.

Williams, J. S., 1973, Fossil distribution across the Middle-Upper Devonian boundary, Portage and Logan Canyons, north-central Utah: Geol. Soc. America Bull., v. 84, no. 5, p. 1699–1703.

Ziegler, Willi, 1962, Taxionomie und Phylogenie Oberdevonischer Conodonten und ihre stratigraphische Bedeutung: Hessisches Landesamt für Bodenforschung Abh. 38, 166 p., 14 pls.

——— 1971, Conodont stratigraphy of the European Devonian, *in* Sweet, W. C., and Bergström, S. M., eds., Symposium on conodont biostratigraphy: Geol. Soc. America Mem. 127, p. 227–284, 6 charts.

Jour. Research U.S. Geol. Survey
Vol. 3, No. 6, Nov.–Dec. 1975, p. 721–731

A LATE HOLOCENE POLLEN RECORD FROM PEARSON'S POND, WEEKS CREEK LANDSLIDE, SAN FRANCISCO PENINSULA, CALIFORNIA

By DAVID P. ADAM, Menlo Park, Calif.

Abstract.—A 210-cm core from Pearson's Pond yielded a pollen record for the past 3 millenia. Prior to A.D. 1000 the pond biota was particularly sensitive to climatic fluctuations. Two wet intervals occur in the pollen record, between 350 B.C. and A.D. 0 and between A.D. 650 and 900. The pollen record suggests that the Weeks Creek landslide may have moved at least twice prior to 3,000 years ago and that the middle part of the slide has been stable since that time. Seasonal changes produce large annual fluctuations in the water table, and climatic changes during the past 3,000 years have produced significant changes in the timing and magnitude of the annual changes. Climatic records such as the one presented here will help us to understand and separate the effects of climate and earthquakes on the landslide history of the Holocene deposits of the San Francisco Bay area.

The interactions between geology and man on the San Francisco peninsula are both politically and economically significant. Tectonic movements along the San Andreas fault system present a continuous threat to lives and property, and landslides, although individually less serious than major earthquakes, are far more frequent and regularly cause property damage (Taylor and Brabb, 1972).

One key to a better understanding of the magnitude and frequency of both landslides and earthquakes lies in a detailed investigation of late Quaternary deposits, including their chronology, depositional and tectonic history, and the record of environmental changes revealed by the fossils that they contain. Despite the economic importance of a thorough understanding of active geologic processes in the San Francisco region, it is only within the past few years that a systematic investigation of the Quaternary deposits of the bay area has begun (Frizzell. 1972). This paper, a part of that study, presents the first Holocene pollen diagram from the bay area, together with a tentative climatic chronology for the past 3,000 years.

Acknowledgments.—Mollusks reported in this paper were identified by D. W. Taylor and Allyn Smith, and vertebrates by D. B. Wake, J. T. Gregory, and C. A. Repenning. David Peterson provided much technical assistance. I thank Mrs. Helen Pearson for granting access to the pond.

SITE DESCRIPTION

The site studied, designated here as Pearson's Pond, is a small pond (fig. 1) on an old landslide near La Honda in San Mateo County, Calif., at an altitude of about 365 m (1,200 ft) in the northern part of the Santa Cruz Mountains (fig. 2).

The vegetation around the pond is largely grassland, but steep slopes support chaparral, and redwood and mixed evergreen forests occur along the stream courses. These plant communities have been described by Thomas (1961). The vegetation is generally very disturbed by man's activities, particularly by logging and grazing, so that little, if any, natural vegetation remains (Thomas, 1961).

Mean annual precipitation at the site is about 900 mm (35 in), most of which falls as rain during a wet season that extends from November through April (Rantz, 1971). Summer fogs are common.

The Weeks Creek landslide (fig. 3) is near the axis of the Weeks Creek syncline in marine strata of the San Lorenzo Formation (Touring, 1959; Brabb and Pampeyan, 1972a) of Eocene and Oligocene age. Brabb and Pampeyan (1972b) have mapped the slide as

FIGURE 1.—**Pearson's Pond**, viewed from the south. The core was taken from bottom sediments at the far edge of the water in the center of the picture. The embankment around the left and far sides of the pond is artificial.

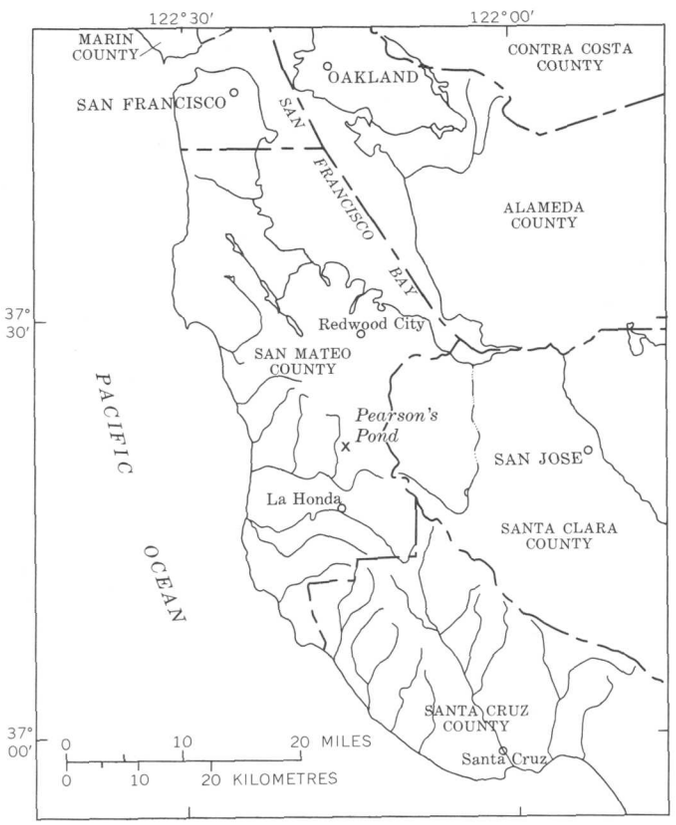

FIGURE 2.—Map showing the location of Pearson's Pond on the San Francisco peninsula.

1,250 m (0.75 mi) long and 500 m (0.3 mi) wide but indicate that older landslide scarps may extend considerably farther up the hill to the east.

Pearson's Pond is just below several slump blocks near the head of the slide. The lower part of the slide appears to be well broken up, with few coherent blocks. The toe of the slide is still active, as evidenced by frequent repairs to California State Highway 84 where it crosses the slide (Close, 1969), but, judging from the fossil record, the part of the slide around the pond appears to have been rather stable for the past 3,000 years.

PROCEDURES

A 210-cm sediment core was recovered from the pond bottom by using a 10-cm piston corer. Forty-nine pollen samples were removed from the core, and the remainder was then divided into 5-cm segments for macrofossil analysis.

The macrofossil samples were disaggregated by boiling in a dilute solution of sodium carbonate (washing soda) and then screened to remove all material finer than 0.25 mm. Not all samples were studied, but the results available assisted in the interpretation of the pollen data.

The pollen samples were processed by acetylation followed by hydrofluoric acid digestion, and the pol-

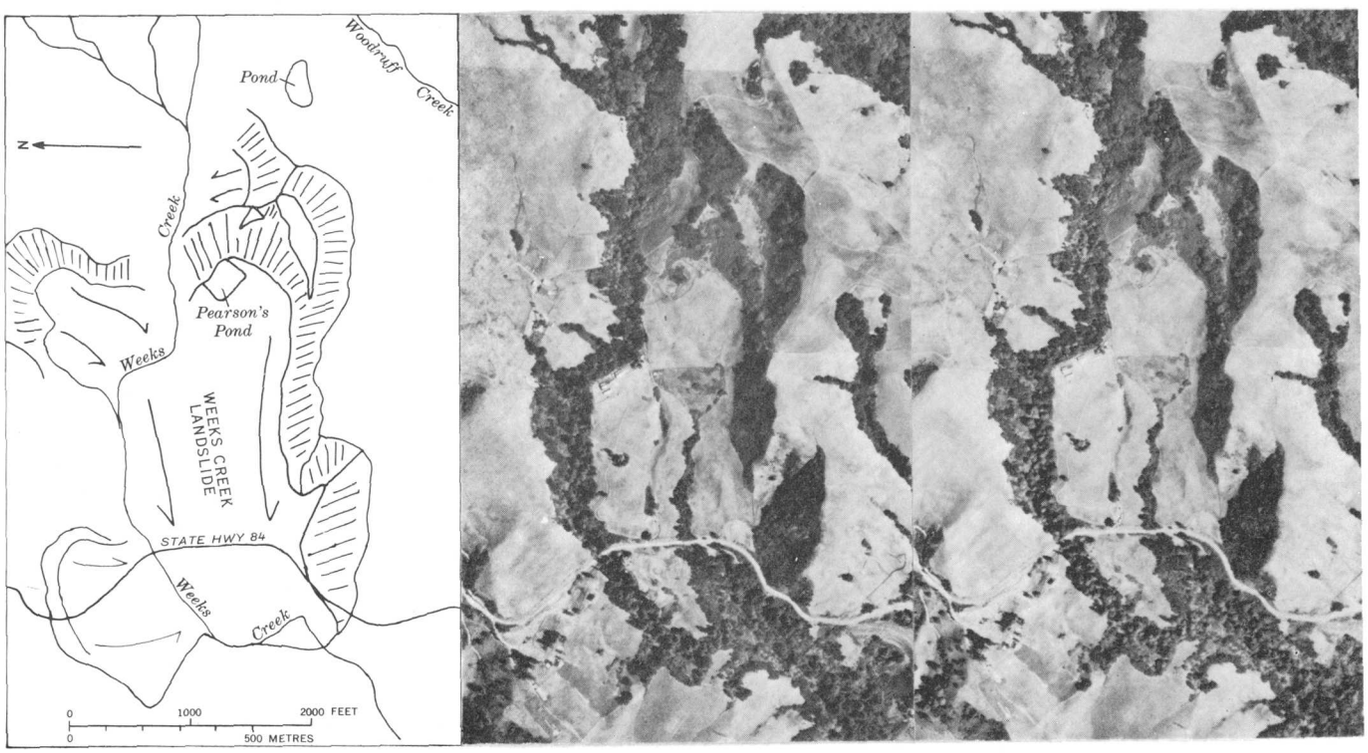

FIGURE 3.—Stereoscopic aerial photographs of Weeks Creek landslide showing location of Pearson's Pond. The line drawing shows only those features relevant to the present investigation. Photography by U.S. Department of Agriculture, 13 October 1963; photographs DDB–3DD–49 and DDB–3DD–50.

len-rich residue from each sample was preserved in silicone oil. Approximately 200 pollen grains were counted for each sample, except for sample 47, which yielded only 56 grains.

Pollen counts were transferred to punched cards for computer processing. The data were converted to percentages, and 95 percent binomial confidence limits were calculated (Mosimann, 1965; Maher, 1972a, b). The pollen diagram was prepared on a digital plotter using a program written by the author.

DATING

Organic carbon fractions of three macrofossil samples (without the sodium carbonate treatment) were submitted for radiocarbon dating, and these yielded ages of 3040±95 B.P. at a depth of 185 to 187 cm (I–6492), 2190±85 B.P. at 127 to 131 cm (I–7768), and 1545±85 B.P. at 107.5 to 112.5 cm (I–7071).[1] By assuming that the rate of sedimentation was uniform between dated horizons and between the uppermost dated sample and the surface, the ages of the various samples were estimated to the nearest decade. These dates are only rough approximations and should not be used uncritically. A list of the pollen samples and their depths, pollen sums, and estimated ages is given in table 1.

STRATIGRAPHY

The sediments consisted of organic muds containing coarse plant debris, mollusk shells, small bones, and generally sparse clastic debris. In addition, some marl coarse enough to be retained by the finest screen used (0.25 mm) was found in samples 34 (149–152 cm) and 38 and 39 (165–173 cm). The amount of coarse plant material in the core also varied considerably; it is nearly absent between 140 and 65 cm but is common both above and below.

The macrofossil samples have not been studied in detail, but the collected remains have been preserved and are available for study. Mollusks vary considerably in size, numbers, and relative proportions of species from level to level and include the following gastropod species:

Gyraulus parvus (Say)
Lymnaea proxima Lea
Menetus centervillensis (Tryon)
Armiger crista (Linnaeus)
Ferrissia fragilis (Tryon)
Planorbella tenuis (Dunker)
Musculium lacustre (Müller)
Succinea? sp.

[1] Radiocarbon dating by Teledyne Isotopes, Westwood, N.J.

TABLE 1.—*Sample data from Pearson's Pond, San Mateo County, Calif.*

[Dates of samples 1–25 are A.D.; dates of samples 26–49 are B.C.]

Sample	Depth (cm)	Pollen sum	Age, in years B.P. estimated to nearest decade (0=A.D. 1950)	Date
1	0	200.	−20	1973
2	5	203.	50	1900
3	10	200.	120	1830
4	15	209.	200	1750
5	20	200.	270	1680
6	25	200.	350	1600
7	30	202.	420	1530
8	35	200.	490	1460
9	40	200.	670	1380
10	45	200.	640	1310
11	50	201.	710	1240
12	55	203.	790	1160
13	60	200.	860	1090
14	67	191.	480	990
15	70	200.	1010	940
16	75	200.	1080	870
17	80	200.	1150	800
18	85	200.	1230	720
19	90	200.	1300	650
20	95	200.	1370	580
21	100	200.	1450	500
22	105	200.	1520	430
23	110	200.	1595±85	350
24	115	200.	1750	200
25	120	202.	1910	40
26	125	200.	2060	110
27	126	199.	2100	150
28	129	200.	2190±85	240
29	135	200.	2280	330
30	140	200.	2350	400
31	142	200.	2380	430
32	146	200.	2440	490
33	148	200.	2470	520
34	150	195.	2500	550
35	155	200.	2580	630
36	157	200.	2610	660
37	160	199.	2650	700
38	165	200.	2730	780
39	170	200.	2800	850
40	175	200.	2880	930
41	178	199.	2920	970
42	180	200.	2950	1000
43	185	200.	3030	1080
44	186	200.	3040±90	1090
45	190	200.	3100	1150
46	195	200.	3170	1220
47	200	56.	3250	1300
48	205	200.	3320	1370
49	210	200.	3400	1450

Vertebrate remains are less common but still numerous and include salamanders of the genus *Taricha*, as well as bones of frogs, snakes, and turtles. No fish remains have been found.

POLLEN TYPES

The plant nomenclature in this paper follows that of Thomas (1961). Departures from standard nomenclature are described below.

The TCT category includes pollen of the families Taxaceae, Cupressaceae, and Taxodiaceae. Most of the grains found had heavy walls and sculpturing and

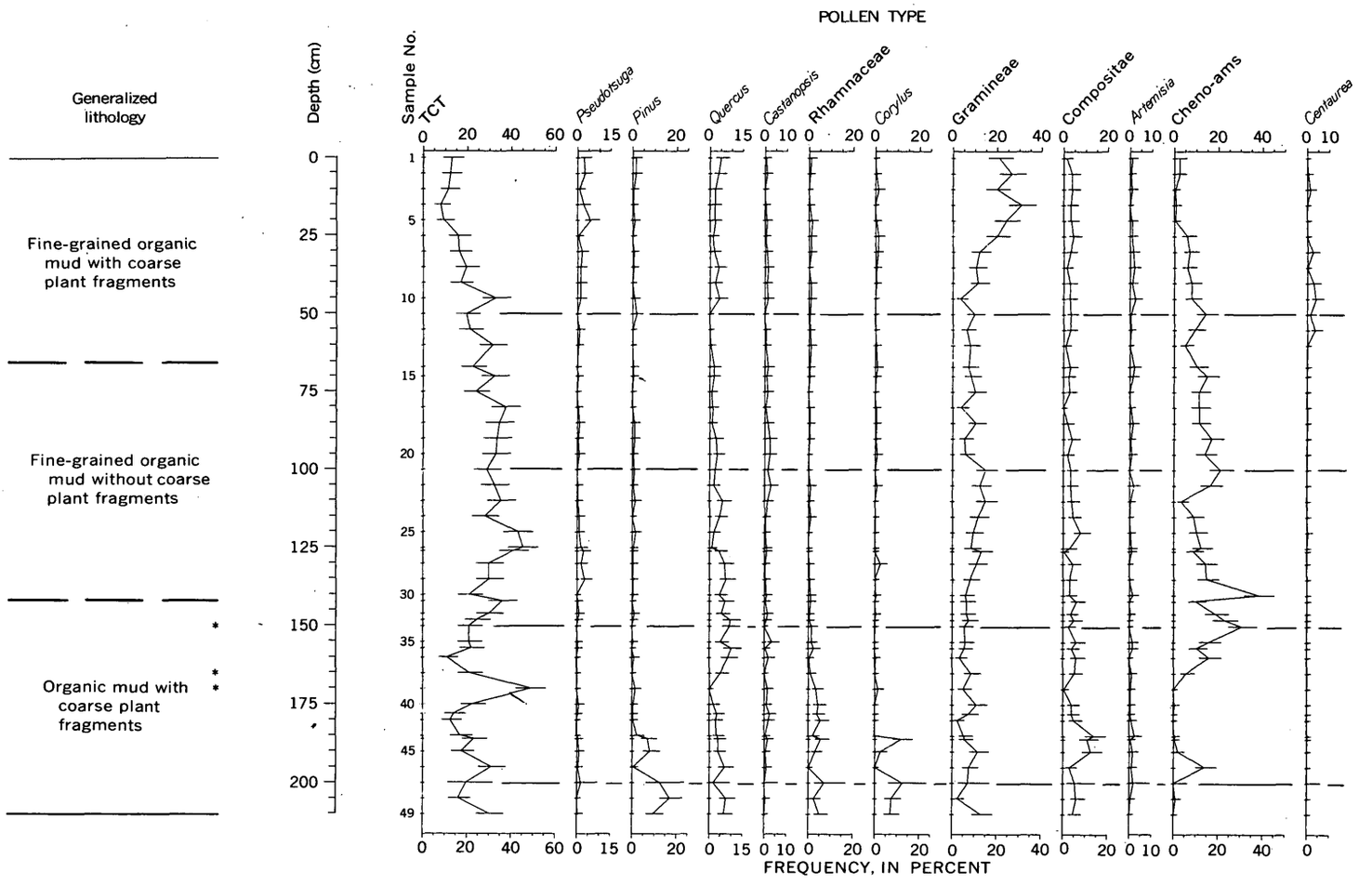

FIGURE 4.—Distribution of pollen from Pearson's Pond, San Mateo County, Calif. TCT category includes pollen of families Taxodiaceae, had no obvious ecological significance and did not seem to vary systematically from level to level in the section, are grouped under isks indicate depths at which marl is found.

probably represent mainly *Sequoia sempervirens*, the coast redwood. Although some grains were of the cupressaceous type, the TCT curve is taken here to be a record of *Sequoia* rather than *Cupressus*.

The cheno-am category includes pollen of the families Chenopodiaceae and Amaranthaceae, and is probably primarily pollen of *Amaranthus californicus*.

The unknown category includes both grains that could be seen but not identified and grains that were damaged or obscured by fine debris that prevented adequate observation.

The pollen of *Nymphaea* (yellow pond lily) found in the Pearson's Pond core is very much smaller than typical *Nymphaea* (=*Nuphar*) pollen and is doubtfully referred to the genus.

The pollen data are shown in table 2. Sixty-one pollen types were recorded, and counts outside the pollen sum were also made of the algae *Pediastrum* and *Botryococcus*. Many of the pollen types were scarce, had no obvious ecological significance, and did not seem to vary systematically from level to level in the section. These types were grouped in a single category of "others" for the pollen diagram, which is shown in figure 4.

LOCAL VERSUS REGIONAL CHANGES

The significance of the changes in pollen content between levels in the Pearson's Pond core depends on whether the pollen record has responded primarily to regional climatic changes or to local environmental changes independent of climate. Several processes that have affected the area are likely to have complicated the response of the fossil record to climatic changes.

Landsliding must have dramatically altered the local vegetation at the time the pond was formed. A large area of bare ground became available for colonization by plants, and the depression now occupied by the pond was created.

These events began a long series of successional changes. Initially, the disturbed sediments of the land-

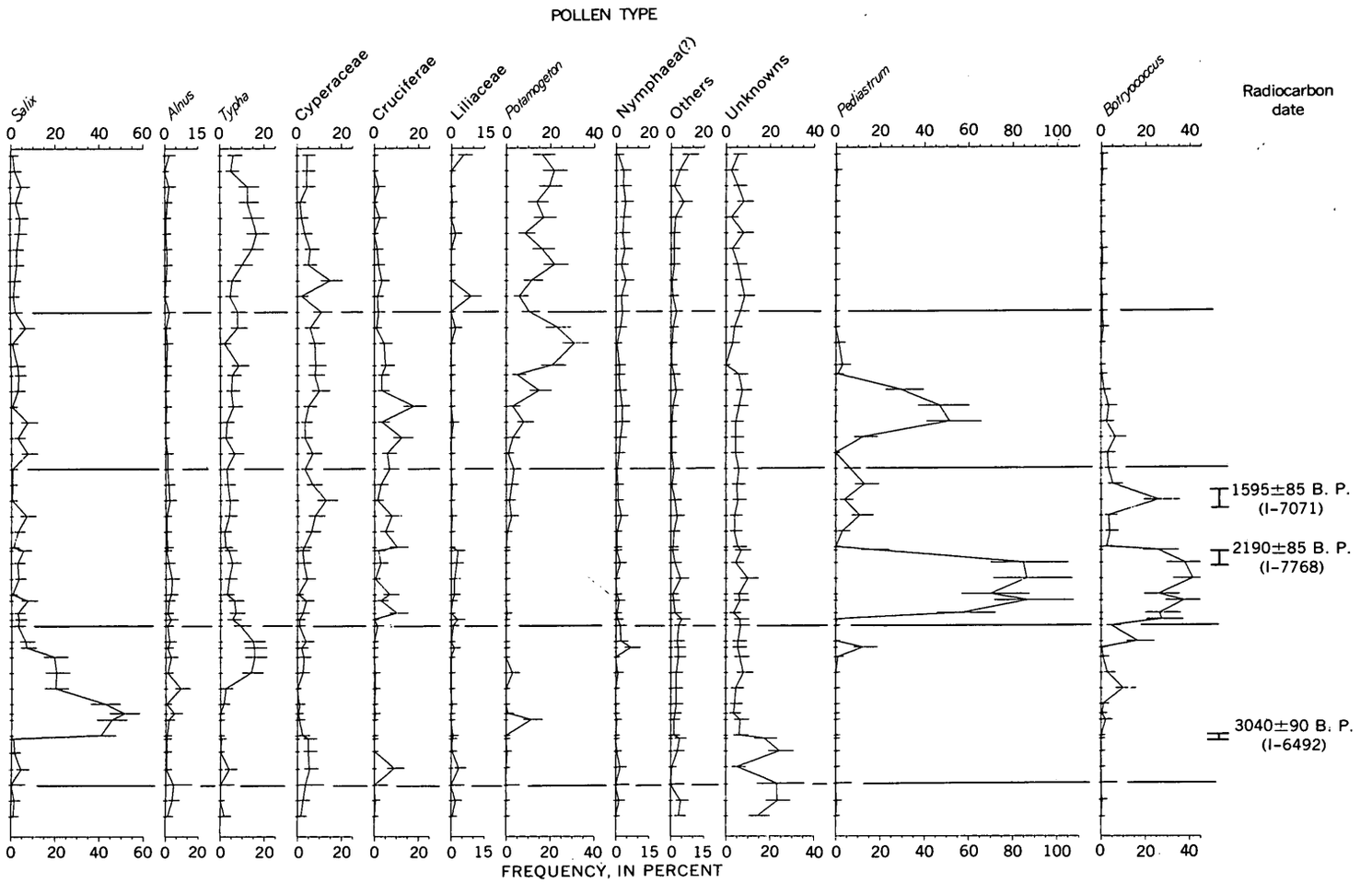

Cupressaceae, and Taxaceae. Cheno-ams include pollen of families Chenopodiaceae and Amaranthaceae. Scarce pollen types, which "Others." Horizontal bars on frequency curves are 95-percent binomial confidence intervals (Maher, 1972b). In sediment column, aster-

slide gave the depression a permeable bottom, but the combined effects of inwashed sediment and accumulating plant matter gradually sealed the bottom and allowed the depression to hold water more effectively. The pond continued to fill with sediment, and a rooted vegetation established itself across the pond once the water depth became shallow enough.

All these local events are reflected in the pollen record and they would presumably be recorded even in the absence of regional climatic changes. To assess fully the relative importance of local versus regional changes, it will be necessary to study other sites in different stages of succession. Such comparative data are rather scarce in California at present; the nearest detailed records of the past 3,000 years are from the Sierra Nevada (Curry, 1969; Adam, 1967; Zauderer, 1973). In the absence of nearby pollen records covering the same time span as the Pearson's Pond core, the best way to extract the climatic information from the fossil record is to look for reversible changes in pollen frequencies that presumably could not result from purely successional changes under a uniform climate.

The earliest pronounced change in the Pearson's Pond pollen record occurred about 3,000 years ago, between the deposition of samples 43 and 44. Samples below this horizon display high frequencies of pine, *Corylus*, and Cyperaceae pollen, giving way abruptly between 185 and 186 cm to very high frequencies of *Salix* (willow) pollen.

It seems likely that the samples below 186 cm represent conditions of intermittent sliding, with final stabilization of the pond occurring at 186 cm. During the early stage of vegetational development on the landslide, the disturbed area was colonized by grasses, Compositae, and Rhamnaceae (probably *Rhamnus californica* growing on the steeper slopes). *Corylus* (hazel) grew along the north margin of the slide along the creek, and some pines were also growing locally. Because pine, *Corylus*, and Rhamnaceae pollen fluctuate

TABLE 2.—*Pollen count, in number of grains, from Pearson's Pond*

Sample No.	1	2	3	4	5	6	7	8	9	10	11	12	13	14	15	16	17	18	19	20
Sample depth in centimetres	0	5	10	15	20	25	30	35	40	45	50	55	60	67	70	75	80	85	90	95
TCT	26	25	23	17	19	32	33	39	34	66	40	43	63	43	65	48	75	69	67	66
Sequoia (included in TCT)	1	0	0	0	2	1	1	1	0	0	0	1	3	0	1	1	0	0	0	2
Pseudotsuga	6	7	2	6	12	1	4	3	3	3	0	2	1	0	1	0	1	2	1	2
Pinus	3	3	1	1	2	0	1	1	0	2	4	0	0	1	1	0	0	2	2	1
Quercus	10	8	5	5	5	3	4	8	5	9	0	0	1	4	4	2	3	2	6	7
Salix	2	4	10	5	9	8	6	6	4	3	5	14	2	6	7	6	1	15	6	15
Alnus	4	0	4	2	1	1	2	2	1	0	4	1	2	1	1	0	1	0	0	2
Castanopsis	1	2	0	1	2	1	2	3	2	3	0	1	1	3	2	3	1	3	5	5
Corylus	0	1	3	0	1	3	2	1	1	0	0	0	1	2	1	0	1	1	1	2
Juglans	0	1	0	1	0	0	0	0	0	0	0	0	0	0	0	0	0	0	0	0
Rhamnaceae	2	1	0	1	3	2	2	0	2	2	1	1	2	1	1	0	1	1	1	0
Rhus	0	0	0	1	0	0	0	0	0	0	0	0	0	0	0	0	0	0	0	0
Betula	0	0	0	1	0	0	1	0	0	0	0	0	0	0	0	0	0	0	0	0
Aesculus	0	0	0	1	0	0	0	0	0	0	0	0	0	0	0	0	0	0	0	0
Sambucus	0	0	0	0	1	0	0	0	0	0	0	0	0	0	0	0	0	0	0	0
Ulmus	0	0	0	0	0	0	0	0	0	0	0	0	0	0	0	0	0	0	0	1
Fraxinus	0	0	0	0	0	0	0	1	0	0	0	0	0	0	0	0	0	0	0	0
Arceuthobium	0	0	0	0	0	0	0	0	0	0	0	0	0	0	0	0	0	0	0	0
Cf. *Cornus*	0	0	0	0	0	0	0	0	0	0	0	0	0	0	0	0	0	0	0	0
Cheno-ams	5	5	1	2	1	12	14	12	16	16	29	19	10	20	30	23	23	23	34	28
Compositae	3	6	8	7	7	8	6	3	6	6	5	5	2	6	5	6	0	4	7	4
Artemisia	2	1	2	0	2	2	3	4	2	5	1	1	0	4	3	0	1	3	1	2
Gramineae	42	54	40	65	48	40	24	21	23	7	20	13	16	14	17	21	8	21	11	12
Plantago	16	1	0	1	1	0	0	0	0	0	0	0	0	0	0	0	0	0	0	0
Liliaceae	11	0	0	1	0	4	0	0	0	18	0	4	0	0	0	0	0	2	0	0
Centaurea	0	1	3	0	0	0	5	0	6	8	3	7	0	0	0	0	0	0	0	0
Polygonaceae	0	3	0	2	0	0	0	0	0	0	0	0	0	0	0	0	1	0	0	0
Umbelliferae	0	1	0	0	1	1	0	1	0	1	1	0	0	0	1	0	1	1	0	0
Caryophyllaceae	0	1	0	1	0	0	0	0	0	0	0	0	0	0	2	0	0	0	0	0
Rubiaceae	0	0	1	0	0	1	0	0	1	0	0	0	0	0	0	2	0	0	0	0
Rosaceae	0	0	1	1	0	0	0	0	0	0	1	0	0	0	1	0	0	0	0	0
Polygonum, Persicaria type	0	0	1	0	0	0	0	0	0	0	0	0	0	0	0	0	0	0	0	0
Caprifoliaceae	0	0	0	1	0	0	0	0	0	0	1	0	0	1	0	0	0	0	0	0
Rumex	0	0	0	1	0	0	0	0	0	0	0	0	0	0	0	0	0	0	0	0
Onagraceae	0	0	0	0	1	0	0	0	0	0	0	0	0	0	0	0	0	0	0	0
Zauschneria	0	0	0	0	0	1	0	0	0	0	0	0	0	0	0	0	0	0	0	0
Ranunculaceae	0	0	0	0	0	0	2	1	0	0	0	1	0	0	0	1	0	0	0	0
Geraniaceae	0	0	0	0	0	0	0	0	0	1	0	1	1	0	0	0	0	0	0	0
Saxifragaceae	0	0	0	0	0	0	0	0	0	0	1	0	0	0	0	0	0	0	0	0
Leguminosae	0	0	0	0	0	0	0	0	0	0	0	0	0	0	0	1	0	0	0	0
Eriogonum	0	0	0	0	0	0	0	0	0	0	0	0	0	0	0	0	0	0	1	0
Convulvulaceae	0	0	0	0	0	0	0	0	0	0	0	0	0	0	0	0	0	0	0	0
Thalictrum	0	0	0	0	0	0	0	0	0	0	0	0	0	0	0	0	0	0	0	0
Labiatae	0	0	0	0	0	0	0	0	0	0	0	0	0	0	0	0	0	0	0	0
Actaea	0	0	0	0	0	0	0	0	0	0	0	0	0	0	0	0	0	0	0	0
Myrica	0	0	0	0	0	0	0	0	0	0	0	0	0	0	0	0	0	0	0	0
Berberis	0	0	0	0	0	0	0	0	0	0	0	0	0	0	0	0	0	0	0	0
Euphorbiaceae	0	0	0	0	0	0	0	0	0	0	0	0	0	0	0	0	0	0	0	0
Papaveraceae	0	0	0	0	0	0	0	0	0	0	0	0	0	0	0	0	0	0	0	0
Ephedra, E. nevadensis type	0	0	0	0	0	0	0	0	0	0	0	0	0	0	0	0	0	0	0	0
Polemoniaceae	0	0	0	0	0	0	0	0	0	0	1	0	0	0	0	0	0	0	0	0
Typha	12	10	25	26	29	33	29	20	11	9	16	16	4	16	11	10	12	6	5	13
Cyperaceae	9	9	9	3	4	7	12	10	30	4	22	12	16	16	16	20	10	7	7	14
Potamogeton	33	44	39	29	34	17	33	44	23	12	21	47	62	40	10	30	6	16	6	2
Nymphaea	2	7	7	9	7	6	8	5	9	5	6	4	1	3	3	4	6	6	4	3
Cruciferae	0	0	4	0	5	0	3	4	7	3	4	2	9	10	7	7	36	7	25	12
Alismataceae	0	0	0	1	0	0	0	0	0	0	0	0	0	0	0	0	0	0	0	0
Zea	0	1	0	0	0	0	0	0	0	0	0	0	0	0	0	0	0	0	0	0
Unknowns	11	5	11	17	5	16	6	11	14	17	13	8	6	0	12	15	12	9	9	9
Others	0	1	0	0	0	1	0	0	0	0	0	0	0	0	0	0	0	0	0	0
Liguliflorae	0	1	0	0	0	0	0	0	0	0	2	1	0	0	0	0	0	0	1	0
Pediastrum	0	1	0	0	0	0	0	0	0	0	0	0	3	6	2	59	94	103	25	0
Botryococcus	1	1	0	0	0	0	1	1	0	1	1	2	0	0	1	3	7	5	13	6

together in the basal section of the core, it is unlikely that the presence of pine pollen can be attributed to long-distance pollen transport. There is also a high frequency of unknowns in the basal sediments; these unknowns may represent either unusual plants that grew on the freshly disturbed landslide, or perhaps reworked grains from the underlying sediments.

The slide may have moved on two separate occasions early in its history. I interpret the segment of the core below 186 cm to represent disturbed conditions just after sliding, but sample 46 (196 cm) resembles conditions higher in the core in several respects, including low frequencies of pine, Rhamnaceae, *Corylus*, and unknowns, as well as high frequencies of chenoams, *Typha*, and Cruciferae. Interpretation of this sample depends upon whether it is part of a conformable sequence or out of place.

If sample 46 is part of a conformable sequence, it suggests that landsliding first established a small depression, and that the initial disturbed conditions had begun to give way to the development of pond vegetation that was interrupted by further landsliding and disturbance of the vegetation. If sample 46 is older than its position in the core indicates, the same interpretation applies, except that the second landsliding event would have disturbed the sediments just enough to confuse the stratigraphy; this seems unlikely.

Possibly, sample 46 is younger than the stratigraphic sequence indicates, and some pollen from higher in the section was introduced at 195 cm, perhaps through a desiccation crack or by an animal stepping in the mud. However, if this were true, then such processes would also have affected samples 44 and 45. I therefore prefer to interpret sample 46 as part

TABLE 2.—*Pollen count, in number of grains, from Pearson's Pond*—Continued

21	22	23	24	25	26	27	28	29	30	31	32	33	34	35	36	37	38	39	40	41	42	43	44	45	46	47	48	49
100	105	110	115	120	125	126	130	135	140	142	146	148	150	155	157	160	165	170	175	178	180	185	186	190	195	200	205	210
58	65	71	56	87	91	82	60	60	42	72	60	49	41	42	44	22	42	98	45	28	25	34	46	35	62	11	32	60
0	0	0	1	2	0	0	0	0	0	0	0	0	0	0	0	0	0	0	0	0	0	0	0	1	0	0	0	0
0	1	1	2	2	4	6	4	7	0	1	2	1	0	1	1	0	0	0	2	1	0	0	1	2	1	1	0	1
2	1	3	0	3	1	1	1	1	1	0	2	1	0	1	0	2	0	3	1	1	1	5	14	16	1	7	34	19
5	4	12	9	4	2	9	14	15	9	14	11	19	18	10	20	17	10	0	4	7	6	7	8	8	14	1	15	13
1	1	1	14	6	2	11	6	7	1	15	6	7	6	13	14	39	41	40	85	102	91	81	2	3	9	0	3	2
2	3	4	1	1	2	1	3	6	5	3	2	5	2	4	2	5	2	14	1	8	3	1	1	1	1	2	6	2
3	6	3	1	1	2	2	1	1	2	1	3	2	0	7	1	4	0	3	2	5	4	1	3	1	2	0	1	0
0	2	0	0	0	0	0	5	0	1	0	1	0	0	0	0	1	0	3	0	0	0	0	24	5	0	7	15	14
0	0	0	0	0	0	0	0	0	0	0	0	0	0	0	0	0	0	0	0	0	0	0	0	2	0	0	0	0
0	2	1	2	0	0	0	1	1	2	2	1	1	3	3	5	1	2	7	9	8	11	4	11	6	0	4	5	10
0	0	0	0	0	0	0	0	0	0	0	0	0	0	0	0	0	0	0	0	0	0	0	0	0	0	0	0	0
0	0	0	0	0	0	0	0	1	0	0	1	0	0	0	0	0	0	0	2	1	1	1	0	0	0	0	0	0
0	0	0	0	0	0	0	0	0	0	0	0	0	0	0	0	0	0	0	0	0	0	0	0	0	0	0	0	0
0	0	0	0	0	0	0	0	0	0	0	0	0	0	0	0	0	0	0	0	0	0	0	0	0	0	0	0	0
0	0	0	0	0	0	0	0	0	0	0	0	0	0	0	0	0	0	0	0	0	0	0	0	1	0	0	0	0
0	0	0	0	0	0	0	0	3	0	0	0	1	0	0	1	0	0	1	0	0	0	0	0	0	0	0	0	0
0	0	0	0	0	0	0	0	1	0	0	0	0	0	0	0	2	0	0	0	0	0	0	0	0	0	0	1	0
0	0	0	0	0	0	0	0	0	0	0	0	0	0	1	0	0	0	0	0	0	0	0	0	0	0	0	0	0
42	33	7	18	21	25	18	29	30	77	20	38	46	60	32	21	32	11	0	1	0	0	1	1	4	28	0	2	0
7	7	8	9	16	6	1	9	6	5	11	7	9	5	11	8	12	10	1	8	8	10	28	21	24	6	3	12	9
0	4	1	0	1	2	2	0	0	3	0	1	0	0	3	3	0	2	1	1	1	2	5	1	3	2	1	1	0
30	25	30	23	19	17	26	22	16	12	13	13	15	11	12	11	7	17	10	22	15	5	11	11	23	15	4	5	26
0	0	0	0	0	0	0	0	0	0	0	0	0	0	0	0	0	0	0	0	0	2	0	2	0	0	0	0	1
0	1	0	1	0	0	6	5	3	3	1	0	6	2	0	3	0	0	0	1	0	0	2	1	1	7	0	4	1
0	0	0	0	1	0	0	0	0	0	0	0	0	0	0	0	0	0	0	0	0	0	0	0	0	0	0	0	0
0	0	0	0	0	0	1	0	0	0	0	0	4	1	0	0	1	0	0	0	0	0	0	2	0	0	0	0	0
1	0	0	2	1	1	0	2	0	1	0	2	0	1	1	0	0	1	2	0	0	0	1	1	0	1	0	1	0
1	0	0	0	0	0	0	2	0	0	0	0	0	0	0	0	1	1	0	0	0	0	0	0	0	0	0	0	0
0	0	0	0	0	0	0	0	0	0	0	0	0	0	1	1	0	1	1	2	0	0	0	0	1	0	0	0	1
0	0	0	0	0	0	0	0	1	0	0	0	1	1	0	0	0	0	0	0	1	0	1	1	2	0	0	1	1
0	0	0	0	0	0	0	0	0	0	0	0	0	2	0	1	1	2	0	0	0	0	0	0	0	0	0	0	1
0	0	0	0	0	0	0	0	0	0	0	0	0	0	1	0	0	0	0	0	0	0	0	0	0	0	0	0	0
0	0	0	0	0	1	0	0	0	0	0	0	0	0	0	0	0	0	0	0	0	0	0	0	0	0	0	2	0
0	0	2	0	0	0	0	0	0	0	0	0	0	0	0	0	0	0	0	0	0	0	0	0	0	0	0	0	0
0	0	0	0	0	0	0	0	0	0	0	0	0	1	0	0	0	0	0	0	0	0	0	0	0	0	0	0	0
0	0	0	0	0	0	0	0	0	0	0	1	1	0	0	0	0	0	0	0	0	0	0	0	0	0	0	2	0
0	1	0	0	0	0	0	0	2	0	0	0	0	0	0	0	0	0	0	0	1	0	0	0	0	0	0	0	0
0	0	0	4	0	0	0	0	0	0	0	0	0	0	0	0	0	0	0	0	0	0	0	0	0	0	0	0	0
0	0	0	0	2	0	0	0	0	0	0	0	0	0	0	0	0	0	0	0	0	0	0	0	0	0	0	0	0
0	0	0	0	0	0	1	0	0	1	0	0	1	0	1	0	2	0	1	1	0	0	0	0	0	0	0	2	1
1	0	0	0	0	0	0	0	0	0	0	0	0	0	0	0	0	0	0	0	0	0	0	0	0	0	0	0	0
0	0	2	0	0	0	0	0	1	0	3	0	1	0	0	0	0	0	0	0	1	0	0	0	0	0	0	0	1
0	0	0	0	0	0	0	0	0	0	0	0	0	0	0	0	0	0	0	0	0	0	0	0	0	0	0	0	0
0	0	0	0	0	0	0	0	0	0	0	0	1	1	0	0	0	0	0	0	0	0	0	0	0	0	0	0	0
0	0	0	0	0	0	0	0	0	0	0	0	0	0	1	0	0	0	0	0	0	0	0	0	0	0	0	0	0
0	0	0	0	0	0	0	0	0	0	0	0	0	0	0	1	0	0	0	0	0	0	0	0	0	0	0	0	0
0	0	0	0	0	0	0	0	0	0	0	0	0	0	0	3	0	0	0	0	0	0	0	0	0	0	0	0	0
0	0	0	0	0	0	0	0	0	0	0	0	0	0	0	0	0	0	0	0	0	0	0	2	0	0	0	0	0
0	0	0	0	0	0	0	0	0	0	0	0	0	0	0	0	0	0	0	0	0	0	0	0	0	0	0	0	1
0	0	0	0	0	0	0	0	0	0	0	0	0	0	0	0	0	0	0	0	0	0	0	0	0	0	0	0	0
6	7	9	8	4	5	8	11	8	6	13	14	11	18	30	31	31	28	5	3	0	0	0	1	0	8	0	0	4
7	14	26	16	13	6	5	6	9	1	8	5	2	2	8	4	6	5	0	2	1	2	5	10	10	11	2	5	3
7	5	3	5	1	0	0	0	0	0	0	1	0	0	0	0	0	6	0	0	2	23	0	0	1	0	0	0	0
1	2	2	5	1	1	1	4	0	1	3	1	2	4	5	14	0	2	0	0	0	1	0	0	1	4	0	3	0
14	6	3	16	10	21	4	6	1	14	6	21	0	3	0	0	0	1	1	0	1	0	0	0	0	18	0	1	0
0	0	0	0	0	0	0	0	0	0	0	0	0	0	0	0	0	0	0	0	0	0	0	0	0	0	0	0	0
0	0	0	0	0	0	0	0	0	0	0	0	0	0	0	0	0	0	0	0	0	0	0	0	0	0	0	0	0
12	10	11	8	8	11	14	9	20	12	13	7	13	13	11	11	13	16	9	8	7	13	12	35	49	10	13	47	29
0	0	0	0	0	0	0	0	0	1	1	0	0	0	0	0	0	0	0	0	0	0	0	0	0	0	0	0	0
0	0	0	0	0	0	0	0	0	0	0	0	1	0	1	0	0	0	0	0	0	0	0	1	1	0	0	0	0
13	26	8	22	6	0	33	170	173	140	174	114	1	0	0	25	2	0	0	0	0	0	0	0	0	0	0	1	0
7	11	52	7	8	5	51	76	83	52	75	53	55	9	33	1	2	6	20	2	1	4	0	0	0	0	0	1	0

of a conformable sequence suggestive of intermittent sliding at the time of formation of the pond.

Above a depth of 185 cm, the pollen record is that of an evolving closed depression under a changing climatic regime. The first phase in the development of the pond was the establishment of a *Salix* (willow) thicket, represented by a peak in the frequency of *Salix* pollen between 160 and 185 cm. The suddenness of the onset of this peak and the lack of parallel responses in other pollen types indicate that this peak resulted primarily from the colonization of the pond depression by willows without any effective competition. Numerous small willows may have initially found favorable growing conditions and produced large amounts of pollen. Eventually, as they began to compete with each other and with the developing pond vegetation, most of them were crowded out. This interpretation is in agreement with Oberlander's (1953) observations of willows on the San Francisco Watershed Reserve about 20 km (12 mi) north-northwest of Pearson's Pond, where he noted that *Salix* is almost exclusively confined to freshly disturbed areas along stream channels.

These early willow thickets were also favored by the ability of willow to survive brief submersion better than its competitors. On the lower parts of the slide today, a few willow thickets occupy closed depressions in which the maximum water depth does not exceed about 50 cm.

The bottom of the pond seems to have been fairly well sealed against percolation by the time the 170-cm level was deposited. This is indicated by precipitated calcium carbonate (calcite) at the 165- and 170-cm levels. This sealing of the pond bottom must have contri-

buted to the decline in willow pollen by increasing the area within the depression that was submerged long enough each year to kill willows or to prevent their establishment. There are at present only three willows at the site (fig. 1). Two of these willows are rooted below the high-water mark (fig. 5). However, they were probably established near the original high-water mark before construction of the embankment (fig. 1) around the lower edge of the pond and were tall enough to escape drowning by the time of the damming. The shoulder on the peak of the willow pollen curve between 160 and 170 cm (fig. 4) indicates that some of the willows at the site may have survived for many years after the bottom became sealed and their roots became annually submerged for long periods.

The development of a true pond vegetation begins at about 165 cm with the onset of the first *Typha* (cattail) peak, together with the reappearance of Cyperaceae pollen and the appearance of *Botryococcus*. From this level upward to a depth of 60 cm or so, aquatic vegetation grew primarily around the edges of the pond and consisted of cattails, sedges, and Cruciferae (probably *Rorippa curvisiliqua*, the western yellow cress). Above 60 cm, a bottom-rooted vegetation including *Potamogeton* spp. and perhaps *Nymphaea* that had been living around the edges of the open water became established across the entire pond, and coarse plant debris became a major fraction of the sediment. Above a depth of 40 cm, *Typha* and *Potamogeton* pollen increase and sedges and Cruciferae decrease, and in the top three samples the sedges replace some of the *Typha* once again. The pollen curve for cheno-ams may be chiefly *Amaranthus californicus*, which grows around the "shores of lakes and ponds after the water has receded" (Thomas, 1961, p. 155). If so, then high frequencies of cheno-am pollen represent periods during which there were large annual fluctuations of water level in the pond. The peak in cheno-am pollen between 126 and 160 cm, together with the low peak in *Quercus* (oak) pollen and the increasing percentages of TCT (mostly *Sequoia*) pollen during the same interval, suggest a wet interval when the local forest expanded at the expense of the grassland and chaparral. At the top of this interval *Pseudotsuga* (Douglas fir) pollen increases slightly but systematically, and the sharp peaks in *Pediastrum* and *Botryococcus* in this part of the core provide further evidence of a wet interval.

FIGURE 5.—Willow (*Salix* sp.) growing below the high-water line at Pearson's Pond. This tree was probably well established before the embankment around the pond was constructed.

These changes in the frequencies of *Pediastrum boryanum* and *Botryococcus braunii* are the most spectacular changes in the fossil record at Pearson's Pond. Pronounced algal blooms appear at depths of 75 to 90 cm and 126 to 146 cm for *Pediastrum*, and a single persistent blooming period of *Botryococcus* is recorded at depths between 126 and 148 cm. In addition to these peaks, scattered samples between 60 and 170 cm contain moderately high frequencies of these algae.

While the meaning of these peaks is of obvious importance in interpreting the history of the pond, it is unfortunately not clear. According to Hutchinson (1967, p. 396), *Pediastrum* is a common dominant in small eutrophic ponds. However, Whiteside (1965) recorded changes in the relative numbers of several species of *Pediastrum* that occurred during the past 20,000 years in Potato Lake in northern Arizona. He noted that the greatest proportion of *P. boryanum* occurred during pluvial times and interpreted this to mean that the lake was oligotrophic during that interval. Chu (1942, p. 302), working with cultures of *P. boryanum*, determined that growth is greatest at a fairly low concentration of nutrients, and Hutchinson (1967, p. 428) stated that optimum growth tempera-

tures for the genus range from 20° to 25°C. Assuming that the peaks of *Pediastrum* frequency represent conditions approaching optimum conditions more closely than do the samples lacking high frequencies, and that the data derived from study of *Pediastrum* in cultures can be extrapolated to natural occurrences, then we may tentatively interpret the *Pediastrum* peaks as representing warm intervals (summers) when the pond contained open water with a fairly low concentration of nutrients. This suggests that the pond overflowed for a greater part of the year during the *Pediastrum*-peak intervals than it did at other times.

The interpretation of the *Botryococcus* record is, if anything, less clear. Hutchinson (1967) repeatedly referred to the genus as "anomalous," and stated that it grows under a wide variety of conditions that defy easy generalization. Two facts are of relevance here: (1) *Botryococcus* floats (Hutchinson, 1967, p. 247), and (2) it tolerates higher concentrations of nutrients and salts than *Pediastrum* (Chu, 1942, p. 147). Both genera appear to require some open water, and at Pearson's Pond both disappeared once the bottom-rooted *Potamogeton* became well established.

The simultaneous peaks of *Pediastrum* and *Botryococcus* may represent an interval during which the pond evaporated from a low nutrient concentration (for the *Pediastrum* peak) to higher concentrations (for the *Botryococcus* peak) during the growing season. If this is so, it suggests a wet winter and spring, with the springs feeding the pond enough water to keep it overflowing well into the summer, so that high nutrient conditions were not reached until after a *Pediastrum* bloom had formed.

The upper *Pediastrum* peak (75–90 cm) is not accompanied by a peak of *Botryococcus*. While the *Pediastrum* peak represents a wet interval, it is not clear whether the interval was relatively wetter or drier than the lower *Pediastrum-Botryococcus* peak. Conditions could have been so much wetter that nutrient concentrations resulting from evaporation never became high enough to support a *Botryococcus* bloom. On the other hand, the pond may have evaporated rapidly enough to prevent a *Botryococcus* bloom after the *Pediastrum* bloom, perhaps because of low spring discharge into the pond. The latter interpretation is in better agreement with the meager paleoclimatic data now available from northern California for the late Holocene (Zauderer, 1970; Curry, 1969; Šercelj and Adam, 1975).

According to this tentative model, dry intervals should be represented by *Botryococcus* frequencies in excess of those for *Pediastrum*. Three samples (34, 38, and 39) display such a pattern and also contain precipitated calcium carbonate (calcite) that indicates considerable evaporation and concentration of dissolved solids in the pond water. The precipitation of carbonate appears to have been the result of uptake of carbon dioxide from the water by plants because the coarsest fraction of the calcite consists of casts of small stems (fig. 6). This suggests that the bottom of pond was sufficiently sealed by the time of deposition of sample 39 to allow the pond water to become highly concentrated, at least with respect to calcite.

Higher in the core, samples at 110 cm and from 120 to 126 cm also show an excess of *Botryococcus* over *Pediastrum*, suggesting a possible dry period from about 1950 to 1550 B.P. (A.D. 0–400). The two wet intervals defined on the basis of the algal record occurred between 1950 and 2300 B.P. (0 to 350 B.C.) and between 1050 and 1300 B.P. (A.D. 650–900).

It must be emphasized that this model for the behavior of *Pediastrum* and *Botryococcus* at Pearson's Pond is only tentative. While the two genera have often been reported in the literature (for example, Raistrick and Blackburn, 1932; Cookson, 1953; Anderson and Kirkland, 1969), little emphasis has been placed on ecological interpretations. *Pediastrum* is generally taken simply as an indicator of fresh water, while *Botryococcus* may represent either fresh or brackish water. Until more fossil records and modern ecological studies are available, the model should be regarded cautiously.

During the interval from approximately 2300 to 1000 B.P. the pond contained open water during the summers, as evidenced by the algal remains and by

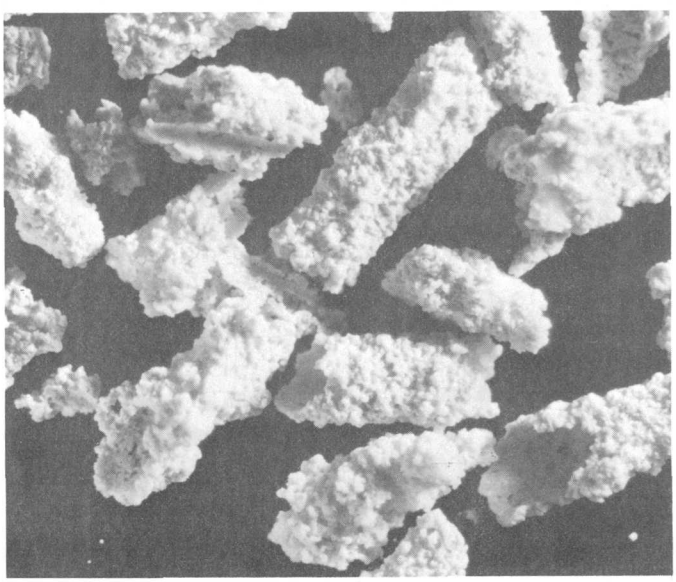

FIGURE 6.—Calcite stem casts from a depth of 170 cm in the Pearson's Pond core. Maximum width of casts is about 1 mm.

the absence of coarse plant debris from the sediments. About 1000 B.P., however, the pondweeds (*Potamogeton* spp.) began to thrive, and coarse plant debris reappeared in the sediments, indicating that a bottom-rooted vegetation displaced the open water that had prevailed earlier. This may have occurred in response to a dry interval or simply as a result of the shallowing of the depression caused by accumulating sediment.

Unfortunately for the present investigation, the development of the bottom-rooted vegetation about 1,000 years ago eliminated the habitats of both *Pediastrum* and *Botryococcus*, for these algae were the most sensitive indicators of changes in climate at Pearson's Pond. Although climatic changes are certain to have occurred on the San Francisco peninsula within the past 1,000 years, it is not possible to detect them with any certainty in the Pearson's Pond core. The most significant changes should have occurred within the past few hundred years, reflecting the most recent glacial advances in the Sierra Nevada (Curry, 1969), but these changes would be expected in the top 20 to 25 cm of the core, where they may have been modified by grazing-induced mixing of the sediments and by changes in the pollen rain influenced by man. The increase in *Pseudotsuga* pollen in the top five samples may reflect climatic change toward wetter conditions because it seems likely that any cultural effect would diminish rather than increase its frequency. Such an interpretation agrees with the interpretation of the *Pediastrum-Botryococcus* peak from 146 to 126 cm, for there is also a small *Pseudotsuga* peak at the top of that interval. Both *Pseudotsuga* peaks occur at the end of periods of high *Quercus* pollen frequency, which suggests that the two peaks may have been caused by similar climatic regimes.

HUMAN INFLUENCES

The only human influences identified in the pollen record are associated with the arrival of Europeans in the area. The major factors influencing the pollen rain appear to be logging and grazing.

The primary effect of logging has been a marked decrease in TCT pollen, representing *Sequoia*, beginning at a depth of 45 cm. It is not certain just when logging began within the *Sequoia* forests that contribute pollen to Pearson's Pond, but Kalenborn (1944) stated that logging in the vicinity of Woodside, about 8 km (5 mi) north of the pond, was well established in 1853.

The historically estimated ages of the human impacts inferred at the top of the core are substantially younger than the ages estimated on the assumption of uniform sedimentation rates (table 1). Several factors may account for this. The uppermost sediments are less compacted than the underlying materials, and this may make the sedimentation rate appear to be higher at the top of the core. The construction of the low dam around the pond may have increased the productivity of the pond or decreased the amount of oxidation before burial of the plant material produced. Finally the cows that use the pond for their water supply may be introducing extra nutrients to the pond through their manure and thus increase its productivity, and they may be more effective than the previous fauna in stirring the upper layers of sediment as they walk across the muddy margins of the pond to get to the water, causing younger sediments to be intruded into the older sediments beneath them.

The effects of grazing appear somewhat later than those of logging. The most conspicuous change is the large increase in Gramineae (grass) pollen above 30 cm. The drop in the frequency of cheno-ams at the top of the core may be a result of the construction of the embankment around the pond or of grazing of the plants by cows. Human impact may also be responsible for the fluctuations in the frequencies of *Typha*, *Potamogeton*, and Cyperaceae pollen in the top 30 cm.

The only exotic plant pollen that appears to be useful as an indicator of European contact is that of *Centaurea*, the star thistle. *Centaurea* pollen appears beginning at 55 cm in the core. This is somewhat below the level at which other evidence for European contact appears and suggests that the plant may have been introduced by the Spanish explorers.

IMPLICATIONS FOR ENVIRONMENTAL GEOLOGY

The Pearson's Pond pollen record demonstrates that there have been climatic changes within the past few millenia of sufficient magnitude to affect the biota of the San Francisco peninsula. It is reasonable to infer that these climatic changes may also have affected the rates of surficial geologic processes, including landsliding. Of course, other factors such as earthquakes may also have affected rates of landsliding.

To illuminate the historical interactions between climate, landslides, and earthquakes it will be necessary to core and date many landslide pond deposits in the San Francisco Bay area. The best cores can be used to extend the climatic record; by dating all cores, it will be possible to determine if particular time periods saw an unusually high number of landslides, and whether these periods were characterized by distinctive climatic regimes. It may then be possible to identify major past earthquakes with past periods of unusually

frequent landsliding, particularly if the climate of the time seems unlikely to have caused extensive landsliding by itself.

Such a study may help to refine our ideas about the relation between climate and landsliding. Intuition suggests that wet intervals should show higher frequencies of sliding than dry intervals, and observation confirms that winter is the landslide season. It is not known, however, whether simple wetness promotes sliding, or if the degree of contrast between the wet and dry seasons is also of importance.

REFERENCES CITED

Adam, D. P., 1967. Late-Pleistocene and Recent palynology in the central Sierra Nevada, California, *in* E. J. Cushing and H. W. Wright, Jr., eds., Quaternary paleoecology: New Haven, Yale Univ. Press, p. 275–301.

Anderson, R. Y.. and Kirkland. D. W., 1969, Paleoecology of the Rita Blanca Lake area: Geol. Soc. America Mem. 113, p. 141–157.

Brabb, E. E., and Pampeyan, E. H., 1972a, Preliminary geologic map of San Mateo County, California: U.S. Geol. Survey Misc. Field Studies Map MF–328.

——— 1972b, Preliminary map of landslide deposits in San Mateo County, California: U.S. Geol. Survey Misc. Field Studies Map MF–344.

Chu, S. P., 1942, The influence of the mineral composition of the medium on the growth of planktonic algae, Part 1—Methods and culture media: Jour. Ecology, v. 30, 284–325.

Close, P. H., III, 1969, Weeks Creek landslide: Stanford Univ., Master's degree research rept., 12 p.

Cookson, I. C., 1953, Records of the occurrence of *Botryococcus braunii, Pediastrum* and the Hystrichosphaerideae in Cainozoic deposits of Australia: Melbourne, Natl. Mus. Victoria, Mem., no. 18, p. 107–122.

Curry, R. R., 1969, Holocene climatic and glacial history of the central Sierra Nevada, California: Geol. Soc. America Spec. Paper 123, p. 1–47.

Frizzell, Virgil, ed., 1972, Unofficial progress report on the U.S. Geological Survey Quaternary studies in the San Francisco Bay area, *in* Guidebook for Friends of the Pleistocene, October 6–8, 1972: 164 p.

Hutchinson, G. E., 1967. A treatise on limnology, volume II—Introduction to lake biology and the limnoplankton: New York, Wiley, 1115 p.

Kalenborn, A. S., 1944, Early lumber industry in San Mateo County: San Mateo County Hist. Assoc. mtg., San Mateo, California, October 19, 1944, paper, 10 p.

Maher, L. J., Jr., 1972a, Absolute pollen diagram of Redrock Lake, Boulder County, Colorado: Quaternary Research, v. 2, p. 531–553.

——— 1972b, Nomograms for computing 0.95 confidence limits of pollen data: Rev. Palaeobotany and Palynology, v. 13, p. 85–93.

Mosimann, J. E., 1965, Statistical methods for the pollen analyst, *in* B. Kummel and D. Raup, eds., Handbook of paleontological techniques: San Francisco, Freeman, p. 636–673.

Oberlander, G. T., 1953, The taxonomy and ecology of the flora of the San Francisco Watershed Reserve: Stanford Univ., Ph. D. thesis, 170 p.

Raistrick, A., and Blackburn, K. B., 1932, The late-glacial and post-glacial periods in the north Pennines. Part III.—The post-glacial peats: Northern Naturalists Union Trans., v. 1, pt. 2, p. 79–103.

Rantz, S. E., 1971, Mean annual precipitation depth-duration-frequency data for the San Francisco Bay region, California: U.S. Geol. Survey open-file rept. 3019–12, 23 p.

Šercelj, Alojz, and Adam, D. P., 1975, A late Holocene pollen diagram from near Lake Tahoe, El Dorado County, California: U.S. Geol. Survey Jour. Research, v. 3, no. 6, p. 737–745.

Taylor, F. A., and Brabb, E. E., 1972, Map showing distribution and cost by counties of structurally damaging landslides in the San Francisco Bay region, California: Winter of 1968–69. U.S. Geol. Survey Misc. Field Studies Map MF–327.

Thomas, J. H., 1961, Flora of the Santa Cruz Mountains of California a manual of the vascular plants: Palo Alto, Stanford Univ. Press, 434 p.

Touring, R. M., 1959, Structure and stratigraphy of the La Honda and San Gregorio quadrangles, San Mateo County, California: Stanford Univ., Ph. D. thesis, 228 p.

Whiteside, M. C., 1965, On the occurrence of *Pediastrum* in lake sediments: Arizona Acad. Sci. Jour., v. 3, p. 144–146.

Zauderer, J. N., 1973, A neoglacial pollen record from Osgood Swamp, California: Tucson, Arizona Univ., M. S. thesis, 48 p.

Jour. Research U.S. Geol. Survey
Vol. 3, No. 6, Nov.–Dec. 1975, p. 733–736

MODERN POLLEN SURFACE SAMPLES—AN ANALYSIS OF SUBSAMPLES

By DAVID P. ADAM and PETER J. MEHRINGER, Jr.,[1]
Menlo Park, Calif., Pullman, Wash.

Abstract.—Multiple subsamples of pollen samples obtained from the modern soil surface at two sites in southern Arizona were individually collected and analyzed to evaluate the practice of mixing subsamples when collecting modern surface samples. Results suggest that at least five subsamples must be mixed in order to avoid collecting a sample that is not representative of the local pollen rain.

The use of surface samples in establishing the pollen deposition of modern vegetation has become a standard interpretive technique for fossil pollen studies. Many sources, including sediments and short cores of lake bottoms, moss polsters, and surface plant detritus and soil have been used throughout the world, particularly in North America (Wright, 1967). In the southwestern United States soil surface samples have long provided the basis for interpretation of alluvial fossil pollen sequences (Martin, 1963).

Because pollen accumulation is in part a result of the depositional environment, the pollen content of the present soil surface at localities approximating the sites of fossil deposition provides the only adequate comparison for alluvial fossil pollen spectra. Similarly, analogs for pollen spectra from cores of lake beds should be sought from present lakes of similar size.

In collecting surface samples, analysts of southwestern pollen have combined subsamples of surface soil so as to avoid the probability of unique or unrepresentative pollen percentages resulting from the proximity of a single point sample to a particular plant. They have attempted to provide an "average" sample for an area of characteristic vegetation or for localities along transects chosen by elevation or distance rather than species composition. There are numerous examples of such pollen transects from western North America (Adam, 1967, figs. 3 and 4; Bent and Wright, 1963, fig. 1; Hevly and others 1965, fig. 12; Maher, 1963, fig. 3; Martin, 1963, fig. 13; Martin, 1964, fig. 25; Mehringer, 1967, fig. 7; Schoenwetter and Eddy, 1964, fig. 21). In all of these, subsamples were mixed during sample collection to minimize the effects of unusual single samples. A theoretical analysis shows that this intuitive method was reasonable.

Assume that a sample is composed of n subsamples of equal size. One may then calculate the effect on the relative frequencies of the various pollen types in that sample when an additional subsample of known composition is added to the group. In the worst possible case the original sample is composed exclusively of pollen type A, and the added subsample consists entirely of pollen type B. In this case, the proportions of A and B in the new sample will be $n/(n+1)$ and $1/(n+1)$, respectively. If we further assume that A represents the true situation and B some departure from this, it follows that the maximum error that can be introduced by a peculiar pinch of dirt to n subsamples is $1/(n+1)$. The more subsamples that are included in the sample, the more reliable the observed frequencies will be.

Acknowledgments.—This work was supported in part by National Science Foundation grants GB–1959 and GB–7797.

METHODS

In February 1964, surface samples were collected from desert, desert grassland, and oak grassland communities of southeastern Arizona (Lowe, 1964) as an aid in interpreting late Quaternary alluvial pollen profiles from the San Pedro Valley, Ariz. (Mehringer and Haynes 1965; Mehringer and others, 1967). Only sites of low relief representing possible areas of slope wash deposition were collected. At each station at least 30 subsamples were taken from an area of relatively uniform vegetation with an estimated diameter of 50 m. Subsamples consisted of the upper 0.5 cm of surface dirt collected on the tip of a trowel. They were placed in a single plastic bag and mixed throughly before extraction. Pollen collection and extraction followed methods described by Mehringer (1967, p. 135–137). Forty-two of these surface samples were utilized for multivariate statistical comparisons of modern and fossil pollen counts (Adam, 1970).

[1] Department of Anthropology, Washington State University, Pullman, Wash. 99163.

In January 1967, we again collected two of the desert grassland surface stations (15 and 29) near Sonoita, Ariz., to observe how multi-pinch samples behave. We were particularly interested in the necessity of combining subsamples and wished to establish the number of subsamples required to adequately characterize soil surface pollen content in the desert grassland. At the two stations 20 subsamples were collected and placed in separate plastic bags for subsequent individual extraction and analysis. Samples were counted using double fixed sums of 200 grains each (Mehringer and Haynes, 1965). The first sum includes all pollen types; cheno-ams (includes families Chenopodiaceae and Amaranthaceae) and Compositae were excluded from the second sum.

RESULTS

Counts of individual subsamples are presented in table 1. In order to determine the full range of possible differences between groups of pooled subsamples, we ranked the observations of a given pollen type from smallest to largest within each locality. The maximum possible frequency that we could have found using n of our 20 subsamples is the average of the n highest frequencies; the minimum is calculated similarly. As n increases, the maximum and minimum possible values converge on the grand mean for all 20 subsamples ($N = 4{,}000$). The grand mean values are considered the "true" values for the site. Results for some of the pollen types are presented in figure 1.

DISCUSSION AND CONCLUSIONS

In sum 1 counts (table 1) cheno-ams are the most variable. Since possible contributors of this pollen type are irregularly distributed and are prolific pollen producers, such variation is expected. Further, the differences between subsamples clearly illustrate that even though the samples were collected in winter, several months after flowering of all species represented at the site, local redeposition by water and wind and the addition of regionally recirculated pollen in dust storms still did not result in uniform surface pollen frequencies.

Grass pollen, the dominant type in all samples, shows less subsample variation. The relatively even distribution of the plants and wind dispersal of this most abundant pollen type produce a regional distribution and a high grass pollen background in all subsamples. The grass pollen variation appears to be primarily the result of constraint produced by the uneven distribution of cheno-ams and Compositae with local variation in grass cover being less important. In sum 2 counts (table 1) the removal of cheno-am and Compositae constraint results in lower standard deviations for grass pollen even though the numbers of grass pollen increase. Grass pollen is an exception in this regard.

The *Quercus* (oak) counts illustrate subsample variation resulting primarily from the relative abundance of local pollen in each subsample. Oak trees are absent from the sites and the long-distance transport of their pollen, along with that of pine and juniper, should result in nearly uniform distribution in the numbers of pollen grains falling on the soil surface within the sample area.

These analyses of 20 subsamples show that each subsample may be a poor reflection of local pollen surface deposition. Further, assuming that the worst possible cases were duplicated in actual sample collection, as many as 10 to 15 subsamples might be required to provide the pooled 20-subsample population estimate. However, this figure is obviously too high as the random selection of such a sample set is improbable. For example, the means of either the first or last five subsamples actually collected fall within the mean and standard deviation of the combined 20 subsamples.

In our surface sample study of southeastern Arizona, at least five subsamples were probably required to characterize the soil surface pollen content of selected sample stations. Ten subsamples would have undoubtedly provided a better estimate and may have been necessary in areas where more species contributed significant amounts of pollen. For example, in our Chihuahuan Desert samples, the decrease in grass pollen, the addition of *Ephedra* as an important contributor, and the increased variability in species distribution between and within sample stations would probably have increased subsample variation. In any case, the minimum of 30 subsamples used for fossil comparisons should have been sufficient to establish deposition of pollen in the soil surface of each sample station even with unusual local irregularities in plant cover. The 1964 and 1967 counts are similar enough to place both samples with others from the open desert grassland of southeastern Arizona. The close agreement after three years may partially result from the fact that each subsample represents several years of pollen accumulation. Collection of samples during the winter would have allowed time for the last season's pollen fall to become partially mixed with that of previous years.

FIGURE 1.—Maximum possible frequency (upper curve) and minimum possible frequency (lower curve) for selected pollen types, plotted against number of 200-grain subsamples averaged together. The two curves converge when all 20 subsamples are included. Shaded zones, 95-percent binomial confidence limits (Mosimann, 1965) plotted about the overall mean (horizontal line) for the entire 4,000-grain sample (narrow band) and for a 200-grain sample (wide band).

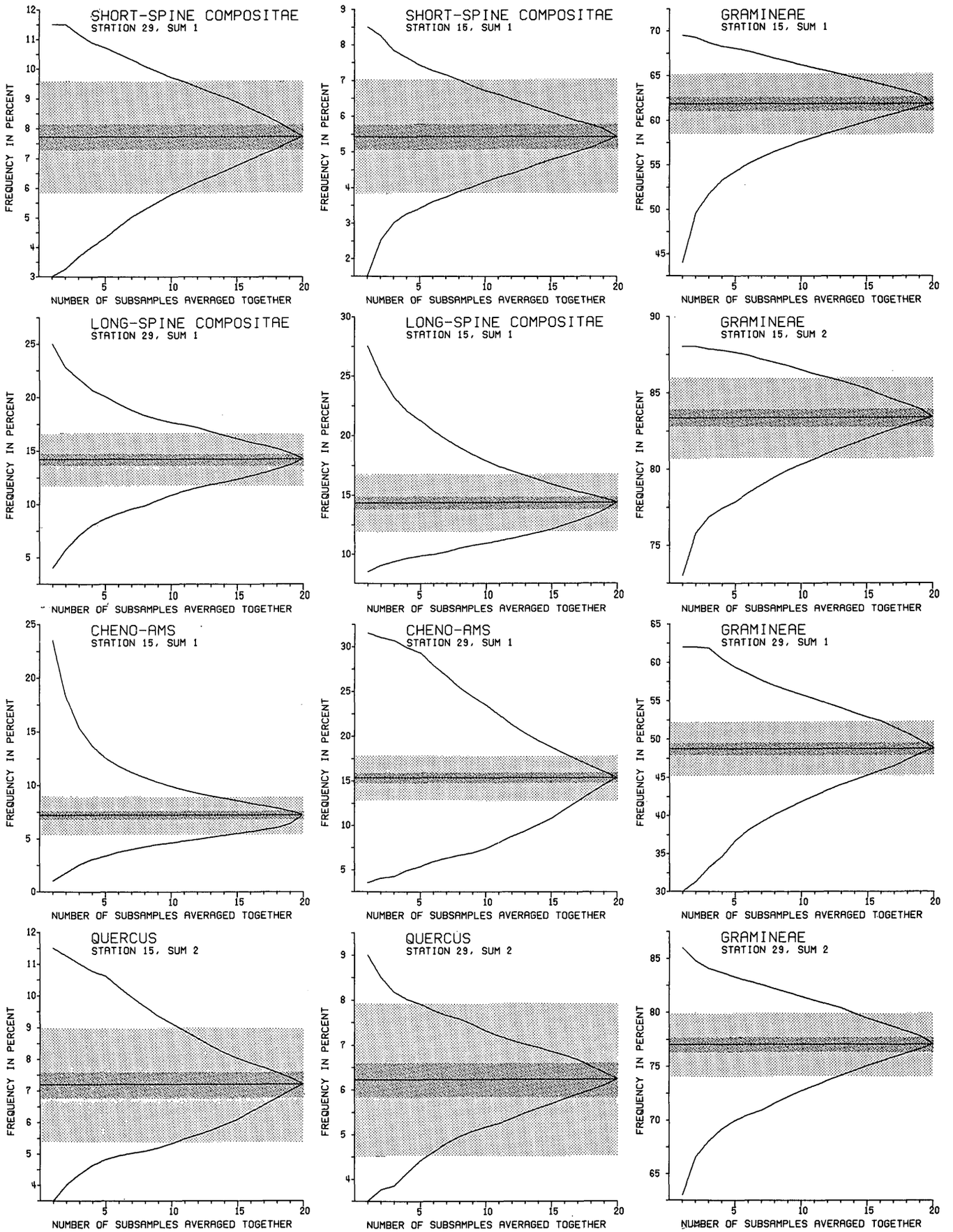
SHORT-SPINE COMPOSITAE
STATION 29, SUM 1
SHORT-SPINE COMPOSITAE
STATION 15, SUM 1
GRAMINEAE
STATION 15, SUM 1
LONG-SPINE COMPOSITAE
STATION 29, SUM 1
LONG-SPINE COMPOSITAE
STATION 15, SUM 1
GRAMINEAE
STATION 15, SUM 2
CHENO-AMS
STATION 15, SUM 1
CHENO-AMS
STATION 29, SUM 1
GRAMINEAE
STATION 29, SUM 1
QUERCUS
STATION 15, SUM 2
QUERCUS
STATION 29, SUM 2
GRAMINEAE
STATION 29, SUM 2
FREQUENCY IN PERCENT
NUMBER OF SUBSAMPLES AVERAGED TOGETHER

TABLE 1.—*Pollen counts of individual subsamples*

[x is the mean; σ is the standard deviation; N is the total number of grains]

Pollen type	1	2	3	4	5	6	7	8	9	10	11	12	13	14	15	16	17	18	19	20	Sum	January 1967 ($x \pm \sigma$)	February 1964
Surface subsamples, station 15, sum 1																							
Pinus	---	3	---	1	1	3	3	4	1	5	3	4	3	2	---	3	3	1	3	1	44	2.2±1.5	3
Quercus	2	6	8	8	8	9	9	11	8	8	16	15	11	14	8	11	12	10	10	15	199	9.9±3.1	7
Juniperus	2	2	3	2	1	---	3	2	2	1	2	4	2	1	1	2	3	1	2	3	39	1.8±1.3	1
Celtis	1	---	---	1	1	2	2	---	1	1	1	2	1	1	1	1	1	2	1	2	22	1.1±1.0	1
Prosopis	2	---	2	2	2	1	---	---	---	1	---	2	1	1	1	---	---	1	3	1	20	1.0±1.0	---
Compositae:																							
Short-spine	12	3	17	11	14	10	16	9	13	7	14	13	8	11	8	8	11	10	9	13	217	10.8±3.2	17
Long-spine	55	45	23	29	32	25	21	25	26	21	21	27	36	19	20	30	25	37	39	17	573	28.6±5.0	27
Cheno-ams	12	2	26	47	15	8	17	19	16	13	13	16	12	9	15	9	5	11	11	12	288	14.4±3.7	22
Gramineae	110	130	112	88	122	134	125	116	128	139	125	116	119	134	138	132	135	123	120	127	2,473	123.6±6.9	112
Euphorbia-type	1	2	2	2	2	1	1	2	1	---	2	1	3	2	4	---	3	1	---	2	32	1.6±1.3	4
Eriogonum	2	2	2	6	---	5	2	4	2	2	1	---	---	2	---	2	1	1	---	2	36	1.8±1.3	2
Other	1	5	5	3	2	2	1	8	2	2	2	---	4	4	4	2	1	2	2	5	57	2.8±1.7	64
Total (N)	200	200	200	200	200	200	200	200	200	200	200	200	200	200	200	200	200	200	200	200	4,000	---	200
Surface subsamples, station 15, sum 2																							
Pinus	---	4	---	2	1	3	7	5	3	7	3	5	4	4	---	5	5	2	3	1	64	3.2±1.8	3
Quercus	7	9	21	23	11	14	11	14	11	11	20	20	22	16	10	13	17	11	12	15	288	14.4±3.7	10
Juniperus	5	2	6	4	1	1	4	2	2	2	2	4	3	1	1	3	4	2	4	5	58	2.9±1.7	2
Celtis	1	---	---	3	2	2	2	---	2	2	2	4	2	1	1	1	2	1	1	3	32	1.6±1.3	2
Prosopis	3	---	4	3	2	1	1	---	---	1	---	2	1	1	2	---	---	1	5	2	29	1.4±1.2	2
Gramineae	176	174	157	146	176	168	167	158	173	171	166	159	158	167	175	171	164	175	170	163	3,334	166.7±5.3	169
Euphorbia-type	1	3	3	2	2	1	1	3	1	---	3	1	4	2	3	1	5	2	3	2	43	2.1±1.6	5
Eriogonum	3	2	3	8	1	5	4	4	2	2	1	1	2	3	---	3	1	1	---	3	49	2.4±1.5	3
Other	4	6	6	9	4	5	3	14	6	4	3	4	4	5	8	3	2	5	2	6	103	5.1±2.2	4
Total (N)	200	200	200	200	200	200	200	200	200	200	200	200	200	200	200	200	200	200	200	200	4,000	---	200
Surface subsamples, station 29, sum 1																							
Pinus	3	2	2	---	1	2	5	2	3	---	3	5	1	2	2	2	7	2	2	4	50	2.5±1.6	5
Quercus	6	10	7	12	9	5	12	4	5	11	7	4	8	8	7	5	6	6	9	10	151	7.5±2.7	7
Juniperus	5	5	2	5	1	3	3	1	2	3	2	4	2	1	4	4	1	4	---	7	59	2.9±1.7	1
Compositae																							
Short-spine	6	9	10	7	16	13	19	15	14	17	23	23	21	20	16	17	14	20	11	18	309	15.4±3.8	21
Long-spine	30	41	30	30	50	35	22	8	35	39	30	29	24	19	24	22	30	15	32	23	568	28.4±4.9	18
Cheno-ams	39	17	61	14	17	9	7	63	14	9	32	54	18	60	55	41	18	30	23	33	614	30.7±5.1	19
Gramineae	99	104	74	124	95	124	123	94	112	108	90	65	105	60	77	91	110	103	101	90	1,949	97.4±7.1	124
Euphorbia-type	5	4	3	---	3	---	3	3	7	6	5	6	10	7	5	5	7	7	4	7	97	4.8±2.2	2
Others	7	8	11	8	8	9	6	10	8	7	8	10	11	23	10	13	7	13	18	8	203	10.1±3.1	3
Total (N)	200	200	200	200	200	200	200	200	200	200	200	200	200	200	200	200	200	200	200	200	4,000	---	200
Surface subsamples, station 29, sum 2																							
Pinus	5	2	8	---	1	3	6	5	4	---	7	7	2	6	3	5	7	5	5	5	86	4.3±2.1	5
Quercus	11	12	18	14	15	8	15	11	10	12	14	14	12	16	13	7	12	8	12	15	249	12.4±3.4	12
Juniperus	5	8	6	7	3	5	4	3	3	4	5	6	4	3	6	6	1	6	---	9	94	4.7±2.1	2
Celtis	2	1	1	3	2	3	2	---	---	1	1	1	5	3	1	3	2	6	2	---	39	1.9±1.4	1
Gramineae	159	163	142	165	167	172	161	158	162	165	147	140	146	126	146	154	155	152	156	145	3,081	154.0±5.9	173
Euphorbia-type	8	5	4	2	4	2	6	6	10	8	11	9	15	14	13	7	14	8	4	10	160	8.0±2.8	3
Other	10	9	21	9	8	7	6	17	11	10	15	23	16	32	18	18	9	15	21	16	291	14.5±3.7	4
Total (N)	200	200	200	200	200	200	200	200	200	200	200	200	200	200	200	200	200	200	200	200	4,000	---	200

REFERENCES CITED

Adam, D. P., 1967, Late-Pleistocene and Recent palynology in the central Sierra Nevada, California, *in* Cushing, E. J., and Wright, H. E., Jr., eds., Quaternary paleoecology: New Haven, Yale Univ. Press, p. 275–301.

——— 1970, Some palynological applications of multivariate statistics: Arizona Univ., Tucson, Ph. D. dissert., 132 p.

Bent, A. M., and Wright, H. E., Jr., 1963, Pollen analyses of surface materials and lake sediments from the Chuska Mountains, New Mexico: Geol. Soc. America Bull., v. 74, p. 491–500.

Hevly, R. H., Mehringer, P. J., Jr., and Yocum, H. G., 1965, Modern pollen rain in the Sonoran Desert: Arizona Acad. Sci. Jour., v. 3, p. 123–135.

Lowe, C. H., ed., 1964, The vertebrates of Arizona: Tucson, Arizona Univ. Press, 259 p.

Maher, L. J., Jr., 1963, Pollen analyses of surface materials from the southern San Juan Mountains, Colorado: Geol. Soc. America Bull., v. 74, p. 1485–1504.

Martin, P. S., 1963, The last 10,000 years: Tucson, Arizona Univ. Press., 87 p.

——— 1964, Pollen analysis and the full-glacial landscape: Research Center Publication No. 3, Fort Burgwin, New Mexico, p. 66–74.

Mehringer, P. J., Jr., 1967, Pollen analysis of the Tule Springs area, Nevada: Nevada State Museum, Anthropological Papers, no. 13, pt. 3, p. 129–200.

Mehringer, P. J., Jr., and Haynes, C. V., Jr., 1965, The pollen evidence for the environment of early man and extinct mammals at the Lehner Mammoth Site, southeastern Arizona: Am. Antiquity, v. 31, p. 17–23.

Mehringer, P. J., Jr., Martin, P. S., and Haynes, C. V., Jr., 1967, Murray Springs, a mid-postglacial pollen record from southern Arizona: Am. Jour. Sci., v. 265, p. 786–797.

Mosimann, J. E., 1965, Statistical techniques for the pollen analyst: multinomial and negative multinomial techniques, *in* Kummel, B., and Raup, D., eds., Handbook of paleontological techniques: San Francisco, W. H. Freeman, p. 636–673.

Schoenwetter, James, and Eddy, F. W., 1964, Alluvial and palynological reconstruction, Navajo Reservoir District: Museum of New Mexico Papers in Anthropology, No. 13, 155 p.

Wright, H. E., Jr., 1967, The use of surface samples in Quaternary pollen analysis: Rev. Paleobotany and Palynology, v. 2, p. 321–330.

Jour. Research U.S. Geol. Survey
Vol. 3, No. 6, Nov.–Dec. 1975, p. 737–745

A LATE HOLOCENE POLLEN DIAGRAM FROM NEAR LAKE TAHOE, EL DORADO COUNTY, CALIFORNIA

By ALOJZ ŠERCELJ [1] and DAVID P. ADAM,
Ljubljana, Yugoslavia, Menlo Park, Calif.

Abstract.—A 2,500-yr pollen record from an alpine meadow in the central Sierra Nevada shows a general agreement with other more detailed pollen records from the late Holocene of California. Tree roots from the site suggest dry conditions at about 1150 and 1350 radiocarbon yr B.P.

This paper describes a pollen record from an alpine wet meadow in the central Sierra Nevada. Several small springs keep the site moist during the dry summer months. The drainage area feeding these springs is rather small, extending from the site to the crest of the range, with the most distant part of the drainage basin only about 0.5 km to the south of the springs. The discharge of the springs, as reflected by peat growth and the pollen record of the surrounding vegetation, should therefore provide a good measure of changes in the precipitation regime at the crest of the Sierra Nevada.

SITE DESCRIPTION

The site (figs. 1–3), which is here designated as Ralston Ridge Bog, is located at the western edge of the valley of Echo Lakes at an altitude of about 2,580 m, less than 250 m from the crest of the Sierra Nevada. Several small springs at the site support boggy vegetation and account for an accumulation of peat. At the lower end of the wet area a natural dam impounds a small pond about 10 to 25 m across. The origin of this dam is uncertain, but it seems to have been formed by accretion of peat, perhaps starting with a fallen log athwart the drainage.

The bedrock beneath and upstream from the site consists of igneous rocks of the Sierra Nevada batholith (Lindgren, 1896), and thus there is little likelihood of finding rebedded pollen.

The present precipitation regime is dominated by heavy winter snows, which fall when large cyclonic storms from the Pacific Ocean are swept over the Sierra Nevada. The orographic lifting that results produces heavy snowfall near the crest of the range, and some snowbanks persist well into August after winters of heavy snowfall. The area above and to the south of Ralston Ridge Bog tends to have a late-melting snow cover; this results both from northern to northwestern exposure and from a forest of mountain hemlock (*Tsuga mertensiana*) that shelters the snow from the sun.

Snowbanks commonly persist from year to year along the nearby east face of the Crystal Range (fig. 1), and some may be permanent. M. H. Clark (oral commun., 1973) reports deposits of both Recess Peak and Matthes Glaciations (see below) on the east side of the Crystal Range, which indicates that local climatic changes during the late Holocene were of sufficient magnitude to produce alternations between glaciation and nonglaciation in the area.

METHODS

The site was sampled during the summers of 1971, 1972, and 1973. The first probing was done with a bucket auger and showed at least 1.5 m of sediment above the pond and the presence of Mazama ash (age 6600 years B.P.) at the site. The following summer a 10-cm core was taken, but the peat was so dense that the corer would not penetrate beyond a depth of 80 cm.

The core, as well as the pollen profile uncovered a year later, was taken from a wet area (fig. 3) between the pond and the springs. The peat in this wet area is very compact and free of roots, and there are no woody plants growing now within several metres of the core site. It was thus of considerable interest that there were woody roots about 1 cm in diameter at several horizons in the core. As this area is now sufficiently wet to prevent woody plants from growing, and the slopes above the site do not appear steep enough to have brought the roots to the site by avalanching, these root horizons were interpreted as representing dry intervals when the summer ground water table was low for a long enough period for woody plants to become established.

[1] Slovenian Academy of Sciences, Ljubljana, Yugoslavia.

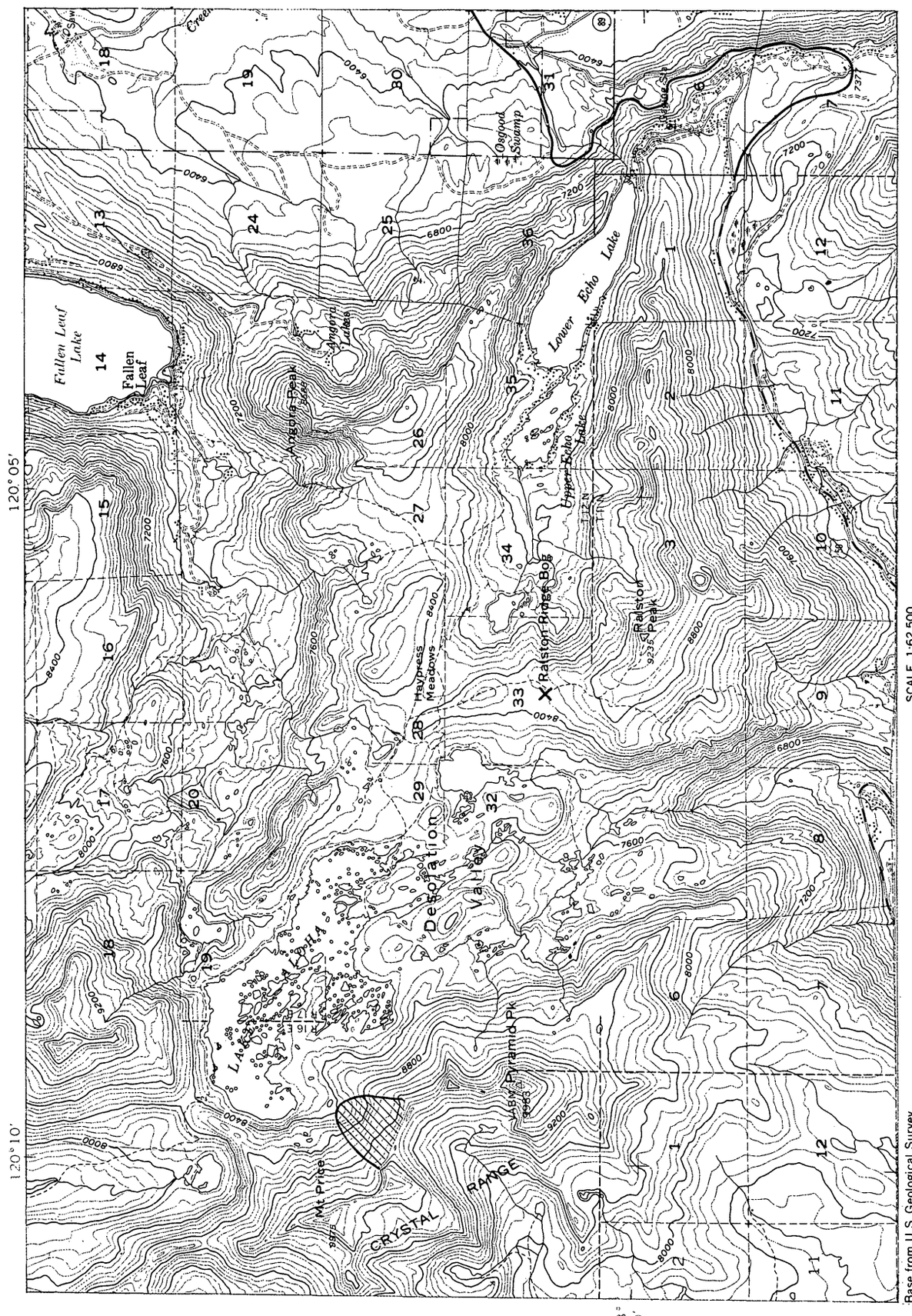

FIGURE 1.—Index map showing location of Ralston Ridge Bog, Echo Lakes valley, and Osgood Swamp. Lined area between Mount Price and Pyramid Peak shows approximate location of Recess Peak glacial deposits.

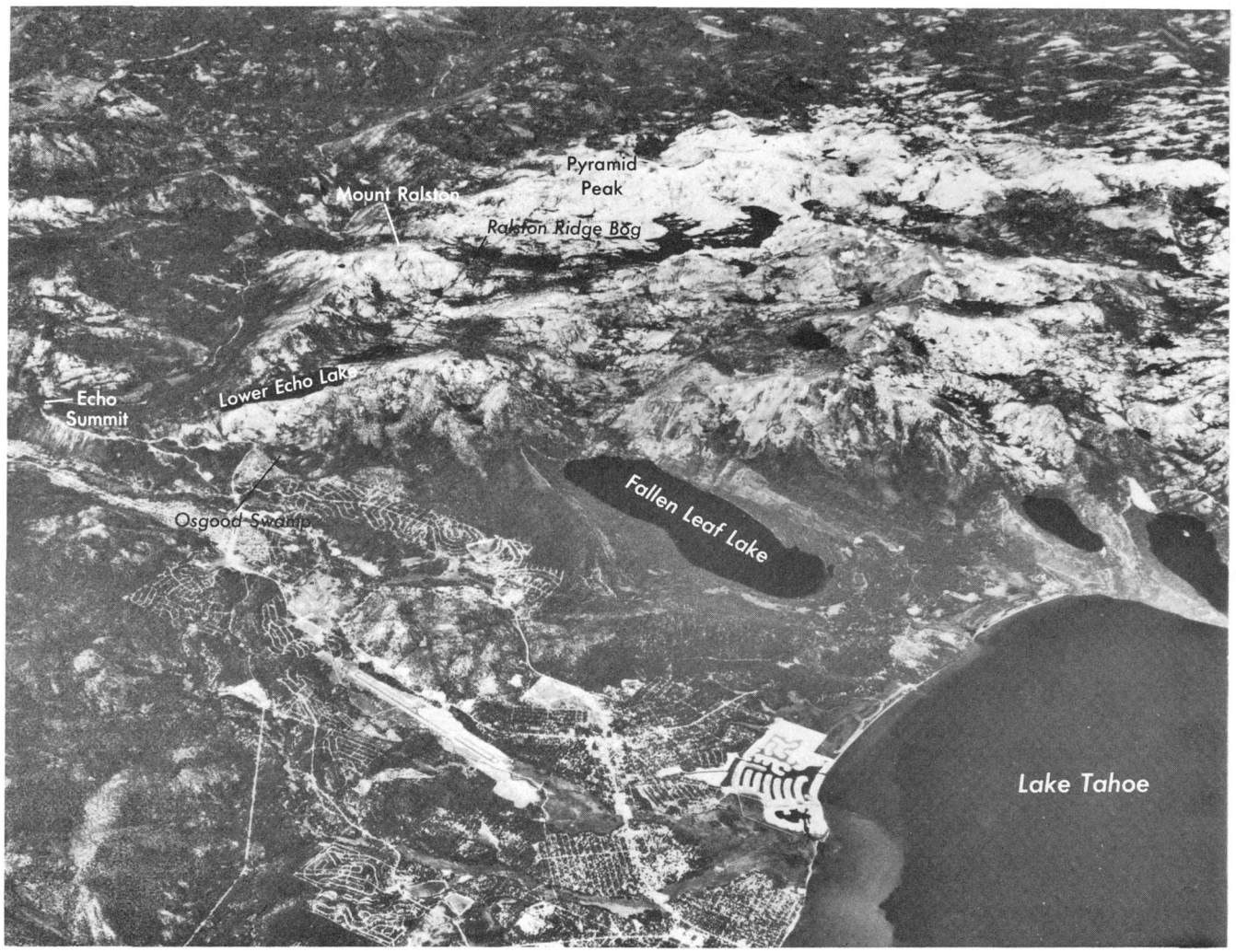

FIGURE 2.—Southwestern part of Lake Tahoe basin. View from the northeast shows the relations of Echo Lakes valley and the Ralston Ridge Bog and Osgood Swamp pollen sites to the crest of the Sierra Nevada (from middle left side to upper right side of photograph). U.S. Geological Survey photograph HA 018L–074, 10 July 1968, taken by U.S. Air Force.

We returned to the site in August 1973 and collected the pollen profile by digging a pit (fig. 3) and removing blocks of sediment from the wall of the pit to a depth of 100 cm. The stratigraphy found is shown in figure 4, and the samples studied are listed in table 1. Eleven pollen samples were removed from the section and extracted by hydrofluoric acid and acetylation. Pollen counts were made using double fixed sums (Mehringer and Haynes, 1965; Adam, 1967). The first sum (200 grains of all pollen) was used to estimate the frequency of pine pollen; the second sum, ranging from 239 to 362 grains of all pollen except pine, was used to estimate the frequency of all other taxa. This procedure departs from that used at nearby Osgood Swamp by Adam (1967, 1970, 1974) in several respects, as follows: (1) We separate pine grains into Haploxylon and Diploxylon groups (2) we separate *Tsuga* from pine, (3) we do not limit the second sum to 100 pollen grains, and (4) we separate *Juniperus* from other Cupressaceae, rather than lump the Cupressaceae into

TABLE 1.—*Pollen samples from Ralston Ridge Bog*

Sample	Zone	Depth (cm)	Pollen (sum 2)	Estimated age, in years	Estimated date of zonal change
1	1a	0–5	293	40 B.P.–A.D. 1910.	
2	1a	11–13	362	290 B.P.–A.D. 1660.	
3	1a	20–22	272	530 B.P.–A.D. 1420.	
4	1a	30–32	278	790 B.P.–A.D. 1160.	
					A.D. 1020.
5	1b	40.5–43	332	1070 B.P.–A.D. 880.	
6	1b	56.5–59	242	1490 B.P.–A.D. 460.	
					A.D. 340.
7	1c	66–68	239	1730 B.P.–A.D. 220.	
8	1c	73–75	277	1910 B.P.–A.D. 40.	
					60 B.C.
9	2	80–82	282	2100 B.P.– 150 B.C.	
10	2	95–97	276	2490 B.P.– 540 B.C.	
11	2	100–102	308	[1] 2595±85 B.P.– 645 B.C.	

[1] Radiocarbon sample I–7556.

FIGURE 3.—Pollen site at the time the pollen profile was collected (21 August 1973). Pollen profile is from pit (foreground). Pond was still overflowing. Crystal Range (background) is a prominent ridge west of the crest of the Sierra Nevada. View to the west.

a single category of TCT that also includes the Taxaceae and the Taxodiaceae. These differences in methods are not important, but they should be kept in mind if figures from this study are compared with Adam's data from Osgood Swamp.

After the pollen counts were made, the data were transferred to punched cards for data processing. The 95-percent binomial confidence limits (Mosimann, 1965; Maher, 1973) for all types were calculated and are shown in figure 4.

A plant list for the Ralston Ridge Bog site and vicinity compiled during the 1973 visit is necessarily incomplete and includes only those plants that were flowering or otherwise identifiable at the time it was made. Many of the observed plants are also recorded in the pollen record, but some are not.

Trees:
- *Pinus murrayana* (Diploxylon type)
- *P. monticola* (Haploxylon type)
- *Tsuga mertensiana*

Shrubs:
- *Salix*
- *Spiraea*
- *Sambucus*
- *Ribes*
- *Arctostaphylos*
- *Kalmia*
- *Vaccinium*

Herbs:
- *Deschampsia*
- *Agrostis*
- *Festuca*
- *Aster*
- *Erigeron*
- *Senecio*
- *Antennaria*
- *Lupinus* (3 spp.)
- *Saxifraga* (2 spp.)
- *Parnassia*
- *Pedicularis*

Herbs—Continued
- *Mimulus*
- *Penstemon*
- *Castilleja*
- *Chimaphila*
- *Epilobium*
- *Chamaenerion*
- *Erythronium*
- *Veratrum*
- *Calochortus*
- *Phlox*
- *Caltha*
- *Sphenosciadium*
- *Oenanthe*
- *Listera*

Marsh plants:
- *Scirpus*
- *Eriophorum*
- *Carex* (2 spp.)
- *Helodea*
- *Polygonum bistortoides*
- *Sphagnum*
- *Hypnum*

Aquatic plants:
- *Sparganium*
- *Callitriche*

POLLEN TYPES

Two types of *Pinus* pollen were distinguished on the basis of bladder morphology. The Haploxylon type grains in this study probably represent mostly *Pinus monticola* (silver or western white pine), and have bladders that are relatively larger than in the Diploxylon type. These grains were usually less than half a sphere as a result of the broad base of insertion of the bladder into the body of the grain, which was either coarsely cristate or at least bore coarse protrusions. The Diploxylon type grains probably represent mostly *Pinus murrayana* (lodgepole pine), had bladders greater than a hemisphere with a finer reticulum, and had a much thinner and more uniform dorsal crest on the body of the grain. Transitional forms were counted as Diploxylon type.

Tsuga mertensiana (mountain hemlock) has inaperturate pollen, but transitional forms range from *Pinus*-like grains to those in which bladders are simple loose fringes. These were separable from *Pinus* because the reticulum of the bladder, if developed, is simple and narrow meshed, with muri that are typically interrupted or punctate. The bladders are not rounded or spherical, but rather intruded and deformed, so that most of them could readily be distinguished from *Pinus* of the Diploxylon type. A single *Tsuga canadensis* type grain with a fringed rudimental corona found in the lowest stratum may represent long-distance transport or possibly an aberrant grain of *Tsuga mertensiana*.

The distinctive size and morphology of *Abies* (fir) pollen made this type easily identifiable, except that fir grains in general showed more damage than other pollen types. The pollen represents either *Abies concolor* or *Abies magnifica*.

Juniperus pollen in this report includes only grains of the *J. communis* type, which is spheroidal to oblong, mostly split, and with both halves somewhat shifted. Other *Juniperus* pollen resembling *J. virginiana* was included in the Cupressaceae, along with *Calocedrus*.

Of the other aboreal pollen, *Pseudotsuga*, with typical laricoid pollen that is rather fragile, is best represented in the lowest strata and probably blew in from a source at a considerably lower elevation. Individual grains of *Taxus*, *Sequoiadendron* (*Sequoia*?), and *Picea* probably also represent long-distance transport.

The few grains of *Quercus* found at the site are most likely to represent *Q. vaccinifolia*, a scrub oak that grows at considerably higher elevations in the Sierra Nevada than other oaks. However, it occurs most frequently in the lower strata along with other pollen types that probably came from distant sources, so some of the *Quercus* grains may represent arboreal oaks.

Water plants are poorly represented except at the base of the section, where *Potamogeton*, *Isoetes*, and Nymphaeaceae occur. In addition, a single tetrad of *Typha latifolia* was found in sample 6.

Several genera of Cyperaceae are represented, and no attempt was made to separate them. Some grains were of the *Eriophorum* type; most sedge grains were damaged because of their thin walls.

Potentilla pollen may have come, at least in part, from *P. palustris*. It was not found in the upper part of the section, nor was the plant found in our survey of the bog vegetation (table 1).

Umbelliferae pollen most probably represents *Oenanthe* and *Sphenosciadium*, which are both common in the present bog vegetation.

Polygonum bistortoides pollen is especially common in the middle of the section. These tricolporate grains closely resemble those of *P. bistorta* but are even larger and have a coarser and thicker sexine. Pori are readily visible. The other *Polygonum* type of grain, found in samples 6 through 8, is much smaller and has a coarsely fringed sexine pattern; it may represent *P. californicum*.

A few grains resembling *Rumex acetosa* found in the two bottom samples may represent Indian or animal impact near the springs or may simply be a result of ground disturbance caused by flooding and deposition of sand on the site.

The relatively high frequency of ericaceous pollen in sample 4 is a result of the local presence of some shrubby species of *Vaccinium* or *Kalmia* at the core site. At this horizon a network of tiny stems occurs within the peat, and these closely resemble stems of *Vaccinium oxycoccos*, although they are a little too thick and not smooth enough to be considered as such.

FOSSIL RECORD

The Ralston Ridge Bog pollen record is generally rather stable, and there is relatively little variability in the pollen percentages. We have therefore relied not only on the pollen record itself for our conclusions, but also on correlations with the more detailed pollen record at nearby Osgood Swamp (Adam, 1967; Zauderer, 1973), using radiocarbon dates from both sites. We have divided the pollen record into four zones using the same system used at Osgood Swamp (Adam, 1967). The Ralston Ridge Bog pollen zones are differentiated mainly on the basis of the pollen curves for *Abies*, Cyperaceae, Umbelliferae, *Polygonum bistortoides*, and Gramineae (table 2).

The major break in the pollen record corresponds to the top of the coarse sands at a depth of 80 cm. Zone 2 (fig. 4) consists of three samples from the sandy layer

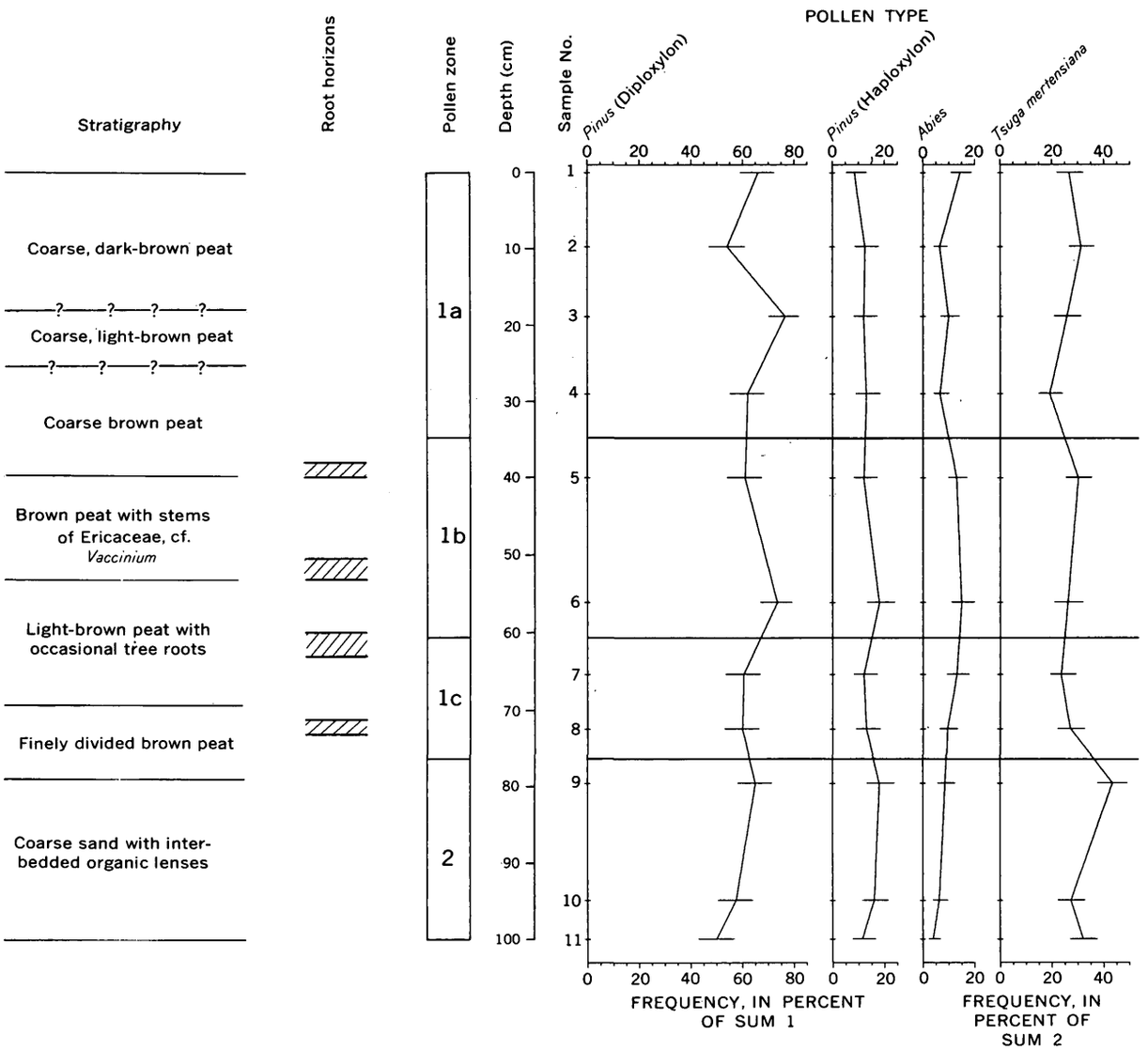

FIGURE 4.—Pollen diagram from Ralston Ridge Bog. Sum 1 includes

TABLE 2.—*Pollen zones at Ralston Ridge Bog and their characteristics*

Zone	Samples	Local maxima	Local minima
1a	1, 2, 3, 4	Cyperaceae	*Abies*
		Umbelliferae	*Polygonum bistortoides*
		Gramineae	
1b	5, 6	*Abies*	Umbelliferae
		Polygonum bistortoides	Gramineae
1c	7, 8	Umbelliferae	*Pinus*, Haploxylon
		Gramineae	
2	9, 10, 11	*Pinus*, Haploxylon	*Abies*
		Tsuga mertensiana	Cyperaceae
		Alnus	Umbelliferae
		Salix	Gramineae
		Potentilla	
		Artemisia	
		Liguliflorae	

and shows high frequencies of *Alnus*, *Salix*, *Potentilla*, *Artemisia*, and Liguliflorae pollen, and low frequencies of *Abies*, Cyperaceae, Umbelliferae, and Gramineae. In addition, several scarce types are found mainly in zone 2, including *Pseudotsuga*, *Taxus*, *Sequoia*, *Acer*, Nymphaeaceae, *Potamogeton*, *Isoetes*, *Rumex*, *Ephedra*, Caryophyllaceae, Saxifragaceae, and *Botrychium*. Taken all together, these occurrences suggest that (1) the aquatic and riparian components of the vegetation during zone 2 time contained plants that are now common only at lower elevations, and (2) local pollen production may have been less than during zone 1 time. Also, the coarse sand interbedded with the organic materials in zone 2 suggests greater rainfall at times when the ground surface was not protected by a snow cover. Either more rain may have fallen during the summer and fall than at present, or there may have been less snow and more rain than at present during the winter.

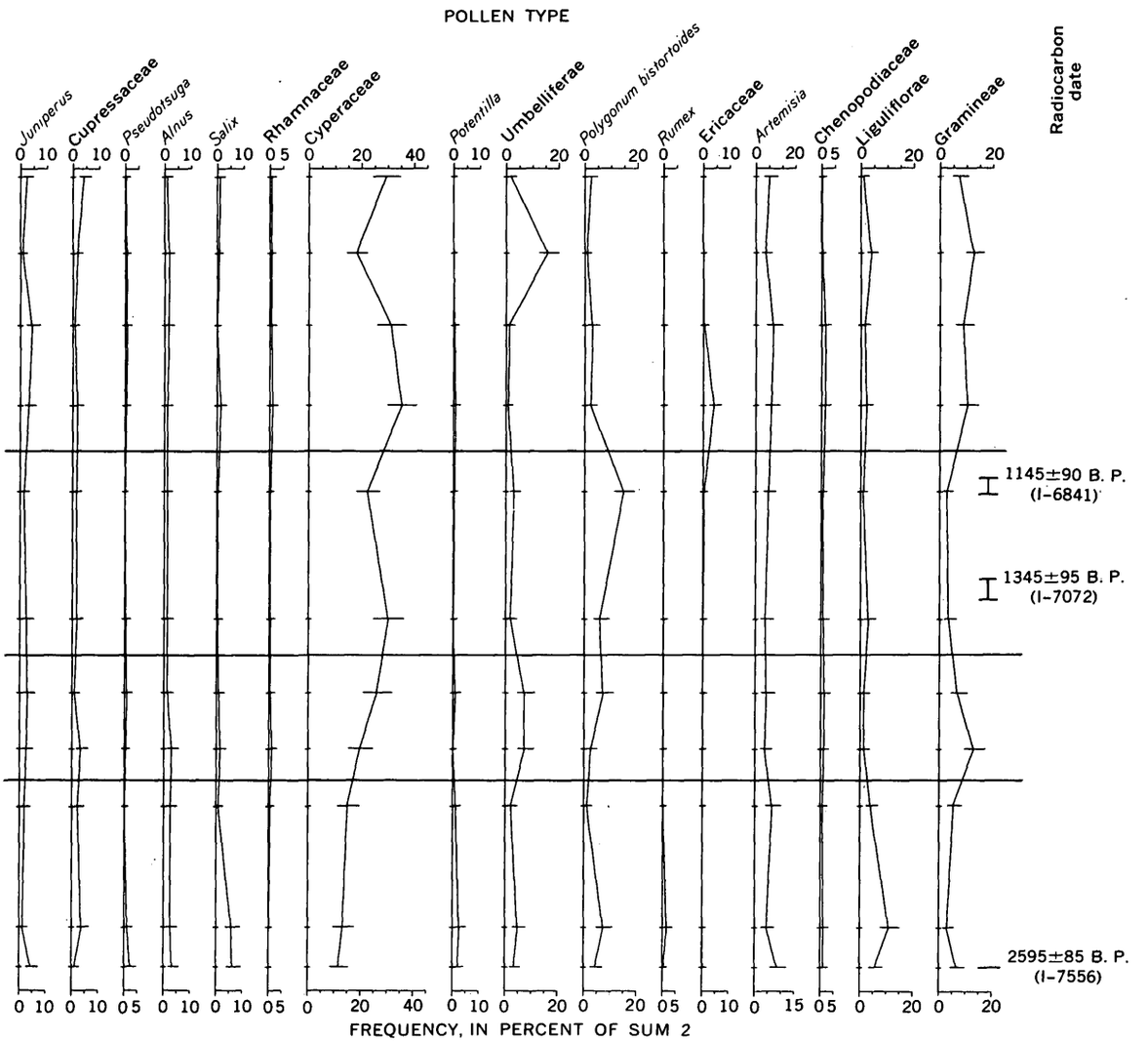

200 grains of all pollen; sum 2 includes all pollen types except pine.

Above zone 2 the deposits are completely organic, and Cyperaceae (sedge) pollen frequencies increase considerably, which we interpret as the result of an increase in the discharge of the springs at the site. There is also a small but systematic increase in *Abies* (fir) pollen.

Zones 1a through 1c are differentiated on the basis of *Abies*, Umbelliferae, *Polygonum bistortoides*, and Gramineae pollen frequencies (table 2). The peaks of Gramineae and Umbelliferae pollen in zones 1a and 1c appear to correlate on the basis of stratigraphic position with the prominent Ericaceae peaks at Osgood Swamp (Zauderer, 1973) and thus represent cool, wet intervals at Ralston Ridge Bog. The *Abies* and *Polygonum bistortoides* pollen peaks, on the other hand, suggest a relatively drier or warmer period during zone 1b.

DATING

Three radiocarbon dates are available from the Ralston Ridge Bog deposits. Two of these, from root horizons in the 1972 core, are discussed below. The third date of 2595±85 B.P. (I–7556) is from wood collected at the base of the pollen section.

As mentioned above, the 1972 core showed several root horizons at depths of 38–40 cm, 50.5–53 cm, 60–63 cm, and 71–73 cm. The upper two of these horizons have been radiocarbon dated at 1145±90 B.P. (I–6841) and 1345±95 B.P. (I–7072), and we assume that these represent periods of relative dryness and decreased spring discharge. The 1972 core was taken about 5 m from the pollen pit, and the ground between the two sites is now rather even, so it seems likely that the dates from the core can be safely extrapolated to

equivalent depths in the pollen section. If that is true, then the dry interval corresponds to samples 5 and 6, in pollen zone 1b. This zone is characterized by high percentages of the pollen of *Abies* and *Polygonum bistortoides* and by low percentages of Gramineae and Umbelliferae.

The lowest root horizon in the core, between 71 and 73 cm, correlates on the basis of depth with pollen zone 1c, which we assume represents cool, wet conditions, whereas the roots correspond to dry conditions. The apparent discrepancy is probably best explained by assuming that the roots were below the ground surface when they grew. The top sample in zone 1c is from a depth of 66–68 cm, and the lowest roots are found between 71 and 73 cm, so that if they grew at a depth of 7 cm or more during the time of zone 1b, they would not be found in zone 1c sediments. Another possibility is that rates of peat formation at the pollen pit and the core site may not have been always parallel.

CORRELATIONS

The Neoglacial sequence in the Sierra Nevada is derived from the detailed work of Birman (1964), who recognized three Neoglacial advances which were designated as Hilgard, Recess Peak, and Matthes Glaciations. Although he believed that all these glaciations followed the postglacial climatic optimum, later workers (Sharp, 1972; Curry, 1969, 1971) believed that the Hilgard was an early postglacial event, or a stade during the Tioga Glaciation (Birkeland and Janda, 1971).

The most detailed work on dating the younger Holocene glacial advances in the Sierra Nevada is by Curry (1969), who relied mainly upon lichenometric dates using *Rhizocarpon* and *Acarospora*. He estimated that the age of the Recess Peak deposits is between 2,000 and 2,700 yr, and that the Matthes moraines postdate A.D. 1550. In addition, he also reported an unnamed glacial advance, not as well defined as the Recess Peak or Matthes, that occurred between A.D. 850 and 1050.

Other information is available from Osgood Swamp, a few kilometres east of Ralston Ridge Bog. The pollen record there (Adam, 1967) shows a pronounced change between Osgood pollen zones 1 and 2a that was interpreted as the onset of the Neoglacial interval; a radiocarbon date of 2,920±200 B.P. (A–544) was obtained near top of pollen zone 2a. (This date is 90 yr greater than originally reported because of a laboratory calibration error discovered after publication (Adam, 1967). The top of the Osgood Swamp section has been restudied in detail by Zauderer (1973) in order to establish a more precise Neoglacial climatic sequence. His results show that during the Neoglacial interval, there were two major peaks in the frequency of Ericaceae pollen, and these are interpreted as responses of the swamp vegetation to the same climatic changes that produced glacial advances in the higher parts of the Sierra Nevada. He dated these peaks in the frequency of Ericaceae pollen by assuming a uniform rate of sedimentation above the Mazama ash layer that occurred at a depth of 125 cm in his core. The Hypsithermal-Neoglacial transition in the core is marked by a sharp drop in *Quercus* pollen between 45 and 47 cm, and the estimated age of the boundary is about 2,430 yr. The Ericaceae maxima occur at depths of 37 cm and 5 cm and have estimated ages of 1,950 yr (A.D. 20) and 260 yr (A.D. 1700), respectively. The second date agrees well with Curry's (1969) estimate of the age of the Matthes Glaciation, but the first date is somewhat younger than both Curry's estimate of the age of the Recess Peak deposits and supporting age estimates of similar Neoglacial deposits elsewhere in western North America (Porter and Denton, 1967; Denton and Karlén, 1973). Several causes may be invoked to account for these discrepancies. Heusser (1960) noted that the Hypsithermal interval lasted longer at lower latitudes in western North America, and Benedict (1973) pointed out that the Neoglacial in the Sierra Nevada apparently postdates the Neoglacial in the Rocky Mountains. There is also the possibility that Curry's lichen growth curves are not yet correctly calibrated.

A final important factor is that there have almost certainly been variations in the rates of sedimentation at Osgood Swamp since the end of the Hypsithermal, and in fact sedimentation may have ceased on at least one occasion. Several stumps have been found in growth position well out from the edge of Osgood Swamp, and one of these has yielded a radiocarbon date of 910±85 B.P. (I–6843), or about A.D. 1040. These trees could only have grown in the position in which they were found during considerably drier conditions than the present, and oxidation of the peat surface may well have slowed the rate of sediment accumulation at that time. This would make underlying strata appear too young when dated using the assumption of a uniform rate of sedimentation.

Adam (1975) described a Holocene pollen sequence covering the last 3,000 yr at Pearson's Pond in San Mateo County, 250 km to the southwest. At that site the identification of the Hypsithermal-Neoglacial boundary is made difficult by changes in the pollen record produced by the landsliding that created the pond and the plant succession that followed, but prominent peaks for both *Pediastrum* and *Botryococ-*

cus occur between 126 and 148 cm in the core, and a radiocarbon date of 2190±85 B.P. at a depth of 129 cm indicates that the Pearson's Pond algal peak is correlative with the lower Ericaceae peak at Osgood Swamp. By again assuming uniform sedimentation rates between radiocarbon dates, the Pearson's Pond algal peak may be dated between about 2470 B.P. and 2100 B.P.

REFERENCES CITED

Adam, D. P., 1967, Late-Pleistocene and Recent palynology in the central Sierra Nevada, California, *in* E. J. Cushing and H. W. Wright, Jr., eds., Quaternary paleoecology: New Haven, Yale Univ. Press, p. 275–301.

——— 1970, Some palynological applications of multivariate statistics: Tucson, Univ. of Arizona, Ph. D. thesis, 140 p.

——— 1974, Palynological applications of principal component and cluster analyses: U.S. Geol. Survey Jour. Research, v. 2, no. 6, p. 727–741.

——— 1975, A late Holocene pollen record from Pearson's Pond, Weeks Creek landslide, San Francisco peninsula, California: U.S. Geol. Survey Jour. Research, v. 3, no. 6.

Benedict, J. B., 1973, Chronology of cirque glaciation, Colorado Front Range: Quaternary Research, v. 3, p. 584–599.

Birkeland, P. W., and Janda, R. J., 1971, Clay mineralogy of soils developed from Quaternary deposits of the eastern Sierra Nevada, California: Geol. Soc. America Bull., v. 82, no. 9, p. 2495–2513.

Birman, J. H., 1964, Glacial geology across the crest of the Sierra Nevada, California: Geol. Soc. America Spec. Paper 75, 80 p.

Curry, R. R., 1969, Holocene climatic and glacial history of the central Sierra Nevada, California: Geol. Soc. America Spec. Paper 123, p. 1–47.

———1971, Glacial and Pleistocene history of the Mammoth Lakes, Sierra, California, a geologic guidebook: Missoula, Univ. Montana, Dept. Geology, Geol. Ser., no. 11, 49 p.

Denton, G. H., and Karlén, Wibjörn, 1973, Holocene climatic variations—their pattern and possible cause: Quaternary Research, v. 3, no. 2, p. 155–205.

Heusser, C. J., 1960, Late-Pleistocene environments of North Pacific North America—an elaboration of late-glacial and postglacial climatic, physiographic, and biotic changes: Am. Geog. Soc. Spec. Pub. 35, 308 p.

Lindgren, Waldemar, 1896, Description of the gold belt; description of the Pyramid Peak quadrangle [Calif.]: U.S. Geol. Survey Geol. Atlas, Folio 31, 8 p.

Maher, L. J., 1973, Nomograms for computing 0.95 confidence limits of pollen data: Rev. Palaeobotany and Palynology, v. 13, p. 85–93.

Mehringer, P. J., Jr., and Haynes, C. V., Jr., 1965, The pollen evidence for the environment of early man and extinct mammals at the Lehner Mammoth Site, southeastern Arizona: Am. Antiquity, v. 31, p. 17–23.

Mosimann, J. E., 1965, Statistical methods for the pollen analyst; multinomial and negative multinomial techniques, *in* Kummel, B., and Raup, D., eds., Handbook of paleontological techniques: San Francisco, Freeman, p. 636–673.

Porter, S. C., and Denton, G. H., 1967, Chronology of Neoglaciation in the North American Cordillera: Am. Jour. Sci., v. 265, p. 177–210.

Sharp, R. P., 1972, Pleistocene glaciation, Bridgeport Basin, California: Geol. Soc. America Bull., v. 83, p. 2233–2260.

Zauderer, J. N., 1973, A neoglacial pollen record from Osgood Swamp, California: Tucson, Univ. of Arizona, M.S. thesis, 48 p.

Jour. Research U.S. Geol. Survey
Vol. 3, No. 6, Nov.–Dec. 1975, p. 747–751

ABSOLUTE AGE OF DISSEMINATED URANINITE IN WHEELER BASIN, GRAND COUNTY, COLORADO

By K. R. LUDWIG and E. J. YOUNG, Denver, Colo.

Abstract.—Uranium and lead isotopic analyses of monazite and uraninite from the disseminated uraninite occurrence at Wheeler Basin, Grand County, Colo., indicate that these minerals formed 1,446±20 m.y. ago. This time correlates well with intrusion of the Silver Plume Granite. The uraninite and monazite were also affected by a later disturbance at 880±130 m.y., but show essentially no effects of subsequent events. This secondary disturbance may have been due to intrusion of dikes related to the Pikes Peak batholith, dated at 1,041±13 m.y. ago.

Uraninite in Precambrian rocks in Wheeler Basin, Grand County, Colo. (fig. 1), is the only known occurrence in the United States of disseminated uraninite of probable metamorphic origin. The occurrence is small, but is similar in many ways to the Rössing deposit in South-West Africa as described by von Backström (1970).

Young and Hauff (1975) concluded from field and petrographic evidence that the uraninite is metamorphic in origin, and attributed its crystallization to the intrusion of a nearby pluton of granite correlated with the Silver Plume Granite, dated at 1,390–1,450 m.y. ago (Peterman and others, 1968); however, they did not observe conclusive evidence of a relation between the granite and the uraninite.

Acknowledgments.—We thank P. L. Hauff for assistance in mineral separation and C. E. Hedge for illuminating discussions on the regional Precambrian geochronology.

GEOLOGIC SETTING

The uraninite occurs in Precambrian metamorphic rocks consisting of migmatized gneiss, mixed gneiss and pegmatite, and small discrete pegmatites. These rocks are probably correlative with the metasedimentary and metavolcanic Idaho Springs Formation, metamorphosed 1,700–1,800 m.y. ago (Peterman and others, 1968). A pluton of granitic rock crops out about 400 ft (130 m) to the south, and probably underlies the metamorphic rocks at the sample locality. This pluton is correlated with the Silver Plume Granite on the basis of its texture and mineralogy. Regional foliation generally strikes northwest and dips northeast at moderate to steep angles. These relations are illustrated by Young and Hauff (1975).

PETROGRAPHY

The uraninite is disseminated in biotite clots in the metamorphic rocks. These clots consist mostly of biotite, sillimanite, and quartz, minor amounts of pyrite, muscovite, monazite, hematite, and uraninite, and trace amounts of zircon, molybdenite, chalcopyrite,

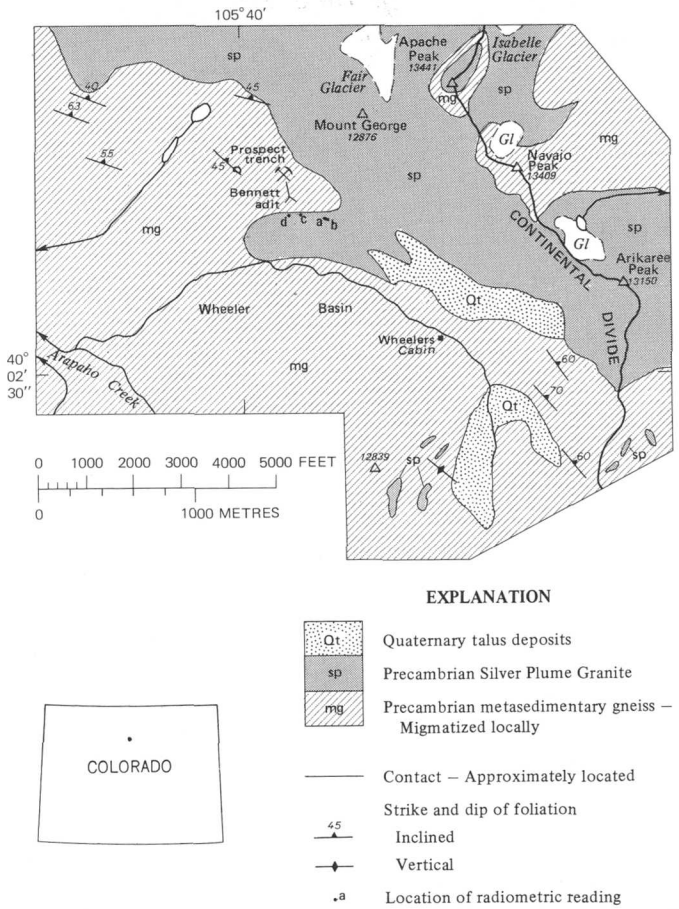

FIGURE 1.—*Geologic sketch map of Wheeler Basin. From Young and Hauff (1975, fig. 1).*

and fluorite. Biotite flakes as much as 5 mm across contain much of the uraninite, which typically occurs as euhedral and anhedral grains from 0.1 to 3 mm in diameter. A more detailed description of the mineralogy and petrography was given by Young and Hauff (1975).

ANALYZED MINERAL SEPARATES

Separates of pure uraninite and nearly pure monazite were obtained by density and magnetic separation from crushed specimens of the biotite clots. The resulting monazite separates (with the exception of sample M2) were then handpicked for clarity and freedom from inclusions. The main impurities were black opaque minerals included in and attached to the monazite grains. The modal abundance of impurities was about 0.5 to 1 percent in the unpicked sample (M2), and about 0.05 to 0.1 percent in the other monazite samples. Some of the opaque impurity may have been uraninite; however, the uniformity of the uranium contents of the four monazite separates (9,470±540 ppm) requires that the abundance of uraninite in the monazite samples be less than about 0.1 percent. The analyzed monazite grains were lemon-yellow, subhedral to anhedral, and about 20 to 100 μm in diameter. The monazite samples weighed 2–5 mg.

The uraninite samples consisted of from one to several grains (about 100 μg total), about 50 μm in diameter. Most grains were moderately well-formed to well-formed black cubes having a submetallic luster. Many of the uraninite grains contained 1 to 5 percent of translucent, yellow and orange-brown minerals near and at the edges of the grains. The orange-brown minerals are probably the curite and fourmarierite identified by X-ray methods by Young and Hauff (1975). The yellow mineral(s) may be schoepite or becquerelite.

ANALYTICAL TECHNIQUES

Monazite samples were dissolved in a few millilitres of hot concentrated HF and $HClO_4$, and uraninite samples in a few millilitres of hot concentrated HNO_3. In an attempt to remove surficial common lead picked up by the uraninite samples during handling, two of the uraninite samples were briefly immersed in a cold HCl wash, and both the washed grains and the HCl wash analyzed.

After digestion, the samples were taken to dryness, redissolved in concentrated HNO_3, and split into weighed aliquots for isotopic composition and concentration determinations. The lead was purified by coprecipitation with barium nitrate (Tatsumoto, 1966) followed by dithizone extraction (Silver and others, 1963), and then loaded onto a single rhenium filament with silica gel and phosphoric acid (modified from Cameron and others, 1969). Laboratory lead contamination was 10 to 20 nanograms per analysis. Uranium was purified using the ion-exchange methods of Tatsumoto (1966), and loaded onto the side filaments of a rhenium triple-filament assembly. Isotope ratios were determined with a 12-inch radius, single-focusing mass spectrometer. Lead isotope ratios were corrected for isotopic discrimination in the mass spectrometer by normalization of concurrently analyzed NBS isotopic standards to the "absolute" values determined by Catanzaro and others (1968). Uncertainties in the lead isotope ratios do not exceed 0.25 percent for ratios <500, 1 percent for ratios between 500 and 10,000, and 4 percent for ratios $>10{,}000$. Concentrations of lead and uranium were determined by isotope dilution, and are reproducible to ±0.5 percent.

RESULTS

When plotted on a concordia diagram (Wetherill, 1956), the data (tables 1, 2) are virtually collinear (fig. 2), and scatter slightly about a line which intersects concordia at $1{,}446^{-10}_{+14}$ m.y. and 880±114 m.y.[1] The line-fitting method of York (1969) was used; errors are the $\pm 2\sigma$ limits. Because of the shallow angle of intersection of the chord with concordia, small systematic errors in concentration determinations significantly affect the position of the intersections. In light of the possibility of systematic errors

[1] Decay constants used for U^{238} and U^{235} were 0.155125×10^{-9}/yr and 0.98485×10^{-9}/yr (Jaffey and others, 1971); with the constants previously in common use (0.15369×10^{-9}/yr and 0.97216×10^{-9}/yr), the intercepts are 1,486 m.y. and 880 m.y.

TABLE 1.—*Analytical data for monazite samples*

Sample	Moles radiogenic Pb/g ($\times10^8$)	Moles U/g ($\times10^8$)	$\frac{Pb^{206}}{Pb^{204}}$	$\frac{Pb^{206}}{Pb^{207}}$	$\frac{Pb^{206}}{Pb^{208}}$	Radiogenic[1] $\frac{Pb^{206}}{Pb^{208}}$	Radiogenic Pb^{207}/Pb^{206} Ratio[1]	Age (m.y.)[2]	Pb^{206}/U^{238} Ratio	Age (m.y.)[2]	Pb^{207}/U^{235} Ratio	Age (m.y.)[2]
M7G	3,026	3,754	20,400	11.004	0.4670	0.4669	0.09020	1,430	0.2512	1,445	3.124	1,439
M7A	3,131	4,125	7,860	10.882	.5072	.5072	.09012	1,428	.2497	1,437	3.103	1,433
M2	3,015	3,992	11,700	10.528	.5795	.5797	.09380	1,504	.2698	1,539	3.490	1,525
M11	3,030	4,046	13,800	10.790	.5365	.5366	.09166	1,461	.2553	1,466	3.226	1,463

[1] Common lead for correction with 206/204=19, 207/204=15.6, 208/204=38.5 (normal laboratory contaminant lead).
[2] Decay constants of $\lambda_{238}=0.155125\times10^{-9}$/yr, $\lambda_{235}=0.98485\times10^{-9}$/yr, $U^{238}/U^{235}=137.88$.

TABLE 2.—*Analytical data for uraninite samples*

Sample	Moles radiogenic Pb in sample ($\times 10^8$)[1]	Moles U in sample ($\times 10^8$)	$\frac{Pb^{206}}{Pb^{204}}$	$\frac{Pb^{206}}{Pb^{207}}$	$\frac{Pb^{206}}{Pb^{208}}$	Radiogenic $\frac{Pb^{208}}{Pb^{206}}$[2]	Radiogenic Pb^{207}/Pb^{206} Ratio[2]	Radiogenic Pb^{207}/Pb^{206} Age (m.y.)[3]	Pb^{206}/U^{238} Ratio	Pb^{206}/U^{238} Age (m.y.)[3]	Pb^{207}/U^{235} Ratio	Pb^{207}/U^{235} Age (m.y.)[3]
U1 (total)[4]	11.21	45.99					0.08720	1,365	0.2243	1,305	2,696	1,327
U11 (total)	8.081	33.09	88,000	11.439	147.39	158	.08726	1,366	.2250	1,308	2.707	1,330
U3 (total)[4]	5.753	24.36					.08645	1,348	.2177	1,270	2.595	1,299
U1 (washed)	11.08	45.10	17,800	11.372	106.88	139	.08715	1,364	.2261	1,314	2.717	1,333
U3 (washed)	5.743	24.32	26,700	11.500	132.67	164	.08644	1,348	.2178	1,270	2.595	1,299
U1 (HCl-wash)	.126	.8929	439.9	8.171	[5]	[5]	.09085	1,443	.1300	788	1.628	981
U3 (HCl-wash)	.0097	.04241	62.73	3.193	[5]	[5]	.09255	1,479	.2098	1,228	2.677	1,322

[1] Samples not weighed because of small size.
[2] Common lead for correction with 206/204=19, 207/204=15.6, 208/204=38.5 (normal laboratory contaminant lead).
[3] Decay constants of $\lambda_{238}=0.155125\times10^{-9}$/yr, $\lambda_{235}=0.98485\times10^{-9}$/yr, $U^{238}/U^{235}=137.88$.
[4] Calculated by adding wash and washed fractions. The 206/204, 206/207, and 206/208 values calculated in this way would not be comparable to the observed ratios given in the table, owing to the effective doubling of the contribution of laboratory contaminant lead in the calculated ratios.
[5] Not determined—spiked with Pb^{208} before extraction.

as large as 0.6 percent in determinations of the uranium to lead ratios, more realistic error assignments are 1,446±20 m.y. and 880±130 m.y.

The virtual collinearity of the monazite and uranite data on the concordia diagram (fig. 2) confirms the petrographic conclusion that the two minerals are cogenetic. The minerals were evidently formed 1,446±20 m.y. ago, and were significantly affected by an event 880±130 m.y. ago. Laramide and later events apparently did not significantly affect either mineral. Uraninite responded to the later disturbance by losing lead, whereas some of the monazite samples evidently lost uranium compared to lead.

It is interesting that, whereas U-Pb isotopic data on zircons from both Silver Plume age plutons and older (1,650–1,820 m.y.) rocks from the southwestern United States show no distinct effect of younger Precambrian events, and all such zircons were apparently affected by Mesozoic-Tertiary disturbances (L. T. Silver, oral commun., 1974), the uraninite and monazite data of this study show the opposite pattern.

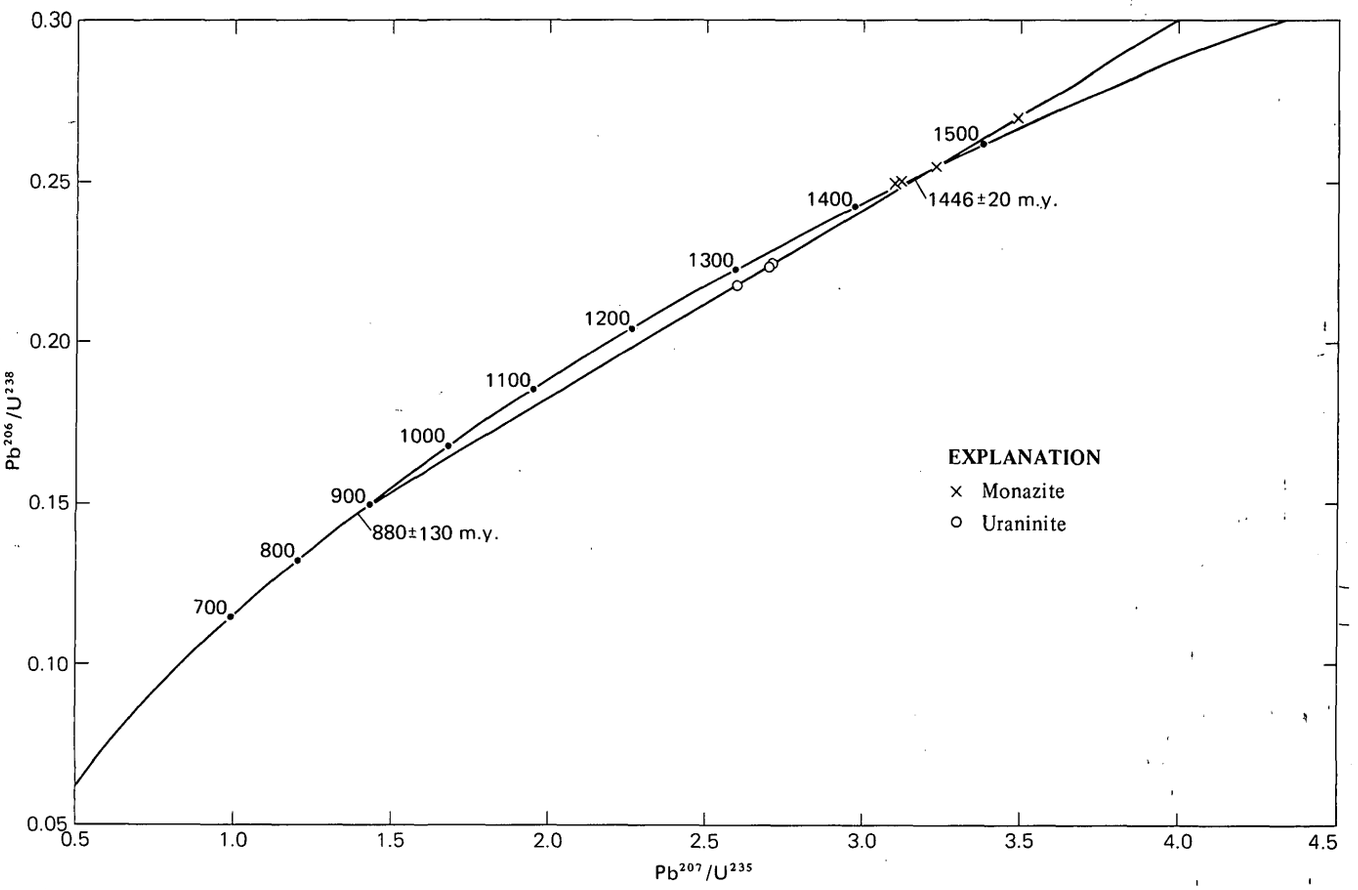

FIGURE 2.—Concordia diagram of monazite and total uraninite data. The best fit intersects concordia at 880±130 m.y. and 1,446±20 m.y.

EFFECT OF HCl WASHING ON URANINITE

The original purpose of the HCl-wash procedure was to preferentially remove surficial, contaminant common lead, without significantly disturbing the actual uraninite lead and uranium. Although the washes did indeed leach lead with a greater proportion of common lead than the wash samples, more complex effects on the lead isotopic compositions of the uraninite samples were also observed. These effects, however, were not great enough to significantly influence the age interpretation just given.

Procedure.—Before digestion in HNO_3, uraninite sample U1 was immersed in cold 2*N* HCl for 20 min and sample U3 in cold 0.05 *N* HCl for 5 min. U^{235} and Pb^{208} spikes were added to the washings, which were then analyzed (table 2).

Washes from both samples contained a small amount of uranium and radiogenic lead; 1.14 percent of the radiogenic Pb^{206} and 1.94 percent of the uranium were leached from sample U1 by the wash, and 0.168 percent of the radiogenic Pb^{206} and 0.174 percent of the uranium from sample U3. The Pb/U ratios of the washes of samples U1 and U3 were, respectively, 42 percent and 3.2 percent lower than the values for the corresponding total samples. This effect could be due merely to differential leaching of lead compared to uranium from a single mineral, or to preferential solution of a lead-free uranium alteration mineral such as schoepite or becquerelite. (The presence of the identified alteration minerals, curite and fourmarierite, cannot account for the observed effect, as they contain essential lead.)

However, the radiogenic Pb^{207}/Pb^{206} values of the HCl washes show analytically significant (though small) differences from the washed samples. The radiogenic Pb^{207}/Pb^{206} value of the HCl wash is 4.1 percent higher for sample U1 and 6.6 percent higher for sample U3 than the corresponding washed sample (table 2). This requires that either (1) the samples have preferentially lost intermediate daughters from the U^{238} decay chain, or (2) the samples contain a phase which sometime in the past lost uranium preferentially to lead, or (3) radiogenic lead from an older system has been incorporated by the samples.

That acid-washings of uraninites can contain lead differing in radiogenic Pb^{207}/Pb^{206} compared to the washed uraninite was observed previously by Banks and Silver (1964), Berglof (1970), and Ludwig (unpub. data, 1974) on uraninites from Phanerozoic uranium deposits. This phenomenon is now being investigated in detail by K. R. Ludwig. The important considerations of this finding to the present study are that (1) the effect is small—neither the location of the intercepts of the chord with concordia nor the fit of the chord to the data is significantly affected by using data from the acid-washed, instead of the total, samples, and (2) though the direction of the effect results in an increase (about 8 m.y.) in the time of the lower intersection if the acid-washed rather than the total uraninite data are used, the choice causes no significant change (less than 1 m.y.) in the time of the upper intersection.

GEOLOGIC SIGNIFICANCE

Young and Hauff (1975) concluded that the intrusion of the granite, which crops out about 400 ft (130 m) from the sample localities, was responsible for the formation of the uraninite and monazite. Silver Plume and related granites have been dated using Rb-Sr methods (Peterman and others, 1968) at 1,390 m.y. to 1,450 m.y. Therefore, the interpretation given by Young and Hauff is supported by the 1,446±20 m.y. apparent age of the uraninite and monazite.

The apparent time of later disturbance, 880±130 m.y., does not correlate precisely with other dated events in the Rocky Mountains, but within analytical error, is close to the 1,041±13 m.y. apparent age determined by Hedge (1970) for the time of intrusion of the Pikes Peak batholith. Major igneous or metamorphic effects related to the Pikes Peak batholith have not been recognized north of the main Pikes Peak plutons, which lie about 50 mi (80 km) southeast of Wheeler Basin. However, about 20 mi (35 km) east of Wheeler Basin granitic dikes of Pikes Peak age have been dated (C. E. Hedge, oral commun., 1974). The local focus of the disturbance recorded by the analyzed uraninite and monazite samples may have been such dikes, possibly exposed and not recognized.

REFERENCES CITED

Backström, J. W. von, 1970, The Rössing uranium deposit near Swakopmund, South West Africa—A preliminary report, *in* Uranium exploration geology: Vienna, Internat. Atomic Energy Agency, Panel Proc. Ser., p. 143–150.

Banks, P. O., and Silver, L. T., 1964, Re-examination of isotopic relationships in Colorado Front Range uranium ores: Geol. Soc. America Bull., v. 75, p. 469–476.

Bergloff, W. R., 1970, Absolute age relationships in selected Colorado Plateau uranium ores: Columbia Univ. Ph. D. thesis, 149 p.

Cameron, A. E., Smith, D. A., and Walker, R. L., 1969, Mass spectrometry of Nanogram-size samples of lead: Anal. Chemistry, v. 41, p. 525–526.

Catanzaro, E. J., Murphy, T. J., Shields, W. R., and Garner, E. L., 1968, Absolute isotopic abundance ratios of common, equal atom, and radiogenic lead isotope standards: Natl. Bur. Standards Jour. Research, A. Physics and Chemistry, v. 72A, p. 261–267.

Hedge, C. E., 1970, Whole-rock Rb-Sr age of the Pikes Peak batholith, Colorado; *in* Geological Survey research 1970: U.S. Geol. Survey Prof. Paper 700–B, p. B86–B89.

Jaffey, A. H., Flynn, K. F., Glendenin, L. E., Bentley, W., and Essling, A. M., 1971, Precision measurement of half-lives and specific activities of ^{235}U and ^{238}U: Phys. Rev. C, v. 4, p. 1889–1906.

Peterman, Z. E., Hedge, C. E., and Braddock, W. A., 1968, Age of Precambrian events in the northeastern front range, Colorado: Jour. Geophys. Research, v. 73, no. 6, p. 2277–2296.

Silver, L. T., McKinney, C. R., Deutsch, S., and Bolinger, J., 1963, Precambrian age determinations in the western San Gabriel Mountains, California: Jour. Geology, v. 71, p. 196–214.

Tatsumoto, M., 1966, Genetic relations of ocean basalts as indicated by lead isotopes: Science, v. 153, p. 1094.

Wetherill, G. W., 1956, Discordant uranium-lead ages: Am. Geophys. Union Trans., v. 36, p. 320–326.

York, D., 1969, Least-squares fitting of a straight line with correlated errors: Earth and Planetary Sci. Letters, v. 5, p. 320–324.

Young, E. J., and Hauff, P. L., 1975, An occurrence of disseminated uraninite in Wheeler Basin, Grand County, Colorado: U.S. Geol. Survey Jour. Research, v. 3, no. 3, p. 305–311.

Jour. Research U.S. Geol. Survey
Vol. 3, No. 6, Nov.–Dec. 1975, p. 753–755

ION-SELECTIVE ELECTRODE DETERMINATION OF IODINE IN ROCKS AND SOILS

By W. H. FICKLIN, Denver, Colo.

Abstract.—Use of an iodide-ion-selective electrode permits rapid and fairly accurate determination of iodine (as iodide) in rocks and soils. When a 1-g sample is used, concentrations as small as 0.5 ppm can be determined with a precision of about 25-percent relative standard deviation. When bromine concentration is greater than 5 ppm, the same method can be used for bromine determination. The procedure merits further investigation as a possible tool in geochemical prospecting.

Existing procedures for the determination of iodine in geological materials lack either adequate sensitivity or speed to analyze the large number of samples that are required for a geochemical exploration program. A reaction between Ce(IV) and As(III) which is catalyzed by iodine was reported by Sandell and Kolthoff (1934, 1937). Schneider and Miller (1965) used this reaction to determine iodine in rocks and soils; they reported several interferences, and therefore conditions must be carefully controlled. Grimaldi and Schnepfe (1971) described a spectrophotometric method that detects as little as 1 ppm of iodine in rocks and soils; this method involves a carbonate sinter, water extraction, and several oxidation-reduction steps. With the iodide-ion electrode method many of the steps can be eliminated. The sensitivity of the electrode allows detection of as little as 0.5 ppm of iodine in a 1-g sample. The function of the electrode was described by Ross (1969, p. 78).

In the precedure described in this paper the sample is sintered in a sodium carbonate-potassium carbonate-magnesium oxide flux that was described by Grimaldi and Schnepfe (1971). The sintered material is leached with water to extract the iodine. An oxidation step converts iodine species to iodate. The solution is acidified; the iodate is reduced to iodide and analyzed by a known addition procedure.

REAGENTS AND APPARATUS

The flux is prepared by mixing equal weights of sodium carbonate and potassium carbonate. To this is added one-fourth weight of magnesium oxide. One gram of crystalline potassium permanganate is placed in a beaker along with 100 ml of demineralized water to make a 1-percent permanganate solution. A 5-percent stannous sulfate solution is prepared by dissolving 5 g stannous sulfate in 50 ml of water; then 50 ml of concentrated sulfuric acid is carefully added. A piece of metallic tin is added to the solution. In place of the stannous sulfate solution, a 5-percent hydroxylamine sulfate solution can be used; this is prepared by adding 5 g of hydroxylamine sulfate to 100 ml of distilled water.

Standard solutions are prepared from reagent-grade sodium iodide. A 1-percent solution of iodide is made by placing 1.18 g of sodium iodide in a 100-ml volumetric flask. The flask is filled up to the mark with distilled, demineralized water. More dilute standards are prepared fresh daily from this. The 1-percent solution is prepared weekly.

An Orion Model 407 specific ion meter is used for the determination of iodide, when coupled with an Orion Model 94–53 iodide-ion selective electrode and a Model 90–01 single-junction reference electrode. The reference electrode is filled with Orion 90–00–01 filling solution.

SAMPLE DISSOLUTION

A 1-g sample is weighed into a Coors No. 01 porcelain crucible, and 5 g of flux is added. The sample and flux must be thoroughly mixed. The sample is then heated in a furnace for 1 h at 700°–750°C. After removal of the sample from the furnace and cooling, about 10 to 15 ml of water is added to loosen the sinter in the crucible. The material is removed from the crucible and placed in a 100-ml beaker; water is added to bring the volume to about 20 ml. The sinter can be loosened by boiling the water in the crucible. When all the sinter has been transferred to the beaker, about 20 ml of concentrated ammonium hydroxide and a piece of zinc are added if silver is present or suspected in the sample; the sample is allowed to stand overnight. If no silver is present the ammonium hydroxide

and zinc can be omitted and only about an hour of waiting is sufficient.

The following day, or hour, the sample is filtered, 3 to 5 drops of 1-percent potassium permanganate are added to the resulting solution, and the solution is boiled for 2 min. When cool, the solution is very carefully acidified with 5 ml of 1:1 sulfuric acid. The solution is cooled to about 23°C, and 1 ml of 5-percent stannous sulfate solution is added. The sample is transferred to a 50-ml volumetric flask and water is added to the mark.

ESTIMATION

Estimation of iodine (as iodide) is done by a method of addition. The iodide-ion electrode and reference electrode are dipped into the test solution. When equilibrium is established the needle of the specific ion meter is set at infinity on the known addition scale. 1 ml of 1-μg/ml iodide solution is added. The reading on the known-increment scale is the amount of iodine in the original sample. If the sample concentration is greater than 5 ppm (0.1 μg/ml in the solution) the needle will not deflect far enough to be on the calibrated part of the scale, and the needle is again set at infinity and 1 ml of 10 μg/ml solution is added. The reading obtained is multiplied by 10 to obtain the original iodine concentration. Because of the first addition, 1 ppm must be subtracted.

DISCUSSION

Some types of samples present special problems. Sulfide-containing samples can possibly allow sulfide species to interfere with the function of the electrode unless the sulfide is removed. This problem is usually eliminated during the sintering process, which oxidizes most of the sulfides. The basic oxidation step with permanganate oxides sulfides and the analysis is done in strongly acidic solution; as a result most of any remaining sulfide is present as hydrogen sulfide.

The function of the sensing electrode is based on the solubility of silver iodide. If a sample contains sufficient silver the electrode responds to that instead of iodide, and so the silver must be removed. This removal is accomplished by the addition of ammonium hydroxide to the basic solution along with a small amount of zinc or tin metal, resulting in the reduction of the silver. Even with this reduction step, care must be taken to ensure that the electrode is responding to iodide and not to silver. The following simple comparison test can identify silver interference. An iodide solution of concentration near the detection limit can be prepared in the same manner as the samples. The potential of this solution is then measured on the millivolt expanded scale of the meter. The questionable solution then is compared to this. If the millivolt reading is more negative than the test solution, the electrode is responding to iodide; if it is several millivolts more positive, it is responding to silver and the test must be done over.

Iodine in rocks and soils is easily detected as iodide by using the ion-selective electrode. Iodine is oxidized to iodate in the alkaline permanganate step. This helps eliminate iodine loss on the acidification of the carbonate solution. Bromide is not oxidized in basic permanganate solution. Because iodide is one of the worst interferences for the bromide electrode and at this point it is now iodate, which does not interfere, it becomes possible to detect bromide in the same solution.

In some circumstances, the same solutions can be used for determining bromine content. The bromide-ion electrode is less sensitive than the iodide-ion electrode, and thus the bromide must be preesnt in amounts of at least 5 ppm. The bromide is detected just after acidification. A drop of alcohol is added to stop the oxidation of bromide in the acidic permanganate solution.

RESULTS

The procedure described is quick and reasonably accurate, and results compare favorably with those obtained by neutron activation analysis (table 1).

TABLE 1.—*Comparison of ion-selective electrode values with those obtained by neutron activation analysis*

[Values in parts per million. Neutron activation analysis (N.A.A.) by Ardith Bartel]

Sample	N.A.A. method	Proposed method		
		Run 1	Run 2	Run 3
Shale samples collected in Missouri by J. J. Connor				
1 -------	19	17.5	17	18
2 -------	19	15.5	14.5	19
Soil samples collected in Missouri by Ronald Tidball				
3 -------	5.53	4.5	3.7	3.6
4 -------	3.08	2.0	2.0	3.3
5 -------	7.3	4.8	5.8	6.0
6 -------	4.44	4.4	4.6	2.4
7 -------	1.08	.5	.9	1.4
8 -------	12.3	7.6	7.4	9.0

Table 2 lists the mean, standard deviation and relative standard deviation obtained for each of the 13 additional samples on repetitive analysis.

Table 1 indicates that accuracy is adequate for the large number of samples to be analyzed in a geochemical exploration study. Table 2 details the precision that can be expected from this method.

Table 3 compares bromine results obtained for three rock samples by the proposed method and by X-ray fluorescence.

TABLE 2.—*Precision of ion-selective electrode analyses for iodine*

Sample	Mean value (ppm)	Standard deviation	Relative standard deviation (percent)	Number of runs
Soil samples collected by Robert Lantz from Cymric oil field, California				
1	8.1	±0.9	11	15
2	1.6	± .4	25	9
3	6.3	± .8	13	10
4	.9	± .3	33	10
5	12	±1.8	15	7
6	2.6	± .3	12	10
7	2.7	± .3	11	8
8	1.4	± .5	36	4
Rock samples collected by J. H. McCarthy, Jr. from copper-producing areas in Arizona				
9	1.5	±0.2	13	9
10	1.5	± .3	20	6
11	5.8	±1.2	21	6
12	9.4	±1.2	13	5
USGS standard rock (dunite)				
DTS-1	0.6	±0.26	43	10

TABLE 3.—*Comparison of bromine values obtained by bromide-ion electrode with those obtained by X-ray fluorescence analysis*

[X-ray fluorescence analyses by James Wahlberg. Samples collected by J. H. McCarthy, Jr., from copper-producing areas in Arizona]

Sample	Analyses (parts per million)	
	By electrode	By X-ray
1	75	70
2	160	150
3	800	750

REFERENCES CITED

Grimaldi, F. S., and Schnepfe, M. M., 1971, Determination of iodine in the ppm range in rocks: Anal. Chim. Acta, v. 53, p. 181–184.

Ross, J. W., Jr., 1969, Solid-state and liquid membrane ion-selective electrodes, *in* Durst, R. A., ed., Ion-selective electrodes: Natl. Bur. Standards Spec. Pub. 314, Chap. 2, p. 57–88.

Sandell, E. B., and Kolthoff, I. M., 1934, Chronometric catalytic method for the determination of micro quantities of iodine: Jour. Am. Chem. Soc., v. 56, no. 1, p. 1426.

——— 1937, Microdetermination of iodine by a catalytic method: Mikrochim. Acta, no. 1, p. 9–25.

Schneider, L. A., and Miller, A. D., 1965, Determination of microamounts of iodine in silicate rocks by a kinetic method: USSR Jour. Anal. Chemistry, v. 20, no. 1, p. 81–86; translation of Zhurnal Analiticheskoi Khimii, v. 20, no. 1, p. 92–97.

ANNUAL INDEX TO VOLUME 3

Journal of Research of the U.S. Geological Survey

[Issue number precedes colon; page number follows colon]

SUBJECT INDEX

AUTHOR INDEX

METRIC-ENGLISH EQUIVALENTS

Metric unit		English equivalent	
Length			
millimetre (mm)	=	0.03937	inch (in)
metre (m)	=	3.28	feet (ft)
kilometre (km)	=	.62	mile (mi)
Area			
square metre (m^2)	=	10.76	square feet (ft^2)
square kilometre (km^2)	=	.386	square mile (mi^2)
hectare (ha)	=	2.47	acres
Volume			
cubic centimetre (cm^3)	=	0.061	cubic inch (in^3)
litre (l)	=	61.03	cubic inches
cubic metre (m^3)	=	35.31	cubic feet (ft^3)
cubic metre	=	.00081	acre-foot (acre-ft)
cubic hectometre (hm^3)	=	810.7	acre-feet
litre	=	2.113	pints (pt)
litre	=	1.06	quarts (qt)
litre	=	.26	gallon (gal)
cubic metre	=	.00026	million gallons (Mgal or 10^6 gal)
cubic metre	=	6.290	barrels (bbl) (1 bbl=42 gal)
Weight			
gram (g)	=	0.035	ounce, avoirdupois (oz avdp)
gram	=	.0022	pound, avoirdupois (lb avdp)
tonne (t)	=	1.1	tons, short (2,000 lb)
tonne	=	.98	ton, long (2,240 lb)
Specific combinations			
kilogram per square centimetre (kg/cm^2)	=	0.96	atmosphere (atm)
kilogram per square centimetre	=	.98	bar (0.9869 atm)
cubic metre per second (m^3/s)	=	35.3	cubic feet per second (ft^3/s)

Metric unit		English equivalent	
Specific combinations—Continued			
litre per second (l/s)	=	.0353	cubic foot per second
cubic metre per second per square kilometre [$(m^3/s)/km^2$]	=	91.47	cubic feet per second per square mile [$(ft^3/s)/mi^2$]
metre per day (m/d)	=	3.28	feet per day (hydraulic conductivity) (ft/d)
metre per kilometre (m/km)	=	5.28	feet per mile (ft/mi)
kilometre per hour (km/h)	=	.9113	foot per second (ft/s)
metre per second (m/s)	=	3.28	feet per second
metre squared per day (m^2/d)	=	10.764	feet squared per day (ft^2/d) (transmissivity)
cubic metre per second (m^3/s)	=	22.826	million gallons per day (Mgal/d)
cubic metre per minute (m^3/min)	=	264.2	gallons per minute (gal/min)
litre per second (l/s)	=	15.85	gallons per minute
litre per second per metre [(l/s)/m]	=	4.83	gallons per minute per foot [(gal/min)/ft]
kilometre per hour (km/h)	=	.62	mile per hour (mi/h)
metre per second (m/s)	=	2.237	miles per hour
gram per cubic centimetre (g/cm^3)	=	62.43	pounds per cubic foot (lb/ft^3)
gram per square centimetre (g/cm^2)	=	2.048	pounds per square foot (lb/ft^2)
gram per square centimetre	=	.0142	pound per square inch (lb/in^2)
Temperature			
degree Celsius (°C)	=	1.8	degrees Fahrenheit (°F)
degrees Celsius (temperature)	=	[(1.8×°C)+32]	degrees Fahrenheit

RECENT PUBLICATIONS OF THE U.S. GEOLOGICAL SURVEY

(The following books may be ordered from the U.S. Geological Survey, 1200 South Eads Street, Arlington, VA 22202 (an authorized agent of the Superintendent of Documents, Government Printing Office). Prepayment is required. Remittances should be sent by check or money order payable to U.S. Geological Survey. Give series designation and number, such as Bulletin 1368–A, and the full title. Prices of Government publications are subject to change. Increases in costs make it necessary for the Superintendent of Documents to increase the selling prices of many publications offered. As it is not feasible for the Superintendent of Documents to correct the prices manually in all the previous announcements and publications stocked, the prices charged on your order may differ from the prices printed in the announcements and publications)

Professional Papers

437–E. Land subsidence due to ground-water withdrawal in the Los Banos-Kettleman City area, California, Part 1. Changes in the hydrologic environment conducive to subsidence, by W. B. Bull and R. E. Miller. 1975. p. E1–E71. $2.05.

708. Ground-water hydraulics, by S. W. Lohman. 1972. 70 p.; plates in pocket. $4.15. (Reprinted 1975.)

716–C. Geology of the southern Himalaya in Hazara, Pakistan, and adjacent areas, by J. A. Calkins, T. W. Offield, S. K. M. Abdullah, and S. Tayyab Ali. 1975. p. C1–C29; plates in pocket. $4.70.

725–B. Generalized geologic framework of the National Reacter Testing Station, Idaho, by R. L. Nace, P. T. Voegeli, J. R. Jones, and Morris Deutsch, edited by Seymour Subitzky. 1975. p. B1–B49; plate in pocket. $2.90.

818–C. The effect of sedimentation and diagenesis on trace element composition of water-laid tuff in the Keg Mountain area, Utah, by D. A. Lindsay. 1975. p. C1–C35. $1.35.

856. Structure and origin of the Koae fault system, Kilauea Volcano, Hawaii, by W. A. Duffield. 1975. 12 p.; plates in pocket. $1.70.

877. The Black Hills–Rapid City flood of June 9–10, 1972: A description of the storm and flood, by F. K. Schwarz, L. A. Hughes, E. M. Hansen, M. S. Petersen, and D. B. Kelly. 1975. 47 p. $1.55.

884 Carboniferous biostratigraphy, northeastern Brooks Range, arctic Alaska, by A. K. Armstrong and B. L. Mamet. 1975. 29 p. $1.25.

889. Precambrian and Lower Ordovician rocks in east-central Idaho. Chapter A, Precambrian Y sedimentary rocks in east-central Idaho, by E. T. Ruppel. Chapter B, Precambrian Z and Lower Ordovician rocks in east-central Idaho, by E. T. Ruppel, R. J. Ross, Jr., and David Schleicher. 1975. 34 p. $1.20.

892. Physical results of research drilling in thermal areas of Yellowstone National Park, Wyo., by D. E. White, R. O. Fournier, L. J. P. Muffler, and A. H. Truesdell. 1975. 70 p. $1.90.

940. Mineral resource perspective 1975. 1975. 24 p. 95¢.

Bulletins

1211–F. Geologic reconnaissance of a proposed powersite on the Maksoutof River near Sitka, southeastern Alaska, by A. A. Wanek. 1975. p. F1–F22; plate in pocket. $1.35.

1309. The geologic story of Isle Royale National Park, by N. K. Huber. 1975. 66 p. $1.20.

1313–E. Automatic interpretation of Schlumberger sounding curves, using modified Dar Zarrouk functions, by A. A. R. Zohdy. 1975. p. E1–E39. 70¢.

1393. The geologic story of Arches National Park, by S. W. Lohman, with graphics by J. R. Stacy. 1974 (1975). 113 p. $2.85.

1395–I. Marine trace fossils in the Upper Jurassic Bluff Sandstone, southeastern Utah, by R. B. O'Sullivan and J. O. Maberry, 1975. p. I1–I12. 45¢.

1395–J. The Supai Group—subdivision and nomenclature, by E. D. McKee. 1975. p. J1–J11. 40¢.

1396. Index of generic names of fossil plants, 1966–1973, by A. M. Blazer. 1975. 54 p. 85¢.

Water-Supply Papers

1473. Study and interpretation of the chemical characteristics of natural water, *second edition*, by J. D. Hem. 1970. 363 p.; plates in pocket. $3.35. (Reprinted 1975.)

2101. Surface water supply of the United States, 1966–70—Part 1, North Atlantic slope basins—Volume 1, Basins from Maine to Connecticut. 1975. 1,123 p. $8.60.

2120. Surface water supply of the United States, 1966–70—Part 7, Lower Mississippi River basin—Volume 1, Lower Mississippi River basin except Arkansas River basin. 1975. 1,278 p. $9.60.

2122. Surface water supply of the United States, 1966–70—Part 8, Western Gulf of Mexico basins—Volume 1, Basins from Mermentau River to Colorado River. 1975. 1,144 p. $8.75.

2133. Surface water supply of the United States, 1966–70—Part 12, Pacific slope basins in Washington—Volume 2, Upper Columbia River basin. 1975. 674 p. $5.50.

2134. Surface water supply of the United States, 1966–70—Part 13, Snake River basin. 1974 (1975). 821 p. $5.50.

2151. Quality of surface waters of the United States, 1970—Part 1, North Atlantic slope basins. 1975. 674 p. $5.55.

2154. Quality of surface waters of the United States, 1970—Parts 4 and 5, St. Lawrence River basin, and Hudson Bay and Upper Mississippi River basins. 1975. 482 p. $4.15.

2155. Quality of surface waters of the United States, 1970—Part 6, Missouri River basin. 554 p. $4.70.

2156. Quality of surface waters of the United States, 1970—Part 7, Lower Mississippi River basin. 1975. 636 p. $5.25.

2171. Ground-water levels in the United States, 1969–73—Southeastern States. 250 p. $2.45.